POLITECNICO DI TORINO

Master's Degree in Physics of Complex Systems

Master's Degree Thesis
developed at the Chair of Entrepreneurial Risks, ETH Zürich

A Statistical Physics approach to financial bubbles: Ising-like modeling of social imitation in an Agent-based multi-asset market

Supervisors

Prof. Didier Sornette

Prof. Luca Dall'Asta

Rebecca Westphal

Candidate

Davide Cividino

Academic year: 2019/2020

Ai miei genitori
Claudia e Pier Luigi,
per tutto

Abstract

From the seventeenth-century Dutch Tulip Bubble and the eighteenth-century South Sea Bubble to the more recent Dotcom Bubble and U.S. Housing Bubble, the economic history has been characterized by bubbles and crashes, booms, and crises of all sorts. To fully understand the financial markets, it is crucial to embrace the fact that the world economy is a constantly evolving multi-agent complex system, that can be studied using the tools of complex systems theory. Among them, the Agent-Based Models (ABMs) are powerful tools to investigate the dynamics of complex systems, and the Statistical Physics has a history of success in modeling systems with a large number of components (in this case the traders) whose collective interactions lead to the emergence of highly not trivial collective phenomena (the bubbles).

The present thesis proposes an extension of an ABM, first introduced by Kaizoji et al. (2015) which is able to reproduce faster-than-exponential bubbles growth together with the "stylized facts" of the financial market. The original model is constituted by two classes of investors: the fundamentalist traders, rational risk-averse traders, and the noise traders guided instead by social imitation and trend following. The traders invest in two assets, one risk-free asset, and one risky asset. The price dynamics is generated imposing the market clearing conditions according to Walras' theory of general equilibrium.

After a review of the original model, we introduce an extension to a multi-asset framework composed of one risk-free asset and many risky assets. First, we address the extension of the fundamentalist traders' class. We then move to the market-clearing conditions, which involves the solution of a complex non-linear system that is addressed with numerical techniques.

The remaining and largest part of the work deals with the extension of the noise traders class. The fundamental feature characterizing it is its Ising-like structure which models the competition between the ordering force of social imitation and the disordering impact of idiosyncratic opinion, hence we largely resort to statistical physics to consider its generalization. We propose four statistical models, deriving the stochastic dynamics characterizing each of them, and discussing their strengths and weaknesses. We consider a Potts model, an O(n) model, a vectorial extension of the BEG model, and an n-state extension of the BEG model. All the models share the same underlying mechanism triggering the bubbles. When the herding propensity parameter exceeds a certain critical threshold, the noise traders class undergoes a phase transition from the disordered state dominated by the idiosyncratic opinion to the ordered state where the class polarizes towards specific investment preferences. This interaction-driven collective behavior leads

to the emergence of the bubbles. A thorough analysis of the phase transition is carried out.

In the last part of the work, we deepen the analysis of the ABM with the O(n) model for the noise traders class. We focus on it due to both the validity of the resulting price time series and the high controllability of its behavior. We first check the model's ability to reproduce the "stylized facts" of financial markets. Then the ABM is applied to understand the mechanism behind the time synchronization of bubbles among the assets. Finally, the dynamic of the returns is compared to the one predicted by the Capital Asset Pricing Model.

Acknowledgements

I am deeply grateful to Prof. Sornette for giving me the opportunity to conclude my academic journey working on my Master's Thesis at his Chair of Entrepreneurial Risks, ETH Zürich. The enlightening conversations with him together with the department breakfast meetings have been unique opportunities for learning and discussing.

My warmest thank goes to Rebecca Westphal for her precious help and generous availability throughout the previous months. I could never thank Rebecca enough for her support and crucial suggestions.

A special thank goes to my internal supervisor Luca dall'Asta and my colleague Matteo Bisardi for the insightful conversations about some implementation aspects of the simulations.

A warmly thank is dedicated to my colleagues, who shared with me the challenging and beautiful adventure of PCS. You are the brightest and most talented people I have ever met, you pushed me to give my best and improve every day.

Naturally, a special thank goes to my lifelong friends, we have shared so much together and you have been always there for me.

My heartfelt thank goes to my parents, Claudia and Pier Luigi to whom this work is dedicated. I owe everything to you, you always encouraged me in my choices and supported me in the difficulties.

I want to give special thought to my grandfathers, Adriano and Mario. I know you would have been happy to see me achieve this goal. You taught me the priceless value of hard work and dedication, deeply believe in what you do and give your best to do it. You have always been and you will always be my role models.

Finally, a special thank goes to you, Carola. You shared with me the challenges of this master and the adventure of this piece of our life, both in the ups and downs. You have colored my life with new bright emotions, and the emotions are all that matters.

Table of Contents

List of Tables

List of Figures

Chapter 1

Introduction

From the seventeenth-century Dutch Tulip Bubble and the eighteenth-century South Sea Bubble to the more recent Dotcom Bubble and U.S. Housing Bubble, the financial and economic history have been characterized by bubbles and crashes, booms, and crises of all sorts.

Despite the very definition of a bubble still being disputed, the impact of such extreme collective phenomena like those aforementioned is undoubtedly dramatic. Understanding the origin of these events is arguably one of the most important problems in economic theory.

Traditional economic and finance theories based on a single representative agent with unbounded rationality fail to explain and predict such phenomena and other empirical facts characterizing financial markets. Indeed, the research in this field is going through a paradigm shift from one representative rational agent towards many diversified interacting agents with heterogeneous expectations and bounded rationality as explained among the others in Lux [1], Arthur et al. [2], Brock and Hommes [3], and Heckman [4].

Numerous empirical evidence has questioned the assumption of fully rational and homogeneous behavior of the investors, as commented in Conlisk [5] and Rubinstein [6]. The developments of behavioral economics have pushed this trend even more. Now it is clear that by reducing all the complexity of the economical and financial world to a single rational representative agent we are missing a central part of the phenomena governing the evolution of such an articulated system. The so-called "stylized facts" of the financial markets, discussed in Cont [7] and Cont [8], emerging statistical regularities observed across a wide range of instruments, markets, and time periods, are difficult to be accommodated and explained in a setting that does not place at the center the role of interactions and heterogeneity.

To fully understand the financial markets, it is crucial to embrace the fact that the world economy is a constantly evolving multi-agent complex system, that can be studied using the tools of complex systems theory. Among them, on the one hand,

the Agent-Based Models (ABMs), as discussed in Axelrod [9], Hommes [10], Chan et al. [11], are powerful tools to investigate the dynamics of complex systems and on the other hand, Statistical Physics has a history of success in modeling systems with a large number of components (in this case the traders) whose collective interactions lead to the emergence of highly non-trivial collective phenomena (in this case the bubbles). Its fruitful application in finance is beautifully reviewed in Sornette [12] Both tools are central to this work.

The present thesis proposes an extension of an ABM, first introduced by Kaizoji et al. [13] which is able to reproduce faster-than-exponential bubbles growth together with "stylized facts" of the financial market.

The original model is constituted of two assets. A risk-free asset, representing a zero-coupon government bond yielding a constant rate of return, and a risky asset, representing a stock paying a dividend to its holders. The latter asset's risk derives from the fact that its rate of return is not known a priori by the investors, depending on the endogenous dynamics of the asset's price and stochastic dividend.

The model features two classes of agents, the fundamentalist traders and the noise traders. The fundamentalists are rational risk-averse traders. Their strategy consists of maximizing, each trading day, their expectation under a Constant Relative Risk Aversion (CRRA) utility function, resulting in the diversification of their investments into a risky and risk-free fraction, as explained in Chiarella et al. [14].

The noise traders, instead are driven by social imitation and trend following, from their original introduction in Lux and Marchesi [15]. At odds with the fundamentalists, each noise trader allocates all his wealth into either the risky asset or the risk-free asset according to a Bernoulli probability distribution, depending on the past prices, through the price momentum, and on the investment preferences of the other traders, through the opinion index. It is this social imitation mechanism that leads to the Ising-like structure of the noise trader class, which will be the central element throughout all the following work.

A wealth dynamics equation governs the time evolution of the traders' wealth. Finally, the two classes of investors interact in the formation of the price of the risky asset through the price equation, where both the fundamentalist and noise investment fractions are present. The price equation is derived from the market-clearing conditions according to Walras' theory of general equilibrium, Walras [16].

After a review of the original model, we introduce an extension to a multi-asset framework characterized by one risk-free asset and many risky assets. Given that in the real financial markets lots of risky assets exist and the portfolio theory is one of the fundamental pillars of modern financial theory, it is clear why we are deeply interested in extending the original setup in this direction. We need to develop an extension for all the components of the model.

First, we address the extension of the dividend process, the wealth dynamics equation, and the fundamentalist traders' class. The fundamentalists solve an optimization problem, this time with respect to many risky investment fractions, that can still be solved analytically. We then move to the generation of the price dynamics, which involves the solution of a complex non-linear system that is addressed with numerical techniques.

The remaining and largest part of the thesis deals with the extension of the noise traders' class, which leaves many possible generalization directions open and requires a deeper theoretical analysis and a careful implementation strategy.

The fundamental feature characterizing the noise traders' class is its Ising-like structure which models the competition between the ordering force of social imitation and the disordering impact of idiosyncratic opinion, hence we largely resort to statistical physics to consider its generalization.

We propose four statistical models for the noise traders' class, deriving the stochastic dynamics characterizing each of them and discussing their strengths and weaknesses. We consider in order a Potts model, an $O(n)$ model, a vectorial extension of the BEG model, and an n-state extension of the BEG model.

Despite their differences, all the models share the same underlying mechanism triggering and generating the bubbles. When the herding propensity parameter exceeds a certain model-dependent critical threshold, the noise traders' class undergoes an actual phase transition from the disordered state dominated by the idiosyncratic opinion to the ordered state where the class polarizes towards specific investment preferences. This interaction-driven collective behavior leads to the emergence of highly non-trivial phenomena, the bubbles. This is a typical feature of complex multi-agent systems.

A thorough analysis of the phase transition and its impact on the price dynamics is carried out. In particular, the trend following behavior of the noise traders is interpreted in a statistical physics fashion as an external field tilting the average opinion. Several tools of complex systems theory are applied to gain theoretical insights into the dynamics of the model, e.g. the stability theory of dynamical systems and the Landau expansion of the free energy.

The core of the present work is constituted by the derivation of a realistic stochastic dynamics for the investments, from each of the aforementioned statistical models. The use of Master Equations and balance conditions characterize the derivation of the simulation algorithms for the market model. Each model is defined by its Hamiltonian, entering in the Boltzmann weight. The latter constitutes the probability distribution associated with the possible configurations of the noise traders class, hence it associates a probability to each possible set of investment decisions the whole pool of traders can undertake. The Boltzmann weight of the model completely determines the statistical properties of the system under analysis.

However, we are interested in modeling the dynamics of the class and not just

its average properties. Hence, the next step for each of the four aforementioned models is to derive the stochastic dynamics characterizing it. We have at disposal a powerful tool to define realistic stochastic dynamics while having complete control of the resulting statistical properties. This tool is constituted by the Markov Chain Monte Carlo (MCMC) theory together with the detailed balance condition which allows us to do exactly what we need, to start from the Boltzmann weight and to obtain through a theoretically solid derivation the transition probabilities which fully determines the stochastic dynamics of the model and therefore the time evolution of the investment decisions of the noise traders.

The implementation of the simulations, which constituted a large part of the work, is done in *C++*. The results of the simulation are stored in a database using the *HDF5* high-performance data library. Then all the analysis of the data and the plotting are performed with *Python*, in particular using the *Matplotlib*, the *Pandas* and the *Seaborn* libraries and accessing the *HDF5* database through the *Python* interfacing library *h5py*.

Another central tool of the work is Decision Theory. Indeed, the analysis of these models unveils a profound connection between the Ising-like structure of the noise traders' class and the Decision Theory framework, in particular concerning the Logit distribution, constituting the theoretical setting in which we can understand the decision process characterizing the investments of this type of agents.

Finally, in the last part of the work, we deepen the analysis of the ABM with the O(n) model for the noise traders' class. We focus on it due to both the validity of the resulting price time series and to the high controllability of its behavior, connected to solid theoretical results on the model itself and the intuitive meaning of its parameters.

We first check the model's ability to reproduce the "stylized facts" of financial markets, in particular, focusing on the hyperbolic decay of the autocorrelation function of the absolute returns in contrast to the exponential decay of the autocorrelation of the signed returns, together with the fat-tailed behavior of the distribution of the returns. Then the analysis is carried out in two main directions. First, the extended ABM is applied to understand the mechanism behind the time synchronization of bubbles among the assets. The second instead deals with the comparison of the dynamics of the resulting returns to the one predicted by the Capital Asset Pricing Model (CAPM).

We close this introduction by presenting the outline of the work. In Chapter 2 we review the original market model setup, but we also expand the analysis presented in the previous works on the model introducing and discussing new points. In particular in section 2.6 we deepen the profound connection between the noise traders class and the Ising model and in section 2.7 we present a new analysis on two features of the original model's transition rates which appear to be fundamental in characterizing a realistic dynamics of the bubbles.

In Chapter 3 we move towards the multi-asset extension of the market model. We first discuss the multiple assets and the extended wealth dynamics in section, then we move to the discussion of the fundamentalist traders class generalization and extension of the market-clearing conditions and the resulting price equations. Finally, we discuss the noise traders' generalization puzzle in section, introducing the approach we will use in the next Chapter to tackle it.

In Chapter 4 we present the core of the present work, constituting by the Statistical Physics's approach to the extension of the noise traders class. We discuss the four statistical models, a Potts model, an $O(n)$ model, a vectorial extension of the BEG model, and an n-state extension of the BEG model and for each of them we derive the characterizing stochastic dynamics and we discuss their strengths and weaknesses.

Finally, in the last Chapter 5 we move to the comparison of the simulation results of the $O(n)$ model with the real financial markets and to its application to investigate interesting financial phenomena. In particular, after having checked the model's ability to reproduce the "stylized facts" of financial markets, we try to gain insights into the mechanism behind the time synchronization of bubbles among the assets. We close the work comparing the dynamics of the resulting returns to the one predicted by the Capital Asset Pricing Model (CAPM).

Chapter 2

The original Market Model

In this Chapter, we review the original market model, first introduced by Kaizoji et al. [13]. We present it in a slightly modified version with respect to the original paper's one, based on the works of Kohrt [17] and Westphal and Sornette [18]. The model has been studied and modified in several directions in Ollikainen [19], Conti [20], Damiani [21], Kopp [22], Drouard [23] and Westphal and Sornette [24].

The market model presented is an Agent-Based Model (ABM), which is able to reproduce faster-than-exponential bubbles growth together with the "stylized facts" of financial market. It is constituted of two assets. A risk-free asset, representing a zero-coupon government bond yielding a constant rate of return, and a risky asset, representing a stock paying a dividend to its holders. The latter asset's risk derives from the fact that its rate of return is not known a priori by the investors, depending on the endogenous dynamics of the asset's price.

The model features two classes of agents, the fundamentalist traders and the noise traders. The fundamentalists are rational risk-averse traders. Their strategy consists in maximizing, each trading day, their expectation under a Constant Relative Risk Aversion (CRRA) utility function, resulting in the diversification of their investments into a risky and a risk-free fraction, as explained in Chiarella et al. [14].

The noise traders, instead are driven by social imitation and trend following, from their original introduction in Lux and Marchesi [15]. At odds with the fundamentalists, each noise trader allocates all his wealth into either the risky asset or the risk-free asset according to a Bernoulli probability distribution, depending on the past prices, through the price momentum, and on the investment preferences of the other traders, through the opinion index. It is this social imitation mechanism that leads to the Ising-like structure of the noise trader class, which will be the central element throughout all the following work.

Both the fundamentalist traders class and the noise traders class can be considered at the aggregate level, yet for different reasons. Each fundamentalist trader

solves the same optimization problem of all the other traders in its class. They all optimize the expectation of the same utility function, they are all characterized by the same constant risk aversion and they all have identical information (price, dividend and long-term expectations of return and standard deviation). Indeed, the whole class can be considered at the aggregate level through a representative agent, whose wealth is equal to the sum of all the wealth of the fundamentalist investors.

The noise traders instead are characterized by the lack of diversification, investing in one asset at a time. Hence, their actual impact on the market dynamics has to be considered at the aggregate level, where the representative noise investor endowed with the total wealth of the class invests into the risk and risk-free assets in factions accounting for the respective proportion of traders.

The two classes of investors interact in the formation of the price of the risky asset through the price equation, where both the fundamentalist and noise investment fractions are present. The price equation is derived from the market-clearing conditions according to Walras' theory of general equilibrium, Walras [16].

In the following, we present in order the various components of the model. We start in section 2.1 from the two assets, in particular the dividend process of the risky one, and the wealth dynamics. Then we move in sections 2.2 and 2.3 to the fundamentalist traders and the noise traders, respectively. Finally, we present in section 2.4 the market-clearing conditions and we derive from them the price equation which governs the dynamics of the price of the risky asset and ultimately the dynamics of the market model.

After having introduced the structure of the original model, we move in section 2.5 to its dynamics. We present in particular the time series resulting from two simulations, introducing the set of parameters used, commenting on some implementation details, and then moving to the time series description. In section 2.6 we unveil the profound connection between the noise traders class and the Ising model, exploiting this correspondence to gain insights into the emergence of the bubbles. Finally, in section 2.7 we present a new analysis on two features of the original model's transition rates which appear to be fundamental in characterizing a realistic dynamics of the bubbles.

2.1 The assets and the wealth dynamics

The model is characterized by two assets, one risk-free and one risky. The risk-free asset represents a zero-coupon government bond yielding a constant rate of return r_f. This risk-free rate of return represents the benchmark interest an investor would expect from an absolutely risk-free investment. In the model r_f is defined such that it represents the daily risk-free rate of return, where the convection is

that the year is composed of 250 trading days.

The risky asset instead represents a stock paying a stochastic dividend. Its intrinsic risk derives both from the stochastic character of its dividend and from the fact that its return rate also depends on the dynamics of its price which is not known a priori. Following the modification of the original model introduced by Kohrt [17], the dividends are determined each trading day by a multiplicative growth process

$$d_t = (1 + r_t^d)d_{t-1}, \tag{2.1}$$

with a stochastic growth factor r_t^d modeled by a normal distribution

$$r_t^d \sim \mathcal{N}(r_d, \sigma_d^2) \tag{2.2}$$

with mean r_d, representing the constant growth of the dividend, and standard deviation σ_d.

The complete dynamics of the dividend process is indeed determined by the i.i.d. Gaussian random variables r_i^d,

$$d_t = d_0 \prod_{i=1}^{t} (1 + r_i^d), \tag{2.3}$$

where d_0 is the initial dividend. The total risky rate of return r_t of the risky asset is defined by two contributions

$$r_t^{tot} = \frac{d_t}{P_{t-1}} + r_t, \tag{2.4}$$

where the first quantity is the dividend yield, the return deriving from the payment of the dividend, while the second is the price rate of return, also called capital return

$$r_t = \frac{P_t}{P_{t-1}} - 1, \tag{2.5}$$

depending on the price dynamics. From expression (2.4), the two sources of risk are clearly identifiable, i.e. the stochastic character of the dividend and the not knowable a priori price dynamics. This enhanced risk with respect to the asset representing the zero-coupon bond, it's called risk premium with respect to r_f. The possibility of a more remunerative investment can push the traders to invest in the risky asset.

As for the quantities already introduced, the evolution of the entire model takes place according to a discrete-time dynamics in which all the quantities change discretely each trading day, then holding their values in the interval $(t, t + 1)$.

We have already commented on the possibility to consider the fundamentalist and noise traders classes at the aggregate level by means of a representative agent.

We will deepen this topic in the next sections. By now, we simply assume, following Kaizoji et al. [13], that each trading day the class of fundamentalist (noise) traders effectively constructs its aggregate portfolio investing a fraction x_t^f (x_t^n) of its wealth W_t^f (W_t^n) in the risky asset and a fraction $1 - x_t^f$ ($1 - x_t^n$) in the risk-free asset. Borrowing and short-selling are not admitted in the market model, hence the risky fractions always satisfy $x_t^{f,n} \in [0,1]$.

According to this description, we can write the wealth dynamics equation for both the fundamentalist and noise classes as

$$W_t^{f,n} = W_{t-1}^{f,n} x_{t-1}^{f,n} \left[1 + \frac{d_t}{P_{t-1}} + r_t \right] + W_{t-1}^{f,n} (1 - x_{t-1}^{f,n})(1 + r_f), \tag{2.6}$$

where the first term accounts for the risky investment while the second for the risk-free one. Reorganizing the terms we obtain the expression

$$W_t^{f,n} = W_{t-1}^{f,n} \left[1 + r_f + x_{t-1}^{f,n} \left(\frac{d_t}{P_{t-1}} + \frac{P_t}{P_{t-1}} - 1 - r_f \right) \right], \tag{2.7}$$

where the quantity

$$r_t^{excess} = \left(\frac{d_t}{P_{t-1}} + \frac{P_t}{P_{t-1}} - 1 - r_f \right) = \left(\frac{d_t}{P_{t-1}} + r_t - r_f \right) \tag{2.8}$$

represents the excess return of the risky asset with respect to risk-free one and clearly shows the fact that the risky asset can be more profitable ($r_t^{excess} > 0$), but also less profitable ($r_t^{excess} < 0$), with respect to the risk-free asset.

2.2 The fundamentalist traders

The introduction of the fundamentalist traders in the original model of Kaizoji et al. [13], follows the work of Chiarella et al. [14] and Brock, Hommes, et al. [25].

The fundamentalist traders are rational risk-averse traders maximizing each trading day their expectation under a Constant Relative Risk Aversion (CRRA) utility function. They are myopic traders only considering one time-step. Each fundamentalist trader solves the same optimization problem of all the other traders in its class, they all optimize the expectation of the same utility function, they are all characterized by the same constant risk aversion and they have the same information about the assets. Indeed, the whole class can be considered at the aggregate level through a representative agent, whose wealth is equal to the sum of all the wealth of the fundamentalist investors. At each trading day t the fundamentalist traders decide the value of their risky fraction maximizing the expected utility function of the future wealth at time $t + 1$

$$x_t^f = \max_{x_t^f} \mathbb{E}_t[U(W_{t+1}^f(x_t^f)]. \tag{2.9}$$

The subscript of the expectation value underline that the expectation is done under the knowledge of available information up to and including time t. The CRRA utility function U is defined according to

$$U(W) = \begin{cases} \log(W) & \gamma = 1 \\ \frac{W^{1-\gamma}}{1-\gamma} & \gamma \neq 1 \end{cases} \tag{2.10}$$

where the constant risk aversion γ follows from

$$\gamma = -W \frac{U''(W)}{U'(W)}. \tag{2.11}$$

The maximization problem has been solved in Chiarella, He, et al. [26], here we report the final (approximated to first order) result

$$x_t^f = \frac{1}{\gamma} \frac{\mathbb{E}_t[r_{t+1}^{excess}]}{\mathrm{Var}_t[r_{t+1}^{excess}]}. \tag{2.12}$$

From the formula it emerges a mean-variance, or in other words, return-risk trade-off. The risky fraction is larger, the larger is the expected excess return of the risky asset and the lower is the uncertainty on its value, measured by its variance. We underline again that the expectation and the variance is computed under the knowledge of available information up to and including time t. We also notice that the risky fraction is independent of the fundamentalist's wealth, property descending from the definition of the Constant Relative Risk Aversion utility function.

The expectation of the excess return can be computed using the definition of the latter as

$$\mathbb{E}_t[r_{t+1}^{excess}] = \mathbb{E}_t\left[\frac{d_{t+1}}{P_t} + r_{t+1} - r_f\right] = \frac{d_t(1+r_d)}{P_t} + \mathbb{E}_t[r_{t+1}] - r_f, \tag{2.13}$$

where in the last passage we used the formula for the growth of the dividend (2.1) and the fact that the risk-free return rate is constant.

Following Kaizoji et al. [13] we also assume that the fundamentalist traders expect a constant return rate

$$\mathbb{E}_t[r_{t+1}] \coloneqq E_r = cst, \tag{2.14}$$

based on the expected behaviour of the risky asset in the long-run, and a constant variance of the return

$$\mathrm{Var}_t[r_{t+1}] \coloneqq \sigma_r^2 = cst. \tag{2.15}$$

The latter quantity is related to the variance of the excess return entering in formula (2.12) by assuming, following Kaizoji et al. [13], Modigliani and Miller [27],

Modigliani and Miller [28], that the dividend policy is independent of the market price and vice-versa and that $P_t \gg \sqrt{\frac{\mathrm{Var}_t[d_{t+1}]}{\mathrm{Var}_t[r_{t+1}]}}$, hence

$$\mathrm{Var}_t[r_{t+1}^{excess}] = \mathrm{Var}_t[r_{t+1}] + \frac{\mathrm{Var}_t[d_{t+1}]}{P_t^2} \approx \mathrm{Var}_t[r_{t+1}] = \sigma_r^2 = cst. \tag{2.16}$$

Then the risky fraction in formula (2.12) becomes

$$x_t^f = \frac{1}{\gamma} \frac{E_r - r_f + \frac{d_t(1+r_d)}{P_t}}{\sigma_r^2}. \tag{2.17}$$

Following Ollikainen [19], we comment on the fact that the fundamentalists allocate their wealth according to the "fundamentals" of the market. Any deviation from the fundamental value of the risky asset represents an opportunity to gain. In particular, we can identify the deviations from the fundamental value in the dividend-price ratio $\frac{d_t}{P_t}$, since the fundamental value is obtained discounting the stream of dividends by the constant factor $(1+r_d)$. Indeed, the strategy of the fundamentalist is buying the risky asset when the dividend-price ratio is high, hence the fundamental value is higher than the market price, and selling it when the ratio is low, hence the market price is higher then the fundamental value. From the expression (2.17), we also notice that the adjustment to the risky fraction are done on top of the constant quantity $\frac{1}{\gamma}\frac{E_r - r_f}{\sigma_r^2}$.

2.3 The noise traders

The noise traders do not implement a rational maximization process, as the fundamentalist traders do, to decide their investment decisions. They are instead driven by social imitation and trend following, allocating each trading day all their wealth into either the risky asset or the risk-free asset.

The setup of the noise traders class follows the work of Lux and Marchesi [15] and their "all-or-nothing" investment strategy accounts for the lack-of-diversification phenomenon, documented among the others in Kelly [29].

Since they are investing in one asset at a time, the noise traders have to be considered at the aggregate level of their class. Indeed, their actual impact on the market dynamics can be represented by the investment decisions of a representative agent, endowed with the total wealth of the class, who invests in the risk and risk-free assets in factions accounting for the respective proportion of traders.

In particular, the fraction of wealth allocated by the representative noise investor into the risky asset is given by

$$x_t^n = \frac{N_t^+}{N_t^+ + N_t^-} \in [0,1], \tag{2.18}$$

where N_t^+ represents the number of noise traders investing in the risky asset, while N_t^- counts the traders investing in the risk-free asset. The total number of traders $N_t^+ + N_t^- = N_n$ is a constant in the dynamics of the model.

We have to comment on the fact that the risky fraction defined in equation (2.18), is valid given that no heterogeneity is present among the noise traders, they all follow the same investment strategy and at each time step they all possess the same fraction of the total wealth of the class, which in the simulation is redistributed at the beginning of the trading day accordingly. We assume that we can neglect the impact on the market of the out-of-average wealth levels of individual noise traders, such that the representative noise trader correctly models the aggregate impact of the investment decisions of the class.

The heterogeneity among the noise traders has been shown to lead to a fat-tailed distribution of the wealth inside the class, through a phenomenon of wealth condensation as explained in Bouchaud and Mézard [30] and Harras et al. [31]. However, following Kaizoji et al. [13], neglecting this heterogeneity is not a restriction in the present model since we are interested only in the aggregated impact of this kind of traders.

The noise trader investment decision process is governed by the social imitation and the trend-following attitudes and is stochastic. The trader can hold either the risky asset or the risk-free one and at each trading day t, can switch between them or hold its previous day position according to a set of transition probabilities. Its investment strategy can be represented by a discrete-time Markov chain, depicted in figure 2.1.

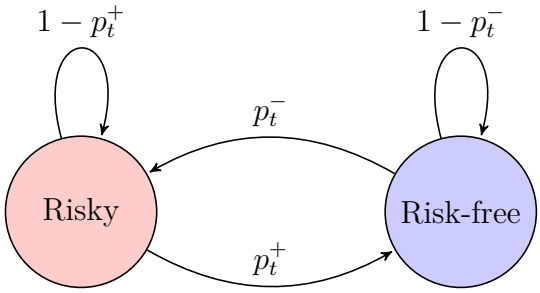

Figure 2.1: Markov chain for the investment decision of a noise trader.

The two possible states of the Markov Chain are constituted by the investment in the risky or risk-free asset. The transition probabilities are as follows. The trader holding the risky asset decides during the trading day t to switch to the risk-free one with probability p_t^+, otherwise he decides to hold its position. Analogously, a trader investing in the risk-free asset can switch to the risky position with probability p_t^- or otherwise hold the present one.

In light of this setup, the number of noise investors holding the risky asset N_t^+

or the risk-free asset N_t^- have to be considered as discrete-time stochastic processes governed by the Markov chain just introduced.

The trend-following and social imitation attitudes of the noise traders are modeled by two terms entering the form of the transition probabilities and hence governing the dynamics of the investment decision. Before describing the form of the probabilities we introduce and analyze the two mechanisms.

The first mechanism of trend-following models the chartist character of this type of investor. They analyze trends in the price of the risky asset and react to its movements. This feature models the impact of technical analysis on the noise traders' investment strategy.

The investors keep track of the price trend through a price momentum indicator, which is the expression for an exponential moving average of past returns. The time dependent price momentum H_t is defined as

$$H_t = \theta H_{t-1} + (1-\theta) r_t = \theta H_{t-1} + (1-\theta)\left(\frac{P_t}{P_{t-1}} - 1\right), \tag{2.19}$$

where $\theta \in [0,1)$ is the memory parameter controlling the characteristic length of the time window of memory of the past returns. In particular we can define $\tau_{memory} = \frac{1}{1-\theta}$ as the characteristic memory time length of the noise traders. Clearly the closer θ is to 1 the longer in the memory, while at the opposite $\theta = 0$ represents the extreme case of a memory of just one trading day.

The second feature characterizing the noise investors is the social imitation attitude. It is this social interaction between the agents endowing the noise traders class with the Ising-like structure, as explained in Harras et al. [31], central in understanding the emergence of bubbles.

The social imitation leads to the polarization of the investment preferences of the class and governs the appearance and dynamics of non-trivial collective phenomena of the investors.

Following Lux and Marchesi [15], in the original model the opinion index s_t measures the polarization of the noise traders class. It is defined as

$$s_t = \frac{N_t^+ - N_t^-}{N_t^+ + N_t^-} \in [-1,1], \tag{2.20}$$

where at denominator we recognize the constant total number of noise investors N_n. The sign of the index represents the attitude towards the risky asset. A positive sign stands for a bullish attitude towards the risky investment, while a negative one represents a bearish attitude of the class. From the definition of this index taking value in the interval $[-1,1]$, the connection of the class with the Statistical Physics Ising model starts to become visible, we will largely deepen it in the following. The opinion index is directly connected to the risky fraction by the formula

$$s_t = 2x_t^n - 1. \tag{2.21}$$

The two mechanisms, governing the noise traders' investment decisions, enter in the transition probabilities. Following Kaizoji et al. [13], the parameters s_t and H_t impact linearly on the transition probabilities. Moreover, at odds with Kaizoji et al. [13], and following the modification presented in Kohrt [17], a bias is introduced accounting for a greater propensity in investing in the risky asset. Finally one last fundamental element is present in the transition probabilities, the herding propensity parameter κ_t. This quantity represents the linear dependence coefficient measuring how much the two mechanism considered impact the transition probability. All in all, the transition rates are defined by

$$p_t^+ = \frac{p_+}{2}\left(1 - \frac{1}{p_+}\kappa_t(s_t + H_t)\right), \tag{2.22}$$

$$p_t^- = \frac{p_-}{2}\left(1 + \frac{1}{p_+}\kappa_t(s_t + H_t)\right). \tag{2.23}$$

The parameters κ_t, p_+ and p_- are chosen such that the probabilities are almost always contained in the interval [0,1]. Yet, we will see in the following that there are situations (the bubbles) in which the probabilities exit this range and indeed are no more consistent. In order to solve this to have well defined transition probabilities, they are redefined including a saturation mechanism

$$p_t^\pm = \begin{cases} \frac{p^\pm}{2}\left(1 \mp \frac{1}{p_+}\kappa_t(s_t + H_t)\right) & \text{if } \frac{p^\pm}{2}\left(1 \mp \frac{1}{p_+}\kappa_t(s_t + H_t)\right) \in [0,1] \\ 0 \quad \text{if } \frac{p^\pm}{2}\left(1 \mp \frac{1}{p_+}\kappa_t(s_t + H_t)\right) < 0 \\ 1 \quad \text{if } \frac{p^\pm}{2}\left(1 \mp \frac{1}{p_+}\kappa_t(s_t + H_t)\right) > 1 \end{cases} \tag{2.24}$$

We now comment further on the quantities entering the transition probabilities. In particular $p_+ < p_-$ are the parameters enforcing the bias towards a greater propensity in investing in the risky asset. The parameter κ_t, representing the magnitude of the herding propensity, will be central in understanding the polarization of the class and the formation of the bubbles. In the present model we will always consider it strictly positive $\kappa_t > 0$, however here we briefly comment on the other two possibilities. A negative herding propensity $\kappa_t < 0$ represents contrarian traders, while $\kappa_t = 0$ characterize the situation where the trend-following and social imitation attitude are absent. In the last scenario, we would have $p_t^+ = \frac{p_+}{2}$ and $p_t^- = \frac{p_-}{2}$, from which the meaning of the parameters p_+ and p_- becomes clear. They govern the length of the time window over which the traders hold the same investment decision in absence of herding behaviour, respectively $t_h^+ = \frac{2}{p_+}$ and $t_h^- = \frac{2}{p_-}$. We will refer to these two parameters as the average holding time of the risky and risk-free asset respectively.

The transition probabilities being defined, we can now write a time evolution equation for the number of traders investing in the two assets. To do so, we notice that each investment decision can be represented by a Bernoulli random variable $\xi(p)$, where the probability p defining its distribution is set equal to one of the transition rates according to the previous asset held by the trader. In particular, the investment decision for a trader previously holding the risky asset is represented by

$$\xi(p_{t-1}^{+}) = \begin{cases} 1 & \text{(switch to risk-free) with probability } p_{t-1}^{+} \\ 0 & \text{(hold risky) otherwise} \end{cases} \tag{2.25}$$

while for the trader previously investing in the risk-free asset

$$\xi(p_{t-1}^{-}) = \begin{cases} 1 & \text{(switch to risky) with probability } p_{t-1}^{-} \\ 0 & \text{(hold risk-free) otherwise} \end{cases} \tag{2.26}$$

Then the time evolution of the numbers of traders investing in the risky asset is described by

$$N_t^{+} = \sum_{k=1}^{N_{t-1}^{-}} \xi_k(p_{t-1}^{-}) + \sum_{k=1}^{N_{t-1}^{+}} [1 - \xi_k(p_{t-1}^{+})], \tag{2.27}$$

where the first sum accounts for the switches towards the risky asset, while the second accounts for the traders holding their previous bullish position. Analogously for the risk-free asset we have

$$N_t^{-} = \sum_{k=1}^{N_{t-1}^{+}} \xi_k(p_{t-1}^{+}) + \sum_{k=1}^{N_{t-1}^{-}} [1 - \xi_k(p_{t-1}^{-})]. \tag{2.28}$$

Finally we can derive also the dynamics of the risky fraction

$$x_t^n = \frac{N_t^{+}}{N_t^{+} + N_t^{-}} = \frac{1}{N_{t-1}^{-} + N_{t-1}^{-}} \left(\sum_{k=1}^{N_{t-1}^{-}} \xi_k(p_{t-1}^{-}) + \sum_{k=1}^{N_{t-1}^{+}} [1 - \xi_k(p_{t-1}^{+})] \right) \tag{2.29}$$

and consequently the dynamics of the opinion index

$$s_t = \frac{N_{t-1}^{+} - N_{t-1}^{-}}{N_t^{+} + N_t^{-}} = \frac{1}{N_{t-1}^{-} + N_{t-1}^{-}} \left(\sum_{k=1}^{N_{t-1}^{-}} [2\xi_k(p_{t-1}^{-}) - 1] + \sum_{k=1}^{N_{t-1}^{+}} [1 - 2\xi_k(p_{t-1}^{+})] \right). \tag{2.30}$$

2.4 The market-clearing conditions and the price equation

In this section, we present the last part of the model, constituted by the market-clearing conditions and the resulting price equation. The two classes of investors

interact in the formation of the price of the risky asset through the price equation, where both the fundamentalist and noise investment fractions are present. We have discussed the aggregate interpretation of both the classes in the previous sections, hence the picture is effectively that of two representative agents endowed with the total wealth of their classes and investing according to the risky and risk-free fractions determined by their respective investment strategies in equation (2.17) for the fundamentalist traders and in equation (2.29) for the noise traders.

The market-clearing conditions are set according to Walras' theory of general equilibrium, Walras [16]. Indeed, since we are in absence of external supply, we have that the risky asset's aggregate excess demand of fundamentalist and noise traders perfectly compensate each other,

$$\Delta D^f_{t-1\to t} + \Delta D^n_{t-1\to t} = 0, \tag{2.31}$$

where $\Delta D^f_{t-1\to t}$ and $D^n_{t-1\to t}$ represent respectively the risky asset's aggregate excess demands of each group. The excess demands can be expressed using the risky fraction of each class as

$$\Delta D^f_{t-1\to t} = W^f_t x^f_t - W^f_{t-1} x^f_{t-1} \frac{P_t}{P_{t-1}}, \tag{2.32}$$

$$\Delta D^n_{t-1\to t} = W^n_t x^n_t - W^n_{t-1} x^n_{t-1} \frac{P_t}{P_{t-1}}. \tag{2.33}$$

Now using the wealth dynamics equation (2.7) we get

$$\Delta D^f_{t-1\to t} = W^f_{t-1} x^f_t \left[1 + r_f + x^f_{t-1}\left(\frac{d_t}{P_{t-1}} + \frac{P_t}{P_{t-1}} - 1 - r_f\right)\right] - W^f_{t-1} x^f_{t-1} \frac{P_t}{P_{t-1}}, \tag{2.34}$$

$$\Delta D^n_{t-1\to t} = W^n_{t-1} x^n_t \left[1 + r_f + x^n_{t-1}\left(\frac{d_t}{P_{t-1}} + \frac{P_t}{P_{t-1}} - 1 - r_f\right)\right] - W^n_{t-1} x^n_{t-1} \frac{P_t}{P_{t-1}}. \tag{2.35}$$

Before imposing the equilibrium condition to derive the price equation, we still need to make explicit the dependence of the fundamentalist's risky fraction on the price P_t at time t,

$$x^f_t = \frac{1}{\gamma} \frac{E_r - r_f + \frac{d_t(1+r_d)}{P_t}}{\sigma^2_r}. \tag{2.36}$$

The noise traders' risky fraction instead, due to the stochastic character of the investment decision process of this type of traders, does not depend on the present price P_t.

Imposing the equilibrium condition (2.31), we obtain a non-trivial equation in the unknown price P_t. Manipulating its expression, in Kohrt [17] it is shown that the equation reduces to a quadratic equation in P_t.

The price equation has the form

$$a_t P_t^2 + b_t P_t + c_t = 0, \tag{2.37}$$

where the parameters are expressed as follows

$$a_t = \frac{1}{P_{t-1}}\left[W_{t-1}^n x_{t-1}^n (x_t^n - 1) + W_{t-1}^f x_{t-1}^f \left(\frac{1}{\gamma}\frac{E_r - r_f}{\sigma_r^2} - 1\right)\right], \tag{2.38}$$

$$b_t = \frac{1}{\gamma}\frac{W_{t-1}^f}{\sigma_r^2}\left\{x_{t-1}^f \frac{d_t(1+r_d)}{P_{t-1}} + (E_r - r_f)\left[x_{t-1}^f\left(\frac{d_t}{P_{t-1}} - 1 - r_f\right) + 1 + r_f\right]\right\} + W_{t-1}^n x_t^n \left[x_{t-1}^n \left(\frac{d_t}{P_{t-1}} - 1 - r_f\right) + 1 + r_f\right], \tag{2.39}$$

$$c_t = W_{t-1}^f \frac{1}{\gamma}\frac{d_t(1+r_d)}{\sigma_r^2}\left[x_{t-1}^f\left(\frac{d_t}{P_{t-1}} - 1 - r_f\right) + 1 + r_f\right]. \tag{2.40}$$

From the condition $x_t^{f,n} \in [0,1]\ \forall t$. it follows that $(x_t^n - 1) < 0$ and $\left(\frac{1}{\gamma}\frac{E_r - r_f}{\sigma_r^2} - 1\right) = (x_{min}^f - 1) < 0$ so that the coefficient $a_t < 0\ \forall t$ is always negative. Moreover, from the positivity of the term $\left(\frac{1}{\gamma}\frac{E_r - r_f}{\sigma_r^2} - 1\right) > 0$ implies the positivity of the coefficients $b_t > 0\ c_t > 0\ \forall t$.

From the conditions on the parameters $a_t < 0$, $b_t > 0$ and $c_t > 0$ we have that the unique physical solution for the price equation is

$$P_t = \frac{-b_t - \sqrt{b_t^2 - 4a_t c_t}}{2a_t}. \tag{2.41}$$

As anticipated, we have that the price equation derived from the market-clearing conditions fully determines the dynamics of the price.

2.5 The dynamics of the model

In the previous sections, we have introduced the various components of the model. Now in this section, we move to the analysis of the resulting dynamics characterizing it. We will first expand the discussion on the quantity κ_t, representing the herding propensity of the noise traders class. Then, we will introduce the set of parameters used in the simulations. We will proceed to present the resulting time series and finally, we will analyze them. Building on the connection with the Ising model we

will deepen the mechanism leading to the emergence of the bubbles, these collective phenomena capable of shaking the entire market.

We start by expanding the discussion on the parameter κ_t. This quantity measures the noise traders' propensity to herd, hence constituting the factor weighing the impact of the trend-following and social imitation attitudes on the investment strategy of these investors. As explained in the original paper by Kaizoji et al. [13], the parameter κ_t accounts for the impact of the economical and geopolitical climate on financial markets.

Two different setups for the herding propensity parameter are outlined in Kaizoji et al. [13]. A stable economical and geopolitical climate, represented by a constant value of $\kappa_t \coloneqq \kappa = cst$ and a varying environment, modeling the impact of a changing world on the financial markets,

$$\kappa_t = \kappa_{t-1} + \eta_\kappa(\mu_k - \kappa_{t-1}) + \sigma_\kappa v_t. \tag{2.42}$$

The above discrete-time equation defines a time-varying stochastic process for κ_t, capturing the dynamical framework of regime-switching characterizing the financial markets, as explained in Lux [1].

Equation (2.42) defines a discrete Ornstein-Uhlenbeck stochastic process, where μ_k represents the mean reversion level towards which the process tends to drift over time. The quantity η_κ represents the mean reversion rate governing the velocity of the reversion process towards μ_k.

Finally, v_t represents a Wiener process, hence the variables v_t are i.i.d. normal random variable $\mathcal{N}(0,1)$. The standard deviation of the Wiener process governing its diffusion is set by σ_κ. We are in presence of a modified random walk, which on top of its stochastic motion tends to revert to the value μ_k, with a greater attraction the farther the process is from that value. The discrete-time version of the Ornstein-Uhlenbeck process is also known as discrete-time autoregressive model (AR(1)).

The Ornstein-Uhlenbeck process is the only non-trivial stationary Gaussian Markovian process, indeed its distribution is fully determined by its first two moments

$$\mathbb{E}[\kappa_t] = \kappa_0 e^{-\eta_\kappa t} + \mu_k(1 - e^{-\eta_\kappa t}), \tag{2.43}$$

$$\mathrm{Cov}[\kappa_s, \kappa_t] = \frac{\sigma_\kappa^2}{2\eta_\kappa}(e^{-\eta_\kappa(t-s)} + e^{-\eta_\kappa(t+s)}) \quad s < t, \tag{2.44}$$

from which we can see that in the long run $t \to +\infty$ the distribution of the process converge to the stationary Gaussian distribution

$$\kappa_t \sim \mathcal{N}\left(\mu_k, \frac{\sigma_\kappa^2}{2\eta_\kappa}\right), \tag{2.45}$$

with mean equal to the mean reversion level μ_k and variance $\frac{\sigma_\kappa^2}{2\eta_\kappa}$.

We now move to the introduction of the set of parameters used for the simulations of the original market model.

2.5.1 The set of parameters

We introduce the set of parameters used to run all the simulations of the original market model. Their values are motivated by real market behavior and are chosen such that one time-step corresponds to roughly one trading day. The set of parameters we use is presented in table 2.1 and is mainly taken from Westphal and Sornette [18]. Discussions on the choice of their values can be found in Kaizoji

	Parameters		
Assets	$r_f = 4 \times 10^{-5}$ $d_0 = 1.6 \times 10^{-4}$	$r_d = 1.6 \times 10^{-4}$ $P_0 = 1$	$\sigma_d = 1.6 \times 10^{-5}$
Fundamentalist traders	$W_0^f = 10^9$ $\sigma_r = 0.02$	$x_0^f = 0.3$	$E_r = 1.6 \times 10^{-4}$
Noise traders	$W_0^n = 10^9$ $\theta = 0.95$ $p^- = 0.200625$	$x_0^f = 0.3$ $H_0 = 1.6 \times 10^{-4}$	$N_n = 1000$ $p^+ = 0.199375$
Herding propensity	$\kappa_0 = \mu_k$ $\sigma_\kappa \approx 0.01$	$\mu_\kappa = 0.98p^+$	$\eta_\kappa \approx 0.11$

Table 2.1: Set of parameters for the original model simulation. Their values are motivated by real markets data and are mainly taken from Westphal and Sornette [18].

et al. [13], Kohrt [17] and Ollikainen [19]. Here we review the main reasons for their choice.

Starting from the analysis of assets' parameters, the daily risk-free rate is set to $r_f = 4 \times 10^{-5}$, which corresponds to an annualized risk-free rate of return $r_f^{annual} \approx r_f \times 250 = 0.01$. Following Kaizoji et al. [13] the dividend process' parameters are calibrated according to Engsted and Pedersen [32]. The average value of the dividend's growth factor is set to $r_d = 1.6 \times 10^{-4}$, corresponding to an annualized value of $r_d^{annual} \approx r_d \times 250 = 0.04$. The standard deviation of the growth rate is instead one order of magnitude smaller $\sigma_d = 1.6 \times 10^{-5}$.

We assume such a small value in order to model a more prominent impact of the stochastic noise traders' behaviour with respect to the stochastic dynamics of

the dividend process. Indeed, in the present model we want to focus primarily on the source of stochasticity coming from the noise traders' strategy and not on the actual dividend structure.

The initial value of the dividend $d_0 = 1.6 \times 10^{-4}$ is set in order that its annualized value is equal to the annual growth rate $d_0^{annual} \approx d_0 \times 250 = 0.04$. Moreover, the initial value of the price is set to an unitary value $P_0 = 1$.

Moving to the traders, we have that both the fundamentalist and the noise investors starts with the same level of wealth $W_0^f = W_0^n = 10^9$ and share the same initial endowment in the risky asset $x_0^f = x_0^n = 0.3$. Regarding the expectation of the fundamentalist on the future dynamics of the returns, we have that they expect an average return equals to the dividend's growth rate $E_r = 1.6 \times 10^{-4} = r_d$ and foresee a standard deviation of the return $\sigma_r = 0.02$.

Moving to the other type of investors, the $N_n = 1000$ noise traders are characterized by a memory length $\tau_{memory} = \frac{1}{1-\theta} = 20$ trading days, roughly one month, which corresponds to a value for the parameter $\theta = 0.95$. The initial price momentum is set to be equal to the average growth rate of the dividend $H_0 = 1.6 \times 10^{-4} = r_d$. Finally, according to Kohrt [17] the parameters introducing the bias towards the risky asset are set equal to $p^+ = 0.199375$ and $p^- = 0.200625$, leading to a higher frequency of positive bubbles with respect to negative ones as observed in real markets.

Moving to the herding propensity, we first comment that the set of parameters already discussed are used for the simulation with both the Ornstein-Uhlenbeck kappa process and the constant one. The constant herding propensity setup is characterized by the constant value $\kappa_t = \kappa_0 = \mu_k$, where as for the varying parameter the mean reversion level is set according to $\mu_\kappa = 0.98p^+$. Besides, for the Ornstein-Uhlenbeck kappa we have two more parameters to calibrate. The mean reversion rate η_κ and the standard deviation of the Wiener process σ_κ are set such that the limiting Gaussian distribution for $t \to +\infty$ has standard deviation of $0.1p^+$ and a deviation of the kappa process two standard deviation above μ_κ will revert within $\Delta T = 20$ trading days. Since the standard deviation of the limiting Gaussian distribution is $\frac{\sigma_\kappa}{\sqrt{2\eta_\kappa}}$, from the first condition we have

$$\sigma_\kappa = 0.1p^+\sqrt{2\eta_\kappa}. \tag{2.46}$$

The parameter η_κ can be fixed according to the second condition. Indeed, from equation (2.43) we can estimate the time ΔT needed by the process to revert to μ_κ in case it is somewhere above the value of p^+, $\kappa_t > p^+$, as

$$\Delta T = \frac{1}{\eta_\kappa} \log\left(\frac{\kappa_t - \mu_\kappa}{p^+ - \mu_\kappa}\right). \tag{2.47}$$

Inverting the expression to have an equation for η_κ, subjected to the aforementioned

condition on ΔT we get

$$\eta_\kappa = \frac{1}{\Delta T}\log\left(\frac{\mu_\kappa + 2\cdot 0.1p^+ - \mu_\kappa}{p^+ - \mu_\kappa}\right) = \frac{1}{20}\log\left(\frac{0.2p^+}{0.02p^+}\right) = \frac{1}{20}\log(10) \approx 0.11. \tag{2.48}$$

Plugging the result for $\eta_\kappa = 0.11$ into (2.46), we get

$$\sigma_\kappa = 0.1p^+\sqrt{2\eta_\kappa} \approx 0.01. \tag{2.49}$$

The parameter representing the constant risk aversion γ of the fundamentalist traders, characterizing their investment strategy (2.17), is not present in 2.1 since is not imposed exogenously but is calculated endogenously at the beginning of each simulation from the other parameters and initial condition. Inverting equation (2.17) evaluated at $t = 0$ the risk aversion is set according to the initial risky investment of the fundamentalist traders as

$$\gamma = \frac{1}{x_0^f}\frac{E_r - r_f + \frac{d_0(1+r_d)}{P_0}}{\sigma_r^2}. \tag{2.50}$$

The risk aversion depends only on the initial dividend-price ratio, on the initial risky fraction and on the expectation on the future dynamics of the returns.

Finally, we comment on the relation between the model's trading day represented by one time-step of the simulation and the real trading day of the financial markets. To connect the two we follow the same reasoning adopted in Ollikainen [19]. The expression for the simulated trading day time in function of the real trading day time is derived imposing the equality between the daily standard deviation of the realized returns in the simulations and the empirical one. The latter is set accordingly to the representative value of daily volatility of the stock markets, which is around $\sigma_{market} \approx 0.01$ as explained in Sornette [33].

First the returns are roughly approximated by a Wiener process, for which the standard deviation depends on time according to $\sigma_t = \sigma_0\sqrt{t}$. Hence, the standard deviations at two different times t_1 and t_1 of a Wiener process are related by the formula

$$\sigma_{t_2} = \sigma_{t_1}\sqrt{\frac{t_2}{t_1}}. \tag{2.51}$$

Using this expression one can express the time corresponding to a simulated trading day in unit of real trading days as

$$\frac{t_{sim}}{t_{market}} = \frac{\sigma_{sim}^2}{\sigma_{market}^2}, \tag{2.52}$$

which leads to

$$t_{sim} = \frac{\sigma_{sim}^2}{0.01^2}, \tag{2.53}$$

whose value expresses the simulated trading day in unit of real days. The simulations are run for $T = 5000$ time-steps, which corresponds to $\frac{T}{250} = 20$ trading years of the model.

2.5.2 Simulation implementation and time series description

In this section, we present the time series resulting from two simulations with the set of parameters introduced in the last section. The only difference between the two is constituted by the herding propensity, the first is characterized by a constant one, the second by an Ornstein-Uhlenbeck one.

Before moving to the presentation of the time series, we spend some time commenting on the computational aspects of the simulation. The code used here to simulate the model was originally written by Kohrt [17], with some modification by Ollikainen [19] and Westphal and Sornette [18]. The core of the model implementation is written in *C++*. Each part of the model, (e.g. the fundamentalist traders, the risky asset, the price equation) is implemented by one specific class, following an object-oriented programming paradigm. To have reproducible results, a pseudo-random number generator with a random seed specified as a run-time parameter is used. The results of the simulation are stored in a database using the *HDF5* high-performance data software library. Then all the analysis of the data and the plotting are performed with *Python*, in particular using the *Matplotlib* library and accessing the *HDF5* database through the *Python* interfacing library *h5py*.

We present in figure 2.2 the time series from a simulation characterized by a constant herding propensity and in figure 2.3 the time series from a simulation featuring an Ornstein-Uhlenbeck κ_t.

We comment now one by one on the eight-time series presented for each simulation, analyzing similarities and differences between the constant kappa (CK) and the Ornstein-Uhlenbeck (OU) kappa setups.

The first panel presents price dynamics. The price time series of the CK simulation is characterized by moderate fluctuations around a roughly linear growth. The linear growth is identifiable with the average exponential growth, being the plot in log-linear scale, of the dividend which indeed features an average constant growth factor r_d. The time series in the OU case is strikingly different. Huge deviations from the fundamental value of the asset, governed by the average dividend growth, are clearly identifiable for example around $t \approx 500$, $t \approx 1800$ and $t \approx 3700$. These rapid build-ups in the graph are exponential hence, being the plot in log-linear scale, these spikes testify a super-exponential growth of the price, characteristic of the dynamics of the bubbles, as commented in Kaizoji et al. [13]. The presence of these endogenous bubbles in the most remarkable feature emerging

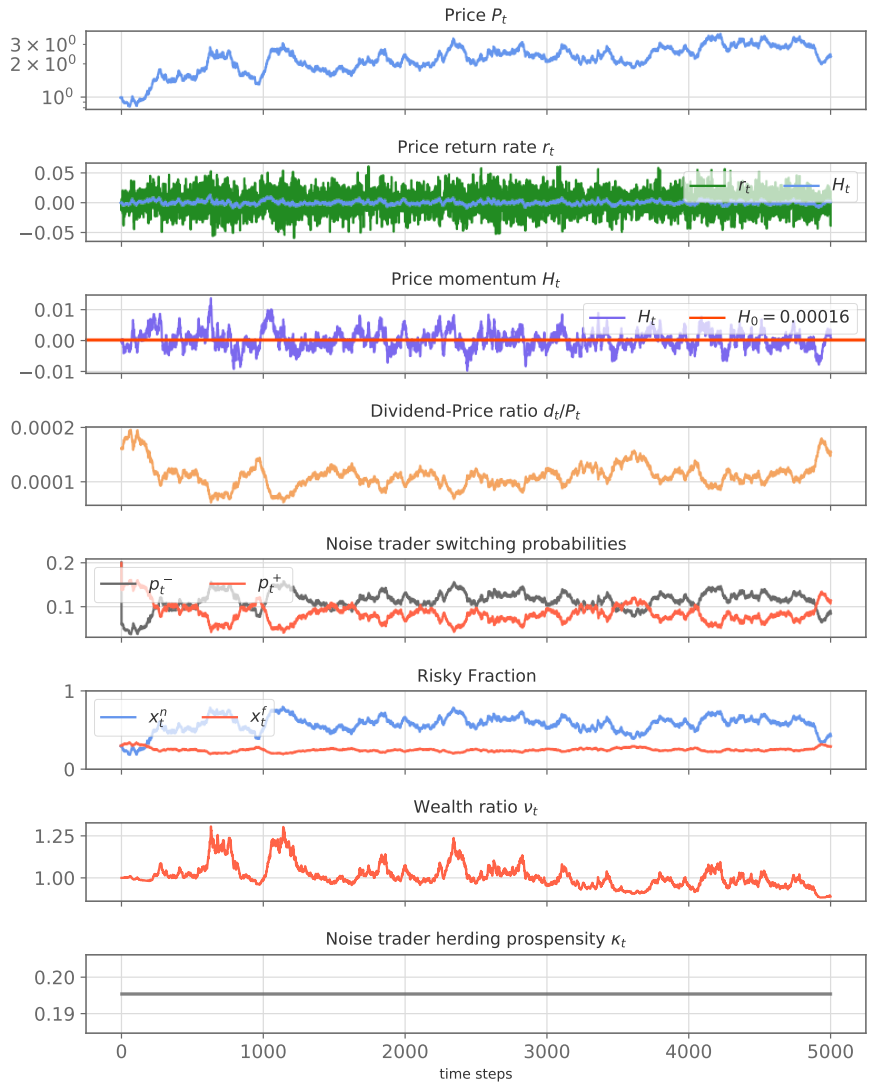

Figure 2.2: Time series of the main quantities characterizing the model's dynamics resulting from a simulation featuring a constant kappa process $\kappa_t = \kappa_0 = 0.98p^+$. The first panel shows the price dynamics P_t in a log-linear plot, the second shows the returns r_t in green and the price momentum H_t in blue. The third panel features again the price momentum H_t in blue and its initial value in red, the fourth shows the dividend-price ratio $\frac{d_t}{P_t}$. The fifth presents the noise traders switching probabilities $p_t^{\pm}$ and the sixth the risky fractions of both the fundamentalist x_t^f (in red) and the noise traders x_t^n (in blue). Finally, the last two panels feature in order, the wealth ratio $\nu_t = \frac{W_t^n}{W_t^f}$ and the constant value for the herding propensity.

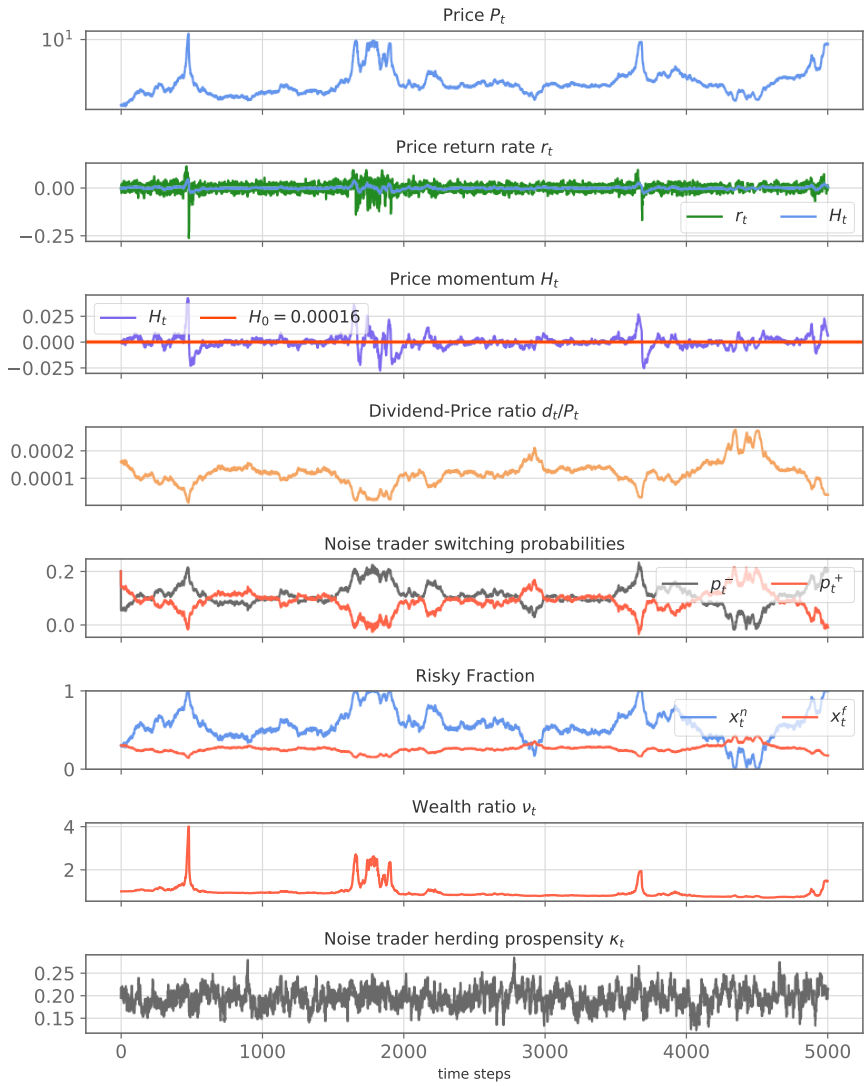

Figure 2.3: Time series of the main quantities characterizing the model's dynamics resulting from a simulation featuring an Ornstein-Uhlenbeck kappa process κ_t. The first panel shows the price dynamics P_t in a log-linear plot, the second shows the returns r_t in green and the price momentum H_t in blue. The third panel features again the price momentum H_t in blue and its initial value in red, the fourth shows the dividend-price ratio $\frac{d_t}{P_t}$. The fifth presents the noise traders switching probabilities $p_t^{\pm}$ and the sixth the risky fractions of both the fundamentalist x_t^f (in red) and the noise traders x_t^n (in blue). Finally, the last two panels feature in order, the wealth ratio $\nu_t = \frac{W_t^n}{W_t^f}$ and the Ornstein-Uhlenbeck kappa process κ_t.

from the simulations and the main difference between the two setups.

This difference manifests itself also in the price return behavior. Indeed, while on the one hand for the CK simulation the daily returns are roughly uniform along the simulation and mainly comprised in the range $[-0.05, +0.05]$, following empirical observations from the tranquil periods of real financial markets, on the other hand, the price returns of the OU simulation shows picks in their absolute value near the price's bubbles. While the range of values of the returns in periods far from the bubbles is similar to the CK one, during the boom and crashed characterizing the bubbles, the returns highly exceed this range.

This is evident also from the third panel presenting the exponential average of the returns. This alternation of tranquil periods to turbulent regimes, characterized by high returns (both positive and negative), is known as volatility clustering and is widely documented in real markets. On the contrary, in the CK simulation, the price momentum has relatively smaller deviations around the initial value of $H_0 = 1.6 \times 10^{-4}$, also representing the average constant growth factor of the dividend.

The fourth frame presents the dividend-price ratio d_t/P_t which for both the simulations represents the mirror image of the price dynamics, as expected from its definition and the small value of the dividend standard deviation σ_d.

Moving to the noise traders switching probabilities, we first notice that they are exactly specular as expected from the constant sum condition to which they are subjected $p_t^+ + p_t^- = \frac{p_+ + p_-}{2} = cst$. More interestingly, we observe that the probability to switch towards the risky asset p_t^- has a correspondent dynamics to the noise traders' risky fraction. It is indeed p_t^- which governs the polarization towards the risky asset and by consequence the value of the risky fraction. Another interesting observation is constituted by the correspondence emerging from a careful analysis, between the fundamentalist's risky fraction and the dividend-price ratio. Recalling equation (2.17), we have indeed that being all the other quantities entering in the formula constant, there exists a perfectly linear relation between the two quantities, with a constant linear coefficient. The last comments are valid for both the simulations.

The main difference in the risky fractions between the CK and the OU setup is represented by the time series of the noise traders' risky endowment x_t^n. While for the CK simulation the oscillations are smaller and its value never exceeds 0.8, for the OU setup the noise traders' risky fraction is characterized by spikes which reaches the limiting value of 1, corresponding to a full polarization of the class towards the risky asset. An analogous phenomenon, yet rarer due to the imposed imbalance between p_+ and p_-, characterize the polarization towards the risk-free asset. We can recognize an example of it near time-step $t \approx 4400$.

These polarizations correspond to values of the switching probability p_t^+ (p_t^- for the negative bubble, where noise traders move in mass towards the risk-free

investment) which tends to the limiting value of 1. During the bubble, the polarization of the class becomes so strong that the probability to sell the risky asset and buy the risky one (the opposite for a negative bubble) becomes extremely small. We are in presence of an irrational wave of enthusiasm, the "irrational exuberance" of the investors described by Shiller [34], which creates a self-reinforcing loop of investment towards the asset undergoing the bubble. Furthermore, there are even periods in which the probability to go against the rest of the class predicted by formulas (2.22) and (2.23) would become negative, as is visible in the fifth panel where the actual p_t^+ and p_t^- predicted by the above formulas are plotted. Whereas, we have modified the definition of the switching probability introducing a saturation mechanism to have well-defined quantities. What happens indeed is that in these periods the probability is saturated to $p_t^- = 0$ ($p_t^+ = 0$ for negative bubbles). The polarization of the class is complete, the noise traders experience the so-called lock-in effect, analyzed in Ollikainen [19], unless this fragile transient equilibrium is broken and the bubble bursts. We will deepen this phenomenon together with the analysis of the full dynamics of the bubble in the next section.

We underline again that all these phenomena characterizing the bubbles are present only in the Ornstein-Uhlenbeck setup. In the next section, we will analyze this fact, unveiling the fundamental importance of the time-varying herding propensity parameter κ_t in the formation of the bubbles. In the meanwhile, we comment that comparing the price dynamics and the noise traders' risky fraction time evolution it becomes clear that it is indeed the stochastic investment strategy of the noise traders characterized by social imitation and trend following that drives the actual dynamics of the price. The correspondence between the two time series is evident. This is true both for the OU setup and the CK one.

We comment finally on the second-last panel featuring the wealth ratio defined by the ratio between the noise traders' total wealth and the fundamentalist's one $\nu_t = \frac{W_t^n}{W_t^f}$. The resulting spikes in this quantity correspond to the bubbles of the price. During these periods both investors get richer thanks to the increasing of the risky asset's price. But while the noise traders invest more in it the more its price rises, the fundamentalist traders follow the opposite strategy reducing the risky fraction. This is understandable in light of the inverse proportionality between x_t^f and P_t mediated by the dividend-price ratio. This reasoning explains the fact that the noise traders become much richer than the fundamentalists during the bubbles.

Nevertheless, from the long-run trend emerging in the wealth ratio we see that at the end of the simulation the fundamentalist's strategy results to be more remunerative than the noise traders one. This concludes the qualitative analysis of the time series.

We still have to give an idea of the typical real time length of one trading day of the simulation. The standard deviation of the realized returns are computed over all the simulation discarding the first 500 time-steps in order to neglect the

misleading phenomena related to the initial equilibration of the market model from the initial conditions. The resulting standard deviations are

$$\sigma_{simm}^{CK} = 0.017 \tag{2.54}$$

for the constant kappa simulation and

$$\sigma_{simm}^{OU} = 0.021 \tag{2.55}$$

for the Ornstein-Uhlenbeck simulation. We comment that these values are in agreement with real markets behavior and motivate ex-post the constant value of the expected standard deviation of $\sigma_r = 0.02$ by the fundamentalist traders.

Now, using formula (2.52) derived in section 2.5.1, we obtain that one trading day of the simulation corresponds to $t_{sim} = 2.89$ real days for the CK simulation and $t_{sim} = 4.41$ for the OU simulation. We underline that these results are just a rough approximation to give an idea of the time length of the simulation. Moreover, the relatively large number of real days for OU simulation has to be understood also considering that the assumed approximation of the returns as a Wiener process is inappropriate during the bubbles periods.

2.5.3 The stylized facts of the financial markets

In this section we close the presentation of the time series, bringing evidence to our claim that the original model is able to reproduce the "stylized facts" of the financial markets. Postponing a wider discussion on the stylized facts to Chapter 5, here following Kaizoji et al. [13], we check the model is able to reproduce two of them, the fat-tailedness of the absolute returns and the long memory in the autocorrelation of the same quantities.

These emerging empirical properties have been observed across a wide range of instruments, markets, and time periods and it is important for a well-grounded representation of the financial markets to be able to reproduce them.

In figure 2.4, we present the autocorrelation function (ACF) of both signed and absolute returns for the two simulations, one characterized by a CK herding propensity 2.2 and the other by an OU one 2.3.

We recall that the l-lag autocorrelation function of a stochastic process X_t is defined at each time τ as

$$ACF_l(X_t)(\tau) = \frac{\mathrm{Cov}[X_t(\tau)X_t(\tau - l)]}{\sqrt{\mathrm{Var}[X_t(\tau)]\mathrm{Var}[X_t(\tau - l)]}}. \tag{2.56}$$

Basically, it is the Pearson correlation between the stochastic process and time-shifted copy of itself by l time-steps. The empirical ACF is computed substituting the covariance and the variances by their empirical counterparts.

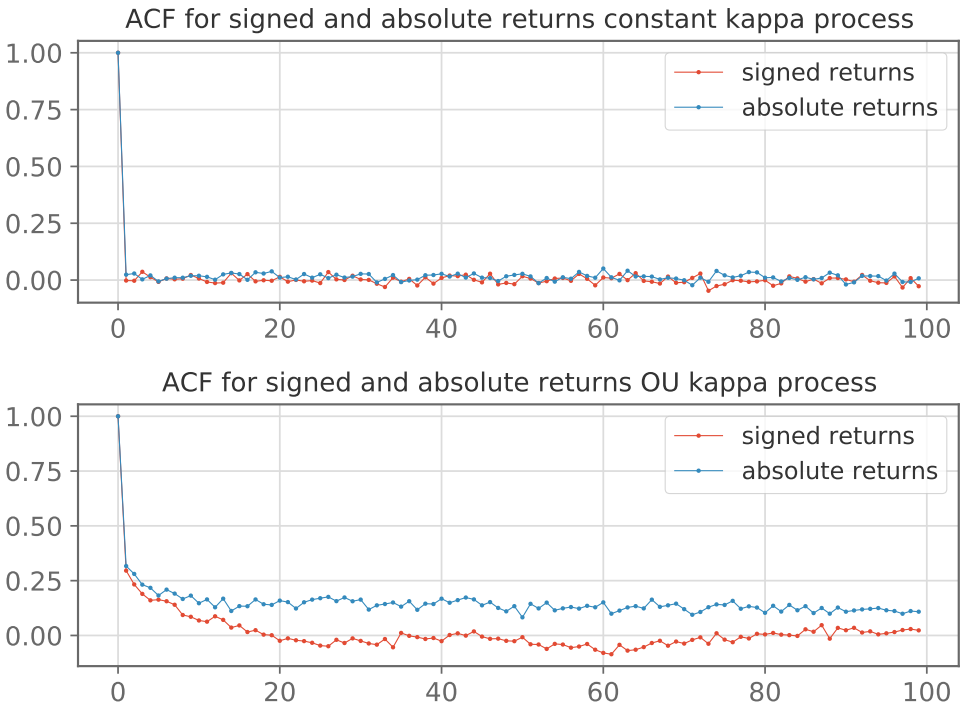

Figure 2.4: The first panel shows the autocorrelation function (ACF) of signed (red) and absolute (blue) returns resulting from the simulation with constant kappa process presented in figure 2.2. The second panel features the ACF from the simulation with OU kappa process presented in figure 2.3. The autocorrelation functions are computed for the data after the 500th trading day in order to exclude possible misleading contributions due to the initial conditions.

Comparing the two panels the difference is remarkable. Indeed, in the case of constant kappa, the ACF for both the signed and absolute returns quickly decays to zero. Whereas, for the OU simulation, while the ACF for the signed returns still decays exponentially fast to zero, the ACF for the absolute returns has a slower hyperbolic decay, in agreement with Kaizoji et al. [13]. As commented in the original paper, the fast decay in the case of signed returns is consistent with an almost absence of arbitrage opportunities in presence of transaction costs, moreover, the slower decay in the case of absolute returns testify the presence of long-memory properties, the signature of the phenomenon of volatility clustering.

This is the quantitative counterpart to the qualitative observation of the phenomenon from just a visual inspection of the returns time series, characterized by the alternation of tranquil periods to turbulent regimes. We have that the OU setup, which gives rise to super-exponential bubbles can correctly reproduce the

stylized facts characterizing the autocorrelation functions, whereas the CK lacking the presence of clear bubbles is not able to do that. This will repeat again for the fat-tailedness of the distribution of absolute returns.

Moving to the latter phenomenon's analysis, we want to compare the realized distribution of absolute returns to the observed leptokurtic behavior of their empirical counterparts. The empirical fat-tail decay of the distribution

$$p(x) \sim x^{-1-\alpha} \tag{2.57}$$

is characterized by an exponent α in the range [2,4]. As shown in figure 2.5, the fitted parameter from the simulated time series falls in this range of values in the case of the Ornstein-Uhlenbeck kappa process, while does not in the case of constant herding propensity.

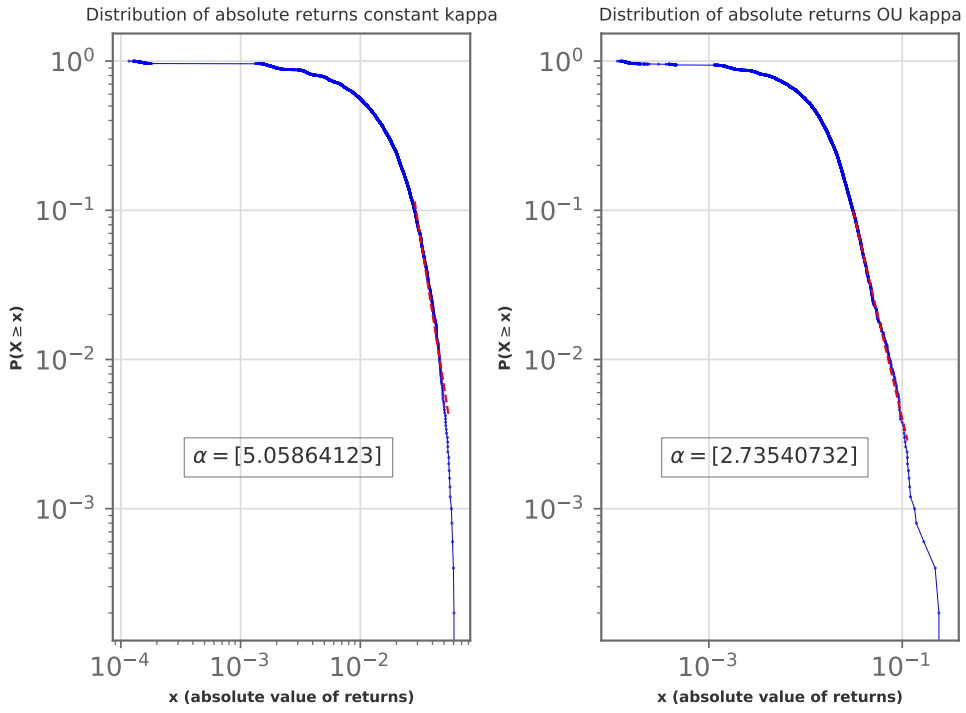

Figure 2.5: Log-log plots of the complementary cumulative distribution functions of the returns for the CK simulation presented in figure 2.2 (on the left) and for the OU simulation presented in figure 2.3 (on the right). The exponent is found fitting data from the last 10th percentile of the cumulative distribution, disregarding the largest ten values. The linear regression line is visible in red.

Again the presence of the bubbles seems to be fundamental in correctly reproducing the stylized facts of the financial markets. Aware of the importance of these

emerging collective phenomena, in the next section, we deepen the analysis of the mechanism triggering and governing their dynamics.

2.6 The bridge between the noise traders class and the Ising model

In this section we comment on the connection between the noise traders class and the Ising model and its importance in understanding the formation of bubbles, building on top of the analyses present in Damiani [21], Kaizoji et al. [13], Harras et al. [31], Ollikainen [19] and Sornette [12] among the others. The fundamental feature characterizing the noise traders class is the competition between the ordering force of social imitation and the disordering impact of idiosyncratic opinion.

One of the key concepts in complex systems theory is the emergence of highly non-trivial collective phenomena from the interactions between a large number of agents. It is the presence of interactions, the crucial element governing these phenomena. It is the interacting character of a group of agents that leads to the emergence of cooperative behaviors.

Statistical Physics has a history of success in modeling and explaining exactly this concept of emergence from interactions and the Ising model represents one of its pillars. Being first introduced as a mathematical model of ferromagnetism in statistical mechanics, its application has now covered the most varied branches of science. In particular, in Sornette [12] the fruitful use of the Ising model in financial economics together with the reasons for this success is beautifully explained.

A clear analogy can be imagined between the interactions of the spins in a ferromagnetic material which tends to align their orientations, while the temperature tends to push the system towards a disordered state, with the social imitation between the noise traders which tends to polarize the class towards a common investment preference, while the stochastic character of the investment decisions favors the idiosyncratic opinion. It is a representation of the never-ending fight between the order (modeled in physics by the minimization of some sort of energy) against the disorder (embodied in physics by the concept of the entropy) characterizing each interacting system, from a ferromagnetic material to a group of investors.

Having introduced this analogy, it is now not surprising that the transition rates defined in formulas (2.22) and (2.23), that we recall here,

$$p_t^+ = \frac{p_+}{2}\left(1 - \frac{1}{p_+}\kappa_t(s_t + H_t)\right), \tag{2.58}$$

$$p_t^- = \frac{p_-}{2}\left(1 + \frac{1}{p_+}\kappa_t(s_t + H_t)\right), \tag{2.59}$$

only based on the assumption of a linear impact of the two phenomenon in analysis, social imitation and trend-following, actually corresponds to the linearized form of the Glauber transition rates, characterizing the well-known Glauber stochastic dynamics of the Ising model first introduced in Glauber [35].

The Glauber transition rates are defined by

$$p_G^+(m,h) = \frac{1}{2}[1 - \tanh(\beta(m+h))] \tag{2.60}$$

and

$$p_G^-(m,h) = \frac{1}{2}[1 + \tanh(\beta(m+h))], \tag{2.61}$$

where m is the average magnetization, h is the external field and β is the inverse temperature. In order to define the quantities entering their expressions and to argument on our strong claim, we have to recall briefly the Ising model definition and what we quantities entering in the above rates represent.

First of all, we underline that the transition rates (2.60) and (2.61) are characteristic of a particular version of the Ising model, the mean-field, or fully-connected one. Hence, we introduce the Hamiltonian, representing the energy of the system, of the fully connected Ising model

$$H_N(\{s_1,\dots,s_N\}) = -\frac{J}{2N}\sum_{i\neq j=1}^{N} s_i s_j - h\sum_{i=1}^{N} s_i. \tag{2.62}$$

The fully-connected Ising model is constituted by N spins s_i which can take value $s_i \in \{-1,1\}$, each of them interacting with all the others. Moreover, an uniform external field h acts on each spin. Finally, J represents the interaction coupling, entering halved in the Hamiltonian since the double sum $\sum_{i\neq j=1}^{N}$ counts twice each interaction.

The equilibrium statistical properties of the model are governed by the standard Boltzmann weight

$$P_{eq}(\{s_1,\dots,s_N\}) = e^{-\beta H_N}, \tag{2.63}$$

where $\beta = \frac{1}{k_B T}$ is the so-called inverse temperature.

The Ising model is a statistical model of an interacting system. Hence, from the theory of Statistical Physics we know that, while the statistical properties are determined by the form of the Hamiltonian, the actual time-evolution dynamics of the model is not fixed a priori. Different dynamics may lead to the same statistical properties and hence to the same Ising model. This is an important point of the discussion and we will come back to it extensively in Chapter 4 together with a deep discussion of the Statistical Physics tools available to define such a dynamics. For the moment, we refer to Glauber [35], where in a groundbreaking work, Glauber introduced the transition rates bearing his name, defining a stochastic dynamics

which correctly generates the statistical properties of the Ising model. The Glauber rates are obtained imposing the detailed balance condition

$$\frac{p(s_i = 1 \to s_i = -1)}{p(s_i = -1 \to s_i = 1)} = \frac{P_{eq}(s_i = -1)}{P_{eq}(s_i = 1)} \tag{2.64}$$

where $p(s_i = 1 \to s_i = -1)$ is the transition probability associated to the spin flip from 1 to -1 of spin $s_i = 1$ and $P(s_i = -1)$ is the Boltzmann weight (2.63) associated to a configuration with the spin $s_i = 1$. Then rearranging the terms we get

$$\frac{p(s_i = 1 \to s_i = -1)}{p(s_i = -1 \to s_i = 1)} = \frac{P_{eq}(s_i = -1)}{P_{eq}(s_i = 1)} = \frac{e^{-\beta(Jm+h)}}{e^{\beta(Jm+h)}} = \frac{1 - \tanh\left(\beta(Jm + h)\right)}{1 + \tanh\left(\beta(Jm + h)\right)}, \tag{2.65}$$

where we have introduced the quantity $m = \frac{\sum_{k=1}^{N} s_k}{N}$, representing the average magnetization. To be rigorous, we have to comment that the third equality in (2.65) is exact only in the limit $N \to +\infty$. Indeed, the actual ratio of the Boltzmann factors, after having simplified the common terms, is given by

$$\frac{P_{eq}(s_i = -1)}{P_{eq}(s_i = 1)} = \frac{e^{-\beta\left(J\left(\frac{\sum_{k\neq i=1}^{N} s_k}{N}\right)+h\right)}}{e^{\beta\left(J\left(\frac{\sum_{k\neq i=1}^{N} s_k}{N}\right)+h\right)}}. \tag{2.66}$$

The sum does not include the spin s_i, yet this difference is negligible in the large N limit, which is the case in the present model. This fact constitutes also the difference between the fully connected version of the Ising model, here presented, and the mean-field one, characterized by the Glauber rates. The fact that this distinction vanish in the large N limits is referred in Statistical Physics as the equivalence of the fully connected and mean-field Ising model in the thermodynamical limit, which is indeed $N \to +\infty$.

Now considering the final ratio in (2.65), we just multiply and divide as a matter of normalization by the same quantity $\frac{1}{2}$ and we finally recognize the Glauber transition rates (2.60), (2.61), which govern the probability of a spin flip in the dynamics of the Ising model,

$$p_G^+(m, h) = \frac{1}{2}[1 - \tanh\left(\beta(Jm + h)\right)], \tag{2.67}$$

$$p_G^-(m, h) = \frac{1}{2}[1 + \tanh\left(\beta(Jm + h)\right)]. \tag{2.68}$$

Linearizing the transition probabilities we get

$$p^+(m, h) = \frac{1}{2}[1 - \beta(Jm + h)] \tag{2.69}$$

and

$$p^{-}(m,h) = \frac{1}{2}[1 + \beta(Jm + h)]. \tag{2.70}$$

The connection with the noise traders transition rates is almost manifest, we just need to multiply both terms by a constant p, which tunes the probability to hold the previous value, while not impacting the statistical properties of the model, since it cancels out in their ratio. We refer again to Chapter 4 for the discussion of this point. We get

$$p^{+}(m,h) = \frac{p}{2}[1 - \beta(Jm + h)] \tag{2.71}$$

and

$$p^{-}(m,h) = \frac{p}{2}[1 + \beta(Jm + h)]. \tag{2.72}$$

Two remaining differences with respects to the rates (2.58) and (2.58) need to be commented. The first is given by the introduction of an asymmetry between the two rates defining a slightly larger value p_{-} for the $p^{-}(m,h)$ with respect to p_{+} for $p^{+}(m,h)$. The second is just a rescaling of β by a factor p_{+}.

The correspondence between the transition rates characterizing the noise traders' investment decision and the Glauber rates is finally manifest and with it the profound connection between the noise traders class and the Ising model.

The Statistical Physics average magnetization m corresponds to the time-dependent opinion index s_t

$$m \Leftrightarrow s_t. \tag{2.73}$$

The external field h applied to each spin corresponds to the time-dependent price momentum H_t influencing the trader decision

$$h \Leftrightarrow H_t. \tag{2.74}$$

The inverse temperature β corresponds to the time-varying herding propensity κ_t

$$\beta \Leftrightarrow \kappa_t. \tag{2.75}$$

Finally, each noise trader is subjected to the social imitation of all the other trader in its class in the same way, independently of the specific investor. We are assuming that the investment decision of each trader impacts the decisions of all the others in the same way. This is represented by a constant homogeneous value of the coupling constant which we set for simplicity to $J = 1$.

What we have just demonstrated is that the noise traders class can be effectively represented by a fully connected Ising model, where each spin s_i represents a noise investor which can alternatively invest in the risky asset ($s_i = 1$) or the risk-free asset ($s_i = -1$). Each noise trader interacts with all the others in the same way and there is a uniform external field constituted by the price momentum which influences each investor in the same way.

Now that the correspondence between the noise class and the Ising model has been established, we can exploit the large corpus of theoretical results on the latter to study and try to explain the emergence of the bubbles in the first.

Indeed, it is the very existence of a phase transition in the Ising model and hence in the noise traders class, which gives rise to the bubbles. The phase transition separates the disordered regime where the idiosyncratic opinion dominates from the ordered regime where the full class polarizes towards one asset, in analogy to the collective alignment of the orientation in the ferromagnetic phase of a magnetic material. When the noise traders class undergoes the phase transition, the average opinion starts to polarize towards one asset, this triggers the bubble's emergence.

Moreover, it is the parameter κ_t correspondent to the inverse temperature β, which governs the phase transition. This explains the presence of the bubbles in the Ornstein-Uhlenbeck setup but not in the case of constant kappa. Indeed, the constant kappa value is set equal to $\kappa = 0.98p^+$, slightly below the critical value β_c corresponding to the critical inverse temperature of the Ising model. We know from Statistical Physics, that the critical point of the fully connected Ising model is at $\beta_c = \frac{1}{J} = 1$, being $J = 1$. Moreover, in the transition rates we have rescaled the kappa process by the factor p^+, hence we expect a phase transition at $\kappa_c = p^+$. In the constant kappa setup, the system remains in the disordered regime throughout the whole simulation, hence no bubbles can emerge. On the contrary, the Ornstein-Uhlenbeck herding propensity fluctuates around the mean reversion level $\mu_\kappa = 0.98p^+$, very close to the critical point, hence sometimes κ_t stochastically enters in the ordered regime, triggering the polarization of the class and ultimately the super-exponential growth of the price.

This effect is further amplified by the price momentum H_t. When the bubbles develop, the price momenta increases following the price dynamics, pushing more and more noise investors to switch to the asset undergoing the bubble. Sometimes this self-reinforcing loop can last until all the traders hold the same asset. At this point the noise traders experience the lock-in effect, the probability to switch to the other asset is saturated to zero.

When the herding propensity reverts to the sub-critical regime the polarization of the noise traders class starts to decrease, the idiosyncratic opinion starts to gain back importance and the noise traders start to switch to the other asset. Focusing for a moment on the case of a positive bubble, this selling phenomenon decreases the price, as an effect the price momentum becomes negative pushing more and more traders to sell the risky asset. The bubble bursts and the price come back to its fundamental value.

In light of this discussion, the name given to the herding propensity κ_t assumes all its meaning. It is this parameter accounting for the impact of a changing economical and geopolitical world on the financial markets to govern the propensity of the traders to herd, according to their social imitation and trend-following

attitudes.

Summarizing, we have demonstrated that it is mainly the noise traders class which triggers the emergence of the bubbles and governs their dynamics, through a polarization phenomenon which constitutes an actual phase transition from the disordered regime dominated by the idiosyncratic opinion to the ordered state characterized by the polarization of the investment preferences. This interaction-driven phase transition is controlled by the herding propensity parameter κ_t, which stochastically enters and exits the ordered regime, triggering the bubbles.

The fruitful connection between the noise traders class and the Ising model will be crucial also in extending the class to the multi-risky-asset framework and will be central throughout all the following work.

We close this Chapter on the original market model presenting in the next section the discussion on two important, "critical" features of the transition rates of the original model. This analysis is not present in any of the previous works on the original model and we think it is important to present it, not only for its significance for the original model itself but also for the resulting implication on the derivation of a new model in the extended framework.

2.7 Two "critical" features of the transition probabilities

In this section, we deepen two features of the original model's transition rates, which appear to be fundamental in characterizing realistic dynamics, in particular regarding the shape of the bubbles. These two crucial points are the average holding time and the linearization of the transition rates. An explicit analysis of them is lacking in the previous works on the original model, moreover, they have to be taken carefully into account in deriving new transition rates and analyzing the applicability of a new model for the multi-asset extension.

The adjective "critical" in the title of the section stands both for the importance of these two features and for their particular relevance near criticality when the kappa process enters the critical regime.

2.7.1 The average holding time

The first feature we analyze is the average holding time, defined as the average number of trading days the noise trader keeps its asset in absence of herding behavior $\kappa_t = 0$. In the original model, the average holding time is controlled by the constant p (or the related p_+ and p_-, which also introduce the imbalance between positive and negative bubbles), which is directly connected to t_h by the

relation

$$t_h = \frac{2}{p}. \tag{2.76}$$

The way the constant p (i.e. p_+, p_-) is introduced in the original model does not introduce modifications to the aforementioned detailed balance condition (2.64) and hence does not impact on the statistical properties of the simulation. In particular, having set a value of $p \approx p_+ \approx p_- \approx 0.2$, the resulting average holding time is given by

$$t_h = \frac{2}{p} \approx 10 \tag{2.77}$$

trading days.

Moreover, we stress that the average holding time should be always taken into account in constructing a new model and a realistic value for t_h should be always set, possibly without introducing errors in the detailed balance condition.

The importance of the parameter t_h representing the average holding time is clear comparing figure 2.6 and figure 2.7.

They represent two simulations of the original model with the same set of parameters, same initial condition, same transition rates, and same random seed. The only difference is the parameter p.

The first is characterized by $p \approx p_+ \approx p_- \approx 0.2$, i.e. $t_h \approx 10$. The second instead has $p \approx p_+ \approx p_- \approx 1$, indeed a less realistic $t_h = 2$. The difference in the modeling accuracy is dramatically evident. In particular, the time series in figure 2.7, characterized by the shorter average holding time, are dominated by an unrealistic oscillating behavior. The price builds up and fall too rapidly, leading to an extremely high frequency in the appearance of the bubbles. The problem is ultimately traced back to the unrealistic oscillating nature of the noise traders' risky fraction.

2.7.2 The linearization of the transition probabilities

The second feature we analyze is the linearization of the transition probabilities. We have commented in the previous section that the transition rates of the original model (2.58) and (2.59),

$$p_t^+ = \frac{p_+}{2}\left(1 - \frac{1}{p_+}\kappa_t(s_t + H_t)\right), \tag{2.78}$$

$$p_t^- = \frac{p_-}{2}\left(1 + \frac{1}{p_+}\kappa_t(s_t + H_t)\right), \tag{2.79}$$

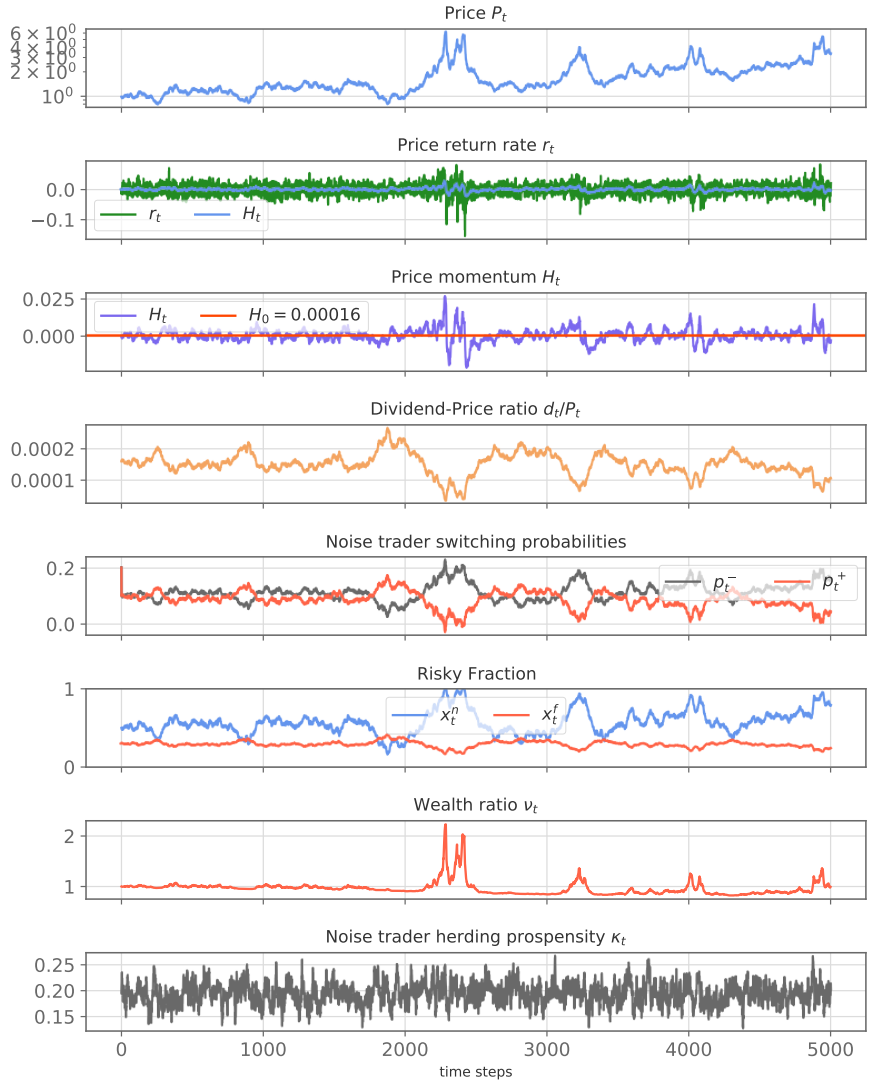

Figure 2.6: Original model Ornstein-Uhlenbeck kappa simulation with $p \approx 0.2$. The figure shows the time series of the standard implementation of the original model.

corresponds to the linearized form of the Glauber transition rates (2.60) and (2.61),

$$p_G^+(m,h) = \frac{1}{2}[1 - \tanh(\beta(m+h))] \tag{2.80}$$

and

$$p_G^-(m,h) = \frac{1}{2}[1 + \tanh(\beta(m+h))]. \tag{2.81}$$

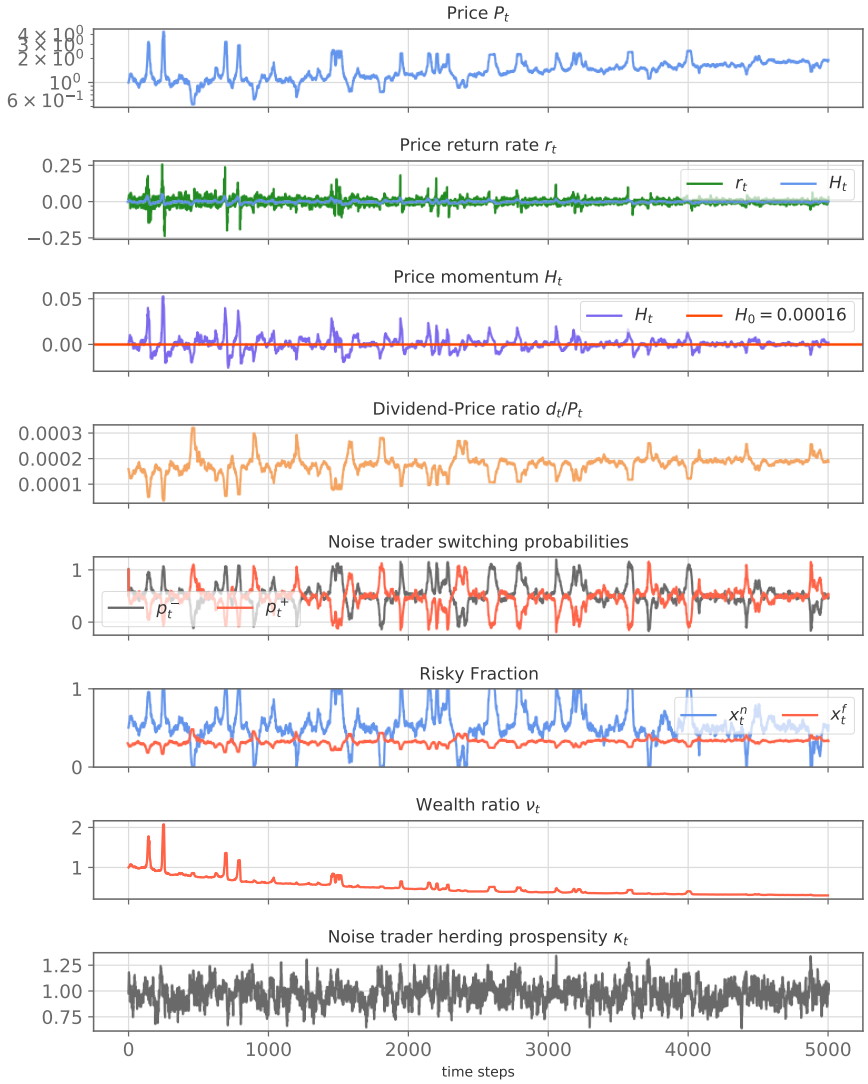

Figure 2.7: Original model Ornstein-Uhlenbeck kappa simulation with $p = 1$. The figure shows the time series of a simulation of the original model with the same set of parameters as the one in figure 2.6, differing only for the value $p = 1$. The loss of modeling accuracy is evident.

One may wonder if the linearization procedure is just an accessory step or represent an indispensable point in defining the transition rates of the model. It turns out that the second is the case since the linearized form is fundamental in defining the correct shape of the bubbles and, for some values of the parameters, their existence itself. The extreme representation of this is evident from figure 2.8 and figure

2.9, where are presented the time series of two simulations of the original model with exactly the same set of parameters, the same initial conditions, and the same random seed, differing only in that the first features the linearized rates and the second the non-linear Glauber rates.

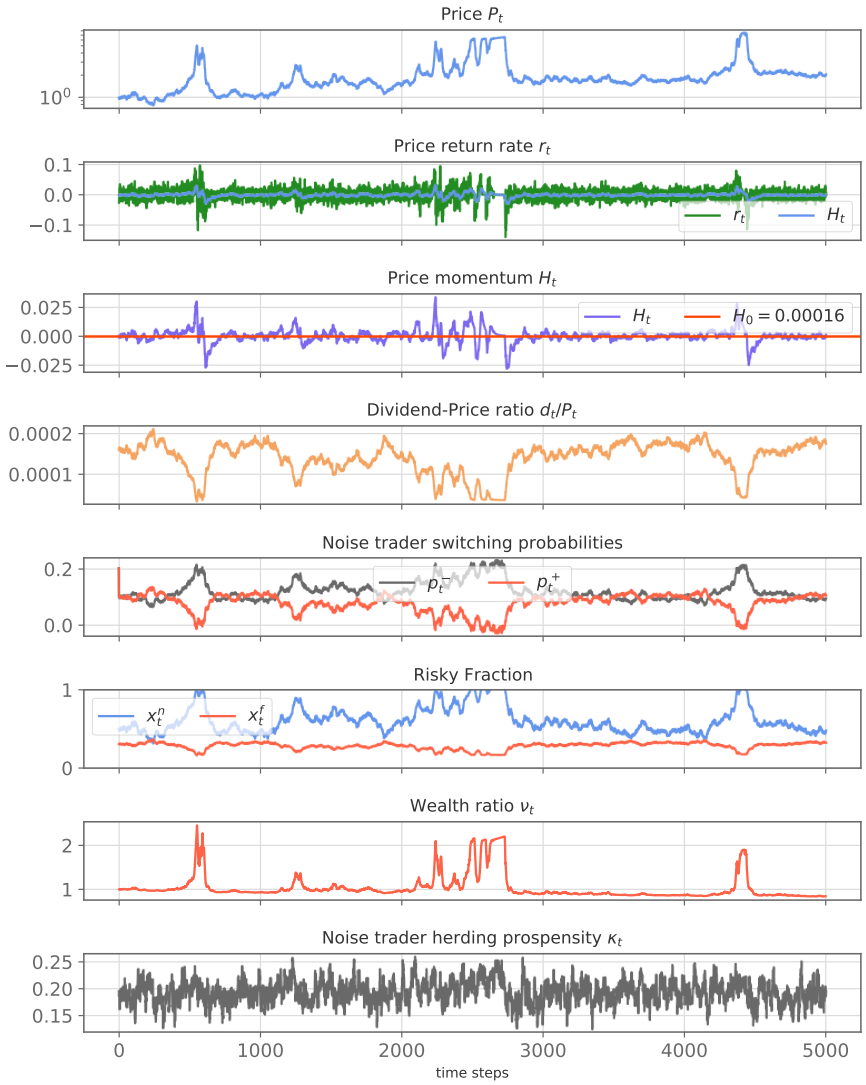

Figure 2.8: Original model Ornstein-Uhlenbeck kappa simulation with linearized rates. The figure shows the time series of the standard implementation of the original model.

Quite remarkably, for the specific set of parameters used the existence itself of clearly recognizable bubbles depends on the linearization procedure. For other sets

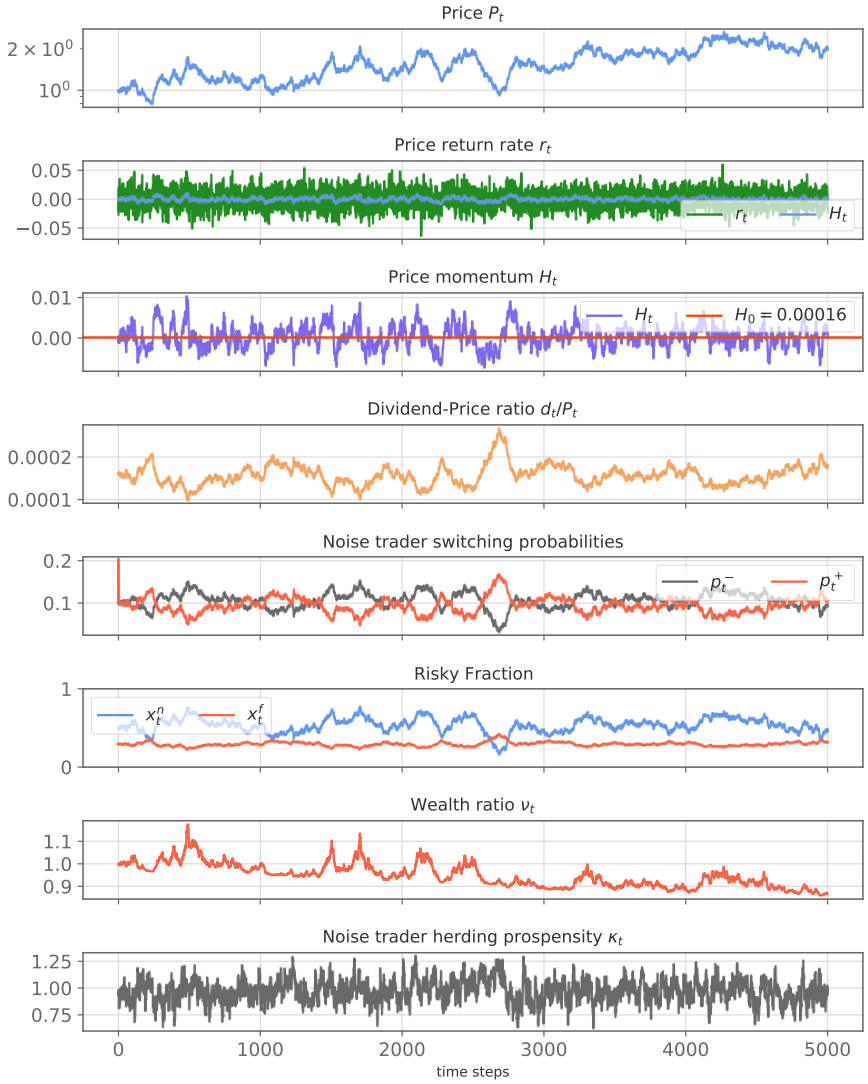

Figure 2.9: Original model Ornstein-Uhlenbeck kappa simulation with non-linear Glauber rates. The figure shows the time series of a simulation of the original model with the same set of parameters as the one in figure 2.8, differing only for the non-linear form of the rates.

of parameters, even if they still exist, the shape of the bubbles appears dramatically different with respect to the linearized case. This can be traced back to the fact that with non-linear rates, the noise traders class never fully polarizes as visible in figure 2.9, at odds with the linear case in figure 2.8.

The explanation of this phenomenon becomes clear analyzing the form of the

transition rates. Indeed, in the non-linear case, a saturation mechanism is already implied by formulas (2.60) and (2.61). When the argument of the hyperbolic tangent increases during a bubble overcoming the value $\frac{1}{2}$, the very form of the function makes the transition probability grows slower and slower. The transition rate eventually tends to the value 1, never reaching it. Instead in the case of linearized probability, the value of 1 is reached linearly for a finite value of the argument. From figure 2.10, the distinct form of the two transition probabilities is clear, and with it the remarkably different behavior of the resulting time series.

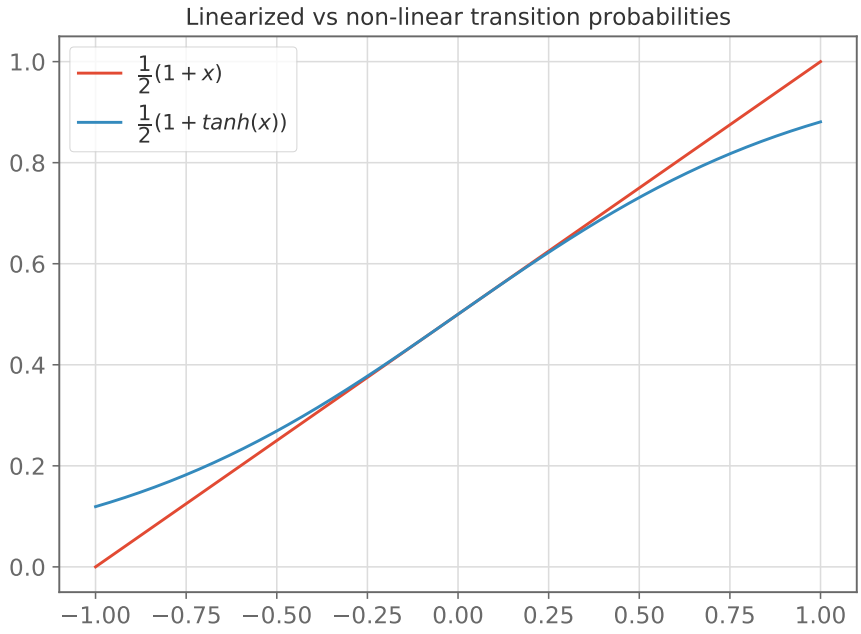

Figure 2.10: Linearized and non-linear forms of the transition probabilities for a range of values $x \in [-1,1]$. The two functions clearly differs for relatively large values of the argument, near -1 and 1.

In conclusion, the linearization of the form of the transition rates derived from the Ising-like model could be a crucial point to take into account when analyzing the applicability of the model.

Chapter 3

Towards the multi-risky-asset extension of the Market Model

After having presented the original model characterized by one risk-free and one risky asset, in this Chapter we move to the primary aim of the present work, the extension to the multi-risky-asset framework. Given that in the real financial markets lots of risky assets exist and the portfolio theory is one of the fundamental pillars of modern financial theory, it is clear why we are deeply interested in extending the original setup in this direction. Will the bubbles still be present in a more realistic model of this kind? And if it will be the case, how will the interplay between their dynamics impact on the properties of the market? Will the bubbles be synchronous or asynchronous? How will the possibility to diversify among different risky assets affect the trader classes' behavior?

The multi-asset nature is a central feature of the financial markets, which has to be taken into account in modeling and studying their complex dynamics. Important works from the literature dealing with the extension of ABMs to the multi-asset framework are constituted by Chiarella et al. [14], Chiarella et al. [36], Böhm and Chiarella [37], Xu et al. [38], Borghesi and Bouchaud [39] and Chen and Huang [40]. In particular, the extension of the original model by Kaizoji et al. [13] has been already addressed in two works, Damiani [21] and Kopp [22].

In the first work, the model has been enlarged to the case of one risk-free and two risky assets. We will discuss the interesting approach used in it, in particular regarding the generalization of the noise traders class. It will be a useful starting point and will inspire the first extension attempts, but eventually, we will detach from it due to the difficulty in scaling the approach to the general n-asset case and being the present work's purpose exactly to develop a well scalable extension in

the number n of risky investments.

The second work, truly remarkable in our opinion, deals instead mainly with the extension of the model to the n-bonds framework, to formulate a fixed income market model. While our approach will be similar regarding the extension of the fundamentalist traders and the price equation, for the noise traders class we will follow a radically different direction. Nevertheless, the comparison of the multi-asset Ising-like modeling we will develop in Chapter 4 to the approaches presented in the aforementioned studies is extremely useful and interesting.

In moving towards the multi-risky-asset (for the sake of conciseness from now on we will omit the adjective risky, being at this point clear our work deals with a multiplicity of risky investments) framework we have to work out the extension of each of the four components of the original model presented in Chapter 2. In this Chapter, we present the multiple assets and the extended wealth dynamics in section 3.1. Then we move to the discussion of the fundamentalist traders class generalization in section 3.2. Then, before moving to the noise traders we present the extension of the market-clearing conditions and the resulting price equations in section 3.1. Finally, we discuss the noise traders' generalization puzzle in section 3.4, introducing the approach we will use in the next Chapter to tackle it.

3.1 The assets and the wealth dynamics

The extended model is constituted of one risk-free asset, still representing a zero-coupon government bond yielding a constant rate of return r_f, and n risky assets, representing n stocks paying stochastic dividends. The first component whose extension needs to be defined is indeed the dividend process, which is substituted by n stochastic processes $d_{k,t}$ with $k \in \{1, \dots, n\}$.

Since we want to allow for the possible interplay between their dynamics, we describe their time evolution through n multiplicative growth processes

$$\begin{cases} d_{1,t} = (1 + r_t^{d,1}) d_{1,t-1} \\ d_{2,t} = (1 + r_t^{d,2}) d_{2,t-1} \\ \quad \vdots \\ d_{n,t} = (1 + r_t^{d,n}) d_{n,t-1} \end{cases} \tag{3.1}$$

where the stochastic growth factors follows a multivariate normal distribution

$$(r_t^{d,1}, r_t^{d,2}, \dots, r_t^{d,n}) \sim \mathcal{N}(\vec{\mu}, \Sigma_d), \tag{3.2}$$

with mean

$$\vec{\mu} = (r_{d,1}, r_{d,2}, \dots, r_{d,n}) \tag{3.3}$$

and covariance matrix Σ_d, the latter governing the relationship between the dividends. As a quick note, we comment that in the simulation the covariance matrix is implemented into a vector of variances and a matrix of correlations, in order to be able to change the variances and the correlations in an independent and easier way. The correlation matrix C_d and the covariance matrix are connected by the relation

$$C_d = (diag(\Sigma_d))^{-\frac{1}{2}} \Sigma_d (diag(\Sigma_d))^{-\frac{1}{2}}, \tag{3.4}$$

where $diag(\Sigma_d)$ represents the diagonal matrix of the variances. We wanted to insist on the implementation of the covariance matrix because the dividend processes represent the component of the model which takes into account the impact of the real economy evolution on the stocks' value.

Even if in the present work we will not deepen this aspect, the possibility to introduce and study the effect of correlations among the dividends represents an interesting simulation playground. Through the correlation matrix C_d and the vector of variances, it is possible to analyze the impact of the correlation coming from the real economy on the price formation mechanism and the synchronization of bubbles.

As a last implementation note, we comment that in the simulation the dividend processes are generated sampling at each time-step the stochastic growth factors in an i.i.d. manner from the multivariate normal distribution (3.2). First, n i.i.d. zero mean and unit variance normal distributions $\mathcal{N}(0,1)$ are sampled. Then the vector of growth factors is obtained through the linear transformation

$$\begin{pmatrix} r_t^{d,1} \\ \vdots \\ r_t^{d,n} \end{pmatrix} = \Sigma_d^{\frac{1}{2}} \begin{pmatrix} \mathcal{N}(0,1) \\ \vdots \\ \mathcal{N}(0,1) \end{pmatrix} + \begin{pmatrix} r_{d,1} \\ \vdots \\ r_{d,n} \end{pmatrix} \tag{3.5}$$

where the matrix $\Sigma_d^{\frac{1}{2}}$ is computed by means of the Cholesky decomposition.

As in the original model the enhanced risk of these assets with respect to the asset representing the zero-coupon bond derives both from the stochastic character of their dividends and from the fact that their returns depend on the prices dynamics, which is not known a priori. This is clear from the expression of the total risky return rates, which in the multi-asset framework reads

$$\vec{r}_t^{tot} = \vec{y}_t^{d} + \vec{r}_t, \tag{3.6}$$

where now the dividend yields $\vec{y}_t^{d}$ and the price returns $\vec{r}_t$ are n-components vectors. In particular the dividend yields vector is defined as

$$\vec{y}_t^{d} = \left(\frac{d_{1,t}}{P_{1,t-1}}, \ldots, \frac{d_{n,t}}{P_{n,t-1}} \right) \tag{3.7}$$

and the price returns vector as

$$\vec{r}_{p,t} = \left(\frac{P_{1,t}}{P_{1,t-1}} - 1, \ldots, \frac{P_{n,t}}{P_{n,t-1}} - 1 \right). \tag{3.8}$$

The fundamentalist and noise traders classes are still considered at the aggregate level by means of two representative agents. The difference is that now both the aggregate portfolios are constituted by n risky fractions $\{x_{1,t}^{f,n}, \ldots, x_{n,t}^{f,n}\}$ and one risk-free fraction $x_{rf,t}^{f,n}$. Borrowing and short-selling are again not admitted in the market model, hence the risky fractions always satisfy $x_{k,t}^{f,n} \in [0,1]$. Also the risk-free fraction satisfies the same constraint $x_{rf,t}^{f,n} \in [0,1]$. Moreover, the fractions are subjected to the condition that they must sum to one at each time step t

$$x_{rf,t}^{f,n} + \sum_{k=1}^{n} x_{k,t}^{f,n} = 1, \tag{3.9}$$

from which we can express the risk-free fraction as

$$x_{rf,t}^{f,n} = 1 - \sum_{k=1}^{n} x_{k,t}^{f,n}. \tag{3.10}$$

According to this description, the wealth dynamics equation generalizes to

$$W_t^{f,n} = W_{t-1}^{f,n} \left[1 + r_f + \sum_{k=1}^{n} x_{k,t-1}^{f,n} \left(\frac{d_{k,t}}{P_{k,t-1}} + \frac{P_{k,t}}{P_{k,t-1}} - 1 - r_f \right) \right], \tag{3.11}$$

where the quantity in parenthesis represents the excess return of the risky asset k with respect to the risk-free return r_f

$$r_t^{k,excess} = \left(\frac{d_{k,t}}{P_{k,t-1}} + \frac{P_{k,t}}{P_{k,t-1}} - 1 - r_f \right), \tag{3.12}$$

measuring the higher profitability ($r_t^{k,excess} > 0$) or lower ($r_t^{k,excess} < 0$), with respect to the risk-free asset.

3.2 The fundamentalist traders

For the extension of the fundamentalist class we refer mainly to Damiani [21], Kopp [22] and Chiarella et al. [14]. We keep the original structure, with rational risk-averse traders who at each time-step maximize the expected CRRA utility function of the future wealth in terms of the risky fractions and for a given level of risk. The difference is that now the number of risky assets in which it is possible to invest is n.

At each time step, each fundamentalist trader constructs its portfolio solving the maximization problem

$$(x^f_{1,t}, \dots, x^f_{n,t}) = \max_{x^f_{1,t},\dots,x^f_{n,t}} E_t[U(W^f_{t+1}(x^f_{1,t}, \dots, x^f_{n,t})], \tag{3.13}$$

where U represents the CRRA utility function with constant risk aversion γ

$$U(W) = \begin{cases} \log(W) & \gamma = 1 \\ \frac{W^{1-\gamma}}{1-\gamma} & \gamma \neq 1 \end{cases} \tag{3.14}$$

Again each fundamentalist trader solves the same optimization problem of all the other traders in its class. Hence, the whole class can be considered at the aggregate level through a representative agent, who solves the same optimization problem (3.13) and whose wealth is equal to the sum of all the wealth of the fundamentalist investors. The maximization problem (3.13) is not trivial and has been solved in Xu et al. [38], here we report the final solution. The fundamentalist portfolio allocation strategy condenses into the equation

$$\begin{pmatrix} x^f_{1,t} \\ \vdots \\ x^f_{n,t} \end{pmatrix} = \frac{1}{\gamma} \mathrm{Cov}^{-1} \begin{pmatrix} E_{r,1} + \frac{d_{1,t}(1+r^{d,1})}{P_{1,t}} - r_f \\ \vdots \\ E_{r,n} + \frac{d_{n,t}(1+r^{d,n})}{P_{n,t}} - r_f \end{pmatrix} \tag{3.15}$$

where Cov^{-1} is the inverse matrix of the expected covariances of the future price returns foresee by the fundamentalist traders, which are assumed equal to the expected covariances of the future excess returns following as for the original model Kaizoji et al. [13], Modigliani and Miller [27] and Modigliani and Miller [28].

We underline the term expected because in the covariance matrix enter the covariances between the risky assets expected by the fundamentalist traders before the effective realization of the random process representing the prices. The expectation of the fundamentalists on the correlations in the future evolution of the prices is then condensed in the matrix Cov which in principle could depend on time, but which we assume, for simplicity, time-independent. In the equation (3.15) enter also the quantities $\{E_{r,1}, \dots, E_{r,n}\}$ which represent the expected price return by the fundamentalist traders.

We notice from the formula that the mean-variance trade-off present in the original model, characterizes also the multi-asset framework. We refer the interested reader to Kopp [22], where two captivating alternative solutions of the optimization problem (3.13) coming from the field of stochastic optimal control are proposed. One is based on the Bellman's dynamic programming approach, the other on the Pontryagin's maximum principle.

Finally, we comment on the fact that the constant risk aversion is endogenously computed at the beginning of the simulation from the initial conditions as

$$\gamma = \frac{E_{r,1} + \frac{d_{1,0}(1+r^{d,1})}{P_{1,0}} - r_f}{\mathrm{Cov}_{1,1}x^f_{1,0} + \ldots + \mathrm{Cov}_{1,n}x^f_{n,0}}, \tag{3.16}$$

which constitutes a natural generalization of the original model's formula (2.50), also adopted in Damiani [21] and Kopp [22].

Before moving to the extension of the noise traders class, which will be also the central topic of the whole Chapter 4 and constitutes the main part of all the present work, in the next section we present the generalization of the market-clearing conditions and the resulting price equations.

3.3 The market-clearing conditions and the price equations

In the original model, the price dynamics is determined from the market-clearing conditions. The market price is set according to Walras's theory of general equilibrium, Walras [16], i.e. at each time-step the supply and the demand must equilibrate.

Setting to zero the aggregate excess demand in the original case of only one risky asset leads to a second-order equation in the unknown P_t. The equation can be explicitly solved giving a unique physical solution, i.e. a positive price, which represents the new price of the risky asset.

Extending the model to n risky assets, the equilibrium condition has to hold at the same time for each asset.

Defining the excess demand from time $t-1$ to t for each risky asset k for the fundamentalists and noise traders classes respectively as

$$\Delta D^{f,k}_{t-1\to t} = W^f_t x^f_{k,t} - W^f_{t-1} x^f_{k,t-1} \frac{P_{k,t}}{P_{k,t-1}} \tag{3.17}$$

and

$$\Delta D^{n,k}_{t-1\to t} = W^n_t x^n_{k,t} - W^n_{t-1} x^n_{k,t-1} \frac{P_{k,t}}{P_{k,t-1}} \tag{3.18}$$

we have that the equilibrium condition translates into the system

$$\begin{cases} \Delta D^{f,1}_{t-1\to t} + \Delta D^{n,1}_{t-1\to t} = 0 \\ \Delta D^{f,2}_{t-1\to t} + \Delta D^{n,2}_{t-1\to t} = 0 \\ \quad\vdots \\ \Delta D^{f,n}_{t-1\to t} + \Delta D^{n,n}_{t-1\to t} = 0 \end{cases} \tag{3.19}$$

The system (3.19) is a system in the n unknowns $P_{1,t}, \ldots, P_{n,t}$.

The increase in complexity is clear. Passing from the one risky asset framework to the n risky asset framework, the price equations change from a single second-order polynomial equation to a complex non-linear system of n equations in n unknowns where each equation is a polynomial equation of degree $n+1$ in all the unknowns. The system is hardly manageable in an analytical way.

We have considered various possible solutions modifying the market-clearing conditions to set the equilibrium in a simpler and more manageable manner with respect to this "detailed equilibrium" conditions. Nevertheless, eventually, we opted for a numerical solution to maintain the original structure of the price equations and the original equilibrium assumption. This turns out to be also the solution adopted in Kopp [22].

Indeed, even if the system is not manageable analytically, it can be tackled with numerical techniques. In particular, we implemented an iterative method using the *C++ GNU Scientific Library (GSL)*, based on the Hybrid algorithm proposed in Powell [41] and Powell [42], derived from the classical Newton–Raphson algorithm. With careful manipulation of the equations and choice of the initial guess (prices in previous time-step as initial conditions), the method consistently converges to the correct physical solution for a wide range of parameters close to the real market quantities. The iterative method is fast and stable, hence we opted to rely on it. Nevertheless, a different way to determine the price dynamics is always possible and the analysis of different equilibrium conditions could be deepened.

3.4 Noise traders: Can Statistical Physics solve the extension puzzle?

We now move to the extension of the last component of the model, the noise traders class. The generalization of the noise traders to the n risky assets framework is extremely delicate and a multiplicity of possibilities can be considered.

As in the original setup, the noise traders do not implement a rational maximization process to decide their investments, as the fundamentalist traders do. They are instead driven by social imitation and trend following. These two attitudes govern their intrinsically stochastic investment strategy.

In Chapter 2 we explained that the fundamental feature characterizing the noise traders class is its Ising-like structure which models the competition between the ordering force of social imitation and the disordering impact of idiosyncratic opinion. We showed that it is this very Ising-like structure that explains the emergence of the bubbles and governs their dynamics. These highly non-trivial collective phenomena emerge through a polarization phenomenon which constitutes an actual phase transition from the disordered state to the order one. We also argued that

this interaction-driven phase transition is controlled by the herding propensity parameter κ_t, which stochastically enters and exits the ordered phase, triggering the bubbles.

Now that we want to move to the multi-asset framework we have to generalize the social imitation and trend following attitudes allowing for many risky assets while preserving the Ising-like structure responsible for the polarization phenomenon governing the bubbles. Many models can be considered to pursue this goal and many factors have to be taken into account in comparing their effectiveness. Should we still rely on the standard Ising model or should we move to the generalizations of it? How should the noise traders' strategy account for the n risky assets? Should they still invest all their wealth into one single asset at a time, or should we allow them to construct a portfolio of different assets and focus on the social imitation and trend following's impact on this stochastic diversification process? Ultimately, which formal rule should we use to define the transition rates, if a systematic rule should be used at all?

The task is challenging. The same extension puzzle has been tackled by Damiani [21] and Kopp [22], hence we start analyzing their approaches. We first mention that we tried to extend the approach of Damiani [21]. Staying on a qualitative explanation, in the latter work the noise traders' model is generalized to the case of one risk-free and two risky assets coupling two distinct Ising models, one for each risky investment. Each of them models the polarization phenomenon towards either one of the risky investment or the risk-free asset. Then, since only one asset of the latter type is present, the two resulting indistinguishable risk-free assets are identified as a unique one. Moreover, the risky assets are connected allowing for switches between them. The model just presented constitutes a discrete-time Markov Chain that we can effectively represent in figure 3.1.

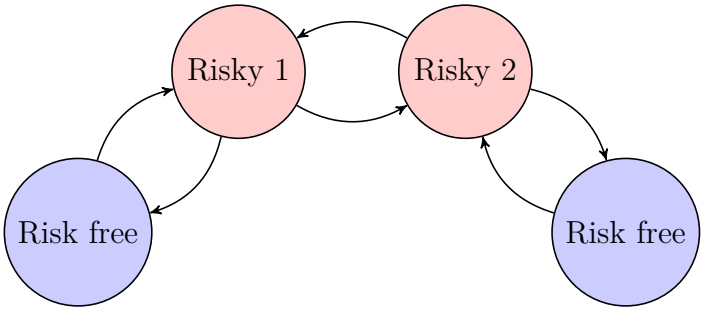

Figure 3.1: Markov chain for the "two coupled Ising" model

In Damiani [21] this setup is shown to still give rise to bubbles, governed basically by the distinct but related phase transitions characterizing the two Ising model. To extend the approach just presented, we considered n Ising model, one for each risky asset, each one representing the possibility for a trader investing in a particular

risky asset to move all his wealth towards the risk-free asset and vice versa. The Ising models are then connected through the risky states by means of a complete graph, i.e. each trader investing in a risky asset, besides the possibility to switch to the risk-free asset or keep its position, has also the possibility to switch to any other risky asset.

The resulting n risk-free assets are then considered indistinguishable, effectively representing one unique risk-free asset, or from the modeling point of view the bond market at the aggregate level.

Again from a dynamical point of view, the scheme presented constitutes a discrete-time Markov chain and a useful graphical representation of it can be made. Figure 3.2 shows the resulting Markov chain in the case of three risky assets.

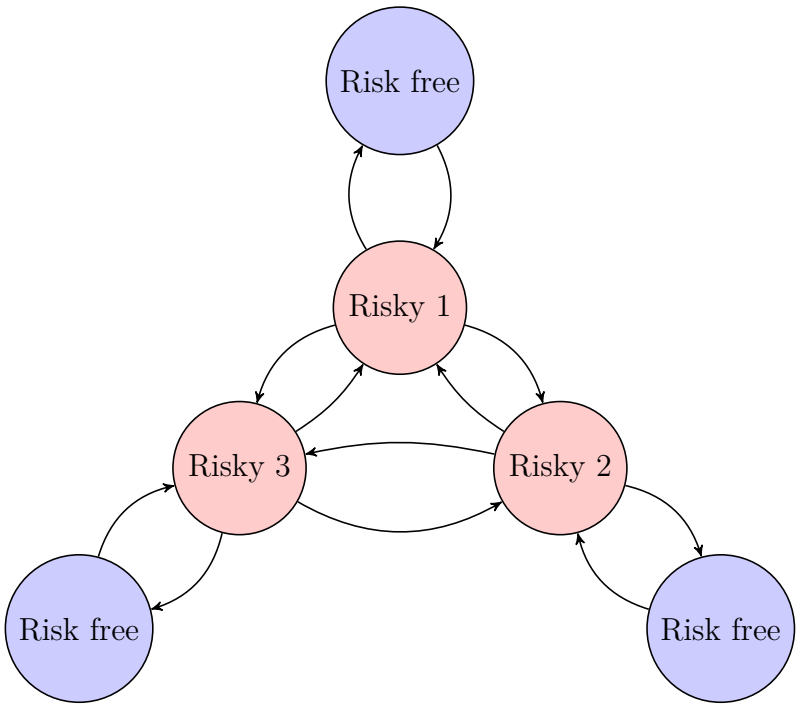

Figure 3.2: Markov chain for the "n ($n = 3$) coupled Ising" model

Eventually, we decided to abandon this approach since growing the number n of risky assets leads to a poorly controllable behavior of the class considered at the aggregate level. The Ising-like structure suggests the form of the transition probabilities between risky and risk-free investments, as in the original setup. Nevertheless, it does not tell us anything about the form of the transition probabilities inside the complete graph. This total freedom in defining the latter rates is a double-edged sword, this large arbitrariness is priced by the lack of control on the emerging statistical property of the system. We will soon come back to this crucial

point.

In the meanwhile, we comment that the other possibility we have considered, which gives rise to a different Markov chain structure is inspired by the solution adopted in Kopp [22]. We can model the transition from the unique risk-free asset towards the risky assets market, i.e. the stock market, considered at the aggregate level and vice-versa through an Ising model and then we can construct a mechanism to specify the investment decision inside the stock market. The resulting Markov chain, again for three risky assets, is represented in figure 3.3.

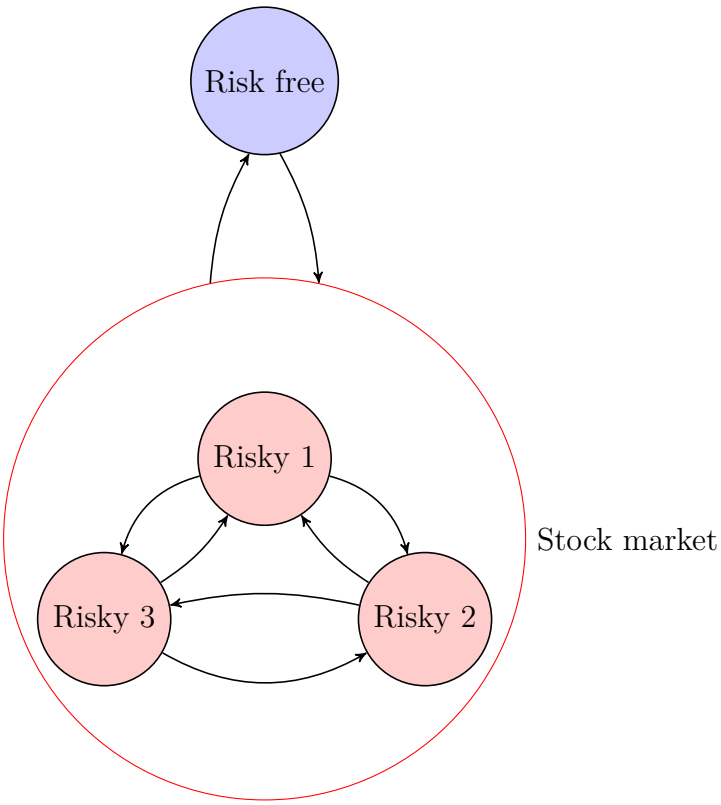

Figure 3.3: Markov chain for the "aggregate stock market" model (with $n = 3$ stocks)

In the following Chapter we will use a radically different approach to construct other models for the noise traders class, here however we explain why we have discarded both the two possibilities just presented.

The two models share the same "microscopic" approach used to derive them. Indeed, we have started to build the models defining a stochastic dynamics, which is completely specified by a discrete-time Markov chain. This approach boils down to defining the possible states, assets in this case, and the transition rates among them which together specify the dynamics of our microscopic agent, the noise

trader. Then we can study the emerging statistical properties of the "macroscopic" system composed by the whole class of noise traders.

The method gives us complete freedom in defining the stochastic dynamics which best models the system under analysis. Yet, in our opinion without other constraints the method would suffer from a major drawback, indeed it would give little or no a priori control, at least quantitatively, on the resulting "macroscopic" statistical properties of the model. The resulting lack of solid theoretical results regarding the emerging statistical properties could be an important problem in modeling a complex system such as the financial market.

For this reason, in the following, we will adopt a different, in some sense specular, approach starting from modeling the statistical property of the noise traders class and then deriving from them the stochastic dynamics governing the time evolution of the investment decisions. Moreover, this is actually the approach underlying the definition of the transition rates in the original model by Kaizoji et al. [13].

Furthermore, we have a strong ally to proceed in this direction. Indeed, a huge amount of work has been done in the field of Statistical Physics to tackle the problem of simulating the stochastic dynamics of a system with specified statistical properties and extremely powerful tools have been developed. We will extensively make use of them. Statistical Physics has a history of success in modeling systems with a large number of components (in this case the traders) whose collective interactions lead to the emergence of highly not trivial collective phenomena (in this case the bubbles).

Basically, in the next Chapter, we will put in the center the Ising-like structure of the noise traders class. We will start from it, trying to generalize the original model framework characterized by the standard Ising model to the multi-asset case.

Fortunately, the Ising model has been extended in many directions to account for the presence of many states. We will largely make use of this rich literature.

In Chapter 4 we will propose four multi-state Ising-like statistical models for the noise traders class, deriving the stochastic dynamics characterizing each of them and discussing their strengths and weaknesses.

Each model has its peculiarities and is able to better depict particular features of the noise traders class we are trying to model. As always in modeling, the trade-off between the accuracy in representing different features of the system under analysis has to be taken into account. We will present in order the four multi-state Ising-like models: a Potts model, an $O(n)$ model, a vectorial extension of the BEG model, and an n-state extension of the BEG model.

Finally, we anticipate that the analysis of these models will unveil a profound connection between the Ising-like modeling of the noise traders and the Decision Theory, in particular concerning the Logit distribution, constituting the theoretical framework in which we can understand the decision process characterizing the investments of this type of agents.

Chapter 4

Ising-like modeling for the extended Noise traders class

We have largely discussed in the last section of the previous Chapter on the difficulties in extending the noise traders class to the multi-asset framework. In this Chapter, we tackle the extension puzzle by applying the tools of Statistical Physics. We have already commented on the effectiveness of Statistical Physics in modeling systems with a large number of components whose collective interactions lead to the emergence of highly non-trivial collective phenomena.

In this Chapter, in particular, we refer to the large literature concerning the multi-state extension of the Ising model to preserve also in the enlarged framework the fundamental Ising-like structure of the noise traders class that we showed to govern the emergence and the dynamics of the bubbles.

As we have already anticipated our approach starts from modeling the "macroscopic" statistical properties of the noise investors through an Ising-like model. We will introduce in order four models of this type: a Potts model, an $O(n)$ model, a vectorial extension of the BEG model, and an n-state extension of the BEG model.

Each model is defined by its Hamiltonian, entering in the Boltzmann weight. The latter constitutes the probability distribution associated with the possible configurations of the noise traders class, hence it associates a probability to each possible set of investment decisions the whole pool of traders can undertake. The Boltzmann weight of the model completely determines the statistical properties of the system under analysis.

However, we are interested in modeling the dynamics of the class and not just its average properties. Hence, the next step for each of the four aforementioned models is to derive the stochastic dynamics characterizing it. From Statistical Physics' theory, we know that different stochastic dynamics can exist that give rise to the same statistical model.

Nevertheless, this is radically different from the situation we where facing in the last Chapter commenting on the total freedom's problem concerning the other extension approaches. In that case, we were referring to this freedom as a double-edged sword, commenting that the resulting lack of solid theoretical results regarding the emerging statistical properties could be an important problem in modeling a complex system such as a financial market.

Instead, now we have at disposal a tool to define realistic stochastic dynamics while having complete control of the resulting statistical properties. This tool is constituted by the Markov Chain Monte Carlo (MCMC) theory together with the detailed balance condition which allows us to do exactly what we need, to start from the Boltzmann weight and to obtain through a theoretically solid derivation the transition probabilities which fully determines the stochastic dynamics of the model and therefore the time evolution of the investment decisions of the noise traders.

We briefly summarize the approach we adopt for each of the four Ising-like models. We start with the Boltzmann weight defined by the Hamiltonian of the particular model under analysis, then we write down the discrete-time Master Equation describing its stochastic dynamics. Applying the detailed balance condition to it we can derive the non-normalized transition probabilities. Finally, we proceed with the normalization obtaining the transition probabilities among the various assets. At this point, the dynamics of the noise traders' investment decision is completely determined by the quantities just computed. The next step is to implement the simulation of the Markov Chain Monte Carlo thus obtained. We will see that this implementation step is in general non-trivial, sometimes constituting a real obstacle to overcome. At this point, we can insert the designed extension of the noise traders class into the whole enlarged model, defined by the components introduced in Chapter 3. We have finally a complete market model extended to the multi-asset framework. Implementing its simulation, we can study the resulting time series and analyze the interesting collective phenomena characterizing them.

One of the most interesting points that will emerge in the following discussion is the profound connection between the transition probabilities derived with this method and the Logit probability distribution. This will create a bridge between the Ising-like modeling of the noise traders and the framework of Decision Theory in which we can understand the decision process of each agent. Building on this connection we will see that all the modeling could be reformulated in terms of the maximization process of a specific deterministic utility function, common to all the agents, in presence of the random impact of the idiosyncratic opinion of each individual. This will allow us to understand how the "macro" statistical properties emerge from the "micro" stochastic decision process of each noise investor.

The whole Chapter is dominated by the application of the tools of Statistical Physics, we will adopt its natural language and we will deepen some important

points insisting in particular on their theoretical implications.

We now move to outline the structure of the Chapter. There are four main sections corresponding to the four Ising-like models analyzed, plus one extra section devoted to a digression on the modeling of the social imitation mechanism in a wider sense, useful for the introduction of the last of the four models.

Here we briefly introduce the four main sections. The detailed presentation of the structure of each section, with the overview of its subsections, is present at the beginning of each of the four parts.

Section 4.1 is dedicated to the Potts model. In particular, we consider a fully connected Potts model with an external field representing the various price momenta. Then, in section 4.2 we present a fully connected $O(n)$ model with a vectorial external field representing the price momenta. In section 4.3 we then move to a vectorial extension of the BEG model. Section 4.4 is instead dedicated to a more general discussion on the task of modeling the social imitation phenomenon in the noise traders class. Finally, in section 4.5 we discuss the last of the four Ising-like statistical models of the Chapter, an n-state extension of the BEG model.

4.1 The Potts model

In this section, we propose a multi-asset extension to the original noise traders class introducing a fully connected Potts model with an external field representing the price momenta.

In subsection 4.1.1 we introduce the Hamiltonian defining the model. In subsection 4.1.2 we derive the transition probabilities and we study their interesting properties, in particular, we find that the resulting transition probabilities coincide with the Logit distribution, thoroughly studied in the Discrete Choice Theory. In the subsection 4.1.3 we present the time series of two simulations and we comment on their qualitative behavior. The time series generated by the implementation of this model are qualitatively and quantitatively very different from the original model ones and very far from real markets' behavior. To understand this unexpected behavior we deepen the theoretical analysis of the model by means of two main tools, the dynamical systems theory to study the mean value equations and the emerging bifurcation diagram, in subsection 4.1.4, and the Landau expansion of the free energy, in subsection 4.1.5. This analysis unveils the reasons for the strange behavior of the time series and points out the limits of applicability of the Potts model in representing the noise traders class. The latter point is addressed in subsection 4.1.6, where we summarize the results found and we comment on the aforementioned limits of applicability, also concerning possible different models which share some features with the Potts' one.

4.1.1 The Potts model on the fully connected graph

To extend the noise traders class to the multi-asset framework we introduce a q-state Potts model with an external field defined on the fully connected graph K_N, with N nodes and $\frac{N(N-1)}{2}$ edges. The number $q = n + 1$, represents the total number of assets, constituted in particular by n risky and one risk-free asset. The Hamiltonian of the model is

$$H_N(\{s_1, \dots, s_N\}) = -\frac{J}{2N} \sum_{i,j=1}^{N} \delta_{s_i,s_j} - \sum_{k=1}^{q} h_k \sum_{i=1}^{N} \delta_{s_i,k} \tag{4.1}$$

where N represents the total number of noise traders. Each noise trader invests all his wealth in only one asset at a time, hence is modeled by a spin which can assume q discrete values $s_i \in \{1, \dots, q\}$. Each value representing the unique asset held by the investor. In particular, the first $n = q - 1$ represent the risky assets, while the last one the risk-free investment. From now on we will refer to s_i both with the terms spin and trader.

Moreover, each noise trader interacts with all the others through a Kronecker delta-like interaction δ_{s_i,s_j}. This interaction models the social imitation attitude of this type of agent. In particular the interaction will be attractive $-\frac{J}{2N}(\delta_{s_i,s_j} = 1) = -\frac{J}{2N}$ in the case of two traders investing in the same asset, or absent in case of different investment decisions $-\frac{J}{2N}(\delta_{s_i,s_j} = 0) = 0$. Basically, the interaction term of the Hamiltonian (4.1) models an effective pairwise force pushing the traders to invest in the same asset. This intuitively motivates the expression modeling the social imitation, but we refer to section 4.4 for a deeper discussion on the topic. Finally, the second attitude characterizing this type of agent, the trend following, is modeled by an external field acting on each spin, i.e. trader, with an intensity-dependent on the state of the spin $h_k\delta_{s_i,k}$. The external field is composed of the price momenta of the risky assets so that the field h "felt" by the investor is constituted exactly by the price momentum corresponding to the asset he is holding.

In the Hamiltonian (4.1) there is a slight difference with respect to the standard form of the Potts model which needs to be clarified. Indeed, the Hamiltonian accounts also for a self-interaction of each spin with itself, being the double sum not subjected to the condition $s_i \neq s_j$, at odds with the standard version of the model. We have allowed for the self-interaction because in the following it will simplify the calculations. The central point is that this modification is negligible in the large N case, which is exactly the present one. This negligible difference is actually what distinguishes the fully connected formulation of the Potts model from the mean-field one, in the finite N regime. Indeed, it can be shown that the fully connected Potts model is equivalent to the mean-field Potts model in the thermodynamical limit $N \to +\infty$. Since it will be useful to compare our results

to the well-known properties of the mean-field models and since we are in a large N regime in which we know that the difference between the two is negligible, we simply slightly modify the fully connected model to extend the equivalence of the two also at finite N. Hence, from now on we will use the two terms, fully connected and mean-field interchangeably, referring always to the Hamiltonian in equation (4.1). We take the standard Boltzmann weight as the equilibrium distribution,

$$P(\{s_1, \ldots, s_N\}) = e^{-\beta H_N}. \tag{4.2}$$

This multivariate distribution, assigning a probability to each possible investments' configuration of the whole class, completely determines the statistical properties of the system.

In the next section, we introduce the procedure to derive from the Boltzmann distribution (4.2) the stochastic dynamics of the noise traders. This procedure, with the proper modifications, will be also applied to derive the transition probabilities of all the other three models we will introduce.

4.1.2 The transition probabilities and their connection to Decision Theory

In order to derive the stochastic dynamics of the statistical model, we construct a Markov Chain Monte Carlo (MCMC) having (4.2) as its equilibrium distribution. The dynamics is completely determined by the transition probabilities. In the next paragraph, we present the derivation of the transition probabilities, while in the following paragraphs we study their properties.

The derivation of the transition probabilities

We start from the discrete-time Master Equation governing the evolution of the time-dependent conditional probability distribution

$$P(s_l \mid \{s_1, \ldots, s_{l-1}, s_{l+1}, \ldots, s_N\}, t) \tag{4.3}$$

of a single spin s_l given all the other spins fixed in their states. From now on $\{s_1, \ldots, s_{l-1}, s_{l+1}, \ldots, s_N\}$ will be considered as fixed parameters each having a specific value among $\{1, \ldots, q\}$. We stress the fact that we have to consider the time evolution of this conditional probability because the time evolution of the full joint probability is not manageable. We also underline the fact that the following derivation relies on the key mean-field assumption, exact (minus an error that is negligible for large N) in the fully connected case, of statistical independence between the spins. This allows us to write

$$P(s_l \mid \{s_1, \ldots, s_{l-1}, s_{l+1}, \ldots, s_N\}, t) = P(s_l, t) \tag{4.4}$$

crucial point in the subsequent passages. The discrete time master equation for the conditional probability to have $s_l = a$ reads

$$\frac{P(s_l = a, t + \Delta t) - P(s_l = a, t)}{\Delta t} = \sum_{\substack{b=1 \\ b \neq a}}^{q} W(b \to a) P(s_l = b, t) - W(a \to b) P(s_l = a, t). \quad (4.5)$$

We will assume an unit time increment $\Delta t = 1$, representing one trading day. The transition rates $W(a \to b)$ have to be understood as conditional rates, having all the spins except s_l fixed. To lighten the notation we denote

$$P(s_l = a \mid \{s_1, \ldots, s_{l-1}, s_{l+1}, \ldots, s_N\}, t) = P(a, t). \quad (4.6)$$

To construct a MCMC for the Potts model we need to sample the desired equilibrium statistical distribution, effectively making the discrete-time derivative equal to zero. This can be done in different ways, here we use the classical detailed balance condition which reads

$$\frac{W(a \to b)}{W(b \to a)} = \frac{P(b)}{P(a)} \quad (4.7)$$

being P the equilibrium Boltzmann weight (4.2) for the Potts model, now independent of time.

At this point, a little theoretical discussion on why we choose the detailed balance condition to set to zero the discrete-time derivative of the Master Equation has to be addressed. What we need to do to proceed with this derivation is just to impose the stationarity condition on the system, expressed indeed by setting to zero the time derivative. The detailed balance condition is just one of the possible choices. It implies, but not vice-versa, the global balance condition, which instead is the actual condition equivalent to the stationarity constraint we want to impose. The global balance condition is expressed by

$$\sum_b W(b \to a) P(b) = \sum_a W(a \to b) P(a) \quad (4.8)$$

In more formal terms, we have that the stationarity condition is necessary and sufficient, hence equivalent, to the global balance condition. Instead, the detailed balance condition is just a more restrictive specific condition, sufficient for the stationarity but not necessary. The detailed balance condition corresponds to the Statistical Physics condition of equilibrium, characterized by spacial and temporal symmetries, where the last in turn corresponds to the reversibility condition of

the equilibrium dynamics. The global balance condition, in the case in which the detailed one is broken, corresponds instead to the stationary out-of-equilibrium systems.

The theoretical discussion on the relationships between detailed balance and global balance is extremely wide and in our opinion represents one of the most interesting and challenging aspects of modern Statistical Physics theory. Nevertheless, a deeper discussion on this topic goes far beyond the scope of this work. We refer in particular to Bouchaud [43], where the author discusses the implication of the relation between the two balance rules for the modeling of financial markets.

In the present work, we can motivate the decision to adopt the detailed balance condition as a way to restrict all the sources of non-equilibrium to the stochastic wandering of the herding propensity parameter κ_t. Since we are interested in the out-of-equilibrium effects deriving from a change in herding propensity κ_t of the noise traders, in turn modeling the changes in geopolitical and economical situation as in Kaizoji et al. [13], we assume the system is constantly pushed out of equilibrium solely by the parameter κ_t. The system tries always to relax to the new equilibrium imposed by that trading day value's of κ_t, but since the parameter is constantly changing the system is always out-of-equilibrium. Moreover, the choice of the detailed balance condition characterize also the definition of the transition probability in the original model introduced in Kaizoji et al. [13] and we want to keep the same structure of the original model from this point of view.

Nevertheless, to conclude this theoretical digression we point out that trying to move from the more restrictive detailed balance to the more general global balance condition can be extremely interesting (and challenging) from the point of view of modeling the extremely complex phenomena characterizing the financial markets. This could be a fruitful direction to pursue in order to push further the study of this model.

Coming back to the main speech, we stress again the fact that the probability $P(a)$ entering in expression (4.7) has to be understood as a conditional probability. Nevertheless, using the definition of conditional probability we can easily switch to the joint probabilities

$$\frac{P(b)}{P(a)} = \frac{P(s_l = b \mid \{s_1, \ldots, s_{l-1}, s_{l+1}, \ldots, s_N\})}{P(s_l = a \mid \{s_1, \ldots, s_{l-1}, s_{l+1}, \ldots, s_N\})} = \frac{\frac{P(s_l=b, \{s_1, \ldots, s_{l-1}, s_{l+1}, \ldots, s_N\})}{P(\{s_1, \ldots, s_{l-1}, s_{l+1}, \ldots, s_N\})}}{\frac{P(s_l=a, \{s_1, \ldots, s_{l-1}, s_{l+1}, \ldots, s_N\})}{P(\{s_1, \ldots, s_{l-1}, s_{l+1}, \ldots, s_N\})}}. \quad (4.9)$$

The denominators simplify and we get the ratio between the joint probabilities, which we can explicitly compute as

$$\frac{P(s_l = b, \{s_1, \ldots, s_{l-1}, s_{l+1}, \ldots, s_N\})}{P(s_l = a, \{s_1, \ldots, s_{l-1}, s_{l+1}, \ldots, s_N\})} = \frac{\frac{1}{Z} e^{-\beta(-\frac{J}{2N}\sum_{i\neq l}\sum_{j\neq l}\delta_{s_i,s_j} - \frac{J}{2N}\sum_j \delta_{s_l=b,s_j} - \frac{J}{2N}\sum_i \delta_{s_i,s_l=b} + \frac{J}{2N}\delta_{s_l=b,s_l=b} - \sum_{k=1}^q h_k(\sum_{i\neq l}\delta_{s_i,k} + \delta_{s_l=b,k}))}}{\frac{1}{Z} e^{-\beta(-\frac{J}{2N}\sum_{i\neq l}\sum_{j\neq l}\delta_{s_i,s_j} - \frac{J}{2N}\sum_j \delta_{s_l=a,s_j} - \frac{J}{2N}\sum_i \delta_{s_i,s_l=a} + \frac{J}{2N}\delta_{s_l=b,s_l=b} - \sum_{k=1}^q h_k(\sum_{i\neq l}\delta_{s_i,k} + \delta_{s_l=a,k}))}}. \tag{4.10}$$

Simplifying the common factors at numerator and denominator we get

$$\begin{aligned}\frac{P(b)}{P(a)} &= e^{-\beta(-\frac{J}{N}\sum_i \delta_{s_i,s_l=b} - \sum_{k=1}^q h_k \delta_{s_l=b,k} + \frac{J}{N}\sum_i \delta_{s_i,s_l=a} - \sum_{k=1}^q h_k \delta_{s_l=a,k})} \\ &= e^{-\beta(-\frac{J}{N}(\sum_i \delta_{s_i,s_l=b} - \sum_i \delta_{s_i,s_l=a}) - (h_b - h_a))} \\ &= e^{\beta(J\frac{\sum_i \delta_{s_i,s_l=b} - \sum_i \delta_{s_i,s_l=a}}{N} + h_b - h_a)}. \end{aligned} \tag{4.11}$$

Now we set $J = 1$, as a remark we note that in order to have a meaningful mean-field assumption we need that all spins interact with the same strength $J = const$. Doing that we effectively drop the topology of the graph representing the interaction between the spins, i.e. the traders. If in the future different interactions strength between the traders, i.e. a non-uniform social imitation strength, will be investigated, it will be necessary to derive the transition rates in a different way, being the mean-field assumption no more justified.

Now we identify the inverse temperature with the herding propensity $\beta = \kappa_t$, as we have done for the original model, and the external field intensities with the corresponding price momenta $h_k = H_k$. Moreover, $\sum_i \delta_{s_i,s_l=a} = N_a$ represents the number of spins in state a, i.e. the number of traders holding the asset a. Here becomes also clear why we had to consider also the self interaction in the Potts model. We then finally get

$$\frac{W(a \to b)}{W(b \to a)} = \frac{P(b)}{P(a)} = e^{\kappa_t(\frac{N_b - N_a}{N} + H_b - H_a)}. \tag{4.12}$$

Now to get the transition rates we have different possibilities. We could use the standard Metropolis-Hastings rule, presented in an historical work by Metropolis et al. [44], i.e. we assume that the transition rate is composed by a move proposal probability $\mathcal{P}$ and a move acceptance probability $\mathcal{A}$

$$W(a \to b) = \mathcal{P}(a \to b)\mathcal{A}(a \to b) \tag{4.13}$$

and assuming the move proposal probability to be uniform on the arrival states, we get from the Metropolis rule

$$\mathcal{A}(a \to b) = min\left\{1, \frac{P(b)\mathcal{P}(b \to a)}{P(a)\mathcal{P}(a \to b)}\right\} = min\left\{1, \frac{P(b)}{P(a)}\right\} \tag{4.14}$$

where in the last equality we have simplified the two uniform probabilities. In our case we get

$$\mathcal{A}(a \to b) = \begin{cases} 1 & \text{if } (\frac{N_b - N_a}{N} + H_b - H_a) > 0 \\ e^{\kappa_t(\frac{N_b - N_a}{N} + H_b - H_a)} & \text{otherwise} \end{cases} \tag{4.15}$$

This would work but it is clearly a very bad modeling of the real actions of the traders, indeed (4.14) and (4.15) define a dynamics where at each time step, each noise trader chooses at random a new asset to switch to and its trade decision is arbitrarily accepted or rejected according to a probability $\mathcal{A}(a \to b)$. For this reason this choice will be discarded.

To construct more realistic dynamics, we need a rejection-less MCMC. Indeed, imposing

$$\mathcal{A}(a \to b) = \mathcal{A}(b \to a) = 1 \tag{4.16}$$

we get

$$min\left\{1, \frac{P(b)\mathcal{P}(b \to a)}{P(a)\mathcal{P}(a \to b)}\right\} = 1 \tag{4.17}$$

from which follows

$$\frac{\mathcal{P}(a \to b)}{\mathcal{P}(b \to a)} = \frac{P(b)}{P(a)} = e^{\kappa_t(\frac{N_b - N_a}{N} + H_b - H_a)}. \tag{4.18}$$

This condition is satisfied, for example, setting

$$\mathcal{P}(a \to b) = e^{\frac{1}{2}\kappa_t(\frac{N_b - N_a}{N} + H_b - H_a)}. \tag{4.19}$$

In this way, we have obtained rejection-less and more realistic moves. From the theory of Markov Chain Monte Carlo, we know that our Markov chain will correctly simulate the dynamics of our Potts model if it satisfies three conditions, i.e. ergodicity, aperiodicity, and respect of probability axioms. The first two descend directly from the method we used to construct the move probabilities. For the third, we already have non-negative transition rates, we have only to ensure that they are correctly normalized to one, that they are indeed well-defined transition

probabilities. We know that a Markov chain is completely determined by its transition matrix T. In our case, it takes the form

$$T = \begin{pmatrix} \mathcal{P}(1 \to 1) & \mathcal{P}(1 \to 2) & \dots & \mathcal{P}(1 \to q) \\ \dots & \dots & \dots & \dots \\ \mathcal{P}(q \to 1) & \mathcal{P}(q \to 2) & \dots & \mathcal{P}(q \to q) \end{pmatrix} \tag{4.20}$$

hence we need to have a matrix normalized by row, ensuring it is a well defined stochastic matrix. The normalization procedure however introduce new terms in the detailed balance condition which have to be taken into account. Indeed, we have

$$\frac{W(a \to b)}{W(b \to a)} = \frac{\mathcal{P}(a \to b)}{\mathcal{P}(b \to a)} = \frac{\frac{1}{Z_1} e^{\frac{1}{2}\kappa_t(\frac{N_b - N_a}{N} + H_b - H_a)}}{\frac{1}{Z_2} e^{\frac{1}{2}\kappa_t(\frac{N_a - N_b}{N} + H_a - H_b)}}, \tag{4.21}$$

where

$$Z_1 = \sum_{k=1}^{q} e^{\frac{\kappa_t}{2}(\frac{N_k - N_a}{N} + H_k - H_a)} \tag{4.22}$$

and

$$Z_2 = \sum_{k=1}^{q} e^{\frac{\kappa_t}{2}(\frac{N_k - N_b}{N} + H_k - H_b)} \tag{4.23}$$

Being Z_1 and Z_2 different, the detailed balance condition is no longer satisfied. Nevertheless, the solution is readily found. We collect from the Z_1 sum a term $e^{\frac{1}{2}\kappa_t(-\frac{N_a}{N} - H_a)}$ common to all the addends and we simplify it with the same term present at the numerator. In an analogous way, we collect from Z_2 a term $e^{\frac{1}{2}\kappa_t(-\frac{N_b}{N} - H_b)}$ and we simplify it. We then get

$$\frac{W(a \to b)}{W(b \to a)} = \frac{\frac{1}{c} e^{\frac{1}{2}\kappa_t(\frac{N_b}{N} + H_b)}}{\frac{1}{c} e^{\frac{1}{2}\kappa_t(\frac{N_a}{N} + H_a)}} = e^{\frac{\kappa_t}{2}(\frac{N_b - N_a}{N} + H_b - H_a)}. \tag{4.24}$$

Unexpectedly the β-like term results halved. This would lead to a doubled critical value of the kappa process in the simulation. The problem is easily solved multiplying by 2 the β-like term.

Doing that we finally get the following transition probability

$$W(a \to b) = \mathcal{P}(a \to b) = \frac{e^{\kappa_t(\frac{N_b - N_a}{N} + H_b - H_a)}}{\sum_{k=1}^{q} e^{\kappa_t(\frac{N_k - N_a}{N} + H_k - H_a)}}. \tag{4.25}$$

Interestingly, $\mathcal{P}(a \to b)$ defines a probability distribution over the arrival states which coincides with the Logit probability distribution. This is once again an example of the connection between the discrete choices models and Ising-like models in modeling social systems, as pointed out in Sornette [12].

The Decision Theory framework: the Logit probability distribution and the transition probabilities

The Logit model of discrete choices has many interesting properties. McFadden has shown in McFadden [45], that the Logit probability distribution actually models individuals who maximize a utility function which has an implicit random idiosyncratic part. Indeed, if each agent makes its choice maximizing

$$s^* = \arg\max_s \{\beta u_s + \eta_s\}, \tag{4.26}$$

where s represents the possible choices, u_s is the deterministic part of the utility function, η_s is a random variable and β plays the role of the inverse temperature, McFadden proved that $P(s^* = s)$ coincides with the Logit distribution if the random variable η_s is distributed according to the Gumbel distribution, with cumulative distribution function

$$F_\eta(x) = e^{-e^{-\frac{x-\mu}{\lambda}}}. \tag{4.27}$$

The choice of the Gumbel distribution is unique in that it leads to the Logit model which satisfies the axiom of independence from irrelevant alternatives. The Logit model has many other interesting properties, but a deeper analysis goes beyond the scope of this thesis.

Having established the equivalence between the transition rates characterizing the noise traders' investment strategy and the Logit distribution we have unveiled the bridge between the present Ising-like model of the noise traders and the framework of Decision Theory in which we can understand the decision process undertaken by each agent. In light of this, all the modeling of the noise traders class can be understood starting from the "micro" stochastic decision process of each noise investor. In particular, in formula (4.26) it is clear how the parameter β which corresponds to the herding propensity κ_t governs the relative importance of the deterministic part of the utility function common to all the traders, hence pushing the traders to polarize towards the same investments, with respect to the random part modeled by the Gumbel distribution representing the importance of the idiosyncratic opinion of each individual. From this decision theory's point of view, the meaning of the herding propensity parameter and the transition between disordered states and a polarized state takes all its meaning.

The properties of the transition probabilities

We comment also on the fact that the transition probabilities (4.25) have another important property, indeed simplifying a common term at numerator and

denominator $e^{\frac{1}{2}\kappa_t(-\frac{N_a}{N}-H_a)}$ we get

$$\mathcal{P}(a \to b) = \frac{e^{\kappa_t(\frac{N_b-N_a}{N}+H_b-H_a)}}{\sum_{k=1}^{q} e^{\kappa_t(\frac{N_k-N_a}{N}+H_k-H_a)}} = \frac{e^{\kappa_t(\frac{N_b}{N}+H_b)}}{\sum_{k=1}^{q} e^{\kappa_t(\frac{N_k}{N}+H_k)}}. \tag{4.28}$$

Remarkably, the transition probability from state a to state b is independent of the initial state a. This could be surprising from a modelistic point of view, but it is actually a typical property of mean-field models and is ultimately connected to the fact that each traders interacts with all the others in the same way ($J = 1$) and that the number of interacting agents is large ($N \gg 1$).

Summarizing, at each time step, i.e. trading day, each noise trader decides to hold its asset or to buy another one according to the probability distribution (4.25) defined over the assets.

It is important to notice that the probability distribution is updated only at the end of the trading day after all the traders have made their decisions, hence each trader decides based on the investment decisions of all the other traders of the previous day. This is motivated from a modeling point of view, but it introduces a problem from a theoretical point of view that needs to be discussed.

Usually, the Markov Chain Monte Carlo used for simulating spin systems proceeds to select one spin or one cluster of spins at random, proposing a move according to a certain proposal probability and then accepting or rejecting the move according to a certain acceptance probability. After each move, all the quantities are then updated according to the new configuration of the system.

The simulation algorithm here proposed is different for at least two reasons. The first is that at each time step all the spins are sequentially updated, so there is not a random choice of the spin to update and the second is that the quantities entering in the transition probabilities are updated only after all the spins have been updated.

The first issue can be understood and the consistency of the method can be proved in the framework of the Gibbs sampling. In this framework, it can be proved that if each component of the vector of spins defining the state of the system is updated sequentially, according to the conditional probability of that spin conditioned to all the others, the Markov chain defined by the full vector of spins considered after all the updates have taken place is correctly sampling the joint probability distribution.

In formulas, given a vector state of spins $(s_1, \ldots, s_{l-1}, s_l, s_{l+1}, \ldots, s_N)$, if at each time step t all the components of the vector are updated, sampling each spin s_l from the conditional probability $P(s_l \mid \{s_1^t, \ldots, s_{l-1}^t, s_{l+1}^{t-1}, \ldots, s_N^{t-1}\})$, then the full vector of updated spins $(s_1^t, \ldots, s_{l-1}^t, s_l^t, s_{l+1}^t, \ldots, s_N^t)$ represents the state at time t of a Markov chain which is correctly sampling the statistical model defined by P, i.e. correctly simulating its dynamics. The key point is that the conditional

probabilities must be updated after each single spin flip as underlined by the time superscripts. This is connected to the second point aforementioned, indeed in our simulation algorithm we are updating the probabilities only at the end of the trading day. Eventually, the method's consistency is assured by the mean-field assumption which allows us to drop the dependence on all the other spins in the conditional probability. This relies on the asymptotic equivalence for $N \to +\infty$ of the fully connected and mean-field Potts models and on the fact that we are indeed in the large N regime.

The average holding time

In this paragraph, we comment on the fact that the dynamics defined by the transition rates (4.25) could lead to an excessively oscillating behavior, where the noise traders change asset at an unrealistically high rate, too far from real markets behavior. For example, discarding for a moment the herding behavior, i.e. setting $\kappa_t = 0$, we would get a probability to hold the asset from one trading day to the next one of $\mathcal{P}(a \to a) = \frac{1}{q}$, which for a large number of assets $q \gg 1$ leads to unrealistic market behavior.

Moreover, in the present implementation, we lack a parameter allowing us to tune the average propensity of each noise trader to hold its asset instead of changing it.

To introduce the holding propensity parameter t_h, we have to break the detailed balance condition, yet in the following, we show that we can quantify the error introduced, proving it is negligible in the not-polarized phase, i.e ordinary regime, but not negligible, yet determinant in the bubble regime when the class becomes polarized.

Indeed, we multiply the holding probability by a constant, chosen to have an average holding time in absence of herding propensity, $\kappa_t = 0$, roughly equals to t_h trading days, where t_h represents the holding propensity parameter. The constant is readily found from

$$t_h = \frac{1}{1 - \mathcal{P}(a \to a)|_{\kappa_t = 0}}, \tag{4.29}$$

from which

$$\mathcal{P}(a \to a)|_{\kappa_t = 0} = 1 - \frac{1}{t_h}, \tag{4.30}$$

hence, using equation (4.28), we get

$$\frac{c}{\sum_{\substack{k=1 \\ k \neq a}}^{q} e^0 + ce^0} = 1 - \frac{1}{t_h}, \tag{4.31}$$

finally

$$c = (t_h - 1)N_{stocks}. \tag{4.32}$$

Inserting this new constant, the transition probabilities change to

$$\mathcal{P}(a \to b) = \frac{(1 + \delta_{a,b}(c-1))e^{\kappa_t(\frac{N_b - N_a}{N} + H_b - H_a)}}{\sum_{k=1}^{q}(1 + \delta_{k,a}(c-1))e^{\kappa_t(\frac{N_k - N_a}{N} + H_k - H_a)}}. \tag{4.33}$$

It follows that the detailed balance condition modifies to

$$\frac{W(a \to b)}{W(b \to a)} = \frac{\mathcal{P}(a \to b)}{\mathcal{P}(b \to a)} = \frac{\frac{(1+\delta_{a,b}(c-1))e^{\kappa_t(\frac{N_b - N_a}{N} + H_b - H_a)}}{\sum_{k=1}^{q}(1+\delta_{k,a}(c-1))e^{\kappa_t(\frac{N_k - N_a}{N} + H_k - H_a)}}}{\frac{(1+\delta_{b,a}(c-1))e^{\kappa_t(\frac{N_a - N_b}{N} + H_a - H_b)}}{\sum_{j=1}^{q}(1+\delta_{j,b}(c-1))e^{\kappa_t(\frac{N_j - N_b}{N} + H_j - H_b)}}}. \tag{4.34}$$

Simplifying the common terms we get

$$\begin{aligned}\frac{W(a \to b)}{W(b \to a)} &= e^{\frac{\kappa_t}{2}(\frac{N_b - N_a}{N} + H_b - H_a)} \frac{\sum_{k=1}^{q}(1 + \delta_{k,a}(c-1))e^{\kappa_t(\frac{N_k}{N} + H_k)}}{\sum_{j=1}^{q}(1 + \delta_{j,b}(c-1))e^{\kappa_t(\frac{N_j}{N} + H_j)}} \\ &= e^{\frac{\kappa_t}{2}(\frac{N_b - N_a}{N} + H_b - H_a)} \frac{x + (c-1)e^{\kappa_t(\frac{N_a}{N} + H_a)}}{x + (c-1)e^{\kappa_t(\frac{N_b}{N} + H_b)}},\end{aligned} \tag{4.35}$$

where in x are collected all the addends in common between numerator and denominator. It is clear that if $c = 1$, i.e. holding probability not tuned, the detailed balance is exactly satisfied. Instead, if we increase the holding probability, $c = (t_h - 1)N_{stocks} > 1$, we introduce an error

$$Error_{a,b} = 1 - \frac{x + (c-1)e^{\kappa_t(\frac{N_a}{N} + H_a)}}{x + (c-1)e^{\kappa_t(\frac{N_b}{N} + H_b)}}. \tag{4.36}$$

The errors depend only on the differences

$$\frac{N_a - N_b}{N} + H_a - H_b \tag{4.37}$$

where (a, b) varies among all the possible couples of assets. Moreover, the errors vanishes (exponentially fast) at the disordered configuration of the noise traders class, where on average $\frac{N_a}{N} \approx \frac{N}{q}$, $H_a \approx H \ \forall a$. Yet, the impact of the errors are not negligible in the ordered configuration characterizing the bubble regimes.

As a last remark, we notice that this approximation is equivalent, for the error neglected, to considering the linearized transition probabilities in the original

model by Kaizoji et al. [13]. However, at odds with the original model the present implementation appears extremely susceptible to the holding propensity parameter t_h, giving unrealistic simulation results for values around the original model one, $t_h = 10$.

4.1.3 Time series description

In this section, we introduce the parameters used for the simulations and we comment on the qualitative behavior of the resulting time series.

Choice of parameters

In 4.1 are present some of the parameters maintained fixed throughout all the subsequent analysis.

	Parameters	
Assets	$q = n + 1 = 5$	$r_f = 4 \times 10^{-5}$
	$r_{d,i} = 1.6 \times 10^{-4}\ \forall i$	$d_{i,0} = 1.6 \times 10^{-4}\ \forall i$
	$P_{i,0} = 1\ \forall i$	$\Sigma^d_{i,i} = 1.6 \times 10^{-5}\ \forall i$
Fundamentalist traders	$W^f_0 = 10^9$	$E_{r,i} = 1.6 \times 10^{-4}\ \forall i$
	$\Sigma^f_{i,i} = 0.0004\ \forall i$	
Noise traders	$W^n_0 = 10^9$	$N_n = 1000$
	$\theta = 0.95$	$H_{i,0} = 1.6 \times 10^{-4}\ \forall i$

Table 4.1: Set of parameters for the simulations of the extended model endowed with a Potts-like noise traders class. Their values constitute the natural generalization of the original models' one being motivated by real markets data and are mainly taken from Westphal and Sornette [18].

In all the subsequent simulations no correlation among the dividend processes for different risky assets is assumed, even if the code is implemented to consider also the possibility of correlated dividend processes.

Regarding the fundamentalist traders, following what we did for the dividends processes, the expected covariance matrix is implemented into a vector of expected variances and a matrix of expected correlations, in order to be able to change the variances and the correlations in an independent and easier way. In the following simulations, the variances are as in the table

$$\Sigma^f_{i,i} = 0.0004 \quad i = 1, \ldots, 4 \tag{4.38}$$

and the correlation matrix is set equal to

$$C^f = \begin{pmatrix} 1.0 & 0.5 & 0.0 & 0.0 \\ 0.5 & 1.0 & 0.0 & 0.0 \\ 0.0 & 0.0 & 1.0 & 0.0 \\ 0.0 & 0.0 & 0.0 & 1.0 \end{pmatrix} \tag{4.39}$$

in order to analyze the impact on the market of a non-zero expected correlation between two assets.

The correlation matrix C^f and the covariance matrix Σ^f are connected by the relation

$$C^f = (diag(\Sigma^f))^{-\frac{1}{2}} \Sigma^f (diag(\Sigma^f))^{-\frac{1}{2}}, \tag{4.40}$$

where $diag(\Sigma^f)$ represents the diagonal matrix of the variances.

The initial investment decisions for fundamentalist and noise traders are as follows

$$\vec{x}_0^f = (0.075,0.075,0.075,0.075,0.7) \tag{4.41}$$

$$\vec{x}_0^n = (0.2,0.2,0.2,0.2,0.2), \tag{4.42}$$

where the last component represents the unique risk-free fraction while the others stand for the $n = 4$ risky assets.

The kappa process properties are instead varied among the two different simulations and presented in the following.

The time series

In this section we present the time series from two different simulations. The first with an Ornstein-Uhlenbeck kappa process defined by

$$\kappa_t - \kappa_{t-1} = \eta(\mu_k - \kappa_{t-1}) + \sigma_k v_t, \tag{4.43}$$

with mean reversion level $\mu_k = 0.98\beta_c$, where β_c represents the theoretical value for the critical inverse temperature of the mean-field q-state Potts model

$$\beta_c = \frac{2(q-1)}{q-2} \log(q-1). \tag{4.44}$$

Which, in our case of $q = 5$, specifies to

$$\beta_c = \frac{2(5-1)}{5-2} \log(5-1) \approx 3.697. \tag{4.45}$$

Moreover, the mean reversion speed η and the step size σ_k are set, as in the original model by Kaizoji et al. [13], such that the Ornstein–Uhlenbeck process has a

standard deviation of $0.1\beta_c$ and a deviation of κ_t two standard deviations above μ_k in the super-critical regime will revert within $\Delta T = 20$, i.e.

$$\eta = \frac{1}{\Delta T} \log \left(\frac{\mu_k + 0.2\beta_c - \mu_k}{\beta_c - \mu_k} \right) \tag{4.46}$$

and

$$\sigma_k = 0.1\beta_c \sqrt{2\eta}. \tag{4.47}$$

The second simulation instead is characterized by a constant kappa in the critical phase

$$\kappa = 3.9 > \beta_c \approx 3.697. \tag{4.48}$$

The resulting time series presents noticeably unexpected features and are presented in figures 4.1, 4.2, 4.3, 4.4, 4.5, 4.6 and 4.7.

The two simulations are characterized by a set of parameters very close to the original model ones, yet the time series are very different and they are very far from the real market behavior. Different sets of parameters produce a more realistic time series but the present ones are useful to explore the key limits of the Potts model. First of all, the exaggerated oscillating behavior of the time series comes from the fact that the probability $P(a \to a)$ to hold the asset is not magnified at all. Nevertheless, this is not the main point, since the behavior can be smoothed multiplying a constant to $P(a \to a)$ as we have previously shown. We have also to stress again that, at odds with the original model, the present implementation appears extremely susceptible to the holding propensity parameter t_h, which for the simulation presented is set equal to one.

Besides the exaggerated oscillating behavior, two main problems emerge. The first is the abrupt change of regime characterizing the bubbles. The second is the unexpected persistence of the ordered (disordered) phase when κ_t exits (enters) the critical region.

The second problem is hardly visible at first sight in the Ornstein-Uhlenbeck kappa process simulation but is evident in the constant kappa simulation, where for a $\kappa_t = 3.9$ above the critical value $\kappa_c \approx 3.697$ the disordered phase persist throughout the simulation. To address these two problems we proceed with a linear stability analysis of the mean value dynamical equations, which is developed in the next subsection.

4.1.4 The mean value dynamical equations approach

In this section, we try to gain insight into the emergence of bubbles studying the dynamical equations of the mean value of the number of noise traders investing

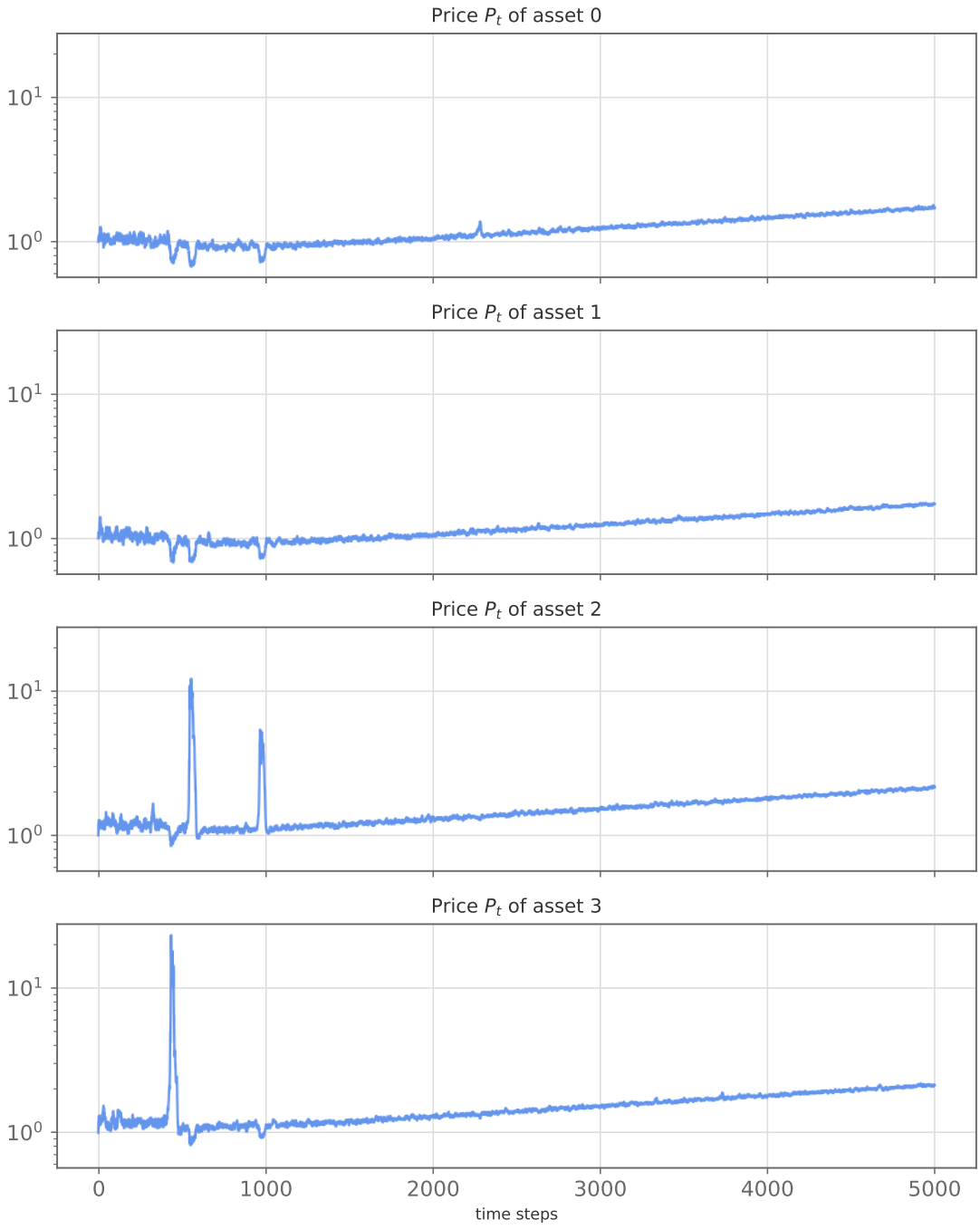

Figure 4.1: Ornstein-Uhlenbeck kappa simulation. The figure shows the time series of the four prices. Three bubbles are clearly identifiable as the peaks in the prices 2 and 3.

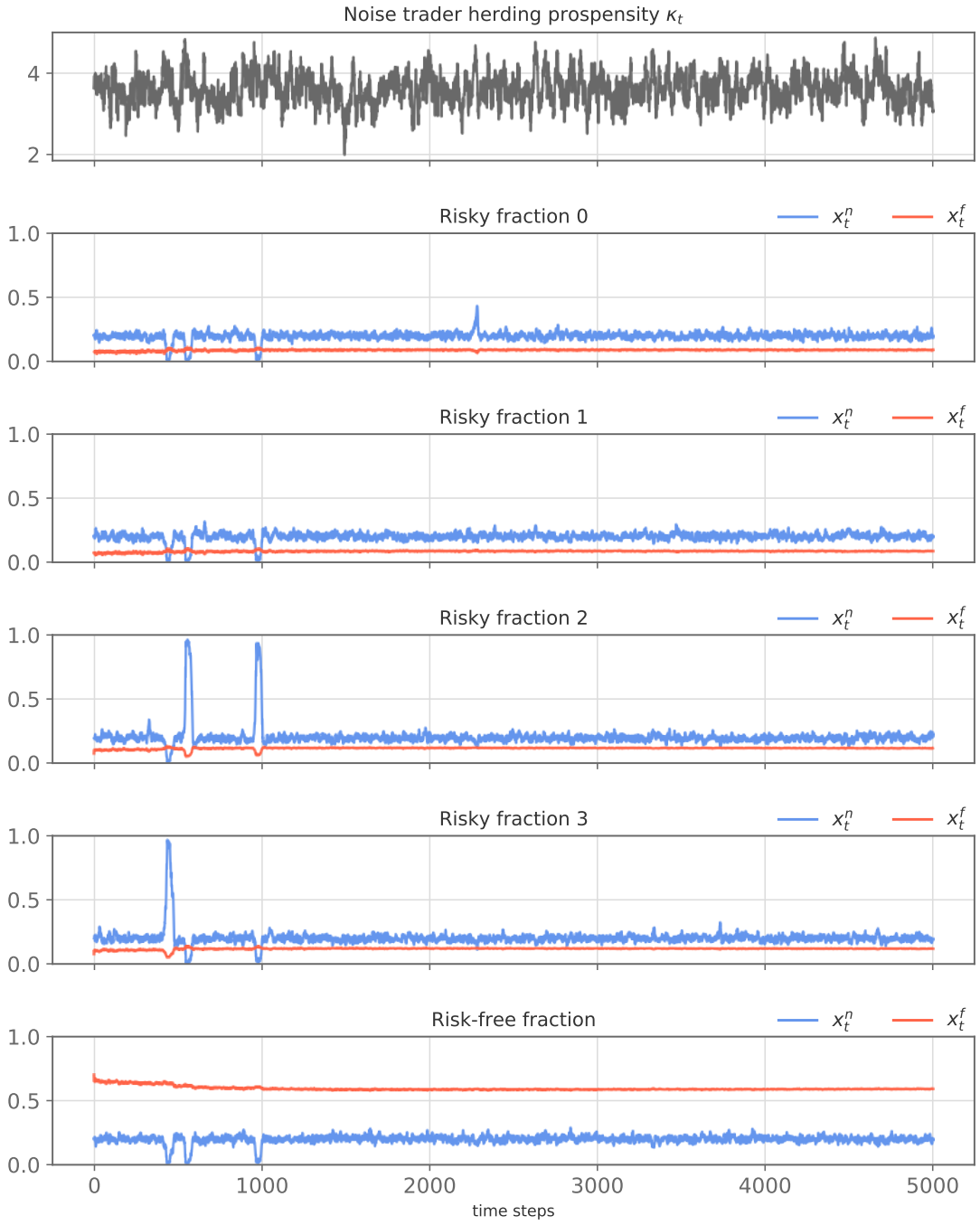

Figure 4.2: Ornstein-Uhlenbeck kappa simulation. The figure shows the time series of the Ornstein-Uhlenbeck kappa process and the time series of both the four risky fractions and the risk-free fraction of the noise traders class at the aggregate level.

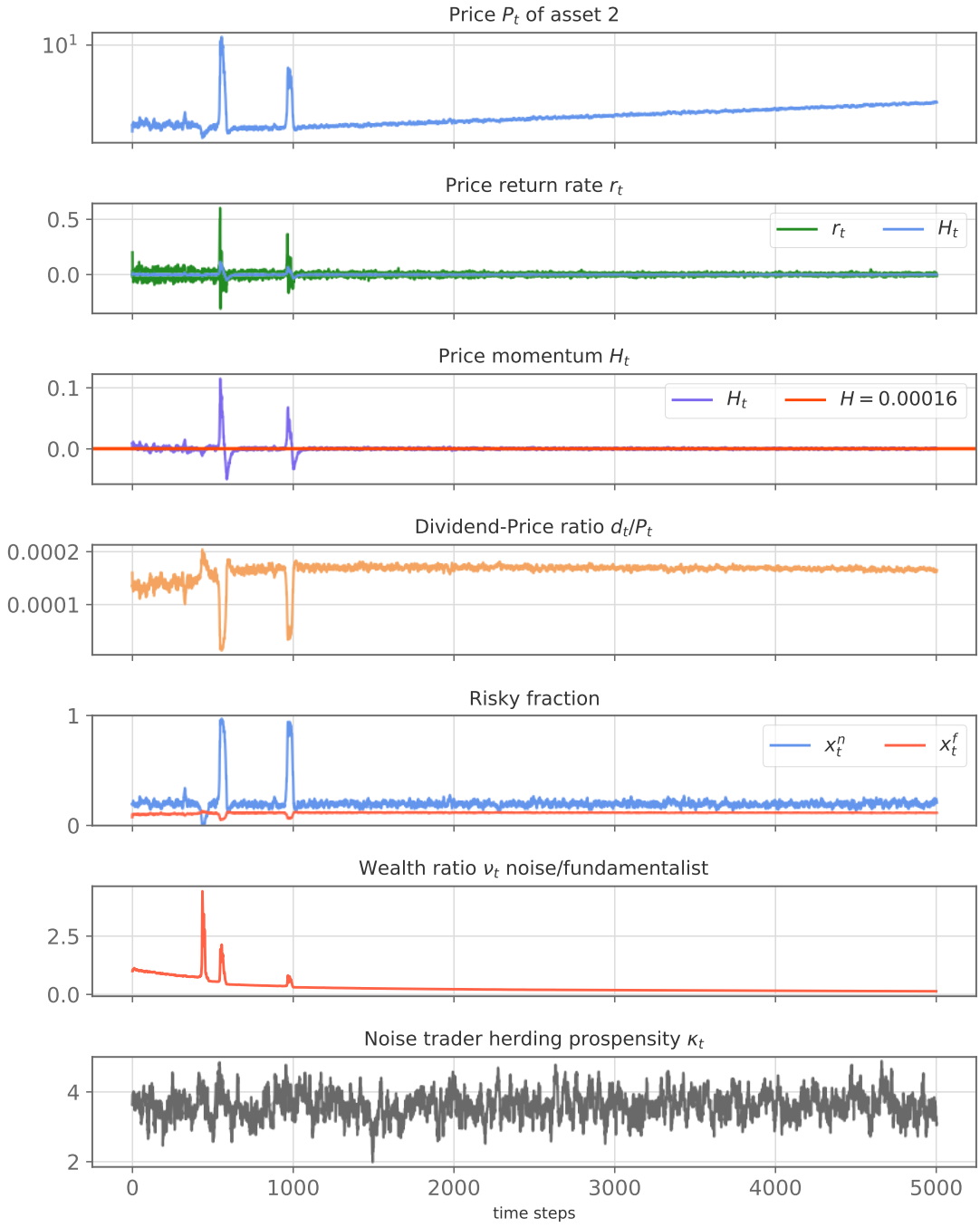

Figure 4.3: Ornstein-Uhlenbeck kappa simulation. The figure shows the detailed time series characterizing the risky asset 2. Two bubbles are clearly identifiable.

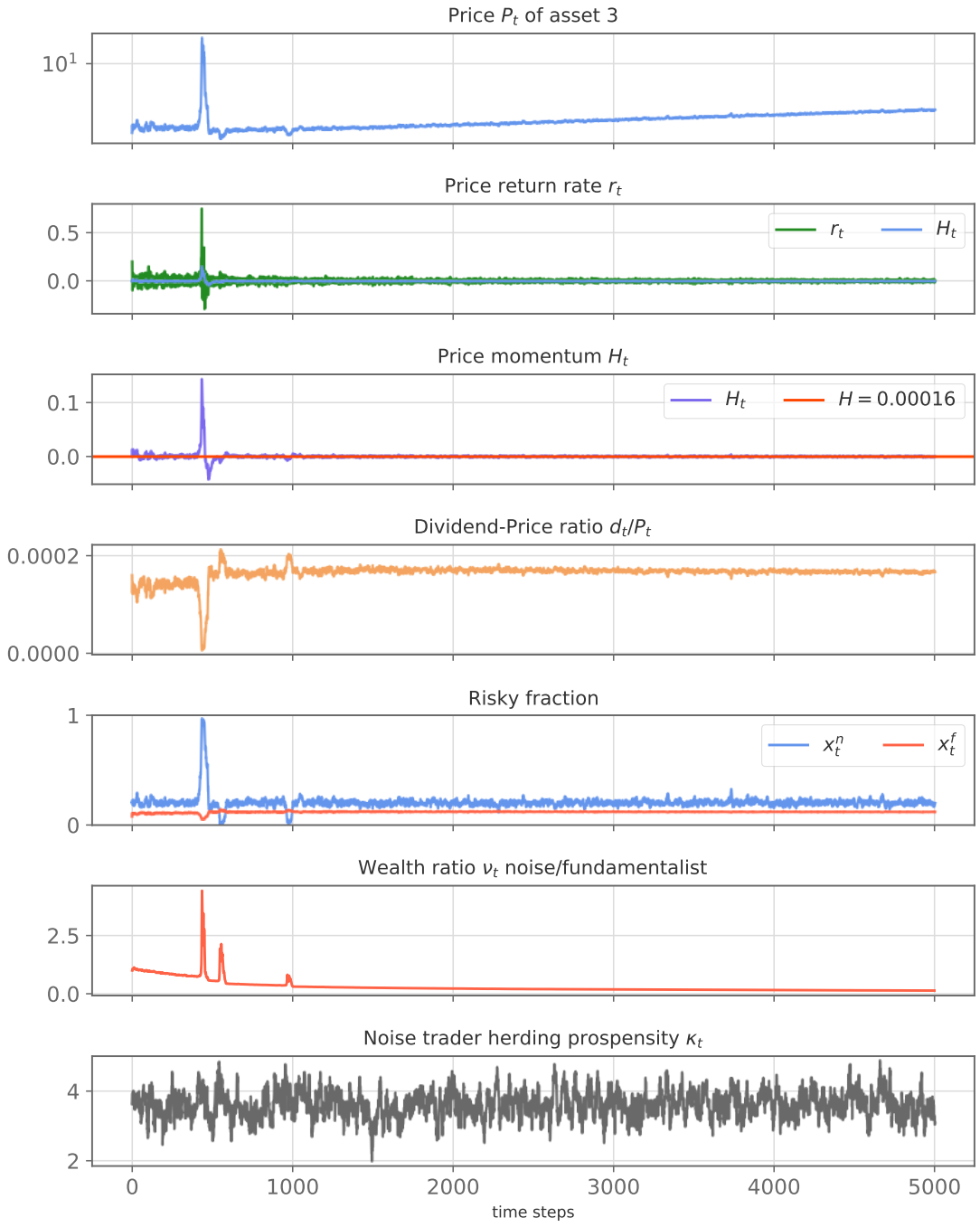

Figure 4.4: Ornstein-Uhlenbeck kappa simulation. The figure shows the detailed time series characterizing the risky asset 3. One bubble is recognizable at the beginning of the simulation.

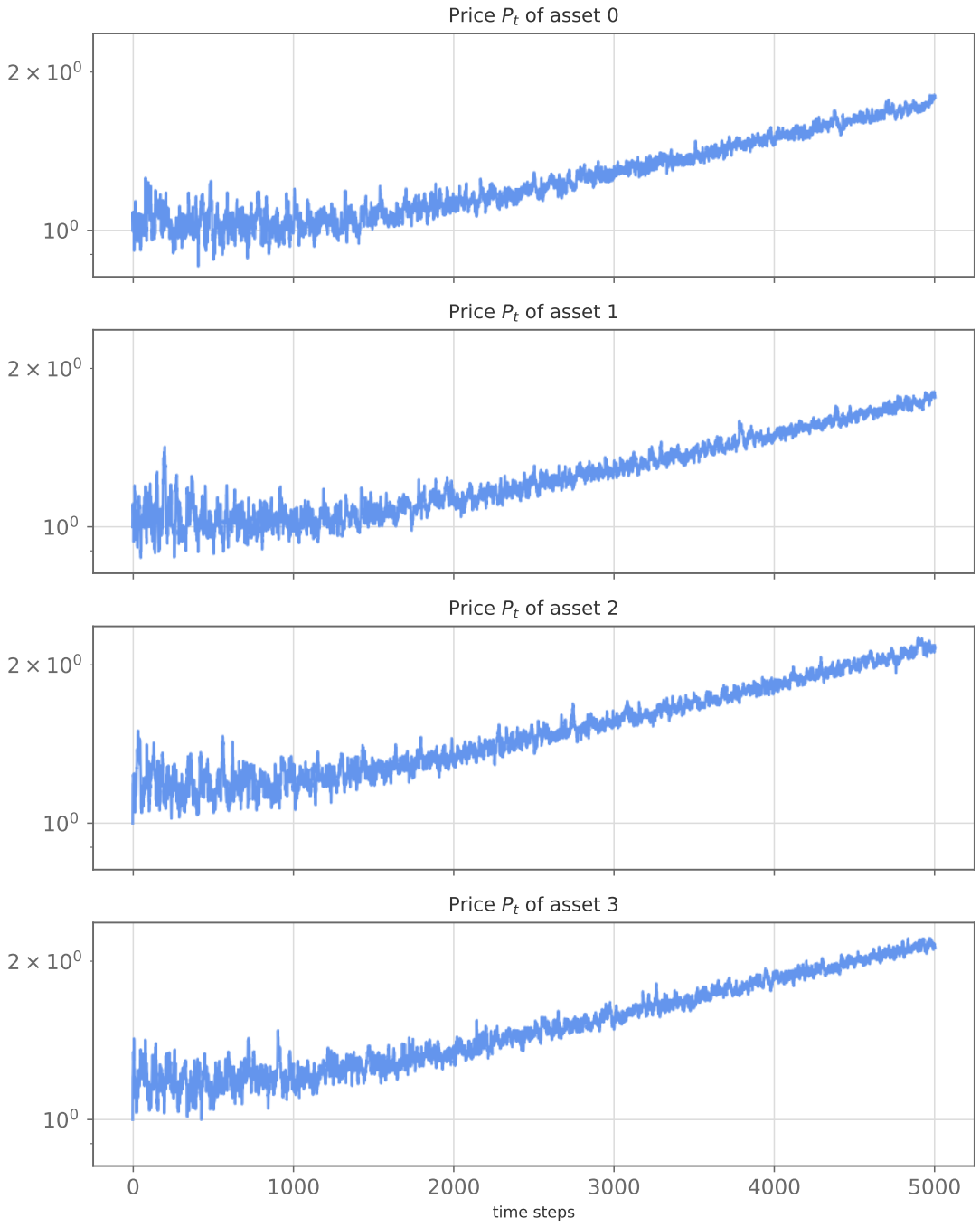

Figure 4.5: Constant kappa simulation. The figure shows the time series of the four prices. Remarkably, even if the noise traders class should be in the ordered regime, since $\kappa = 3.9 > \beta_c$, there are no signs of bubbles.

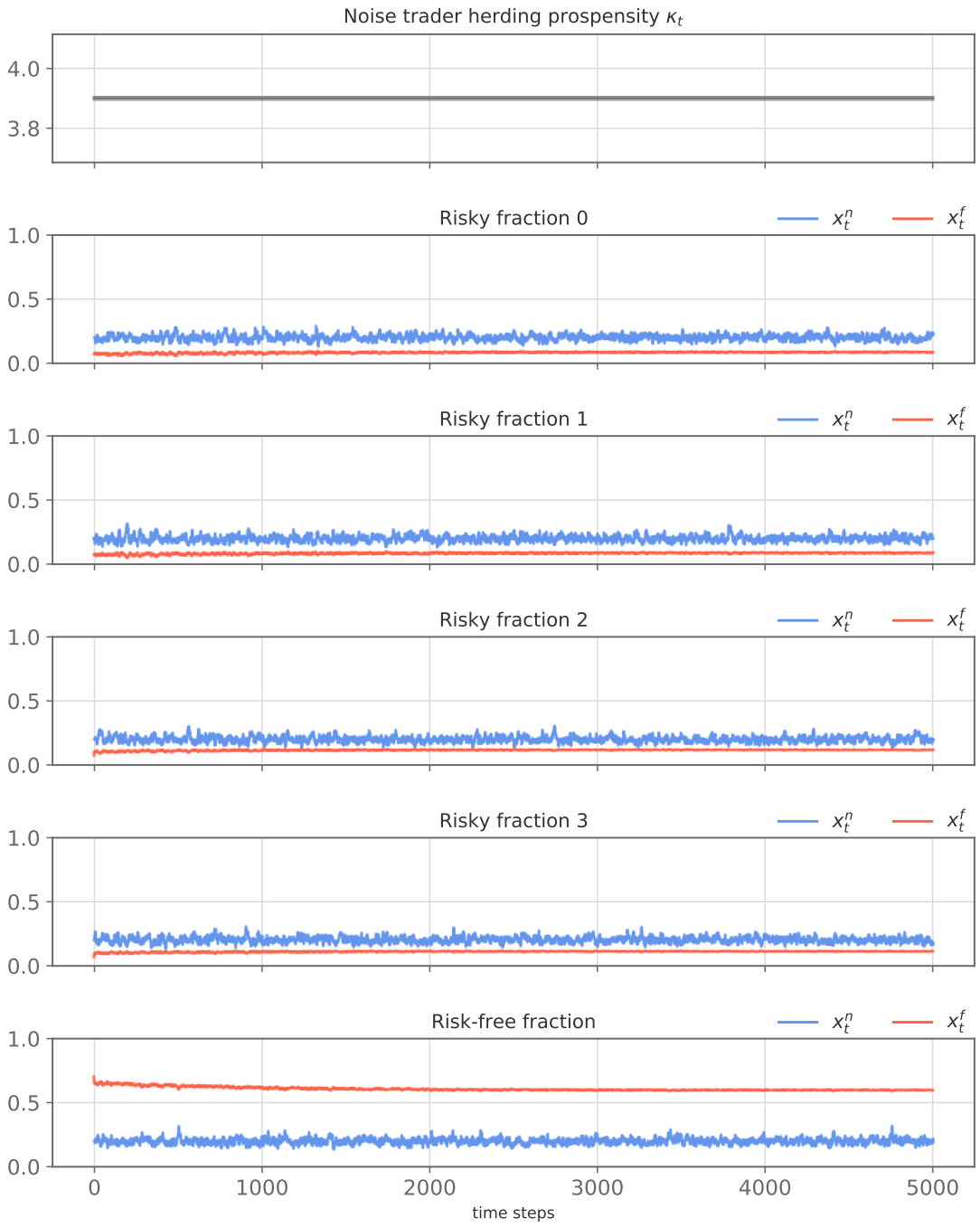

Figure 4.6: Constant kappa simulation. The figure shows the time series of both the four risky fractions and the risk-free fraction of the noise traders class at the aggregate level. Remarkably, even if the noise traders class should be in the ordered regime, since $\kappa = 3.9 > \beta_c$, there are no signs of bubbles

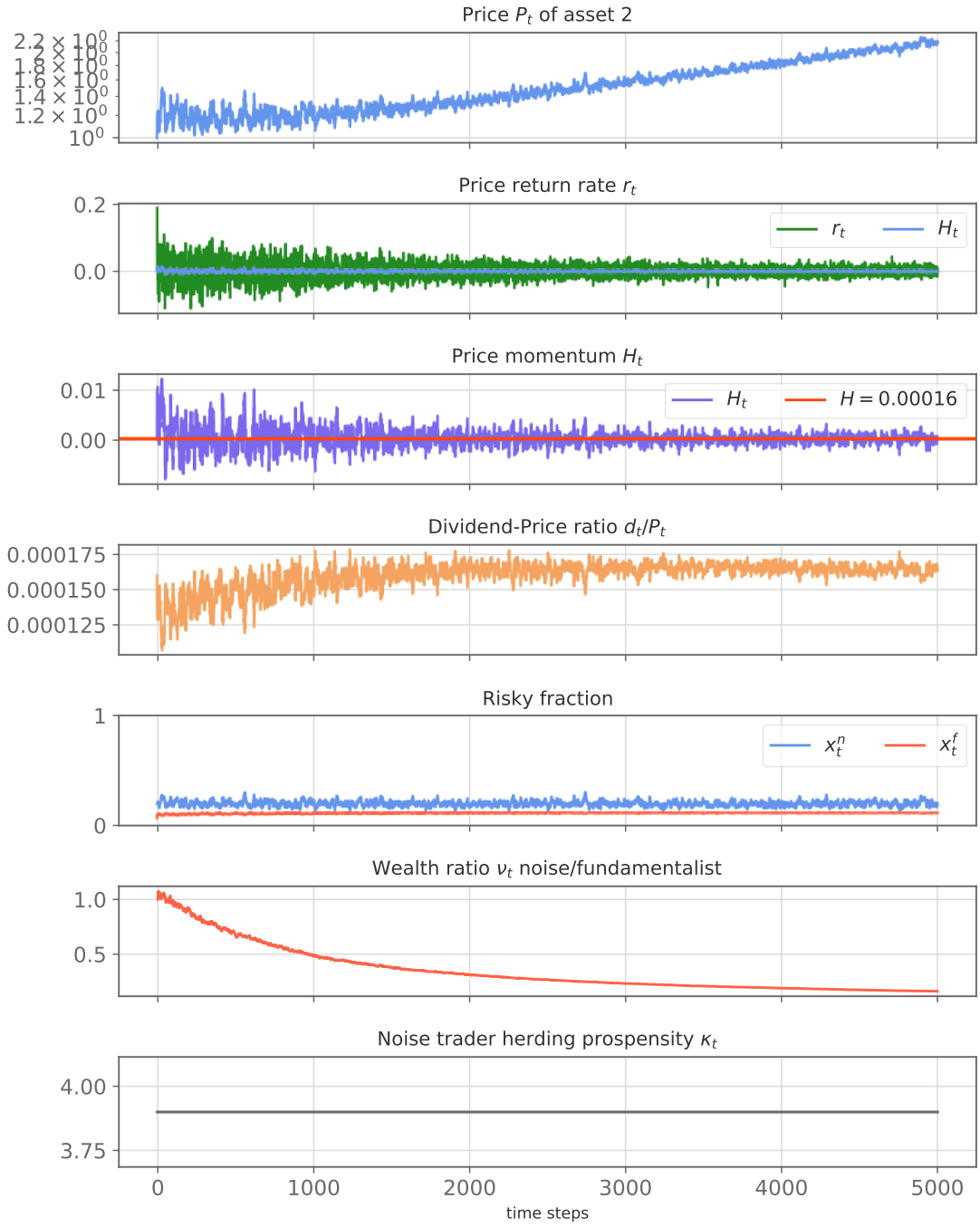

Figure 4.7: Constant kappa simulation. The figure shows the detailed time series characterizing the risky asset 2. No bubble is present.

in each asset. To derive the set of differential equations, we first define the mean value of the number of noise traders investing in the asset a

$$n_a = \left\langle \sum_{i=1}^{N} \delta_{s_i,a} \right\rangle. \tag{4.49}$$

The average value of each Kronecker delta function reads

$$\langle \delta_{s_i,a} \rangle = P(s_i = a, t) = P(s_i = a \mid \{s_1, \ldots, s_{i-1}, s_{i+1}, \ldots, s_N\}, t), \tag{4.50}$$

where in the last step we used again the crucial mean-field assumption. Since we know the time evolution of the conditional probability through the Master Equation we can write

$$\begin{aligned}
\frac{dn_a}{dt} &= \sum_{i=1}^{N} \frac{d}{dt} P(s_i = a \mid \{s_1, \ldots, s_{i-1}, s_{i+1}, \ldots, s_N\}, t) \\
&= \sum_{i=1}^{N} \Bigg(\sum_{\substack{b=1 \\ b\neq a}}^{q} W(b \to a) P(s_l = b \mid \{s_1, \ldots, s_{l-1}, s_{l+1}, \ldots, s_N\}, t) \\
&\quad - W(a \to b) P(s_l = a \mid \{s_1, \ldots, s_{l-1}, s_{l+1}, \ldots, s_N\}, t) \Bigg) \\
&= \sum_{\substack{b=1 \\ b\neq a}}^{q} W(b \to a) \sum_{i=1}^{N} P(s_l = b \mid \{s_1, \ldots, s_{l-1}, s_{l+1}, \ldots, s_N\}, t) \\
&\quad - \sum_{\substack{b=1 \\ b\neq a}}^{q} W(a \to b) \sum_{i=1}^{N} P(s_l = a \mid \{s_1, \ldots, s_{l-1}, s_{l+1}, \ldots, s_N\}, t).
\end{aligned} \tag{4.51}$$

Identifying the mean values n_a and n_b we finally get the mean value dynamical equation

$$\frac{dn_a}{dt} = \sum_{\substack{b=1 \\ b\neq a}}^{q} \Big(W(b \to a) n_b - W(a \to b) n_a \Big). \tag{4.52}$$

Actually we have a system of q mean value dynamical equations one for each asset. Substituting the expression (4.25) for the transition probabilities we get

$$\frac{dn_a}{dt} = \sum_{\substack{b=1 \\ b\neq a}}^{q} \left(\frac{1}{Z_b} e^{\kappa_t (\frac{n_a - n_b}{N} + H_a - H_b)} n_b - \frac{1}{Z_a} e^{\kappa_t (\frac{n_b - n_a}{N} + H_b - H_a)} n_a \right) \quad a = 1, \ldots, q, \tag{4.53}$$

where the transition probabilities are written in terms of the mean values and Z_b and Z_a are the normalisation constants. We use two different indices for them to underline they are different.

Equation (4.53) can be rewritten, simplifying the common terms at numerator and denominator, as

$$\frac{dn_a}{dt} = \sum_{\substack{b=1 \\ b\neq a}}^{q} \left(\frac{e^{\kappa_t(\frac{n_a}{N}+H_a)}}{\sum_{k=1}^{q} e^{\kappa_t(\frac{n_k}{N}+H_k)}} n_b - \frac{e^{\kappa_t(\frac{n_b}{N}+H_b)}}{\sum_{j=1}^{q} e^{\kappa_t(\frac{n_j}{N}+H_j)}} n_a \right) \quad a = 1, \ldots, q, \tag{4.54}$$

The set of equations (4.54) defines a system of q non-linear ordinary differential equations in the q unknowns $n_1, \ldots, n_q$. To study the dynamical properties of the mean value equations we proceed with the linear stability analysis of the system. In order to do that we have to compute the Jacobian matrix of the system. We write the system in the compact form

$$\frac{dn_a}{dt} = f_a(n_a, \{n_i\}_{i\neq a}) \quad a = 1, \ldots, q. \tag{4.55}$$

After collecting the common denominator, we get

$$f_a = \sum_{\substack{b=1 \\ b\neq a}}^{q} \frac{1}{\sum_{k=1}^{q} e^{\kappa_t(\frac{n_k}{N}+H_k)}} \left(e^{\kappa_t(\frac{n_a}{N}+H_a)} n_b - e^{\kappa_t(\frac{n_b}{N}+H_b)} n_a \right). \tag{4.56}$$

We compute the derivatives of f_a as

$$\begin{aligned} \frac{\partial f_a}{\partial n_a} = \frac{1}{(\sum_{k=1}^{q} e^{\kappa_t(\frac{n_k}{N}+H_k)})^2} \sum_{\substack{b=1 \\ b\neq a}}^{q} \Bigg(& (\frac{\kappa_t}{N} e^{\kappa_t(\frac{n_a}{N}+H_a)} n_b - e^{\kappa_t(\frac{n_b}{N}+H_b)})(\sum_{k=1}^{q} e^{\kappa_t(\frac{n_k}{N}+H_k)}) \\ & - (e^{\kappa_t(\frac{n_a}{N}+H_a)} n_b - e^{\kappa_t(\frac{n_b}{N}+H_b)} n_a) \frac{\kappa_t}{N} e^{\kappa_t(\frac{n_a}{N}+H_a)} \Bigg), \end{aligned} \tag{4.57}$$

$$\begin{aligned} \frac{\partial f_a}{\partial n_i} = \frac{1}{(\sum_{k=1}^{q} e^{\kappa_t(\frac{n_k}{N}+H_k)})^2} \Bigg(& - (\frac{\kappa_t}{N} e^{\kappa_t(\frac{n_i}{N}+H_i)} n_a - e^{\kappa_t(\frac{n_a}{N}+H_a)})(\sum_{k=1}^{q} e^{\kappa_t(\frac{n_k}{N}+H_k)}) \\ & - \sum_{\substack{b=1 \\ b\neq a}}^{q} (e^{\kappa_t(\frac{n_a}{N}+H_a)} n_b - e^{\kappa_t(\frac{n_b}{N}+H_b)} n_a) \frac{\kappa_t}{N} e^{\kappa_t(\frac{n_i}{N}+H_i)} \Bigg) \quad i \neq a. \end{aligned} \tag{4.58}$$

We focus on the fixed point of the system (4.54) $n_i = \frac{N}{q} \ \forall i$, which represent the disordered state fixed point and we study its stability for varying κ_t. To further

simplify the picture we arbitrarily consider the fixed point for the price momentum $H_i = H \ \forall i$ and we get

$$\left.\frac{\partial f_a}{\partial n_a}\right|_{\frac{N}{q},H} = \sum_{\substack{b=1 \\ b\neq a}}^{q} \frac{1}{q}\left(\frac{\kappa_t}{q} - 1\right) = \frac{q-1}{q}\left(\frac{\kappa_t}{q} - 1\right), \tag{4.59}$$

$$\left.\frac{\partial f_a}{\partial n_i}\right|_{\frac{N}{q},H} = -\frac{1}{q}\left(\frac{\kappa_t}{q} - 1\right). \tag{4.60}$$

The Jacobian of the system evaluated at the fixed point reads

$$J\Big|_{\frac{N}{q},H} = \frac{1}{q}\left(\frac{\kappa_t}{q} - 1\right)\begin{pmatrix} q-1 & -1 & -1 & \dots & -1 \\ -1 & q-1 & -1 & \dots & -1 \\ \dots & \dots & \dots & \dots & \dots \\ -1 & -1 & -1 & \dots & q-1 \end{pmatrix} \tag{4.61}$$

Neglecting for a moment the multiplicative constant we have that the eigenvalues of the matrix are $\lambda_1 = 0$ with multiplicity 1 and $\lambda_{2,\dots,q} = q$ with multiplicity q. Considering also the multiplicative constant we can identify a change of stability of the disordered fixed point at $\kappa_c = q$. For $\kappa_t < q$ all the eigenvalues are non-positive pointing out to a stable fixed point. For $\kappa_t > q$ the eigenvalues become positive and the fixed point loses its stability.

This is an interesting result, because we found a change of stability at a critical value different from the standard value of the mean-field Potts model $\beta_c = \frac{2(q-1)}{q-2}\log(q-1)$. However, we have to underline that the presence of a zero-valued eigenvalue denotes that we are in presence of a marginal case. Hence, from the theory of dynamical systems, we don't have any theorem stating that the stability results of linear analysis well represent the true stability of the full non-linear systems. Stated otherwise, the linearization results could be wrong.

Nevertheless, the previous result is an interesting clue driving us to study the critical behavior of the model employing other techniques, both numerical and analytical. Before doing that in the following paragraph, we mention that we tried to go to the second order in the stability analysis, computing the Hessian matrix H_a for each component f_a of the system. However, the Hessian seems not to do add any new information about the aforementioned change of stability or about other changes of stability.

Numerical analysis of the bifurcation diagram

The fact that the standard critical inverse temperature of the mean-field Potts model $\beta_c = \frac{2(q-1)}{q-2}\log(q-1)$ does not emerge from this stability analysis, is an interesting unexpected point.

This pushed us to try to study the stability phase diagram numerically, varying the constant kappa parameter and the initial conditions through different simulations. In the literature there are several works addressing exactly the change of stability problem and the presence of metastable states, we cite among them Cuff et al. [46], Kirkpatrick and Wolynes [47], Ostilli and Mukhamedov [48], and Thirumalai and Kirkpatrick [49]. The simulations, by now, are in accord with the results from the literature.

We refer to Ostilli and Mukhamedov [48] for a complete bifurcation diagram. In a few words, from the bifurcation diagram we identify two changes of stability, one occurring at $\kappa_t = \frac{2(q-1)}{q-2}\log(q-1)$ with a pitchfork subcritical bifurcation which correspond to a first-order transition and another one at $\kappa_t = q$.

This picture unveils the main reason for the problems of the simulation. First, being the phase transition of first-order, i.e. discontinuous, the time series jumps discontinuously in the simulation and the bubbles do not grow continuously as it happens for the original Ising model, which features a second-order phase transition. Instead, the discontinuous jump leads to a full polarization of the noise traders class in few trading days, characterizing the bubbles as real changes of regime.

Moreover, a second problem adds to the first, the particular phase transition of the mean-field Potts model is characterized by the presence of metastable states. Starting from a disordered state below the critical kappa, when the κ_t enters in the critical region, even if from a statistical point of view the thermodynamical equilibrium has changed, from a dynamical point of view the system remains frozen in a metastable disordered state until a sufficiently strong stochastic perturbation breaks the metastability and the system jumps discontinuously to the new ordered state, or κ_t becomes greater than q exiting the metastability region and the metastable state ceases to be locally stable.

The same problem is present when vice-versa κ_t decreases from the critical region to the disordered region, the system could remain ordered even below the critical temperature.

To deepen the analysis of the metastability region, in the next section we study the system with a classical tool of Statistical Physics, the Landau expansion of the free energy.

4.1.5 The Landau expansion approach

For this section we refer to [50]. We recall that the Hamiltonian of our model is

$$H_N(\{s_1,\dots,s_N\}) = -\frac{1}{2N}\sum_{i,j=1}^{N}\delta_{s_i,s_j} - \sum_{k=1}^{q}H_k\sum_{i=1}^{N}\delta_{s_i,k}. \tag{4.62}$$

As an approximation we neglect the external field part of the Hamiltonian, hence in the following analysis we consider the approximated Hamiltonian

$$H_N(\{s_1,\dots,s_N\}) = -\frac{1}{2N}\sum_{i,j=1}^{N}\delta_{s_i,s_j}. \tag{4.63}$$

We recall that the free energy is defined as

$$F = \langle H\rangle - TS \tag{4.64}$$

where $\langle H\rangle$ represents the average total energy of the system, T is the temperature, which in our case we can define as $T = \frac{1}{\kappa_t k_B}$ with k_B being the Boltzmann constant and S is the thermodynamical entropy.

From the mean-field assumption, it follows that

$$P(\{s_1,\dots,s_N\}) = P(s_1)P(s_2)\cdots P(s_N). \tag{4.65}$$

We expect that the disordered phase is characterised by $P(s_i) = \frac{1}{q}\ \forall i$. Instead in the ordered phase, the probability that a noise trader holds a particular asset, say for example the asset number 1, is higher than the others. From this reasoning and to then work out a Landau expansion we introduce an order parameter m and we assume, following a variational method, that the probability for the single noise trader reads

$$P(s_i) = \begin{cases} \frac{1+(q-1)m}{q} & s_i = 1 \\ \frac{1-m}{q} & s_i = 2,\dots,q \end{cases} \tag{4.66}$$

where

$$m \in \left[-\frac{1}{q-1},1\right]. \tag{4.67}$$

As a remark, we underline that the asset number 1 has nothing special and we could choose any other asset. Making this arbitrary choice we are effectively breaking the symmetry of the system, a necessary step in this derivation.

Using (4.66) we can compute the average value of the delta-like interaction term

$$\begin{aligned}\langle\delta_{s_i,s_j}\rangle &= \sum_{s_i=1}^{q}\sum_{s_j=1}^{q}\delta_{s_i,s_j}P(s_i)P(s_j) = \sum_{s_i=1}^{q}(P(s_i))^2 \\ &= \left(\frac{1+(q-1)m}{q}\right)^2 + (q-1)\left(\frac{1-m}{q}\right)^2 = \frac{1+(q-1)m^2}{q}.\end{aligned} \tag{4.68}$$

Using this result we can compute the average total energy as

$$\langle H \rangle = -\frac{1}{2N} N^2 \frac{1 + (q-1)m^2}{q}. \tag{4.69}$$

The entropy term is readily computed from the definition of Shannon entropy as

$$S = -k_B N \left(\frac{1 + (q-1)m}{q} \log \frac{1 + (q-1)m}{q} + (q-1) \frac{1-m}{q} \log \frac{1-m}{q} \right). \tag{4.70}$$

Hence the variational free energy reads

$$\begin{aligned} F = \langle H \rangle - TS = & -\frac{1}{2N} N^2 \frac{1 + (q-1)m^2}{q} \\ & + \frac{1}{\kappa_t} N \left(\frac{1 + (q-1)m}{q} \log \frac{1 + (q-1)m}{q} + (q-1) \frac{1-m}{q} \log \frac{1-m}{q} \right). \end{aligned} \tag{4.71}$$

From which the variational free energy density per spin easily follows

$$\begin{aligned} f(m) = \frac{F}{N} = & -\frac{1}{2} \frac{1 + (q-1)m^2}{q} \\ & + \frac{1}{\kappa_t} \left(\frac{1 + (q-1)m}{q} \log \frac{1 + (q-1)m}{q} + (q-1) \frac{1-m}{q} \log \frac{1-m}{q} \right). \end{aligned} \tag{4.72}$$

We are finally able to compute the Landau expansion of the free energy density, which is a Taylor expansion in powers of m.

$$f(m) = f_0 + f_2 m^2 + f_3 m^3 + f_4 m^4 + \dots \tag{4.73}$$

Expanding up to the fourth order the logarithms present in the entropy expression and collecting the terms we get

$$f_0 = -\frac{1}{2q} - \frac{1}{\kappa_t} \log q, \tag{4.74}$$

$$f_2 = \frac{(q-1)(\frac{q}{\kappa_t} - 1)}{2q}, \tag{4.75}$$

$$f_3 = -\frac{1}{6} \frac{1}{\kappa_t} (q-1)(q-2), \tag{4.76}$$

$$f_4 = \frac{1}{12}\frac{1}{\kappa_t}(q-1)(q^2-3q+3). \tag{4.77}$$

We are interested in the presence of absolute and relative minima of the free energy, corresponding respectively to stable and metastable thermodynamical configurations of the system. The four coefficients are sufficient to identify the interesting minima and their nature. Indeed, while the zeroth-order term represents only a shift of the free energy, the fourth-order term being always positive ensures the presence of at least one minimum in the allowed range of m values. Being f_3 always negative and considering the change of sign of f_2 at $\kappa_t = q$ the picture which emerges is the following. For $\kappa_t > q$ the only (absolute) minimum is at a positive value of $m > 0$. At $\kappa_t = q$, a new local minimum appears at $m = 0$, while the minimum at $m > 0$ remains the absolute thermodynamical stable minimum. At a critical value $\kappa_c > q$ to be determined, a first-order phase transition takes place, with the minimum at $m = 0$ becoming the absolute one. The value κ_c can be determined from the conditions characterising the transition

$$f(m_c) = f(0), \tag{4.78}$$

$$\left.\frac{df}{dm}\right|_{m_c} = 0, \tag{4.79}$$

which lead to

$$\kappa_c = \frac{2(q-1)}{q-2}\log(q-1), \tag{4.80}$$

the standard critical inverse temperature for the mean-field Potts model and

$$m_c = \frac{q-2}{q-1}. \tag{4.81}$$

This picture is in agreement with the results from the linear stability analysis, confirming the presence of metastable states and a region of metastability of the disordered state, for values of κ_t in the interval

$$\frac{2(q-1)}{q-2}\log(q-1) < \kappa_t < q, \tag{4.82}$$

which divides the stable and unstable regions.

4.1.6 Limits of applicability of the Potts model

In this section we summarize the results found, pointing out the limits of applicability of the Potts model in modeling the noise trader class.

Both the mean value dynamical equation approach and the Landau expansion approach have shown the presence of metastable states characterizing the range of κ_t near the critical value. Even if, from a thermodynamical point of view, the thermodynamical stable equilibrium is always unique, from a dynamical point of view, the presence of metastable states, i.e. local minima of the free energy, is not negligible. As we have shown, simulating the dynamics of the system with a varying κ_t, the system can get stuck in local minima of the free energy leading to the persistence of the ordered (disordered) phase even outside (inside) the critical region. To address this problem, one could imagine (as we tried) to "delete" the metastable region, effectively making the κ_t process jumping the entire metastable region with some if conditions in the code, this would solve the problem of the metastable states but won't solve, rather will aggravate the second main problem concerning the applicability of the Potts model, the discontinuous character of the transition.

From the previous analysis, in particular, considering the bifurcation diagram, we see that the metastable region for the disordered state

$$\frac{2(q-1)}{q-2}\log(q-1) < \kappa_t < q, \tag{4.83}$$

is smaller the smaller is q. In the limiting case of $q = 2$, the metastable region disappears and the two change of stability points merge. From a dynamical theory point of view, the character of the bifurcation changes, the subcritical pitchfork bifurcation becomes a supercritical pitchfork bifurcation. The first-order discontinuous transition becomes a second-order continuous one. In the limiting case of $q = 2$ the Potts model reduces to the Ising model and, considering the linearized form of the resulting transition probabilities, we get the original implementation of the noise traders class. The different qualitative behavior of the time series of the present implementation with respect to the original model is ultimately related to the different character, first-order or second-order, of the underlying phase transition.

This is also a warning in choosing in the future new models for the noise traders class. Indeed, leaving the safe haven of the second-order continuous transition of the Ising model, many other models present first-order phase transitions which will lead to abrupt changes of regime in the time series instead of nice smooth bubbles. Hence, a preliminary study of the phase transition and the bifurcation diagram of the model will be needed.

Possible directions for further analysis

The last paragraph concludes the analysis of the limits of the Potts model, nevertheless, something more could be done. For example, a parametric scan of the stability phase portrait could be worked out to quantitatively confirm the qualitative analysis of the bifurcation diagram.

Some play with the code and parameters of the Ornstein–Uhlenbeck kappa process could be done to find the best parameter settings to see, still discontinuous but nicer bubbles, which could have a meaning for real markets modeling or could be useful to compare to the results of the future models that will be considered.

But probably the most interesting further analysis which could be done is the study of the rich physical picture which emerges considering also negative value for the kappa process, i.e. contrarian noise traders. We found an extremely interesting analysis in Ostilli and Mukhamedov [51], addressing exactly the dynamical behavior of the mean-field Potts model in presence of anti-ferromagnetic couplings. In a few words, in presence of anti-ferromagnetic couplings for a particular range of parameters the system never reaches the unique thermodynamical Boltzmann equilibrium settling instead on a period-2 stable trajectory. This is a peculiar effect of the discrete-time dynamics, in contrast to the continuous-time dynamics for which this strange behavior does not emerge. This is not the only peculiar behavior of the discrete-time anti-ferromagnetic dynamics and the paper points out many other effects coming from the discrete nature of time characterizing the model.

We report a comment present in the paper, underlining the importance of this discrete nature of time: *"We stress also that the discrete-time dynamics we shall focus on, is not meant as an approximation of the continuous-time dynamics (as is instead usually done for practical simulations). There are infinitely many remarkable examples where the dynamics is intrinsically discrete. Whereas only a continuous-time dynamics can represent some description of a system of physical particles each other interacting via a physical medium, a discrete- time dynamics can represent a system of agents which interact via, e.g., exchange of information taking place at discrete random times, as in fact occurs in the actual world, especially in social or economical contexts, but also in ecosystems"*

Considering negative values for the kappa process in our simulations we found indeed peculiar oscillating behaviors of all the quantities.

This analysis goes far beyond the scope of this thesis but we report it because it is engaging and challenging from a physical and mathematical point of view and could be useful also from the modelization point of view.

As a last comment, we notice that in Ollikainen [19] the same oscillating behavior is found and analyzed in the case of the standard Ising model (indeed the Ising model correspond to a Potts model with $q = 2$). Yet, the work concludes by stating that: *"The exact mechanism behind the oscillating phase is still unknown.*

This is a question for future work". The interesting analysis present in Ostilli and Mukhamedov [51] could be a satisfying theoretical explanation of this phenomenon.

4.2 The O(n) model

In this section, we move to a different Ising-like statistical model to represent the noise traders class: the $O(n)$ model, also known as n-vector model. In subsection 4.2.1 we introduce a fully connected version of the $O(n)$ model with a vectorial external field representing all the price momenta. This time the resulting transition rates derived in section 4.2.2 constitute a complicate multivariate probability distribution, still resembling however a continuous version of the Logit distribution, from which is difficult to sample. Two different approaches are then presented to construct a sampling procedure to simulate the model.

The first is presented in section 4.2.3 and is based on the McFadden result for the Logit distribution. It is based on an interesting connection between the Ising-like modeling of the noise traders class and the Decision Theory's framework in which we can understand the decision process of each investor. Nevertheless, the resulting algorithm is particularly expensive from a computational point of view. In section 4.2.4 we then move to the second method, which exploits the geometrical symmetries of the distribution to generate samples in a rejection-less manner. The method is constituted by two steps. In the first, we sample an angle theta from a univariate distribution and then in the second we sample uniformly at random from a particular hypersphere $\mathbb{S}^{n-2}$, a subset of the original space of choices $\mathbb{S}^{n-1}$. This second method is promising, being fast and well scalable with the number of risky assets. The simulations presented are obtained with its implementation.

In section 4.2.5 the portfolio interpretation of the spin vector $\vec{S}_i$ is discussed. Two main possible interpretations emerge. In the first, the first $n-1$ components represent the risky assets, while the last component represents the unique risk-free asset. In the second, that in our opinion is more promising, the negative components represent at the aggregate level the risk-free asset, while the positive represents the respective risky assets.

The time series resulting from the $O(n)$ model are presented is section 4.2.6. They are encouraging in terms of a realistic description of the market behavior, at least from a qualitative point of view. Quantitatively some problems have to be further analyzed, in particular, a problem regarding the critical value κ_c for the kappa process, which will be also extensively discussed in the next Chapter.

4.2.1 The O(n) model on the fully connected graph

To model the noise traders class in the multi-asset framework we introduce an $O(n)$ model with an external field of price momenta. We will discuss two slightly different

versions of the model. One where the first $n-1$ components of the spin vector represent the risky assets, while the last component represents the unique risk-free asset. The other where each positive component of the spin vector represents a risky asset while the risk-free asset is accounted for by the negative components at the aggregate level. In each version the number n will assume a different meaning, in the first case representing the total number of assets, hence the number of stocks plus one, instead in the second case being equal to only the number of risky investments.

To fix the ideas, we start by considering the first version of the model, postponing the discussion of the second version to a later section. Hence, in the present case, n = number of stocks + 1 represents the total number of risky and risk-free assets. The model is defined on the fully connected graph K_N, with N nodes and $\frac{N(N-1)}{2}$ edges.

The Hamiltonian of the model is

$$H_N(\{\vec{S}_1, \dots, \vec{S}_N\}) = -\frac{J}{2N} \sum_{i,j=1}^{N} \vec{S}_i \cdot \vec{S}_j - \sum_{i=1}^{N} \vec{h} \cdot \vec{S}_i, \tag{4.84}$$

where the spin

$$\vec{S}_i = (s_{i1}, \dots, s_{in}) \in \mathbb{S}^{n-1} \tag{4.85}$$

lives on the $(n-1)$-sphere and represents the portfolio allocation of noise trader i. More precisely,

$$s_{ia}^2 = x_{ia} \quad a = 1, \dots, n. \tag{4.86}$$

The squared component s_{ia}^2 of the spin vector represents the fraction of wealth x_{ia} invested by the trader i in the asset a. The modeling is consistent since $\vec{S}_i$ satisfies $\|\vec{S}_i\| = 1$, therefore at each time step the investment fractions for each noise trader correctly sum to one,

$$\sum_{a=1}^{n} x_{ia} = 1. \tag{4.87}$$

As an implementation note, we assume that the first $n-1$ components represent the risky assets, while the last component represents the unique risk-free asset.

The interpretation of the components of the spin is a delicate point and different modeling strategies can be applied. This issue will be deepened in the following.

Each spin, i.e. noise trader, we will use as usual the two terms interchangeably, interacts with all the others, and, at odds with the classical $O(n)$ model, also with itself. This will be useful later on and in any case, this introduces a negligible correction to the Hamiltonian for large N. This negligible correction corresponds to the one introduced for the Potts model and we refer to section 4.1.1 for the detailed discussion of it. As in the case of the Potts model, it can be shown that in the thermodynamical limit $N \to +\infty$, the fully connected $O(n)$ model is equivalent to

the mean-field $O(n)$ model. From now on we will use the two terms interchangeably since we are in a large N regime.

Finally, a vectorial external field $\vec{h}$ acts on each spin. It models the trend following attitude of the noise investors. In particular, we have that each component of the vector h corresponds to the price momentum associated with the respective asset $h_k = H_k$, where we have defined a fictitious price momentum of the risk-free asset and we have set it to zero $h_n = H_n = 0$ for simplicity. Its actual value should be $H_n = r_f$ but the difference, being just a rescaling of the risky price momenta, is negligible.

As for the Potts model we take the standard Boltzmann weight as the equilibrium distribution,

$$P(\{\vec{S}_1, \ldots, \vec{S}_N\}) = e^{-\beta H_N}, \tag{4.88}$$

fully describing the statistical properties of the model. In the next section we apply the method already used in the case of the Potts model, to derive the transition probabilities characterizing the stochastic dynamics of the $O(n)$ model and hence defining the investments' dynamics of the noise traders class.

4.2.2 The transition probabilities

The derivation of the transition probabilities follows closely the passages of the derivation for the Potts model. To easily compare the two derivations we use the same notation.

Again, as in the case of the Potts model, one important point has to be preliminarily considered before constructing the MCMC. Indeed, the algorithm we are going to construct is different from the standard MCMC algorithms used for simulating spin systems for two main reasons that we briefly review in the next section.

Parallel update vs random update in the MCMC algorithms

Usually, the Markov Chain Monte Carlo used for simulating spin systems proceeds to select one spin or one cluster of spins at random, proposing a move according to a certain proposal probability and then accepting or rejecting the move according to a certain acceptance probability.

After each move, all the quantities are then updated according to the new configuration of the system.

In the setup we will derive instead, at each time-step all the spins are updated in parallel, considering sequentially all the spins inside the same time-step, without any random choice of one single spin to update. Moreover, all the quantities entering the transition probabilities are updated only after all the traders have

made their decisions, hence each trader decides based on the investment decisions of all the other traders of the previous day, i.e. after all the spins have been updated.

As explained in the Potts model's Chapter, in particular in subsection 4.1.2 the sequential update's validity can be proved in the framework of the Gibbs sampling. Indeed, if each component of the vector of spins defining the state of the system is updated according to the conditional probability of that spin conditioned to all the others, the Markov chain defined by the full vector of spins considered after all the updates have taken place is correctly sampling the joint probability distribution.

If at each time step t all the components of the vector

$$(\vec{S}_1, \ldots, \vec{S}_{l-1}, \vec{S}_l, \vec{S}_{l+1}, \ldots, \vec{S}_N) \tag{4.89}$$

are updated, sampling each spin $\vec{S}_l$ from the conditional probability

$$P(\vec{S}_l \mid \{\vec{S}_1^t, \ldots, \vec{S}_{l-1}^t, \vec{S}_{l+1}^{t-1}, \ldots, \vec{S}_N^{t-1}\}), \tag{4.90}$$

then the full vector of updated spins $(\vec{S}_1^t, \ldots, \vec{S}_{l-1}^t, \vec{S}_l^t, \vec{S}_{l+1}^t, \ldots, \vec{S}_N^t)$ represents a correct sample of the statistical model defined by P, i.e. is correctly simulating its dynamics. The key point is that the conditional probabilities must be updated after each single spin flip as underlined by the time superscripts. This is connected to the second point aforementioned, indeed in our simulation algorithm we are updating the probabilities only at the end of the trading day. Eventually, as explained in subsection 4.1.2, the method's consistency is assured by the mean-field assumption which allows us to drop the dependence on all the other spins in the conditional probability. This relies on the asymptotic equivalence for $N \to +\infty$ of the fully connected and mean-field $O(n)$ models and on the fact we are in the large $N \gg 1$ case.

The derivation of the transition probabilities

We start again from the discrete-time Master Equation governing the evolution of the time-dependent conditional probability distribution

$$P(\vec{S}_l \mid \{\vec{S}_1, \ldots, \vec{S}_{l-1}, \vec{S}_{l+1}, \ldots, \vec{S}_N\}, t) \tag{4.91}$$

of a single spin $\vec{S}_l$ given all the others. As for the Potts model, from now on $\{\vec{S}_1, \ldots, \vec{S}_{l-1}, \vec{S}_{l+1}, \ldots, \vec{S}_N\}$ will be considered as fixed parameters, each having a specific value, this time on the $(n-1)$-sphere $\mathbb{S}^{n-1}$.

From the mean-field assumption it follows

$$P(\vec{S}_l \mid \{\vec{S}_1, \ldots, \vec{S}_{l-1}, \vec{S}_{l+1}, \ldots, \vec{S}_N\}, t) = P(\vec{S}_l, t). \tag{4.92}$$

The discrete-time master equation for the conditional probability to have $\vec{S}_l = \vec{A} \in \mathbb{S}^{n-1}$ reads

$$\frac{P(\vec{S}_l = \vec{A}, t+\Delta t) - P(\vec{S}_l = \vec{A}, t)}{\Delta t} = \int_{\vec{B}\in\mathbb{S}^{n-1}} W(\vec{B}\to\vec{A})P(\vec{S}_l = \vec{B}, t) - W(\vec{A}\to\vec{B})P(\vec{S}_l = \vec{A}, t). \quad (4.93)$$

We assume again an unit time increment $\Delta t = 1$, corresponding to one trading day. As for the Potts model, to effectively set the discrete-time derivative equal to zero we use the detailed balance condition which in this case reads

$$\frac{W(\vec{A}\to\vec{B})}{W(\vec{B}\to\vec{A})} = \frac{P(\vec{B})}{P(\vec{A})}. \quad (4.94)$$

We refer to the discussion in subsection 4.1.2 to motivate our choice in using the detailed balance, instead of other balance conditions, e.g. the global balance presented in the aforementioned subsection.

Using the definition of conditional probability we can easily switch to the joint probabilities

$$\frac{P(\vec{B})}{P(\vec{A})} = \frac{P(\vec{S}_l = \vec{B} \mid \{\vec{S}_1,\dots,\vec{S}_{l-1},\vec{S}_{l+1},\dots,\vec{S}_N\}}{P(\vec{S}_l = \vec{A} \mid \{\vec{S}_1,\dots,\vec{S}_{l-1},\vec{S}_{l+1},\dots,\vec{S}_N\}} = \frac{\frac{P(\vec{S}_l=\vec{B},\{\vec{S}_1,\dots,\vec{S}_{l-1},\vec{S}_{l+1},\dots,\vec{S}_N\}}{P(\{\vec{S}_1,\dots,\vec{S}_{l-1},\vec{S}_{l+1},\dots,\vec{S}_N\})}}{\frac{P(\vec{S}_l=\vec{A},\{\vec{S}_1,\dots,\vec{S}_{l-1},\vec{S}_{l+1},\dots,\vec{S}_N\}}{P(\{\vec{S}_1,\dots,\vec{S}_{l-1},\vec{S}_{l+1},\dots,\vec{S}_N\})}}. \quad (4.95)$$

Simplifying the denominators we get the ratio between the joint probabilities, which we can explicitly compute as

$$\frac{P(\vec{S}_l = \vec{B}, \{\vec{S}_1,\dots,\vec{S}_{l-1},\vec{S}_{l+1},\dots,\vec{S}_N\}}{P(\vec{S}_l = \vec{A}, \{\vec{S}_1,\dots,\vec{S}_{l-1},\vec{S}_{l+1},\dots,\vec{S}_N\}} = \frac{\frac{1}{Z}e^{-\beta(-\frac{J}{2N}\sum_{i\neq l}\sum_{j\neq l}\vec{S}_i\cdot\vec{S}_j - \frac{J}{2N}\sum_j \vec{B}\cdot\vec{S}_j - \frac{J}{2N}\sum_i \vec{S}_i\cdot\vec{B} + \frac{J}{2N}\vec{B}\cdot\vec{B} - \sum_{i\neq l}\vec{h}\cdot\vec{S}_i - \vec{h}\cdot\vec{B})}}{\frac{1}{Z}e^{-\beta(-\frac{J}{2N}\sum_{i\neq l}\sum_{j\neq l}\vec{S}_i\cdot\vec{S}_j - \frac{J}{2N}\sum_j \vec{A}\cdot\vec{S}_j - \frac{J}{2N}\sum_i \vec{S}_i\cdot\vec{A} + \frac{J}{2N}\vec{A}\cdot\vec{A} - \sum_{i\neq l}\vec{h}\cdot\vec{S}_i - \vec{h}\cdot\vec{A})}}. \quad (4.96)$$

Simplifying the common factors at numerator and denominator we get

$$\begin{aligned}\frac{P(\vec{B})}{P(\vec{A})} &= e^{-\beta(-\frac{J}{N}\sum_i \vec{S}_i\cdot\vec{B} - \vec{h}\cdot\vec{B} + \frac{J}{N}\sum_i \vec{S}_i\cdot\vec{A} - \vec{h}\cdot\vec{A})} \\ &= e^{-\beta(-\frac{J}{N}(\sum_i \vec{S}_i\cdot\vec{B} - \sum_i \vec{S}_i\cdot\vec{A}) - (\vec{h}\cdot\vec{B} - \vec{h}\cdot\vec{A}))} \\ &= e^{\beta(J\frac{\sum_i \vec{S}_i\cdot(\vec{B}-\vec{A})}{N} + \vec{h}\cdot(\vec{B}-\vec{A}))}. \quad (4.97)\end{aligned}$$

We set $J = 1$ and we identify the inverse temperature with the herding propensity $\beta = \kappa_t$. The external field vector components are set equal to the corresponding price momenta $h_k = H_k$, where the price momentum of the risk-free asset is set to zero. We then finally get

$$\frac{W(\vec{A} \to \vec{B})}{W(\vec{B} \to \vec{A})} = \frac{P(\vec{B})}{P(\vec{A})} = e^{\kappa_t (\frac{\sum_i \vec{S}_i \cdot (\vec{B} - \vec{A})}{N} + \vec{H} \cdot (\vec{B} - \vec{A}))}. \tag{4.98}$$

Now to get the transition rates we have different possibilities. We again discard, as for the Potts model's case, the standard Metropolis-Hastings rule proposed in Metropolis et al. [44] due to the unrealistic modeling we would obtain.

To construct a more realistic rejection-less MCMC we impose

$$\frac{\mathcal{P}(\vec{A} \to \vec{B})}{\mathcal{P}(\vec{B} \to \vec{A})} = \frac{P(\vec{B})}{P(\vec{A})} = e^{\kappa_t \left(\frac{\sum_i \vec{S}_i \cdot (\vec{B} - \vec{A})}{N} + \vec{H} \cdot (\vec{B} - \vec{A}) \right)}. \tag{4.99}$$

This condition is satisfied setting

$$\mathcal{P}(\vec{A} \to \vec{B}) = e^{\kappa_t \left(\frac{\sum_i \vec{S}_i \cdot \vec{B}}{N} + \vec{H} \cdot \vec{B} \right)}. \tag{4.100}$$

The ergodicity and the aperiodicity of the MCMC constructed descend directly from the method used to derive it. We only need to correctly normalize the resulting transition rates. Normalizing we finally get the following transition probability

$$W(\vec{A} \to \vec{B}) = \mathcal{P}(\vec{A} \to \vec{B}) = \frac{e^{\kappa_t \left(\frac{\sum_i \vec{S}_i \cdot \vec{B}}{N} + \vec{H} \cdot \vec{B} \right)}}{\int_{\vec{K} \in \mathbb{S}^{n-1}} e^{\kappa_t \left(\frac{\sum_i \vec{S}_i \cdot \vec{K}}{N} + \vec{H} \cdot \vec{K} \right)}}. \tag{4.101}$$

To generate the dynamics of our model we have to sample realizations of the random vector $\vec{B} = (B_1, \ldots, B_n)$ from the multivariate probability distribution (4.101). Unfortunately, constructing a sampling procedure is difficult due to the high dimensionality of the distribution and to the non-trivial relation between the components of the random vector $\sum_{k=1}^{n} B_k^2 = 1$.

We mention that first, we tried to apply unsuccessfully two methods to attack the problem, the rejection sampling and the copula method. On the one hand, rejection sampling has been discarded due to its possible inefficiency caused by a high rejection ratio connected to the high dimensionality. The method suffers from the so-called curse of dimensionality.

On the other hand, the possibility to construct a copula function of the n correlated random variable B_k, appears soon unfeasible due to their non-trivial relation $\sum_{k=1}^{n} B_k^2 = 1$.

The approach we develop in the next section to tackle the problem starts from noting that the form of the probability distribution (4.101) coincides with a

continuous version of the Logit probability distribution for the arrival states. The Logit distribution is throughout used and studied in the discrete choice theory. In our case the space of choices is continuous, the choices live on the $(n-1)$-sphere, $\vec{B} \in \mathbb{S}^{n-1}$. As for the Potts model's case, this is once again an example of the connection between the discrete choices models and the Ising-like models in modeling social systems, as pointed out in Sornette [12].

We finally comment on the fact that the transition probabilities (4.101) have the remarkable property that the transition probability from state $\vec{A}$ to state $\vec{B}$ is independent of the initial state $\vec{A}$. This is a typical property of mean-field models.

4.2.3 Discretization and McFadden result approach

McFadden has shown in McFadden [45], that the Logit probability distribution actually models individuals who maximize a utility function that has an implicit random idiosyncratic part distributed according to the Gumbel distribution. Indeed, if each agent makes its choice maximizing

$$s^* = \arg\max_s \{\beta u_s + \eta_s\}, \tag{4.102}$$

where s represents one of the possible choices, u_s is the deterministic part of the utility function, η_s is a Gumbel random variable and β plays the role of the inverse temperature, McFadden has proved that $P(s^* = s)$ coincides with the Logit distribution.

Now we take advantage of this result to construct a sampling procedure for the multivariate probability distribution (4.101). If we discretize the space of choices $\mathbb{S}^{n-1}$ we end up exactly with a Logit distribution and instead of sampling the choices directly from the probability density function we can model each decision as a maximization problem

$$\vec{B}^* = \arg\max_{\vec{B} \in \mathbb{S}^{n-1}} \{\kappa_t u_{\vec{B}} + \eta_{\vec{B}}\}. \tag{4.103}$$

Where in our case the utility function is

$$u_{\vec{B}} = \left(\frac{\sum_i \vec{S}_i}{N} + \vec{H} \right) \cdot \vec{B}. \tag{4.104}$$

We used a subscript for the Gumbel distribution $\eta_{\vec{B}}$ to stress the fact that we have to use a different realization of the Gumbel distribution for each possible decision $\vec{B}$.

There are different ways to discretize the space of choices $\mathbb{S}^{n-1}$. We decided to consider choices sampled from a uniform distribution on the hypersphere. To do so, we generate samples from n i.i.d. zero mean and unit variance Normal distributions

$\mathcal{N}(0,1)$. Now, due to the spherical symmetry property of the multivariate normal distribution, we have the beautiful result, as pointed out by many sources as for example in Muller [52], that the random vector

$$\vec{B} = \frac{1}{\|(\mathcal{N}_1(0,1), \dots \mathcal{N}_n(0,1))\|} \left(\mathcal{N}_1(0,1), \dots \mathcal{N}_n(0,1) \right) \tag{4.105}$$

is distributed uniformly at random on the $(n-1)$-sphere. Due to the finite number of points we consider on the hypersphere, the sum over all the vectors representing the points could not be the zero vector. We then enforce it considering for each vector also the corresponding symmetric one with respect to the origin, i.e. with all components with opposite signs.

Summarizing, at the beginning of the simulation we generate the uniform discretization of the space of choices $\mathbb{S}^{n-1}$ with the following algorithm. The discretization will be kept fixed throughout the whole simulation to preserve the detailed balance condition.

Algorithm 1: Uniform discretization of the space of choices $\mathbb{S}^{n-1}$

Result: N_{points} vectors (choices) uniformly distributed on the hypersphere
for $(i = 0; i < \frac{N_{points}}{2}; i++)$ **do**
  for $(k = 0; k < n; k++)$ **do**
    $B_k = \mathcal{N}(0,1)$;
  end
  $r = \sqrt{\sum_{k=0}^{n-1} B_k}$;
  $\frac{1}{r}(B_0, \dots, B_{n-1})$ is a new point on $\mathbb{S}^{n-1}$;
  $\frac{1}{r}(-B_0, \dots, -B_{n-1})$ is a new point on $\mathbb{S}^{n-1}$;
end

Moreover, at each time-step, the trading decisions of the noise traders, i.e. reallocation of their portfolios, are generated according to the following algorithm.

Algorithm 2: Trading decisions of the noise traders

Result: Noise traders dynamics satisfying detailed balance
$\vec{M} = (\frac{\sum_i \vec{S}_i}{N} + \vec{H})$ (compute average magnetization + external field);
for *each noise trader* i **do**
  for $(i = 0; i < N_{points}; i++)$ **do**
    generate i.i.d. Gumbel RV $\eta_{\vec{B}}$;
  end
  $choice_i = \arg\max_{\vec{B}} \{\kappa_t \vec{M} \cdot \vec{B} + \eta_{\vec{B}}\}$
end

It is clear that also this procedure suffers from the curse of dimensionality. The computational cost of the simulation is exponential in the number N_{points} used to discretize the hypersphere and clearly a large number of points is needed to have a good uniform distribution and a realistic simulation. Nevertheless, the simulations presented in the following are run with a number of points of the order of the thousands, which gives already good results in terms of the uniform distribution on the hypersphere. The problem aggravates with an increasing number of risky assets, i.e. increasing dimensionality n.

Besides the computational problems, this method worth presenting because gives an interesting interpretation of the modeling of the noise trader's decision process we are building.

Indeed, modeling the trading decisions with the multivariate distribution (4.101), we are modeling traders which due to their herding behavior tend to "align" their portfolio allocation to the average portfolio allocation of the aggregate class of traders to which they are in contact to. The herding behavior represents the deterministic part of the utility optimization, which we can consider the rational part of the choice process undertaken by each agent. In absence of clear information, imitate others can be the unique rational strategy possible. The Gumbel random variable instead models the random idiosyncratic part, peculiar of each trader, which enters in the decision process.

To overcome the computational problems of the present method, in the next subsection we derive a different algorithm to generate the stochastic dynamics governed by the transition rates (4.101).

4.2.4 A new sampling algorithm

In this subsection we propose a different sampling algorithm to overcome the drawbacks of the method proposed in the last subsection. We focus in particular on the task of sampling from the linearized form of the probability distribution (4.101). Indeed, from the discussion presented in subsection 2.7.2 on the importance of the linearization step in the original model, we know that it is significant to be able to test the simulation of the model also with the linearized form of the transition probabilities. Nevertheless, the method we present in this section is directly applicable also to the non-linear form of the transition rates with just a minor implementation modification. To fix the ideas, we focus from now on, on the linearized form of the transition probabilities, hence we start from the non-normalized form of the transition rates

$$W(\vec{A} \to \vec{B}) = \mathcal{P}(\vec{A} \to \vec{B}) = e^{\kappa_t \left(\frac{\sum_i \vec{s}_i}{N} + \vec{H} \right) \cdot \vec{B}} \tag{4.106}$$

and linearizing it, we obtain

$$1 + \kappa_t \left(\frac{\sum_i \vec{S}_i}{N} + \vec{H} \right) \cdot \vec{B}. \tag{4.107}$$

We are back to the problem of sampling a multivariate probability distribution for the random vector $\vec{B}$ subjected to the non-trivial constraint

$$\vec{B} = (B_1, \ldots, B_n) \quad \sum_{k=1}^{n} B_k^2 = 1. \tag{4.108}$$

Moreover, this time we cannot use the "McFadden trick" since we have linearized the form of the distribution.

Yet, the density function (4.107) has interesting symmetry properties, which we will exploit to propose a sampling algorithm.

We first make explicit the symmetry property of the dot product entering the density function, expressing it in terms of the angle θ between the vector

$$\vec{M} \coloneqq \frac{\sum_i \vec{S}_i}{N} + \vec{H} \tag{4.109}$$

and the vector $\vec{B}$. It is always possible to define a unique angle between two vectors in any inner product space and in particular in the Euclidean space $\mathbb{R}^n$ to which our vector belongs to. Hence, we can write

$$P(\theta) = 1 + \kappa_t \|\vec{M}\| \|\vec{B}\| \cos\theta. \tag{4.110}$$

The norm of $\vec{B}$ is exactly equals to one, since $\vec{B} \in \mathbb{S}^{n-1}$, hence the expression simplifies to

$$P(\theta) = 1 + \kappa_t \|\vec{M}\| \cos\theta. \tag{4.111}$$

The probability distribution effectively depends only on one variable

$$\theta \in [0, 2\pi). \tag{4.112}$$

The sets of equiprobable choices, i.e. equiprobable vectors $\vec{B}$, are defined by the conditions

$$\begin{cases} \frac{1}{\|\vec{M}\|} \vec{M} \cdot \vec{B} = \cos\theta \\ \|\vec{B}\| = 1 \end{cases} \tag{4.113}$$

The second condition enforces the choice vectors to belong to the $(n-1)$-sphere. The first condition instead defines an hyperplane in $\mathbb{R}^n$, in fact it can be written as

$$m_1 b_1 + m_2 b_2 + \ldots + m_n b_n = \cos\theta, \tag{4.114}$$

where $m_1, \ldots, m_n$ are fixed coefficients. We now use a beautiful geometric property, indeed the intersection of a $(n-1)$-sphere and a n-dimensional hyperplane, is still a hypersphere, yet of one less dimension. Indeed, the system (4.113) defines a $(n-2)$-sphere in $\mathbb{R}^n$, with centre

$$\vec{C} = \cos\theta \frac{1}{\|\vec{M}\|} \vec{M} \tag{4.115}$$

and radius

$$r = \sqrt{1 - \cos^2\theta} = \sin\theta. \tag{4.116}$$

This fact will be crucial in constructing the sampling algorithm.

First of all, we focus on the angle θ. The expression (4.111) is not yet a well-defined probability distribution. Indeed, for some range of θ values and for large κ_t and $\|\vec{M}\|$, the expression becomes negative. To handle it we simply set equal to zero the probability of the θ values for which (4.111) becomes negative. The error introduced in this way is small and it is equivalent to the linearization error introduced considering only the linear term instead of the full non-linear distribution (4.106). Moreover, the probability distribution obtained has to be normalized.

Both problems can be overcome with rejection sampling. At odds with the rejection sampling applied to (4.101), the method this time does not suffer from the curse of dimensionality since we are dealing with a univariate distribution.

We sample from (4.111) with the following algorithm.

Algorithm 3: Rejection sampling from the $P(\theta)$ distribution

Result: An angle θ sampled from $P(\theta)$
while $(u * (1 + \kappa_t \|\vec{M}\|)) > (1 + \kappa_t \|\vec{M}\| \cos(\theta))$ **do**
  $\theta = Uniform(0,1) * 2\pi$;
  $u = Uniform(0,1)$
end
return θ;

We keep drawing uniformly at random angles $\theta \in [0,2\pi)$ until the value of the probability density function computed for that specific angle is greater than a uniform RV times the maximum of the distribution, i.e. $1 + \kappa_t \|\vec{M}\|$. Then the value of θ is correctly sampled from (4.111).

We can imagine pictorially the method in the following way. We draw a rectangle $[0,1) \times [0,2\pi)$, then we superimpose the graph of the density function, even if not always positive and not normalized. Now, we pick uniformly at random points from the rectangle, if the point stays below the graph, its x-coordinate is a valid

sample for θ. Points for which the graph is negative are never chosen, indeed we are effectively setting their probability to zero.

Now that we have correctly sampled a value for the angle, we have to choose a vector uniformly at random from the equiprobable set defined by that angle. Fortunately, the set is just a hypersphere $\mathbb{S}^{n-2}$ and we have already presented in formula (4.105) and in Algorithm 1 a way to generate uniformly at random a vector on a hypersphere. Indeed, the vector

$$\vec{\mathcal{B}}^*_{n-1} = \frac{1}{\|(\mathcal{N}_1(0,1), \dots \mathcal{N}_{n-1}(0,1))\|} \Big(\mathcal{N}_1(0,1), \dots \mathcal{N}_{n-1}(0,1) \Big) \tag{4.117}$$

will be uniformly distributed on $\mathbb{S}^{n-2}$. To have a vector in $\mathbb{R}^n$ we have to add one extra zero component, for example at the beginning of the vector, effectively increasing its dimensionality by one. The new vector is

$$\vec{\mathcal{B}}^*_{n} = \frac{1}{\|(\mathcal{N}_1(0,1), \dots \mathcal{N}_{n-1}(0,1))\|} \Big(0, \mathcal{N}_2(0,1), \dots \mathcal{N}_{n}(0,1) \Big). \tag{4.118}$$

Moreover, the hypersphere has to be translated and its radius rescaled following (4.115) and (4.116). Finally, one last important step has to be worked out. The $\mathbb{S}^{n-2}$ hypersphere will correctly represent the intersection between the higher dimensional $\mathbb{S}^{n-1}$ hypersphere and the hyperplane only after it will be rotated in such a way that the unit versor, corresponding to the extra component added in (4.118), will be rotated to the direction of the normalized vector $\frac{1}{\|\vec{M}\|}\vec{M}$.

We have to construct the orthogonal matrix R representing the rotation of the unit versor

$$\vec{X} = (1, 0, 0, \dots, 0), \tag{4.119}$$

to the direction of the vector $\frac{1}{\|\vec{M}\|}\vec{M}$. The matrix R has to satisfy

$$\frac{1}{\|\vec{M}\|}\vec{M} = R\vec{X}. \tag{4.120}$$

In two or three dimensions, such a rotation is given by the standard matrices containing sine and cosine functions. For example, in two dimension the rotation matrix would be

$$R_{n=2} = \begin{pmatrix} \cos\theta & -\sin\theta \\ \sin\theta & \cos\theta \end{pmatrix} \tag{4.121}$$

where θ is the angle between the two vectors.

In the general case of n dimension finding an efficient and numerical stable algorithm is not an easy task. There are many strategies to attack the problem, one is based on the Householder reflection matrices, another one on the Gram–Schmidt

orthonormalization process. Here we use an approach based on Givens rotations and to construct the algorithm we thoroughly refer to Zhelezov [53].

Eventually, the choice vector $\vec{B}$ sampled from the distribution (4.107), representing the noise trader's portfolio reallocation, is given by

$$\vec{B} = \sin\theta R\vec{\mathcal{B}}_n^* + \cos\theta \frac{1}{\|\vec{M}\|}\vec{M}. \tag{4.122}$$

Summarizing, the sampling algorithm is as follows.

Algorithm 4: Simulating the investment choice for a noise trader

Result: A vector $\vec{B}$ representing the new portfolio
sample an angle θ from $P(\theta)$ using Algorithm 3;
sample uniformly at random a vector $\vec{\mathcal{B}}_{n-1}^*$ on $\mathbb{S}^{n-2}$;
$\vec{\mathcal{B}}_n^* = (0, \vec{\mathcal{B}}_{n-1}^*) \in \mathbb{S}^{n-1}$;
construct the rotation matrix R following [53];
$\vec{B} = \sin\theta R\vec{\mathcal{B}}_n^* + \cos\theta \frac{1}{\|\vec{M}\|}\vec{M}$;
return $\vec{B}$;

As a final comment, we underline that the algorithm developed applies directly also to the case of non-linear transition probability. It is sufficient to modify the form of the univariate distribution from which we sample the angle theta. All the subsequent steps concerning the sampling from the hypersphere $\mathbb{S}^{n-2}$ are not affected at all.

The average holding time

In the last implementation of the stochastic dynamics for the $O(n)$ model no parameter to control the average holding time is present. From the discussion in section 2.7.1 we know it is a crucial quantity in defining a realistic form of the bubbles. Hence in this section, we introduce a parameter to modify the average holding time in the $O(n)$ algorithm just presented.

Before sampling an angle θ from the probability distribution (4.111) which represents for a noise trader the reallocation of its portfolio, we take into account the status-quo bias which could push the noise trader to maintain its present portfolio composition through a Bernoulli random variable.

Each trading day, before proceeding with its trading decisions, the noise trader first decides if to perform any trading moves at all or to just be inactive on the financial market for that day and hold its previous portfolio allocation position which he considers solid and profitable.

The trader decides to be active in the financial market and modifies its portfolio allocation with a probability

$$P(active) = \min\left\{1, \frac{1}{t_h}\left(1 + \frac{\kappa_t}{n}\|\vec{M}\|\right)\right\} \tag{4.123}$$

The probability to be inactive and hold the previous portfolio allocation is clearly

$$P(holding) = 1 - P(active). \tag{4.124}$$

The parameter t_h represents again the average number of trading days the noise traders keep its asset in absence of herding behaviour. In this way, we can directly control the trading frequency and the intensity of the oscillating behavior of the time series characterizing the resulting market dynamics.

The Algorithm 4 modifies to

Algorithm 5: Simulating the investment choice for a noise trader with average holding time parameter

Result: A vector $\vec{B}$ representing the investment choice
if $Uniform(0,1) > \frac{1}{t_h}(1 + \frac{\kappa_t}{n}\|\vec{M}\|)$ **then**
  $\vec{B}$ =previous portfolio allocation;
else
  Sample an angle θ from $P(\theta)$ using Algorithm 3;
  Sample uniformly at random a vector $\vec{\mathcal{B}}^*_{n-1}$ on $\mathbb{S}^{n-2}$;
  $\vec{\mathcal{B}}^*_n = (0, \vec{\mathcal{B}}^*_{n-1}) \in \mathbb{S}^{n-1}$;
  Construct the rotation matrix R following [53];
  $\vec{B} = \sin\theta R\vec{\mathcal{B}}^*_n + \cos\theta\frac{1}{\|\vec{M}\|}\vec{M}$;
end
return $\vec{B}$;

We close this paragraph commenting on the fact that this approach to introduce the average holding time parameter t_h easily applies also to the simulation method based on the McFadden result, presented in subsection 4.2.3. We just model the trader's decision to be active or inactive before the implementation of the "McFadden's maximization problem", through the same Bernoulli trial expressed by the equation (4.123).

The approach presented to impose the average holding time is rather general and an analogous Bernoulli trial can be implemented in the case of the Potts model, hence solving the problem presented in subsection 4.1.2. Clearly, in that case the term entering in the minimum, defining the probability to be active, has to be properly modified. The same approach is also applicable to the following models we are going to present, as we will explicitly point out.

4.2.5 The portfolio interpretation of the spin vector

We recall that in the present implementation, the spin

$$\vec{S}_i = (s_{i1}, \dots, s_{in}) \in \mathbb{S}^{n-1} \tag{4.125}$$

represents the portfolio allocation of noise trader i. More precisely,

$$s_{ia}^2 = x_{ia} \quad a = 1, \dots, n, \tag{4.126}$$

i.e. the squared component a of the spin vector represents the fraction of wealth x_{ia} invested by the trader i in the asset a. The modeling is consistent since $\vec{S}_i$ satisfies $\|\vec{S}_i\| = 1$, at each time step the investment fractions for each noise trader correctly sum to one,

$$\sum_{a=1}^{n} x_{ia} = 1. \tag{4.127}$$

We notice that in the present implementation, the first $n-1$ components represent the risky assets, while the last component represents the unique risk-free asset.

This interpretation presents two main problems, the first is that it is introducing a degeneracy in the portfolio representation. Indeed, the spins

$$\vec{S}_i = (s_{i1}, \dots, s_{in}) \tag{4.128}$$

and

$$-\vec{S}_i = (-s_{i1}, \dots, -s_{in}) \tag{4.129}$$

represent the same portfolio. This does not have any relevant effect in the model, the statistical properties are not affected at all by this interpretation of the spins, yet this represents an unmotivated introduction of a degeneracy from a modelistic point of view. The second problem, which is instead not negligible, is the inconsistent effect of the sign of the external field, i.e. the price momentum, on the noise traders' strategy. Unexpectedly, this seems to not have an impact on the realism of the resulting time series, but in any case, this is a problem that has to be solved.

One possible solution is to consider the action of the external field not as the standard dot product

$$\vec{H} \cdot \vec{S} \tag{4.130}$$

but as the dot product where the components of the spin are taken in absolute value

$$\vec{H} \cdot \vec{S}_{abs} = \sum_{k=1}^{n} H_k |S_k|. \tag{4.131}$$

Another promising solution is to change the interpretation of the spin $\vec{S}$. The action of the external field price momenta is consistent if the components of the vectors interpretation is such that

$$s_{ia}^2 = x_{ia} \quad \text{if } s_{ia} \geq 0 \tag{4.132}$$

represents the risky fraction invested in a, if s_{ia} is non-negative. Instead the sum of all the negative components at the aggregate level represent the risk-free fraction

$$\sum_{a:s_{ia}<0}^{n} s_{ia}^2 = x_f. \tag{4.133}$$

The condition

$$\sum_{a=1}^{n} x_{ia} = 1. \tag{4.134}$$

is still satisfied. We underline that in this interpretation the number of components of the spin is exactly equal to the number of risky assets, n = number of stocks. The risk-free asset is taken into account at the aggregate level by the negative components. Moreover, as a final remark, we comment that in this last interpretation the ABM endowed with the $O(n = 1)$ model actually corresponds to the original market model. This $O(n = 1)$ model is indeed equivalent to the standard Ising model characterizing the original formulation of the noise traders class. This as opposed to the previous interpretation we have considered, indeed the $O(n = 2)$ model with one component for the risky asset and one for the risk-free one is not equivalent to the Ising structure of the original setup.

4.2.6 Time series description

In this section, we introduce the parameters used for the simulation and we comment on the qualitative behavior of the resulting time series.

Choice of parameters

In table 4.2 are present some of the parameters maintained fixed throughout all the subsequent analysis.

As for the Potts model, no correlation among the dividend processes is assumed. Regarding the fundamentalist traders, the expected covariance matrix implementation is divided into a vector of expected variances and a matrix of expected correlations. Their values coincides with the Potts model ones. The variances are as in the table

$$\Sigma_{i,i}^f = 0.0004 \quad i = 1, \ldots, 4 \tag{4.135}$$

and the correlation matrix is set equal to

$$C^f = \begin{pmatrix} 1.0 & 0.5 & 0.0 & 0.0 \\ 0.5 & 1.0 & 0.0 & 0.0 \\ 0.0 & 0.0 & 1.0 & 0.0 \\ 0.0 & 0.0 & 0.0 & 1.0 \end{pmatrix} \tag{4.136}$$

	Parameters	
Assets	$N_{stocks} = 4$	$r_f = 4 \times 10^{-5}$
	$r_{d,i} = 1.6 \times 10^{-4}\ \forall i$	$d_{i,0} = 1.6 \times 10^{-4}\ \forall i$
	$P_{i,0} = 1\ \forall i$	$\Sigma^d_{i,i} = 1.6 \times 10^{-5}\ \forall i$
Fundamentalist traders	$W^f_0 = 10^9$	$E_{r,i} = 1.6 \times 10^{-4}\ \forall i$
	$\Sigma^f_{i,i} = 0.0004\ \forall i$	
Noise traders	$W^n_0 = 10^9$	$N_n = 1000$
	$\theta = 0.95$	$H_{i,0} = 1.6 \times 10^{-4}\ \forall i$

Table 4.2: Set of parameters for the simulations of the extended model endowed with a $O(n)$-like noise traders class. Their values constitute the natural generalization of the original models' one being motivated by real markets data and are mainly taken from Westphal and Sornette [18].

The initial investment decisions for fundamentalist and noise traders are as follows

$$\vec{x}^f_0 = (0.075,0.075,0.075,0.075,0.7) \tag{4.137}$$

$$\vec{x}^n_0 = (0.2,0.2,0.2,0.2,0.2), \tag{4.138}$$

where the last component represents the unique risk-free fraction while the others stand for the $n = 4$ risky assets.

Finally, an average holding time of ten trading days is imposed with the parameter $t_h = 10$.

The time series

In this section we present the time series from two different simulations. Both of the simulations are characterized by an Ornstein-Uhlenbeck kappa process defined by

$$\kappa_t - \kappa_{t-1} = \eta(\mu_k - \kappa_{t-1}) + \sigma_k v_t, \tag{4.139}$$

with mean reversion level $\mu_k = 0.98\beta_c$, where β_c represents the theoretical value for the critical inverse temperature of the mean-field $O(n)$ model

$$\beta_c = n. \tag{4.140}$$

Moreover, the mean reversion speed η and the step size σ_k are set, as in the original model, such that the Ornstein–Uhlenbeck process has a standard deviation of $0.1\beta_c$

and a deviation of κ_t two standard deviations above μ_k in the super-critical regime will revert within $\Delta T = 20$, i.e.

$$\eta = \frac{1}{\Delta T} \log \left(\frac{\mu_k + 0.2\beta_c - \mu_k}{\beta_c - \mu_k} \right) \tag{4.141}$$

and

$$\sigma_k = 0.1\beta_c \sqrt{2\eta}. \tag{4.142}$$

The two simulation differ only for the interpretation of the spin vector as explained in section 4.2.5. The first one is characterized by the interpretation with $n = N_{stocks}+1$ components, where the spin

$$\vec{S}_i = (s_{i1}, \ldots, s_{in}) \in \mathbb{S}^{n-1} \tag{4.143}$$

representing the portfolio allocation of noise trader i, has the meaning

$$s_{ia}^2 = x_{ia} \quad a = 1, \ldots, n, \tag{4.144}$$

i.e. the squared component a of the spin vector represents the fraction of wealth x_{ia} invested by the trader i in the asset a. Hence, in this case

$$n = \beta_c = 5. \tag{4.145}$$

In the second simulation instead

$$s_{ia}^2 = x_{ia} \quad \text{if } s_{ia} \geq 0 \tag{4.146}$$

represents the risky fraction invested in a, if s_{ia} is non-negative. Instead the sum of all the negative components at the aggregate level represent the risk-free fraction

$$\sum_{a:s_{ia}<0}^{n} s_{ia}^2 = x_f. \tag{4.147}$$

Hence, in this case

$$n = \beta_c = 4. \tag{4.148}$$

Moreover, the two simulations share also the same random seed. To distinguish between the two simulations we will refer in the following to the first version, with the risk-free asset represented by the last component of the vector, as "$n = N_{stocks} + 1$" version, while we will refer to the second one, with the risk-free fraction accounted at the aggregate level by the negative components, as "$n = N_{stocks}$" version. The simulation results are qualitatively similar and are presented in figure 4.8, 4.9, 4.10, and 4.11.

Figure 4.8: Ornstein-Uhlenbeck kappa simulation, "$n = N_{stocks} + 1$" version. The figure shows the time series of the four prices. The simulation is characterized by 5-components spin vectors, where the last component represents the risk-free asset.

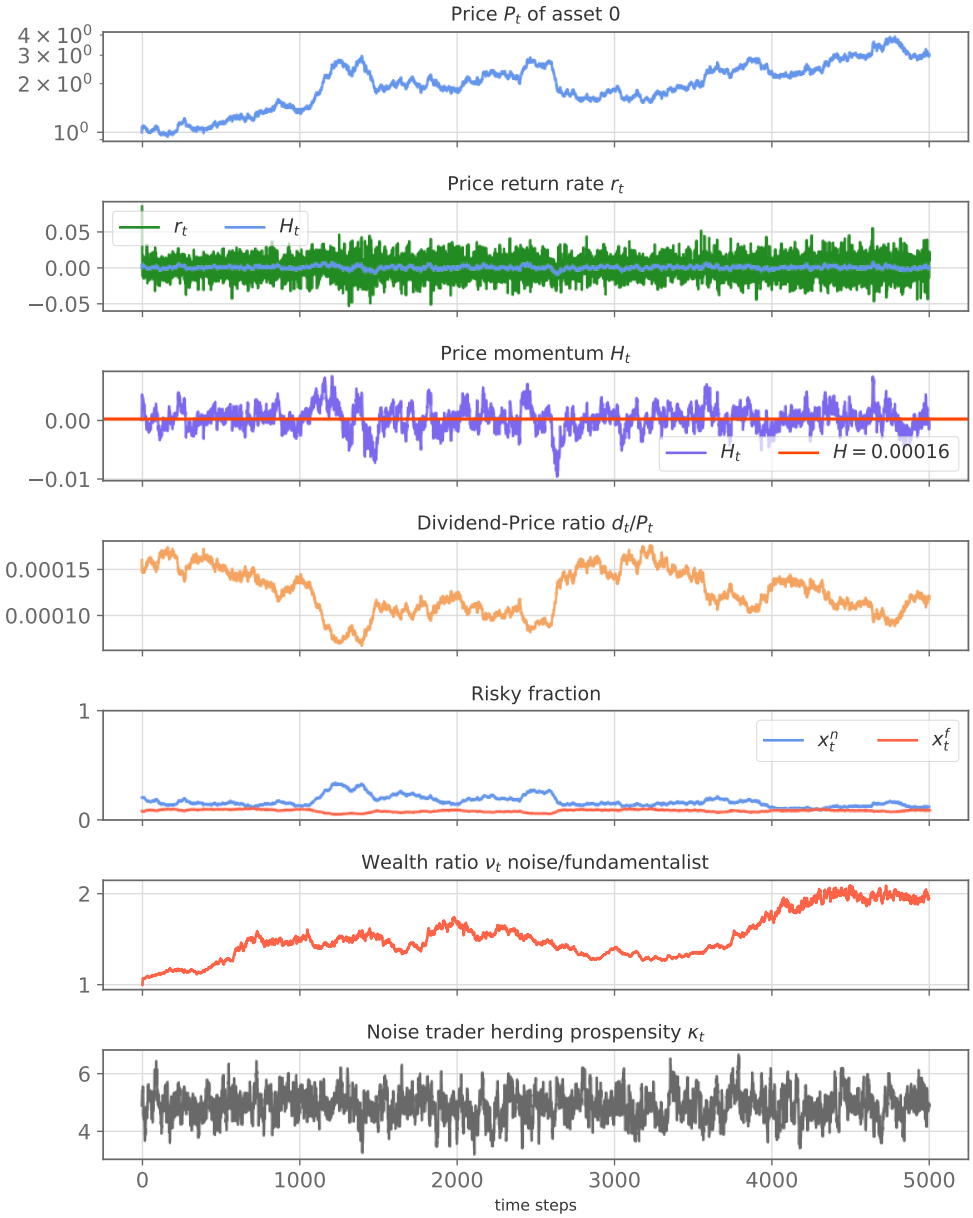

Figure 4.9: Ornstein-Uhlenbeck kappa simulation, "$n = N_{stocks} + 1$" version. The figure shows the time series of the Ornstein-Uhlenbeck kappa process and the time series of both the four risky fractions and the risk-free fraction of the noise traders class at the aggregate level. The simulation is characterized by 5-components spin vectors, where the last component represents the risk-free asset.

Figure 4.10: Ornstein-Uhlenbeck kappa simulation "$n = N_{stocks}$" version. The figure shows the time series of the four prices. The simulation is characterized by 4-components spin vectors, where the negative components at the aggregate level represents the risk-free asset.

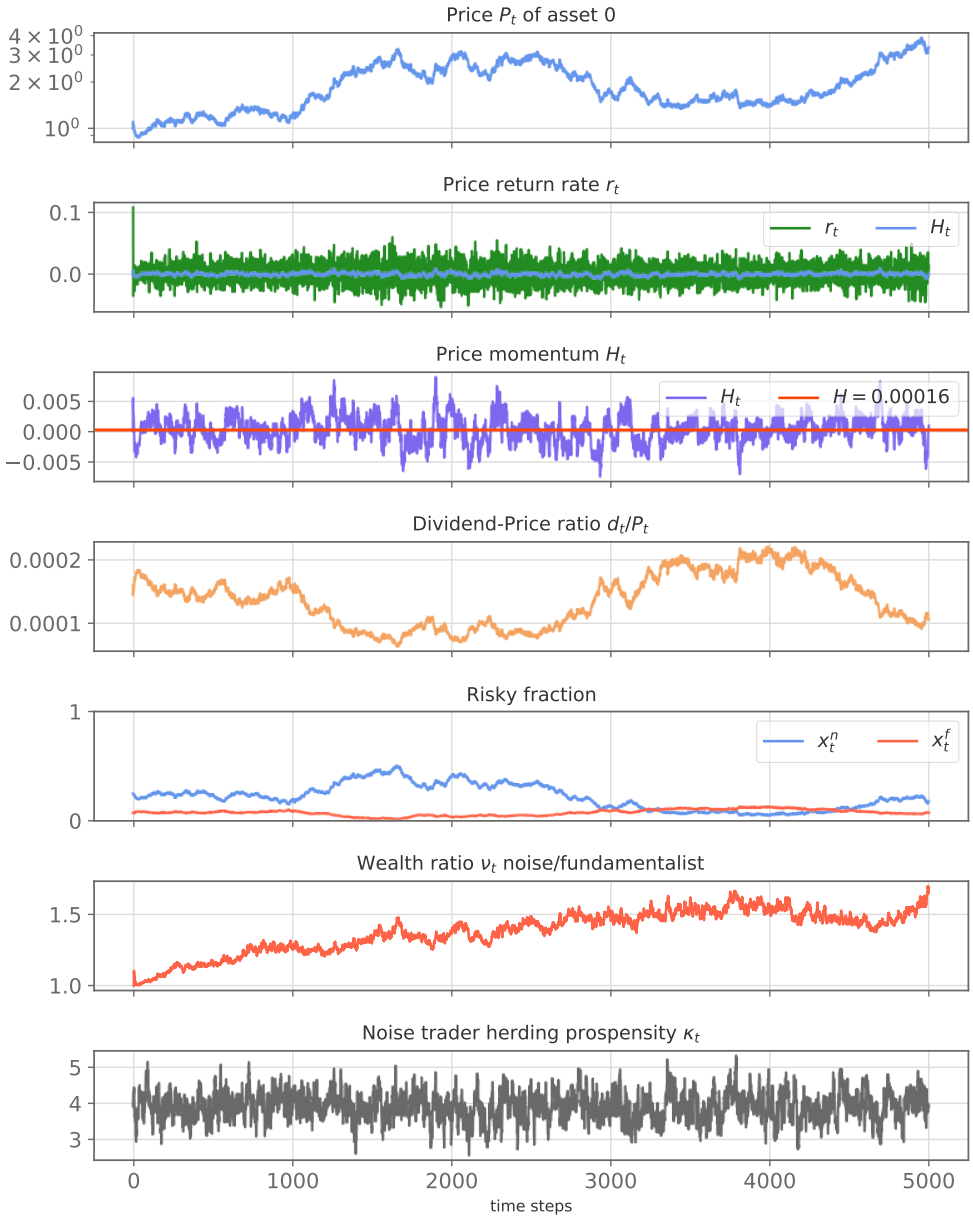

Figure 4.11: Ornstein-Uhlenbeck kappa simulation "$n = N_{stocks}$" version. The figure shows the time series of the Ornstein-Uhlenbeck kappa process and the time series of both the four risky fractions and the risk-free fraction of the noise traders class at the aggregate level. The simulation is characterized by 4-components spin vectors, where the negative components at the aggregate level represents the risk-free asset.

Most important the resulting time series are much more realistic than the Potts model ones. Yet, the bubbles are a delicate point. We can recognize some bubbles in the time series, but with respect to the original model their intensity, in particular, their height is much smaller in the order of magnitude.

The main problem which emerges from the times series is that the noise traders class, even if the polarization phenomenon is clearly present, never fully polarizes. The maximum polarization is around $x \approx 0.5$, too small to have bubbles of intensity comparable with the original model ones.

After an extensive analysis of the problem, the main point emerging is summarized by figure 4.12.

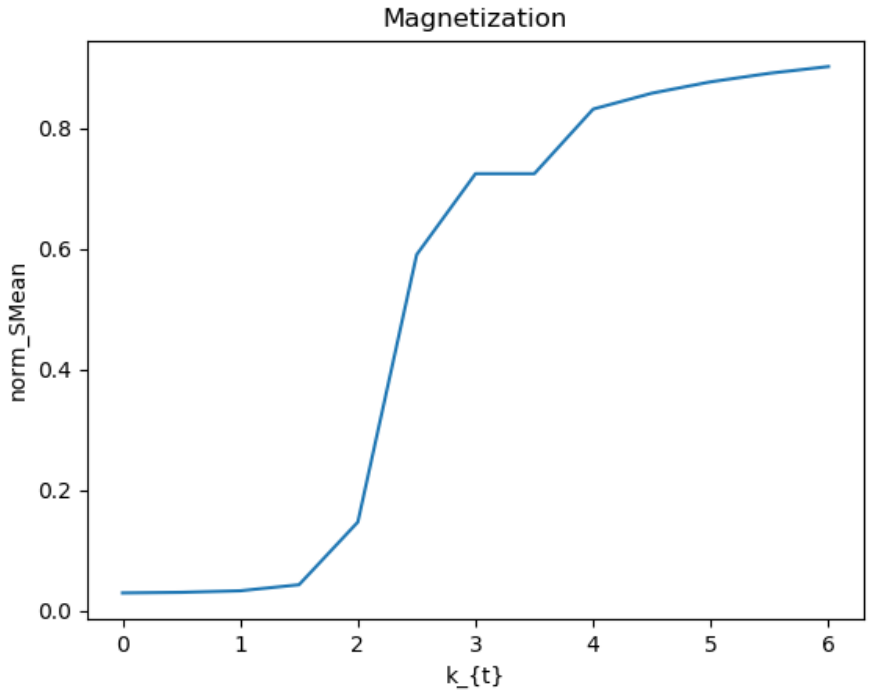

Figure 4.12: Average magnetization characterizing the constant kappa simulations for various κ values.

In figure 4.12, the average magnetization emerging in different constant kappa simulation is plotted. The average magnetization is defined as the time average over all the simulation of the value of the norm of the mean spin vector.

The simulations used to realize the plot of the average magnetization are all characterized by the "$n = N_{stocks} + 1$" version of the model (nevertheless, we find the same behavior with the other "$n = N_{stocks}$" version). Indeed, we expect that the critical kappa for these simulations is $\kappa_c = n = 5$.

Figure 4.13: Ornstein-Uhlenbeck kappa simulation "$n = N_{stocks}$" version with $\mu_k = 0.98 \cdot 2$. The figure shows the time series of the four prices. The simulation is characterized by 4-components spin vectors, where the negative components at the aggregate level represents the risk-free asset. Moreover the parameters are slightly modified with respect to the other simulations, in particular the main difference is in the mean reversion level of the kappa process $\mu_k = 0.98 \cdot 2$.

Instead, unexpectedly the transition happens around a value $\kappa_c \approx 2$. The problem represents the main issue in the applicability of this model. We will extensively discuss it in Chapter 5, hence we refer to it for a broader analysis.

Nevertheless, setting the mean value of the Ornstein-Uhlenbeck kappa process $\mu_k \approx 0.98 \cdot 2$ and varying a little bit the parameters, we obtain promising time series in terms of qualitative realistic behavior emerging from the implementation of the simulation. They are presented in figure 4.13.

4.3 A vectorial extension of the BEG model

In this section, we present a different Ising-like model for the noise traders, a vectorial extension of the BEG model. We start from the classical Blume-Emery-Griffiths (BEG) model, introduced in Blume et al. [54] and first used to model the superfluid transition of ^{3}He - ^{4}He mixtures, and we generalize it to the case of n-vector spins.

In subsection 4.3.1 we introduce the Hamiltonian of the statistical model, explaining its connections to the noise traders class. Then in subsection 4.3.2, as we have done for the Potts and $O(n)$ models, we derive the transition probabilities characterizing the stochastic dynamics of the present model and defining the investments' dynamics of the noise traders class. In doing so, we will find interesting analogies with both the $O(n)$ model and the standard Ising model. We will exploit these analogies to proceed with the derivation, yet at one point we will face a problem in normalizing consistently the transition probability derived. To find a solution to this non-trivial problem we will have to present section 4.4 and 4.5.

4.3.1 The vectorial extension of the BEG model on the fully connected graph

To model the noise traders class we consider a n-vector extension of the BEG model with an external field and Van der Waals-like interactions. In our case, $n =$ number of stocks represents the total number of risky assets.

The model is defined on the fully connected graph K_N, with N nodes and $\frac{N(N-1)}{2}$ edges. The Hamiltonian of the model is

$$H_N(\{\vec{S}_1, \dots, \vec{S}_N\}) = -\frac{J}{2N} \sum_{i,j=1}^{N} \vec{S}_i \cdot \vec{S}_j - \sum_{i=1}^{N} \vec{h} \cdot \vec{S}_i - \mu \sum_{i=1}^{N} \vec{S}_i^2 - \frac{K}{2N} \sum_{i,j=1}^{N} \vec{S}_i^2 \vec{S}_j^2, \quad (4.149)$$

where the spin

$$\vec{S}_i = (s_{i1}, \dots, s_{in}) \in \mathbb{S}^{n-1} \cup \vec{O} \quad (4.150)$$

lives on the $(n-1)$-sphere plus a point representing the null vector $(0, \dots, 0)$.

The spin vector represents the portfolio allocation of noise trader i as in the $O(n)$ model, but at odds with it, also the null vector is a valid state for the spin and represents a trader investing only in the risk-free asset. More precisely,

$$s_{ia}^2 = x_{ia} \quad a = 1, \ldots, n, \tag{4.151}$$

i.e. the squared component a of the spin vector represents the fraction of wealth x_{ia} invested by the trader i in the asset a.

The trader can alternatively decide to invest in the stock market constructing a portfolio modeled by the vector $\vec{S}_i \in \mathbb{S}^{n-1}$ satisfying $\|\vec{S}_i\| = 1$, or can decide to invest all its wealth in the risk-free asset, being effectively represented by the null vector

$$\vec{O} = (0, \ldots, 0). \tag{4.152}$$

We notice that the first two terms of the Hamiltonian coincide exactly with the $O(n)$ Hamiltonian (4.84). We will fruitfully exploit this fact since many results and computations done for the $O(n)$ model will be useful in this derivation.

4.3.2 The transition probabilities

As for the Potts and the $O(n)$ models, we want to construct the stochastic dynamics characterizing the statistical model defined by the probability distribution

$$P(\{\vec{S}_1, \ldots, \vec{S}_N\}) = e^{-\beta H_N}. \tag{4.153}$$

The stochastic dynamics is defined by the transition rates and as usual, we derive them starting from the discrete-time Master equation and effectively setting to zero the time derivative through the detailed balance condition.

All the theoretical consideration regarding the consistency of the MCMC we are going to derive are the same as for the case of the Potts and $O(n)$ models and for them, we refer to sections 4.1.2 and 4.2.2.

The derivation of the transition probabilities

There are two kinds of moves for which we have to compute the respective transition rates. The moves representing a reallocation of the trader portfolio and the moves representing the traders entering or exiting the stocks market moving from or to the risk-free asset.

The first kind of moves are modeled by a rotation of the spin on the hypersphere $\mathbb{S}^{n-1}$. The detailed balance condition for them reads

$$\frac{W(\vec{A} \to \vec{B})}{W(\vec{B} \to \vec{A})} = \frac{P(\vec{B})}{P(\vec{A})}. \tag{4.154}$$

Remarkably we notice that being the norm of the vector equals to one both before and after the move, the third and fourth terms of the Hamiltonian are not affected by the move and the corresponding terms in $P(\vec{A})$ and $P(\vec{B})$ exactly simplify. The ratio defining the detailed balance condition (4.156) coincides exactly with the one for the $O(n)$ model. The same derivation as in section 4.2.2 leads to the $O(n)$ result

$$W(\vec{A} \to \vec{B}) = \mathcal{P}(\vec{A} \to \vec{B}) = \frac{e^{\kappa_t \left(\frac{\sum_i \vec{S}_i \cdot \vec{B}}{N} + \vec{H} \cdot \vec{B} \right)}}{\int_{\vec{K} \in \mathbb{S}^{n-1}} e^{\kappa_t \left(\frac{\sum_i \vec{S}_i \cdot \vec{K}}{N} + \vec{H} \cdot \vec{K} \right)}}. \tag{4.155}$$

The second kind of moves is instead different. The choices of a trader to enter or exit the stock market are modeled by a move from the null vector to a point of the hypersphere and vice versa respectively. The detailed balance condition for this kind of moves reads

$$\frac{W(\vec{A} \to \vec{O})}{W(\vec{O} \to \vec{A})} = \frac{P(\vec{O})}{P(\vec{A})}. \tag{4.156}$$

Using the definition of conditional probability we get

$$\frac{P(\vec{O})}{P(\vec{A})} = \frac{P(\vec{S}_l = \vec{O} \mid \{\vec{S}_1, \ldots, \vec{S}_{l-1}, \vec{S}_{l+1}, \ldots, \vec{S}_N\}}{P(\vec{S}_l = \vec{A} \mid \{\vec{S}_1, \ldots, \vec{S}_{l-1}, \vec{S}_{l+1}, \ldots, \vec{S}_N\}} = \frac{\frac{P(\vec{S}_l = \vec{O}, \{\vec{S}_1, \ldots, \vec{S}_{l-1}, \vec{S}_{l+1}, \ldots, \vec{S}_N\}}{P(\{\vec{S}_1, \ldots, \vec{S}_{l-1}, \vec{S}_{l+1}, \ldots, \vec{S}_N\})}}{\frac{P(\vec{S}_l = \vec{A}, \{\vec{S}_1, \ldots, \vec{S}_{l-1}, \vec{S}_{l+1}, \ldots, \vec{S}_N\}}{P(\{\vec{S}_1, \ldots, \vec{S}_{l-1}, \vec{S}_{l+1}, \ldots, \vec{S}_N\})}}. \tag{4.157}$$

Simplifying the denominators we get the ratio between the joint probabilities, which we can explicitly compute as

$$\begin{aligned}
&\frac{P(\vec{S}_l = \vec{O}, \{\vec{S}_1, \ldots, \vec{S}_{l-1}, \vec{S}_{l+1}, \ldots, \vec{S}_N\}}{P(\vec{S}_l = \vec{A}, \{\vec{S}_1, \ldots, \vec{S}_{l-1}, \vec{S}_{l+1}, \ldots, \vec{S}_N\}} \\
&\quad = \frac{\frac{1}{Z} e^{-\beta(-\frac{J}{2N} \sum_{i \neq l} \sum_{j \neq l} \vec{S}_i \cdot \vec{S}_j - \frac{J}{2N} \sum_j \vec{O} \cdot \vec{S}_j - \frac{J}{2N} \sum_i \vec{S}_i \cdot \vec{O} + \frac{J}{2N} \vec{O} \cdot \vec{O} - \sum_{i \neq l} \vec{h} \cdot \vec{S}_i - \vec{h} \cdot \vec{O})}}{\frac{1}{Z} e^{-\beta(-\frac{J}{2N} \sum_{i \neq l} \sum_{j \neq l} \vec{S}_i \cdot \vec{S}_j - \frac{J}{2N} \sum_j \vec{A} \cdot \vec{S}_j - \frac{J}{2N} \sum_i \vec{S}_i \cdot \vec{A} + \frac{J}{2N} \vec{A} \cdot \vec{A} - \sum_{i \neq l} \vec{h} \cdot \vec{S}_i - \vec{h} \cdot \vec{A})}} \\
&\quad \cdot \frac{e^{-\beta(-\mu \sum_{i \neq l} \vec{S}_i^2 - \mu \vec{O}^2 - \frac{K}{2N} \sum_{i \neq l} \sum_{j \neq l} \vec{S}_i^2 \vec{S}_j^2 - \frac{K}{2N} \sum_j \vec{O}^2 \vec{S}_j^2 - \frac{K}{2N} \sum_i \vec{S}_i^2 \vec{O} + \frac{K}{2N} \vec{O}^2 \vec{O}^2)}}{e^{-\beta(-\mu \sum_{i \neq l} \vec{S}_i^2 - \mu \vec{A}^2 - \frac{K}{2N} \sum_{i \neq l} \sum_{j \neq l} \vec{S}_i^2 \vec{S}_j^2 - \frac{K}{2N} \sum_j \vec{A}^2 \vec{S}_j^2 - \frac{K}{2N} \sum_i \vec{S}_i^2 \vec{A} + \frac{K}{2N} \vec{A}^2 \vec{A}^2)}}.
\end{aligned} \tag{4.158}$$

Simplifying the common factors at numerator and denominator and neglecting $\frac{J}{2N}$ and $\frac{K}{2N}$, negligible for large N, we get

$$\frac{P(\vec{O})}{P(\vec{A})} = e^{-\beta \left(J \frac{\sum_i \vec{S}_i \cdot \vec{A}}{N} + \vec{h} \cdot \vec{A} + \mu + \frac{K}{N} \sum_i \vec{S}_i^2 \right)}. \tag{4.159}$$

We set $J = 1$ and $K = 1$ and we identify the inverse temperature with the herding propensity $\beta = \kappa_t$. The external field vector components are set equal to the corresponding price momenta $h_k = H_k$. We then finally get

$$\frac{W(\vec{A} \to \vec{O})}{W(\vec{O} \to \vec{A})} = \frac{P(\vec{O})}{P(\vec{A})} = e^{\kappa_t \left(-\left(\frac{\sum_i \vec{S}_i}{N} + \vec{h} \right) \cdot \vec{A} - \left(\mu + \frac{\sum_i \vec{S}_i^2}{N} \right) \right)}. \tag{4.160}$$

Expression (4.160) can be further elaborated as

$$\frac{1}{e^{\kappa_t \left(\left(\frac{\sum_i \vec{S}_i}{N} + \vec{h} \right) \cdot \vec{A} \right)}} e^{-\kappa_t \left(\mu + \frac{\sum_i \vec{S}_i^2}{N} \right)} = \frac{1}{e^{\kappa_t \left(\left(\frac{\sum_i \vec{S}_i}{N} + \vec{h} \right) \cdot \vec{A} \right)}} \cdot \frac{e^{-\frac{\kappa_t}{2} \left(\mu + \frac{\sum_i \vec{S}_i^2}{N} \right)}}{e^{\frac{\kappa_t}{2} \left(\mu + \frac{\sum_i \vec{S}_i^2}{N} \right)}}. \tag{4.161}$$

Now we apply the "Glauber trick" to the second ratio in the last passage. Indeed, by means of the identity

$$\frac{e^{-x}}{e^{x}} = \frac{1 - \tanh x}{1 + \tanh x} \tag{4.162}$$

we finally get

$$\frac{W(\vec{A} \to \vec{O})}{W(\vec{O} \to \vec{A})} = \frac{1}{e^{\kappa_t \left(\left(\frac{\sum_i \vec{S}_i}{N} + \vec{h} \right) \cdot \vec{A} \right)}} \cdot \frac{\frac{1}{2} \left(1 - \tanh \frac{\kappa_t}{2} \left(\mu + \frac{\sum_i \vec{S}_i^2}{N} \right) \right)}{\frac{1}{2} \left(1 + \tanh \frac{\kappa_t}{2} \left(\mu + \frac{\sum_i \vec{S}_i^2}{N} \right) \right)} \tag{4.163}$$

We recognize in the second ratio the classical Glauber transition rates for a mean-field Ising model with a uniform constant external field μ and a halved coupling intensity $K = \frac{J_{Ising}}{2}$, where J_{Ising} is the coupling of the standard mean-field Ising model. This is not surprising, since the third and fourth elements on the Hamiltonian (4.149) are actually an effective mean-field Ising model

$$H_{3,4}(\{\vec{S}_1, \ldots, \vec{S}_N\}) = -\mu \sum_{i=1}^{N} \vec{S}_i^2 - \frac{K}{2N} \sum_{i,j=1}^{N} \vec{S}_i^2 \vec{S}_j^2 = -\mu \sum_{i=1}^{N} s_i - \frac{K}{2N} \sum_{i,j=1}^{N} s_i s_j, \tag{4.164}$$

where the spins takes values $s_i = 0{,}1$. More precisely, $s_i = 0$ represents a trader investing in the risk-free asset while $s_i = 1$ represents a trader investing in the stock market. Moreover, $s_i^+ - s_i^- = 1 - 0 = 1$, i.e. half the value for the classical Ising model, from which the effective halving of the coupling intensity.

The first ratio in (4.163) instead exactly coincides with the rates characterizing the $O(n)$ model.

However, splitting the expression (4.163) into two well-defined transition probabilities is not an easy task. In particular, correctly considering the normalization of the probabilities represents a tricky point.

The solution we have adopted implies a different interpretation of the spin vector and a slightly different derivation of the transition rates. We will present it in the following.

Before that, in the next section, we focus on the modeling of the social imitation phenomenon between the traders and their relation with the portfolio interpretation of the spin. This is a fundamental point in the construction of our model. By now we have considered it implicitly every time we have introduced a new Hamiltonian. In the next section, we focus explicitly on it, both for its importance for the aforementioned alternative derivation and its stand-alone significance for the modeling effectiveness.

4.4 The social imitation mechanism in the noise traders class

In this section, we focus on the modeling of the social imitation phenomenon between the traders and its relation with the portfolio interpretation of the spin.

Fundamentally, the concept underlying every possible modeling of the social imitation mechanism among two noise traders is constituted by the minimization of some sort of distance between their investment decisions.

The problem of defining the best representation of the imitation behavior boils down to defining the best representation of the investment decisions and associating to it the correct notion of distance, the two being closely related.

In absolute generality, what we are searching for is a distance, also called a metric, which mathematically is a function

$$d : X \times X \to [0, +\infty), \tag{4.165}$$

which associates to each pair of elements from a set X, in our case the set of the investment representations, a non-negative real number and which just need to satisfy the three axioms of distance, i.e.

- $d(x, y) = 0 \leftrightarrow x = y$ Identity of indiscernibles,
- $d(x, y) = d(y, x)$ Symmetry,
- $d(x, y) < d(x, z) + d(z, y)$ Triangle inequality.

This gives a huge freedom in defining the function d and indeed a large number of metrics have been thoroughly studied.

For example in the Potts model analyzed in section 4.1, each noise trader decides at each time step to invest all his wealth into a single asset, then the natural representation of its investment is simply a q-state spin where q = number of assets.

In this setting, a natural choice of the distance between the investments of different traders, which the imitation mechanism tends to minimize, is the discrete distance, defined by

$$d(s_i, s_j) = \begin{cases} 1 & \text{if } s_i = s_j \\ 0 & \text{if } s_i \neq s_j. \end{cases} \tag{4.166}$$

The discrete distance together with a q-state representation of the investment decision gives rise to the Kronecker delta interaction term, characteristic of the Potts Hamiltonian

$$-\frac{J}{2N} \sum_{i,j=1}^{N} \delta_{s_i,s_j}. \tag{4.167}$$

Moving from a picture in which each trader holds just one asset at a time, to a setting where each trader can diversify its investment constructing a portfolio of different assets, the modeling is less straightforward and multiple possibilities are present.

Quite confidently we can affirm that we need a vector with many components to take into account the various investment fractions, both risky and risk-free. Yet, the best way in which the portfolio representation is implemented through the various components is not clear a priori. We have already partly addressed this issue in section 4.2.5, here we deepen its analysis.

Both in the $O(n)$ model and in the BEG model the social imitation phenomenon characterizing the noise traders class is modeled by the maximization of the dot product between the spins. For example, considering two noise traders i and j, the social imitation mechanism among them tends to "align" their investment decision, effectively maximizing the dot product between the two vectors representing their portfolios.

This dot product maximization process, modeling the social imitation, justifies the presence of the term

$$-\frac{J}{2N} \sum_{i,j=1}^{N} \vec{S}_i \cdot \vec{S}_j \tag{4.168}$$

in the Hamiltonian of the system, indeed the principle of energy minimization in this case implies exactly the maximization of the dot products. From this, also the presence of the minus sign appears clear.

This seems a rather natural choice in modeling the social imitation mechanism, yet a deeper analysis is important since this point represents one of the features at the foundation of the model itself.

Indeed, we have considered different possible solutions characterized by the different representation of the investment decisions and different distances. Among

them, we have in particular considered an interesting distance, which is the Hamming distance. Studied in the context of information theory and coding theory, the Hamming distance counts the number of different symbols at corresponding positions between two strings of equal length.

In section 4.2.5 we have discussed how the interpretation of the spin vector

$$\vec{S}_i = (s_{i1}, \ldots, s_{in}) \in \mathbb{S}^{n-1} \tag{4.169}$$

where the squared component a of the spin vector represents the fraction of wealth x_{ia} invested by the trader i in the asset a and the first $n-1$ components represent the risky assets, while the last component represents the unique risk-free asset

$$s_{ia}^2 = x_{ia} \quad a = 1, \ldots, n, \tag{4.170}$$

suffers from an unmotivated degeneracy in the portfolio representation and, more seriously, from an inconsistency with the sign of the price momenta external field.

As a possible solution we have proposed a different promising interpretation where the components of the vector

$$s_{ia}^2 = x_{ia} \quad \text{if } s_{ia} \geq 0 \tag{4.171}$$

represents the risky fraction invested in a, if s_{ia} is non-negative. Instead the sum of all the negative components at the aggregate level represents the risk-free fraction

$$\sum_{a:s_{ia}<0}^{n} s_{ia}^2 = x_f. \tag{4.172}$$

With the Hamming distance we can propose a radically different solution. We define the n-components spin vector

$$\vec{S}_i = (s_{i1}, \ldots, s_{in}), \tag{4.173}$$

where each component represents a risky asset and can assume values

$$s_{ia} = \begin{cases} 1 & \text{if the trader } i \text{ invests in risky asset } a \\ -1 & \text{otherwise.} \end{cases} \tag{4.174}$$

With this definition of the spin vector, the Hamming distance becomes the proper measure of the distance between the two investment decisions, counting the number of assets for which the choice to invest or not differs among the two traders. In this picture, all the -1 components contribute to defining at the aggregate level the wealth invested in the risk-free asset.

Despite its interesting properties, this modeling suffers from a major drawback, indeed a clear notion of investment fractions in the various risky assets is missing

and a trivial interpretation where the wealth is uniformly split among the different assets, with the -1 accounting at the aggregate level for the risk-free asset, seems inappropriate.

We have considered other spin representations with different distances, like the L_1 distance or the Chebyshev distance, but in our opinion, they are less effective from the modelization point of view with respect to the Euclidean metric, which is the actual distance underlying the dot product between the spin vectors as we will show in the following.

The Euclidean distance is induced by the standard Euclidean norm

$$d(\vec{X},\vec{Y}) = \|\vec{X}-\vec{Y}\| = \sqrt{(x_1-y_1)^2+\cdots+(x_n-y_n)^2}. \tag{4.175}$$

It is easy to show that the minimization of the distance between two spin vectors is equivalent to the maximization of their dot product, indeed considering the squared Euclidean distance we have

$$(d(\vec{S_i},\vec{S_j}))^2 = \|\vec{S_i}-\vec{S_j}\|^2 = (\vec{S_i}-\vec{S_j})\cdot(\vec{S_i}-\vec{S_j}) = \|\vec{S_i}\|^2+\|\vec{S_j}\|^2-2\vec{S_i}\cdot\vec{S_j} \tag{4.176}$$

which in case of spins living on the $n-1$-sphere becomes

$$(d(\vec{S_i},\vec{S_j}))^2 = 2(1-\vec{S_i}\cdot\vec{S_j}). \tag{4.177}$$

The factor 2 and the additive constant do not affect the minimization procedure, hence the minimum for the distance is obtained maximizing the dot product.

In the next section, we move back to the vectorial BEG model and instead of trying to change the notion of distance implied in the modeling of the social imitation, we focus on the constraints in the definition of the spin vector and modifying them we propose an alternative to the $O(n)$ model. This choice will result in the fourth statistical model of the present Chapter.

4.5 A n-state extension of the BEG model

We come back to the extension of the BEG model presented in section 4.3 and, as anticipated in that section, we modify the definition of the spin vector to be able to explicitly compute the transition rates and to have a model giving rise to an interesting dynamics.

In subsection 4.5.1 we introduce the modified Hamiltonian of the n-state extension. In subsection 4.5.2 we derive the transition probabilities, commenting on their interesting connection with the Potts model and the Logit distribution. Then, in the subsection 4.5.3, we deepen again one recurrent topic of this Chapter, the average holding time. Finally, in subsection 4.5.4 we present the resulting time series and we comment on them.

4.5.1 The n-state extension of the BEG model on the fully connected graph

Starting from the Hamiltonian of the vectorial BEG model

$$H_N(\{\vec{S}_1,\ldots,\vec{S}_N\}) = -\frac{J}{2N}\sum_{i,j=1}^{N}\vec{S}_i\cdot\vec{S}_j - \sum_{i=1}^{N}\vec{h}\cdot\vec{S}_i - \mu\sum_{i=1}^{N}\vec{S}_i^2 - \frac{K}{2N}\sum_{i,j=1}^{N}\vec{S}_i^2\vec{S}_j^2 \quad (4.178)$$

we modify the definition of the spin

$$\vec{S}_i = (s_{i1},\ldots,s_{in}) \quad (4.179)$$

assuming that the vector can have either only one component equal to 1

$$\vec{S}_i = (0,1,0,\ldots,0) \quad (4.180)$$

representing a trader investing all its wealth in that specific risky asset, or all the components equal to zero

$$\vec{S}_i = (0,\ldots,0) \quad (4.181)$$

representing a trader investing in the risk-free asset. In this setting the n components of the vector represent the n risky assets.

With this new definition of the spin, the first two terms in the Hamiltonian become equivalent to the Potts model Hamiltonian

$$H_N(\{\vec{S}_1,\ldots,\vec{S}_N\}) = -\frac{J}{2N}\sum_{i,j=1}^{N}\delta_{z_i,z_j} - \sum_{k=1}^{n}h_k\sum_{i=1}^{N}\delta_{z_i,k} - \mu\sum_{i=1}^{N}\vec{S}_i^2 - \frac{K}{2N}\sum_{i,j=1}^{N}\vec{S}_i^2\vec{S}_j^2, \quad (4.182)$$

where the new variable z_i is either equal to the number of the unique non-zero component of the spin or is equal to zero in the case of a trader investing in the risk-free asset.

4.5.2 The transition probabilities

Following the same approach used for the other models, we derive the transition rates starting from the discrete-time Master Equation and then imposing the detailed balance condition. As in the derivation for the vectorial BEG model in section 4.3.2, we have to consider two kinds of moves.

The first being constituted by the reallocation of the investment inside the stock market, when the traders decide to switch from one risky asset to another one.

For this kind of moves, the detailed balance condition reads

$$\frac{W(z_i = a \to z_i = b)}{W(z_i = b \to z_i = a)} = \frac{P(z_i = b)}{P(z_i = a)}. \tag{4.183}$$

Noting that the third and fourth terms are not affected by a change of value of the spin variable z_i as long as it remains non-zero, expression (4.183) becomes

$$\frac{P(z_i = b)}{P(z_i = a)} = \frac{\frac{1}{Z}e^{-\beta(-\frac{J}{2N}\sum_{i\neq l}\sum_{j\neq l}\delta_{z_i,z_j}-\frac{J}{2N}\sum_j\delta_{z_l=b,z_j}-\frac{J}{2N}\sum_i\delta_{z_i,z_l=b}+\frac{J}{2N}\delta_{z_l=b,z_l=b})}}{\frac{1}{Z}e^{-\beta(-\frac{J}{2N}\sum_{i\neq l}\sum_{j\neq l}\delta_{z_i,z_j}-\frac{J}{2N}\sum_j\delta_{z_l=a,z_j}-\frac{J}{2N}\sum_i\delta_{z_i,z_l=a}+\frac{J}{2N}\delta_{z_l=b,z_l=b})}} \cdot \frac{e^{-\beta(-\sum_{k=1}^{q}h_k(\sum_{i\neq l}\delta_{z_i,k}+\delta_{z_l=b,k}))}}{e^{-\beta(-\sum_{k=1}^{q}h_k(\sum_{i\neq l}\delta_{z_i,k}+\delta_{z_l=a,k}))}}. \tag{4.184}$$

Which exactly coincides with the Potts model result. Indeed simplifying the common terms we get

$$\frac{P(z_i = b)}{P(z_i = a)} = e^{\beta(J\frac{\sum_i\delta_{z_i,z_l=b}-\sum_i\delta_{z_i,z_l=a}}{N}+h_b-h_a)}. \tag{4.185}$$

Splitting the exponential among the two transition rates and normalizing them to obtain well defined transition probabilities we get exactly the same result as for the Potts model, i.e. the Logit probability distribution

$$W(a \to b) = \frac{e^{\kappa_t(\frac{N_b}{N}+H_b)}}{\sum_{k=1}^{n}e^{\kappa_t(\frac{N_k}{N}+H_k)}}, \tag{4.186}$$

where N_b is equal to the number of noise traders investing in that specific risky asset and we have identified the vectorial external field with the vector of price momenta $\vec{h} = \vec{H}$.

The second possible kind of move is constituted by the moves from a risky asset to the risk-free asset and vice versa. Following the calculation for the vectorial BEG model in section 4.3.2, we have

$$\frac{W(z_i = a \to z_i = 0)}{W(z_i = 0 \to z_i = a)} = \frac{P(z_i = 0)}{P(z_i = a)} = e^{\kappa_t\left(-\left(\frac{N_a}{N}+H_a\right)-\left(\mu+\frac{\sum_i\vec{S}_i^2}{N}\right)\right)}. \tag{4.187}$$

Thanks to the effective Kronecker delta interactions, at odds with the corresponding expression for the vectorial BEG model (4.160), in formula (4.187) no dot product between vectorial quantities is present. This solves the problems related to the definition of the transition probabilities. Indeed splitting the rates

$$\frac{W(z_i = a \to z_i = 0)}{W(z_i = 0 \to z_i = a)} = \frac{1}{e^{\kappa_t\left(\frac{N_a}{N}+H_a\right)}} \cdot e^{\kappa_t\left(-\left(\mu+\frac{\sum_i\vec{S}_i^2}{N}\right)\right)} \tag{4.188}$$

we can identify the transition probabilities

$$W(z_i = a \to z_i = 0) = e^{\kappa_t\left(-\left(\mu+\frac{\sum_i \vec{S}_i^2}{N}\right)\right)} \tag{4.189}$$

and

$$W(z_i = 0 \to z_i = a) = e^{\kappa_t\left(\frac{N_a}{N}+H_a\right)}. \tag{4.190}$$

We now have to correctly normalize the probability distribution not only over all the risky assets but also over the risk-free asset. This was the main problem in the previous derivation for the vectorial BEG model, this time instead the result is readily found. For the risky assets we have

$$W(a \to b) = \frac{e^{\kappa_t(\frac{N_b}{N}+H_b)}}{\sum_{k=1}^{n} e^{\kappa_t(\frac{N_k}{N}+H_k)} + e^{\kappa_t\left(-\left(\mu+\frac{\sum_i \vec{S}_i^2}{N}\right)\right)}} \quad b \in 1,\dots,n \tag{4.191}$$

while for the risk-free asset we have

$$W(a \to 0) = \frac{e^{\kappa_t\left(-\left(\mu+\frac{\sum_i \vec{S}_i^2}{N}\right)\right)}}{\sum_{k=1}^{n} e^{\kappa_t(\frac{N_k}{N}+H_k)} + e^{\kappa_t\left(-\left(\mu+\frac{\sum_i \vec{S}_i^2}{N}\right)\right)}}. \tag{4.192}$$

We can represent both the expression in a unique form, defining

$$N_0 = -\sum_{i=1}^{N} \vec{S}_i^{\,2} \quad H_0 = -\mu \tag{4.193}$$

we get

$$W(a \to b) = \frac{e^{\kappa_t(\frac{N_b}{N}+H_b)}}{\sum_{k=0}^{n} e^{\kappa_t(\frac{N_k}{N}+H_k)}} \quad b \in 0,\dots,n \tag{4.194}$$

which is noticeably another Logit distribution over the possible investment choices.

4.5.3 The average holding time

We now discuss the implementation in the present model of the average holding time parameter t_h, which we recall to be the average number of trading days the noise trader holds its asset in absence of herding behavior. It gives us also the possibility to discuss a general issue in the implementation of this parameter.

We follow what we have done for the $O(n)$ model, i.e. each trading day, before proceeding with its trading decisions, the noise trader first decides if perform any trading moves at all or to just be inactive for that day holding its previous portfolio allocation.

The trader decides to be active with probability

$$P(active) = \min\left\{1, \frac{1}{t_h}\left(1 + \frac{\kappa_t}{\mu_k}\right)\right\} \tag{4.195}$$

where μ_k is the mean reversion level of the kappa process.

Now it comes the crucial implementation point, indeed if the trader decides to be active one could expect that the probability from which the trading decision is sampled does not take into account the asset the trader was previously holding. Yet, in this case the form of the probability distribution would break the detailed balance, indeed we would have

$$\mathcal{P}(a \to b) = P(active) \cdot \frac{e^{\kappa_t(\frac{N_b}{N} + H_b)}}{\sum_{\substack{k=0 \\ k \neq a}}^{n} e^{\kappa_t(\frac{N_k}{N} + H_k)}} \quad b \in 0, \ldots, n \tag{4.196}$$

and

$$\mathcal{P}(b \to a) = P(active) \cdot \frac{e^{\kappa_t(\frac{N_a}{N} + H_a)}}{\sum_{\substack{k=0 \\ k \neq b}}^{n} e^{\kappa_t(\frac{N_k}{N} + H_k)}} \quad a \in 0, \ldots, n \tag{4.197}$$

and the detailed balance condition would not be satisfied, since the two different normalization constants would not cancel out. Basically, the error introduced in this way would be equivalent to the error studied for the Potts model in section 4.1.2, when the parameter t_h was introduced by means of the constant $c = (t_h - 1)N_{stocks}$, which was breaking the detailed balance.

The solution is straightforward, after having sampled from a Bernoulli random variable with parameter $P(active)$, if the trader has decided to be active, its trading decision is sampled from the full probability distribution including also the asset previously held.

This is actually what has been done for the $O(n)$ model, but if in that case the probability $\mathcal{P}(\vec{A} \to \vec{A})$ had zero measure, this time the probability to hold the previous position even if the trader has decided to move is finite and need to be motivated. Nevertheless, this is reasonable from a modelization point of view, since the trader can decide a priori at the beginning of the trading day to hold its position whatever happens or can decide to actively trade but by the end of the day figure out that its previous investment decision was the best.

4.5.4 Time series description

In this section, we present a time series resulting from the implementation of the model.

Choice of parameters

The set of parameters is similar to the other models' simulations, with small differences.

	Parameters	
Assets	$n = N_{stocks} = 4$	$r_f = 4 \times 10^{-5}$
	$r_{d,i} = 1.6 \times 10^{-4}\ \forall i$	$d_{i,0} = 1.6 \times 10^{-4}\ \forall i$
	$P_{i,0} = 1\ \forall i$	$\Sigma^d_{i,i} = 1.6 \times 10^{-5}\ \forall i$
Fundamentalist traders	$W^f_0 = 10^9$	$E_{r,i} = 1.6 \times 10^{-4}\ \forall i$
	$\Sigma^f_{i,i} = 0.0004\ \forall i$	
Noise traders	$W^n_0 = 10^9$	$N_n = 1000$
	$\theta = 0.95$	$H_{i,0} = 1.6 \times 10^{-4}\ \forall i$
	$\mu = -0.5$	

Table 4.3: Set of parameters for the simulations of the extended model endowed with a n-state BEG model-like noise traders class. Their values constitute the natural generalization of the original models' one being motivated by real markets data and are mainly taken from Westphal and Sornette [18].

No correlation among the dividend processes for different risky assets is assumed. Regarding the fundamentalist traders we have

$$\Sigma^f_{i,i} = 0.0004 \quad i = 1, \ldots, 4 \tag{4.198}$$

and the correlation matrix is set equal to

$$C^f = \begin{pmatrix} 1.0 & 0.5 & 0.0 & 0.0 \\ 0.5 & 1.0 & 0.0 & 0.0 \\ 0.0 & 0.0 & 1.0 & 0.0 \\ 0.0 & 0.0 & 0.0 & 1.0 \end{pmatrix} \tag{4.199}$$

The initial investment decisions for fundamentalist and noise traders are as follows

$$x^f_0 = (0.075, 0.075, 0.075, 0.075, 0.7) \tag{4.200}$$

and

$$x^n_0 = (0.2, 0.2, 0.2, 0.2, 0.2), \tag{4.201}$$

where the last component represents the risk-free asset. The simulation is characterized by an Ornstein-Uhlenbeck kappa process defined by

$$\kappa_t - \kappa_{t-1} = \eta(\mu_k - \kappa_{t-1}) + \sigma_k v_t, \tag{4.202}$$

with mean reversion level $\mu_k = 0.98c$, where for this time series $c = 3.4$. Moreover, the mean reversion speed η and the step size σ_k are set, as in the original model [13], such that the Ornstein–Uhlenbeck process has a standard deviation of $0.1c$ and a deviation of κ_t two standard deviations above μ_k in the super-critical regime will revert within $\Delta T = 20$, i.e.

$$\eta = \frac{1}{\Delta T} \log \left(\frac{\mu_k + 0.2c - \mu_k}{c - \mu_k} \right) \tag{4.203}$$

and

$$\sigma_k = 0.1c\sqrt{2\eta}. \tag{4.204}$$

Finally an average holding time of ten trading days is imposed with the parameter $t_h = 10$.

The time series

The resulting time series, presented in figures 4.14, 4.15, 4.16, and 4.17, are interesting. Several bubbles in different assets are clearly identifiable.

Yet, an unrealistic behavior is present at the beginning of the time series, when in the first trading days the noise traders, who were investing in the risk-free asset, due to the initial condition, moves in mass towards the stock market. This phenomenon is governed by the μ parameter, which represents a measure of the risk aversion of the noise traders, minus the risk aversion to be more precise.

This is also introductory to the fundamental new feature of the present model with respect to the previous ones, an extra degree of freedom constituted by the μ parameter. The average number of noise traders investing in the risk-free asset can be tuned through this parameter, which not by chance is the equivalent of the chemical potential in the physical interpretation of the BEG model.

This concludes the presentation of the n-state extension of the BEG model and with it the present Chapter concerning the Ising-like modeling of the extended noise traders class. In this Chapter, we have proposed and analyzed four Ising-like statistical models for the noise traders, in order: a Potts model, an $O(n)$ model, a vectorial extension of the BEG model, and an n-state extension of the BEG model. We have derived their stochastic dynamics and we have discussed their strengths and weaknesses in modeling the investments' dynamics of the noise traders. In the next Chapter, we will compare the four models, to focus on one of them, in order to move to the comparison of the simulation results to the real financial markets and to the application of the model to investigate interesting financial phenomena.

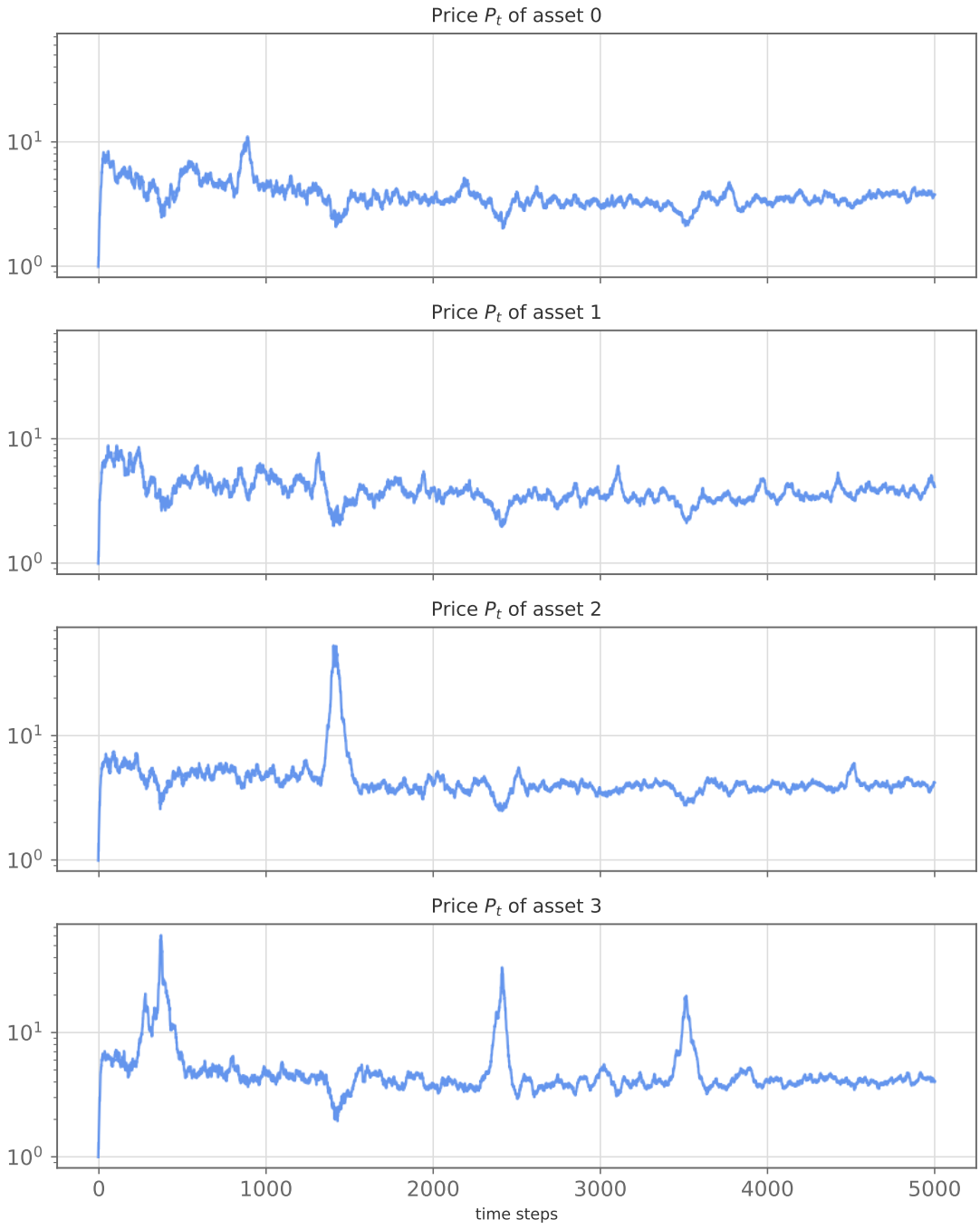

Figure 4.14: Ornstein-Uhlenbeck kappa simulation for the n-state BEG model. The figure shows the time series of the four prices. Several bubbles are clearly identifiable

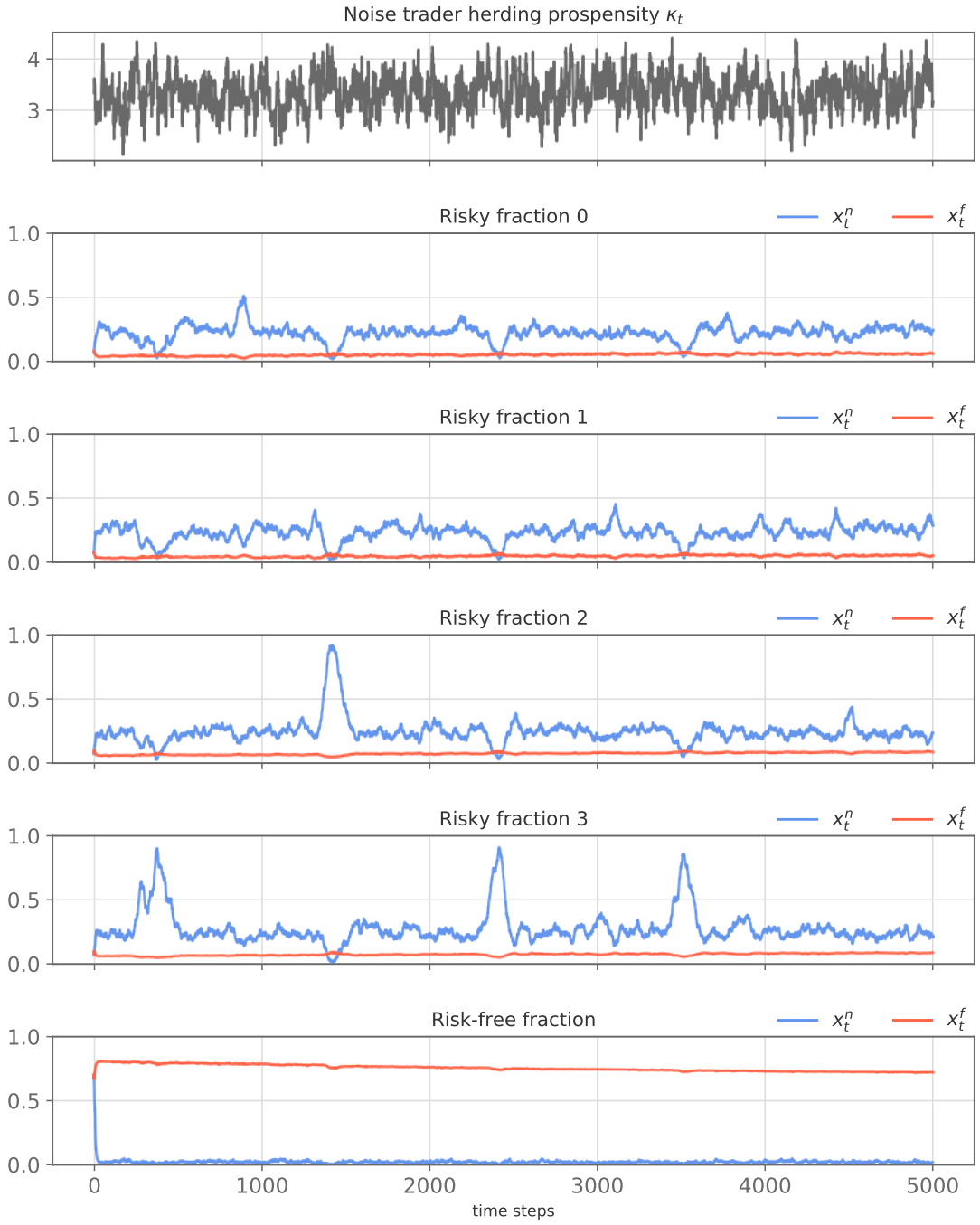

Figure 4.15: Ornstein-Uhlenbeck kappa simulation for the n-state BEG model. The figure shows the time series of the Ornstein-Uhlenbeck kappa process and the time series of both the four risky fractions and the risk-free fraction of the noise traders class at the aggregate level.

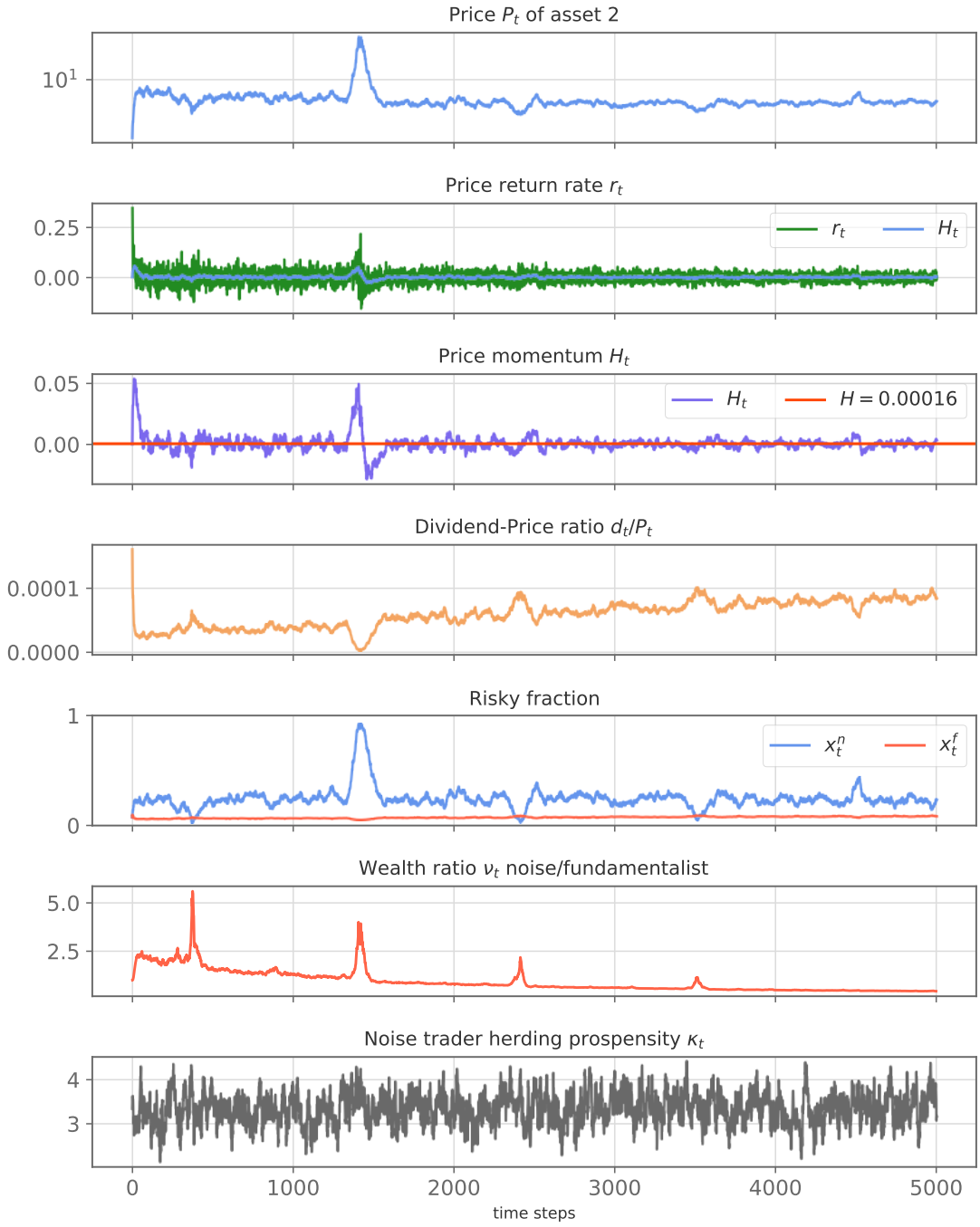

Figure 4.16: Ornstein-Uhlenbeck kappa simulation for the n-state BEG model. The figure shows the detailed time series characterizing the risky asset 2.

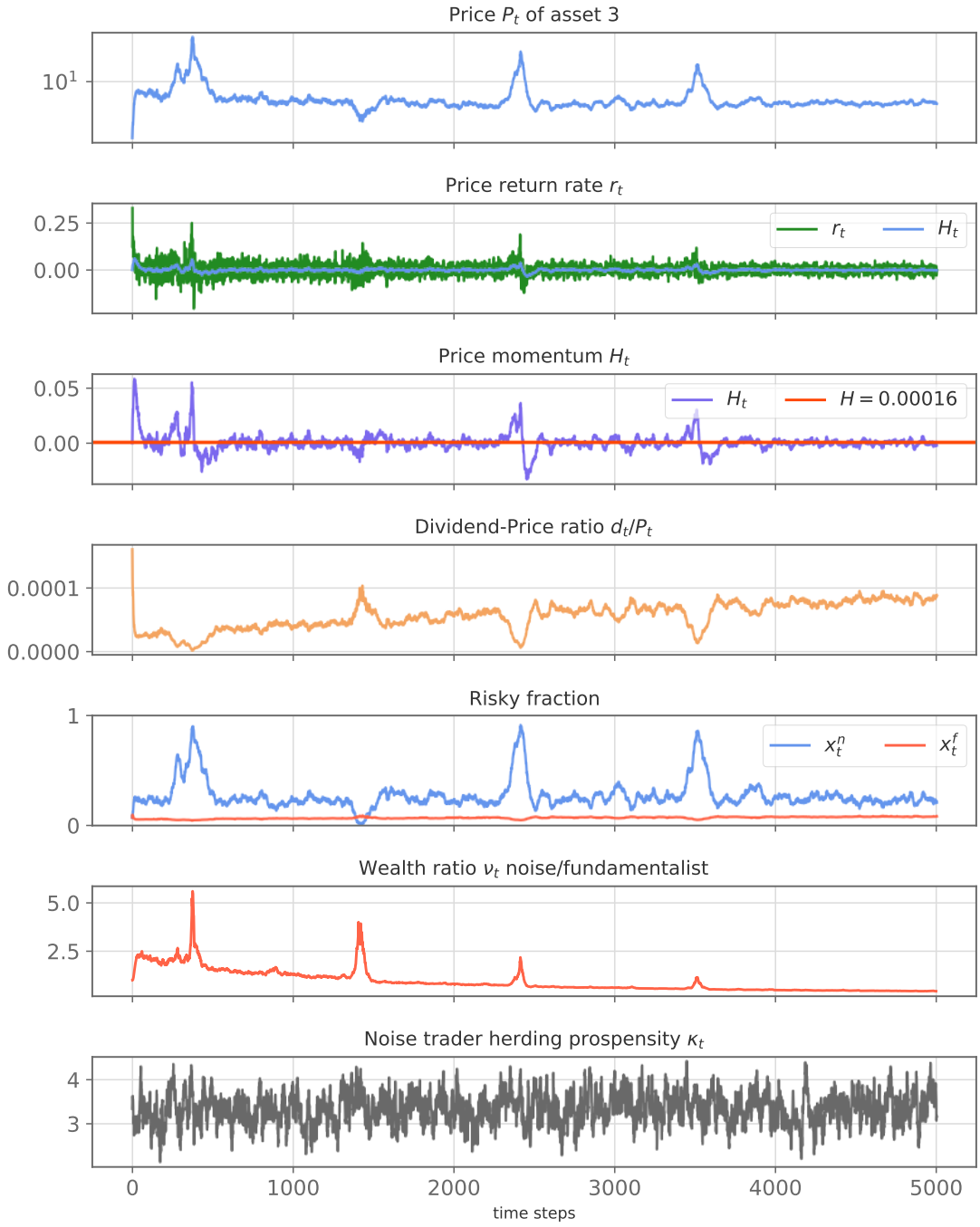

Figure 4.17: Ornstein-Uhlenbeck kappa simulation for the n-state BEG model. The figure shows the detailed time series characterizing the risky asset 3.

Chapter 5

The extended Market Model with the O(n) Noise traders class

In the last Chapter, we have introduced four Ising-like statistical models for the noise traders class. We have considered in order: a Potts model, an $O(n)$ model, a vectorial extension of the BEG model, and an n-state extension of the BEG model.

Despite their differences, all of them share the same underlying mechanism triggering and generating the bubbles. This mechanism is the same mechanism characterizing the original model and that we have deeply discussed in section 2.6. When the herding propensity parameter exceeds a certain model-dependent critical threshold, the noise traders class undergoes an actual phase transition from the disordered state, dominated by the idiosyncratic opinion to the ordered state where the class polarizes towards specific investment preferences. This interaction-driven collective behavior leads to the emergence of highly non-trivial phenomena, the bubbles. This is a typical feature of complex multi-agent systems.

Each model has its strengths and weaknesses, we have addressed many of them in the last Chapter. We now want to move to the comparison of the simulation results with the real financial markets and to the application of the model to investigate interesting financial phenomena.

To proceed in this direction we have to choose the model that best suits the modelization goal, constituting the finest middle way between modelization accuracy and manageability.

In section 5.1 we address this topic, comparing the four setups presented and deciding on the one that, in our opinion, best fits the aforementioned requirements. The selected one turns out to be the $O(n)$ model, in particular in the version where the sum of all the negative components at the aggregate level represents the

risk-free fraction. We decide to focus on it due to both the validity of the resulting price time series and to the high controllability of its behavior, connected to solid theoretical results on the model itself and the intuitive meaning of its parameters.

Nevertheless, in modeling not all that glitters is gold. We can metaphorically say that modeling, like life, is a constant balancing act. We will never find the perfect model, but we have to search for useful imperfect ones. In this situation, we have a further representation of this point. Indeed, despite this model represents the most solid one from a theoretical point of view and gives rise to a realistic and interesting dynamics, we have to address one problem in its implementation. We have already mentioned it in subsection 4.2.6, it is a problem regarding the critical point resulting from the simulations of the $O(n)$ model. We can't hide the dust under the carpet and, before moving to the application part, we will deeply discuss the topic in section 5.2. Nevertheless, we will see that despite the problem, the $O(n)$ model is still extremely valid, and that, always keeping in mind this implementation detail, we can move safely and solidly to its application. We will show that this implementation detail does not affect at all the properties of the resulting dynamics.

Reassured by this analysis, we finally move to the application part. In section 5.3 we first check the model's ability to reproduce the stylized facts of financial markets, in particular, focusing on the fat-tailed behavior of the distribution of the absolute returns in subsection 5.3.1, together with the hyperbolic decay of the autocorrelation function of the absolute returns, discussed in subsection 5.3.2.

Then the analysis is carried out in two main directions. First, in section 5.4, the extended ABM is applied to understand the mechanism behind the time synchronization of bubbles among the assets. Then in section 5.5, we present the comparison of the dynamics of the resulting returns to the one predicted by the Capital Asset Pricing Model (CAPM).

5.1 Comparison between the models

In the last Chapter we have discussed four Ising-like models to represent the noise traders class: a Potts model, an $O(n)$ model, a vectorial extension of the BEG model, and an n-state extension of the BEG model. In this section, we compare their effectiveness from the point of view of modeling a real financial market.

This is also the occasion to present a quick digression on the computational aspects of the simulations of the extended ABMs characterized by the various setups for the noise traders class. Despite the differences between them characterizing the implementation of the noise investors, they all share the same implementation regarding the other components of the market model. A large part of the work carried out in the thesis has been dedicated to the extension of the original *C++*

code written by Kohrt [17], with some modification by Ollikainen [19] and Westphal and Sornette [18], to take into accounts the enlarged multi-asset framework. The core of the extended model is still written in *C++*, following an object-oriented programming paradigm where each part of the model, (e.g. the fundamentalist traders, the risky asset, the price equation) corresponds to one specific class.

One of the advantages of such a coding strategy is that we can switch from one model with a particular structure of the noise traders class, to another one, just changing the header file in which the noise traders' strategy is implemented. Indeed, one header file for each of the Ising-like models is present.

Moreover, to have reproducible results, as for the original setup, a pseudo-random number generator with a random seed specified as a run-time parameter is used. The results of the simulation are still stored in a database using the *HDF5* high-performance data software library. Then all the analysis of the data and the plotting are performed with *Python*, in particular using the *Matplotlib*, the *Pandas* and the *Seaborn* libraries and accessing the *HDF5* database through the *Python* interfacing library *h5py*.

Coming back to the main discussion we start from the analysis of the first model presented in section 4.1, the Potts one.

As we have already discussed in subsection 4.1.6 the Potts model presents two main limits of applicability. First, it features a first-order phase transition, hence in the simulations the time series jump discontinuously and the bubbles do not grow continuously as it happens for the original Ising model, which features a second-order phase transition. Instead, the discontinuous jumps lead to a full polarization of the noise traders class in few trading days, characterizing the bubbles as unrealistic changes of regime.

Moreover, a second problem adds to the first, the particular phase transition of the mean-field Potts model is characterized by the presence of metastable states. Starting from a disordered (ordered) state below (above) the critical kappa, when the κ_t enters in the supercritical (subcritical) region, even if from a statistical point of view the thermodynamical equilibrium has changed, from a dynamical point of view the system remains frozen in a metastable disordered (ordered) state until a sufficiently strong stochastic perturbation breaks the metastability and the system jumps discontinuously to the new ordered (disordered) state, or κ_t becomes greater (smaller) than q exiting the metastability region and the metastable state ceases to be locally stable.

These two points represent real obstacles to obtain a realistic dynamics of the market model, a fortiori given that these are two intrinsic features of the statistical model under analysis. Given these facts, we will not select the Potts model in view of the application's part.

We have already anticipated that we will select the $O(n)$ model, but before moving to it we first comment on the two versions of the BEG model.

Only the second of these two versions give rise to real implementable transition probabilities. Indeed, we recall that the transition probabilities derived from the vectorial extension of the BEG model, presented in 4.3, were characterized by huge difficulties in performing a correct normalization procedure of them. Moreover, this was the very problem that pushed us to move to sections 4.4 and 4.5, and eventually to present the second extension of the BEG model.

Discarded the first version of the extended BEG model, we then move to the aforementioned second one, presented in section 4.5. This time the transition rates can be easily normalized and the stochastic dynamics generated by them can be implemented. The resulting time series presented in subsection 4.5.4 are realistic and present several bubbles in the different assets. Moreover, the model features a further important parameter with respect to the previous ones, the μ parameter. It represents a measure of the risk aversion of the noise traders, a risk seeking parameter to be more precise. The average number of noise traders investing in the risk-free asset can be tuned through this parameter.

On the one hand, this is an interesting possibility, since the presence of μ allows the explicit modeling of a risk aversion trait for the noise traders. On the other hand, this quantity represents a further degree of freedom for which the empirical calibration is difficult. The presence of this parameter results, through the Hamiltonian 4.178 in which it enters, in a complex Statistical Physics picture, characterized by phase transitions of different natures (first and second-order) depending on the value of the parameters entering in the Hamiltonian, together with the presence of another important object studied in Statistical Physics, a tricritical point.

The complex picture emerging would require a large theoretical investigation with the tools of Statistical Physics (e.g. the linear stability analysis of the mean value dynamical equations, introduced in subsection 4.1.4, and the Landau approach, discussed in subsection 4.1.5), to clarify the important properties that could have an impact on the dynamics of the bubbles. The task would be challenging and time-consuming, but also extremely interesting from a theoretical point of view.

Nonetheless, this goes beyond the scope of the present work, indeed at this point, we want to favor a model which is both effective in generating realistic time series and highly controllable, to be able to use it as a sharp and flexible instrument in the analysis of complex financial phenomena, how are the bubbles.

Proceeding with this latter model would be forced and clumsy, given the little theoretical mastery that we have on it and the presence of a further parameter that should be deeply discussed and motivated from a modelization point of view. On the other hand, we have an extremely effective model, on which we have a large theoretical knowledge and an intuitive motivation for its parameters, it is the $O(n)$ model. At this point it is clear why we decided to proceed with it, postponing the anyway interesting discussion on the n-state BEG model to a future work.

Summarizing, after careful analysis, we decided to work with the $O(n)$ model due to both the validity of the resulting price time series and to the high controllability of its behavior, connected to solid theoretical results on the model itself and the intuitive meaning of its parameters.

In particular, we decided to proceed with the the version of the $O(n)$ model where the sum of all the negative components at the aggregate level represents the risk-free fraction. This interpretation of the spin vector is more consistent with respect to the one with $n-1$ risky components and the last one risk-free. First, because it does not introduce any unmotivated degeneracy in the portfolio's representation and it does take into account the sign of the price momentum in a coherent way. Moreover, it is easier to be understood intuitively from the point of view of bullish vs bearish attitudes towards the assets and does not consider the risk-free asset in the same way as any other risky asset, which would be bad from a modelization point of view.

We now briefly review the $O(n)$ model presented in section 4.2 underlining the characteristic of the spin vector's interpretation we use.

The Hamiltonian of the model is

$$H_N(\{\vec{S}_1, \ldots, \vec{S}_N\}) = -\frac{J}{2N} \sum_{i,j=1}^{N} \vec{S}_i \cdot \vec{S}_j - \sum_{i=1}^{N} \vec{H} \cdot \vec{S}_i \tag{5.1}$$

where the spin

$$\vec{S}_i = (s_{i1}, \ldots, s_{in}) \in \mathbb{S}^{n-1} \tag{5.2}$$

lives on the $(n-1)$-sphere and represents the portfolio allocation of noise trader i. More precisely,

$$s_{ia}^2 = x_{ia} \quad \text{if } s_{ia} \geq 0 \tag{5.3}$$

represents the risky fraction invested in a, if s_{ia} is non-negative. Instead the sum of all the negative components at the aggregate level represent the risk-free fraction

$$\sum_{a:s_{ia}<0}^{n} s_{ia}^2 = x_f. \tag{5.4}$$

The modeling is consistent since $\vec{S}_i$ satisfies $\|\vec{S}_i\| = 1$, i.e. at each time step the investment fractions for each noise trader correctly sum to one,

$$\sum_{a=1}^{n} x_{ia} = 1. \tag{5.5}$$

We notice that in this interpretation n = number of stocks. A vectorial external field $\vec{h}$ of price momenta acts on each spin, in particular, H_k represents the price momentum of the risky asset k.

In section 4.2.2 we have derived the transition rates defining the stochastic dynamics of the model. We report here the final result of the derivation, the transition probability from a portfolio $\vec{A}$ to a different portfolio $\vec{B}$ is given by

$$W(\vec{A} \to \vec{B}) = \mathcal{P}(\vec{A} \to \vec{B}) = \frac{e^{\kappa_t \left(\frac{\sum_i \vec{S}_i \cdot \vec{B}}{N} + \vec{H} \cdot \vec{B} \right)}}{\int_{\vec{K} \in \mathbb{S}^{n-1}} e^{\kappa_t \left(\frac{\sum_i \vec{S}_i \cdot \vec{K}}{N} + \vec{H} \cdot \vec{K} \right)}}. \tag{5.6}$$

Generating the stochastic dynamics from these transition rates is a delicate task as already largely discussed in sections 4.2.2. We have presented two methods to derive an algorithm to sample from this multivariate distribution and hence to implement the simulation of the noise traders class dynamics.

In particular in subsection 4.2.3, we have presented a method based on the McFadden result for the Logit distribution, while in subsection 4.2.4, we have presented a method exploiting the geometric symmetries of the multivariate distribution.

Generating the stochastic dynamics of the $O(n)$ model from this multivariate probability density is a delicate point. Moreover, as anticipated, we need to tackle directly a problem regarding the second approach we have set aside so far. This will be the main topic of the next section.

5.2 Generating the stochastic dynamics of the O(n) model: McFadden result approach vs geometric symmetries approach

The stochastic dynamics characterizing the noise traders investment's decisions in the $O(n)$ setup is governed by the transition probabilities

$$W(\vec{A} \to \vec{B}) = \mathcal{P}(\vec{A} \to \vec{B}) = \frac{e^{\kappa_t \left(\frac{\sum_i \vec{S}_i \cdot \vec{B}}{N} + \vec{H} \cdot \vec{B} \right)}}{\int_{\vec{K} \in \mathbb{S}^{n-1}} e^{\kappa_t \left(\frac{\sum_i \vec{S}_i \cdot \vec{K}}{N} + \vec{H} \cdot \vec{K} \right)}}. \tag{5.7}$$

To generate the dynamics of our model we have to sample realizations of the random vector $\vec{B} = (B_1, \ldots, B_n)$ from the multivariate probability distribution (5.7). Unfortunately, constructing a sampling procedure is difficult due to the high dimensionality of the distribution and to the non-trivial relation between the components of the random vector $\sum_{k=1}^{n} B_k^2 = 1$. In subsection 4.2.3 and 4.2.4, we have proposed two methods to address this task.

The first method based on the McFadden result for the Logit distribution, despite the interesting connection with Decision Theory upon which has been built,

is really expensive from a computational point of view and hence not well scalable in the number of assets.

To react to this problem, we have developed the second method based instead on the symmetry properties of the multivariate probability distribution (5.7). This second method has been proved promising, being fast and well scalable with the number of risky assets. Indeed, all the simulations of the $O(n)$ model presented in section 4.2 were obtained with its implementation.

Nevertheless, at the end of the aforementioned section, in particular in subsection 4.2.6 we have commented that the main problem emerging from the times series was that the noise traders class, even if the polarization phenomenon was clearly present, never fully polarized. The maximum polarization was around $x \approx 0.5$, too small to have bubbles of intensity compared with the original model ones. Eventually, we have led back the problem to the fact that unexpectedly the phase transition happened around a value $\kappa_c \approx 2$, even if the model was featuring $n = 5$ components and hence we would have expected a critical value $\kappa_c = 5$. We have said that we couldn't hide the dust under the carpet and, before moving to the application of the model, we should have discussed deeply this problem. The time to do that has come.

We briefly recall here the ideas under the formulation of the simulation method based on the symmetry properties of the transition probabilities. In particular, at odds with the derivation presented in subsection 4.2.4, here we focus on the case of non-linear rates, showing that the resulting algorithm is completely equivalent.

The method is constituted by two steps. In the first, we sample an angle theta from a univariate distribution and then in the second we sample uniformly at random from a particular hypersphere $\mathbb{S}^{n-2}$, a subset of the original space of choices $\mathbb{S}^{n-1}$.

We first make explicit the symmetry property of the dot product entering the non-normalized form of the density function (5.7), expressing it in terms of the angle θ between the vector

$$\vec{M} := \frac{\sum_i \vec{S}_i}{N} + \vec{H} \tag{5.8}$$

and the vector $\vec{B}$. It is always possible to define a unique angle between two vectors in any inner product space and in particular in the Euclidean space $\mathbb{R}^n$ to which our vector belongs to. Hence, we can write

$$P(\theta) = e^{\kappa_t \|\vec{M}\| \cos\theta}, \tag{5.9}$$

since the norm of $\vec{B}$ is exactly equals to one.

The sets of equiprobable choices, i.e. equiprobable vectors $\vec{B}$, are defined by the

conditions

$$\begin{cases} \frac{1}{\|\vec{M}\|}\vec{M}\cdot\vec{B} = \cos\theta \\ \|\vec{B}\| = 1 \end{cases} \tag{5.10}$$

the first defining an hyperplane in $\mathbb{R}^n$, the second a $(n-1)$-sphere.

We proceed using the beautiful geometric property that the intersection of a $(n-1)$-sphere and a n-dimensional hyperplane, is still a hypersphere, yet of one less dimension. Indeed, the system (5.10) defines a $(n-2)$-sphere in $\mathbb{R}^n$, with centre

$$\vec{C} = \cos\theta\frac{1}{\|\vec{M}\|}\vec{M} \tag{5.11}$$

and radius

$$r = \sqrt{1-\cos^2\theta} = \sin\theta. \tag{5.12}$$

First of all, we focus on the angle θ. This time the expression (5.9) is always non-negative. Hence, we can directly sample from it with rejection sampling without introducing any approximation. The rejection sampling method is presented in the following algorithm.

Algorithm 6: Rejection sampling from the non-linear $P(\theta)$ distribution

Result: An angle θ sampled from $P(\theta)$
while $(u * e^{\kappa_t\|\vec{M}\|}) > e^{\kappa_t\|\vec{M}\|\cos\theta}$ **do**
  $\theta = Uniform(0,1) * 2\pi$;
  $u = Uniform(0,1)$
end
return θ;

We can notice that we only difference compared to algorithm 3, is constituted by the argument of the while condition. Ultimately, this is the only difference between the non-linear and the linearized probabilities implementations.

Now that we have correctly sampled the value for the angle, we have to choose a vector uniformly at random from the equiprobable set defined by that angle. The method to do that has been detailed presented in subsection 4.2.4, here we review the main points. We generate uniformly at random a vector on the hypersphere $\mathbb{S}^{n-2}$ through algorithm 1. The resulting vector

$$\vec{\mathcal{B}}^*_{n-1} = \frac{1}{\|(\mathcal{N}_1(0,1),\dots\mathcal{N}_{n-1}(0,1))\|}\Big(\mathcal{N}_1(0,1),\dots\mathcal{N}_{n-1}(0,1)\Big) \tag{5.13}$$

is uniformly distributed on $\mathbb{S}^{n-2}$. We add one extra zero component at the beginning of the vector to have a vector in $\mathbb{R}^n$. The new vector is

$$\vec{\mathcal{B}}^*_{n} = \frac{1}{\|(\mathcal{N}_1(0,1),\dots\mathcal{N}_{n-1}(0,1))\|}\Big(0,\mathcal{N}_2(0,1),\dots\mathcal{N}_{n}(0,1)\Big). \tag{5.14}$$

Moreover, the hypersphere has to be translated and its radius rescaled following (5.11) and (5.12). Finally, the $\mathbb{S}^{n-2}$ hypersphere will correctly represent the intersection between the higher dimensional $\mathbb{S}^{n-1}$ hypersphere and the hyperplane only after it will be rotated in such a way that the unit versor, corresponding to the extra component added in (5.14), will be rotated to the direction of the normalized vector $\frac{1}{\|\vec{M}\|}\vec{M}$.

We construct the orthogonal matrix R representing the rotation of the unit versor

$$\vec{X} = (1, 0, 0, \ldots, 0), \tag{5.15}$$

to the direction of the vector $\frac{1}{\|\vec{M}\|}\vec{M}$ using an approach based on Givens rotations, for which we thoroughly refer to Zhelezov [53].

Eventually, the choice vector $\vec{B}$ sampled from the distribution (4.107), representing the noise trader's portfolio reallocation, is given by

$$\vec{B} = \sin\theta R\vec{\mathcal{B}}^*_n + \cos\theta\frac{1}{\|\vec{M}\|}\vec{M}. \tag{5.16}$$

Summarizing, the sampling algorithm is as follows.

Algorithm 7: Simulating the investment choice for a noise trader (non-linear transition probabilities)

Result: A vector $\vec{B}$ representing the new portfolio
sample an angle θ from $P(\theta)$ using Algorithm 6;
sample uniformly at random a vector $\vec{\mathcal{B}}^*_{n-1}$ on $\mathbb{S}^{n-2}$;
$\vec{\mathcal{B}}^*_n = (0, \vec{\mathcal{B}}^*_{n-1}) \in \mathbb{S}^{n-1}$;
construct the rotation matrix R following [53];
$\vec{B} = \sin\theta R\vec{\mathcal{B}}^*_n + \cos\theta\frac{1}{\|\vec{M}\|}\vec{M}$;
return $\vec{B}$;

The derivation appears to be solid and the algorithm performs very well. Nevertheless, as commented in subsection 4.2.6, albeit modeling in the correct way the phase transition characterizing the noise traders class, the algorithm locates it at an incorrect value κ_c.

Comparing figures 5.1, 5.2, 5.3, and 5.4, the problem is clear.

The plots are obtained from simulations characterized by a constant value of the kappa process κ, reported on the abscissa. Moreover, we have set to zero the external field effectively decoupling the noise traders class from the rest of the market model. Doing that, the part of the model representing the noise traders becomes completely equivalent to a fully-connected $O(n)$ model without an external field. Hence, the resulting dynamics is effectively the actual dynamics

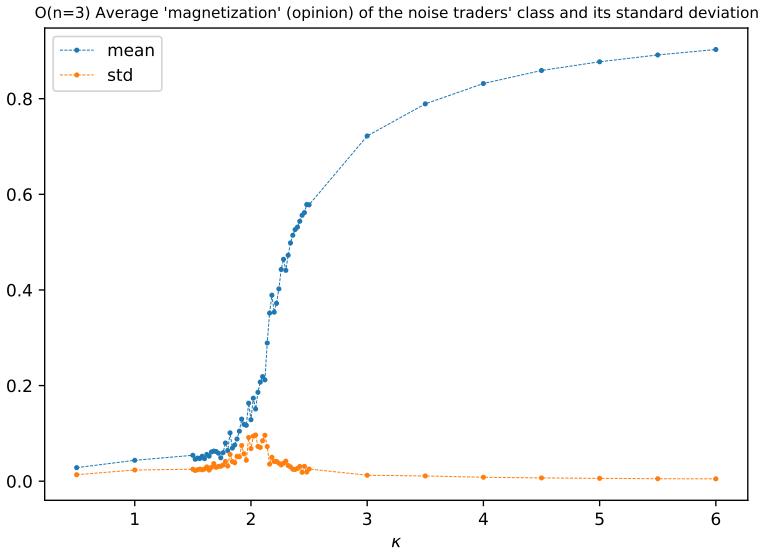

Figure 5.1: Time-average and standard deviation of the magnetization (norm of the mean spin vector of that trading day) of the noise traders class, characterizing the constant kappa simulations for various κ values. The model simulated is the $O(n = 3)$, using the geometric symmetries approach.

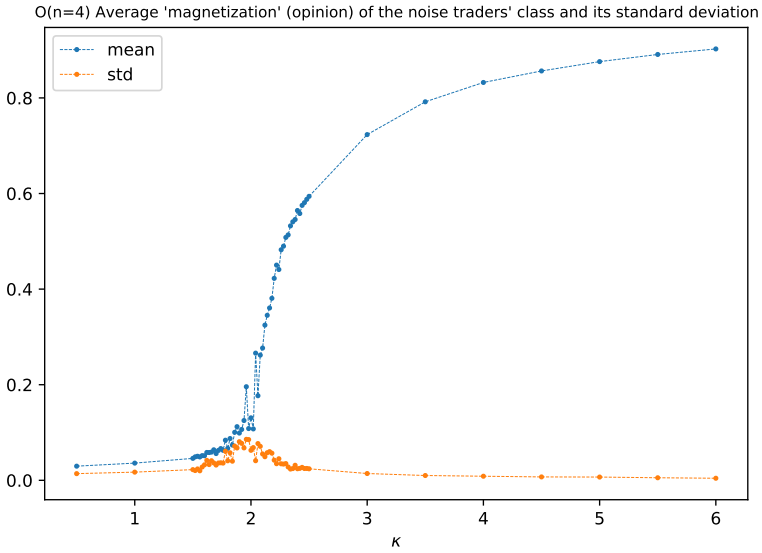

Figure 5.2: $O(n = 4)$ geometric symmetries approach. We refer to figure 5.1 for a detailed description.

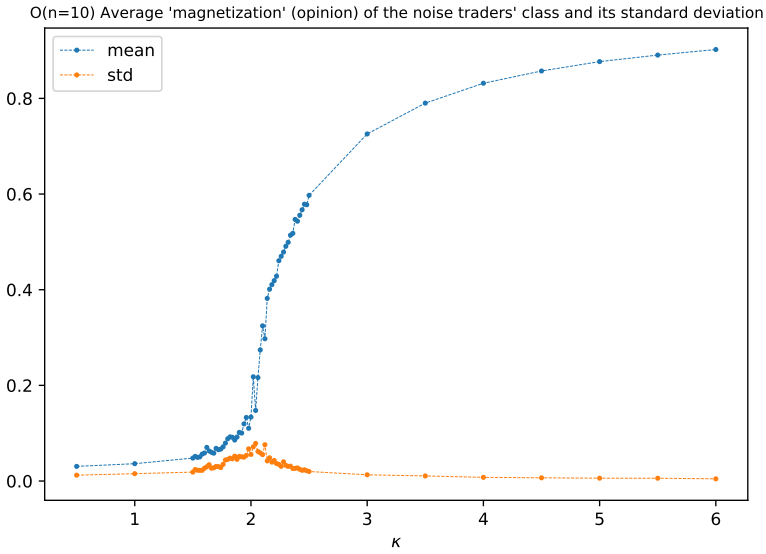

Figure 5.3: $O(n = 10)$ geometric symmetries approach. We refer to figure 5.1 for a detailed description.

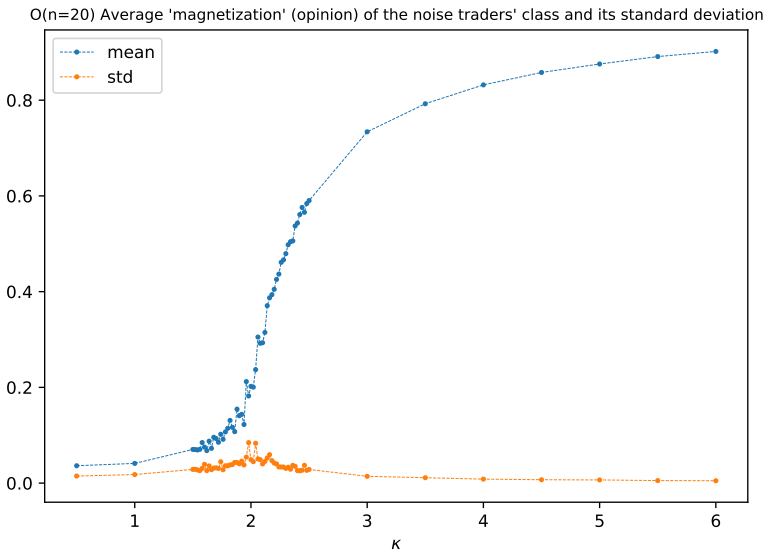

Figure 5.4: $O(n = 20)$ geometric symmetries approach. We refer to figure 5.1 for a detailed description.

of the Statistical Physics' $O(n)$ model. Having "cleaned" the simulation from the effects coming from the other parts of the model (e.g. dividend processes,

fundamentalist traders, price equations) we can focus on the problem concerning the $O(n)$ model simulation, being certain that it is not influenced by other factors.

Indeed, we observe that the proposed algorithm can correctly reproduce the phase transition characterizing the model. The mean magnetization is defined as the time-average over all the simulation's steps of the value of the spin vector's norm (i.e. average opinion of the class for that day). This time-average presents the correct behavior expected from Statistical Physics theory. A zero value in the subcritical region (here the small but non-zero value is due to the finite size effects) and an increase starting from the critical point representing the phase transition. Also, the shape of the curve is in good qualitative agreement with the theoretical one. Moreover, the phase transition is correctly marked by an increase in the standard deviation of the spin's vector norm.

Despite this good agreement with the results expected from the theory, we notice that the phase transition is located always at the same value of $\kappa_c = 2$, instead of the expected value $\kappa_{c,theory} = n$ fixed by the number of components of the spins characterizing the model.

This is something unexpected. Given the apparent correctness of the derivation of the algorithm, we initially supposed the problem could be related to an error in the coding implementation of the method.

Therefore, we moved to a detailed analysis of the code. To gain insight into the dynamics generated, we worked out a way to have a visual representation of the simulated noise traders' decision. After some implementation work in *Python* together with some *Bash* scripts, we effectively represented the actual dynamics of the investment choices of the noise traders class in the case of $n = 3$ components, i.e. risky assets. Indeed, in the case of $O(n = 3)$ we can plot the decision of the traders as three-dimensional unit vectors on the $\mathbb{S}^2$ hypersphere, the viewable three-dimensional sphere.

First, we have been able to plot the actual set of equiprobable choices generated by the second part of the algorithm at a fixed angle theta. We plotted it to exclude the chance that some errors in the code could give rise to the definition of an incorrect set of equiprobable choices in each trading decision process. Conversely, figures 5.5 and 5.6 show that the method correctly generates, as set of equiprobable choices, a circle. Which is indeed the intersection of a $(3-1)$-sphere $\mathbb{S}^2$ and a 3-dimensional hyperplane (a three-dimensional sphere and plane), i.e. a hypersphere of one less dimension $\mathbb{S}^1$ (a circle).

After a careful analysis of the code, no implementation error has been found. We then moved to test more deeply the theoretical derivation of the method. First, we examined again the correctness of the form of the transition probabilities (5.7). An error in its expression would invalidate a priori any subsequent sampling procedure.

In order to have an independent check of its validity, we repeated the constant kappa simulations' experiment presented in figures 5.1, 5.2, 5.3, and 5.4, for the $O(n)$

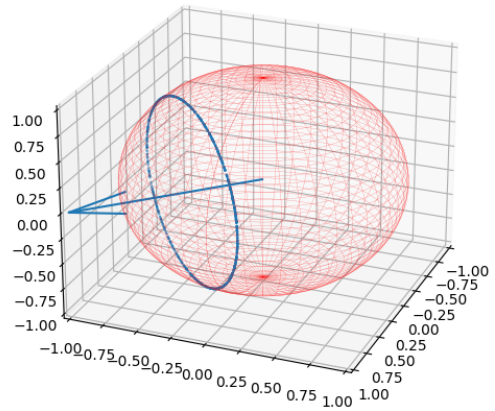

Figure 5.5: Set of equiprobable choices at fixed theta. Each point represents one of the 1000 choices sampled for a given value of theta. The blue vector constitutes the average spin vector $\vec{M}$. We observe that the choices correctly distributes uniformly on a circle around $\vec{M}$.

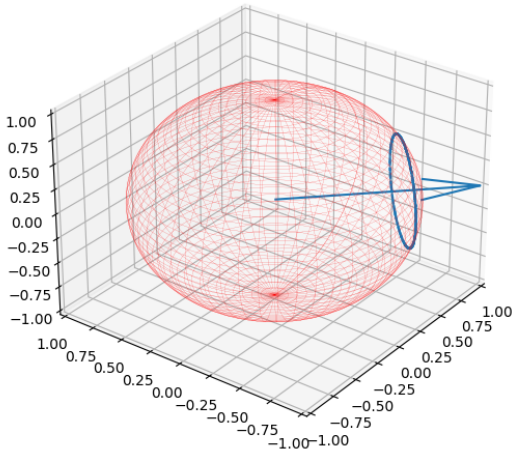

Figure 5.6: Another set of equiprobable choice at a fixed value of theta (different from figure 5.5). Again the choices correctly distributes uniformly on a circle around $\vec{M}$. The value of theta is smaller, hence the circle has a smaller radius.

model simulated with the McFadden result's method. Again we set the external field to zero, decoupling the noise traders class from the rest of the model to be certain that no external factor influenced the results. The resulting time-average

and standard deviation plots of the norm of the mean spin vector are presented in figures 5.7 and 5.8. Remarkably, the phase transitions are present at the correct critical values. In particular $\kappa_c \approx 4$ for the $O(n = 4)$ model and $\kappa_c \approx 10$ for the $O(n = 10)$ model, the negligible differences attributable to the finite size effects.

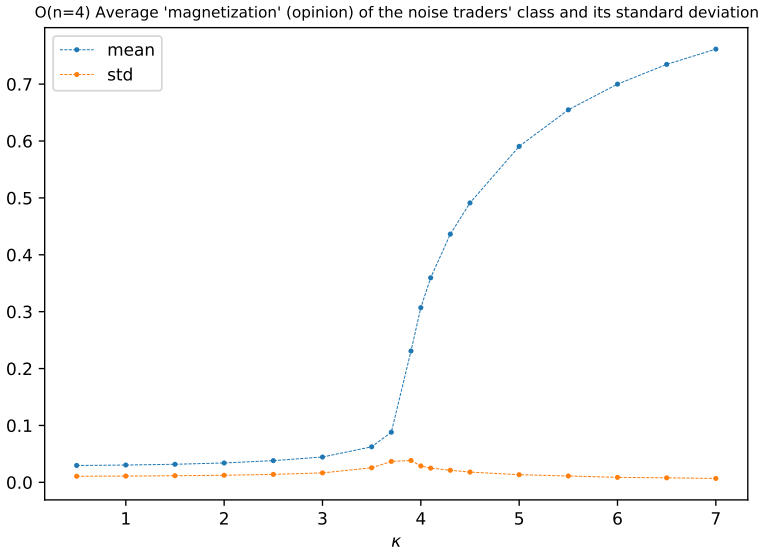

Figure 5.7: $O(n = 4)$ McFadden result's approach. Time-average and standard deviation of the magnetization (norm of the mean spin vector of that trading day) of the noise traders class, characterizing the constant kappa simulations for various κ values. The model simulated is the $O(n = 4)$, using the McFadden result's approach.

The interpretation is clear. The transition probabilities form is the correct one characterizing the stochastic dynamics of the $O(n)$ model. The problem concerns only the derivation of the method based on the symmetries approach.

We thoroughly analyzed the derivation and the implementation of the latter method, but surprisingly no error has been found. At the time of writing the problem in the symmetry-based algorithm has not been identified and the author would be extremely grateful to anyone who could spot the problem or give a hint for its individuation.

Nevertheless, as we have commented, the phase transition is correctly modeled and the dynamics of the $O(n)$ model are correctly generated minus a rescaling of the parameter κ by a factor $\frac{1}{n}$. The only problem in the simulation of the model is constituted by this effective rescaling. Comparing the results of the two method's application, we have observed that none of the properties of the dynamics of the model is affected by the aforementioned issue. Given this absence of any further

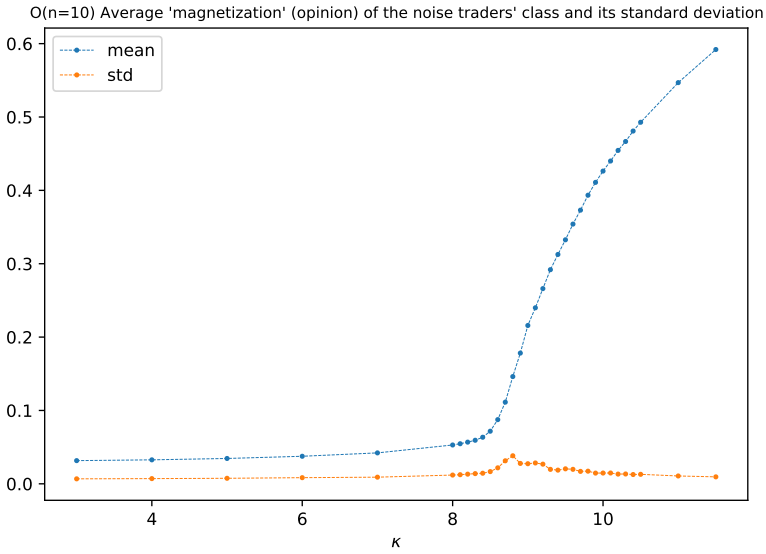

Figure 5.8: $O(n = 10)$ McFadden result's approach. We refer to figure 5.7 for a detailed description.

impact on the simulation of the noise traders with respect to this acceptable point (it is just a matter of remembering that the critical point is effectively rescaled to be always located at $\kappa_c = 2$ for any n), and pushed by the effectiveness of the algorithm from the point of view of both computational efficiency and realistic time series, we decide to rely on it for the following application of the market model.

We stress again that the resulting time series are not affected by the aforementioned problem, we just have to keep in mind this discussion.

As a final representation of the critical value's rescaling problem, we present the visualization of the actual dynamics of the noise traders' decisions. In particular, in figures 5.9, 5.10, and 5.11, we present all the one thousand noise traders' investment choices for the trading days 0, 2 and 6 respectively, taken from a simulation of $O(n = 3)$ model with a constant kappa value $\kappa = 2.5$ above the actual critical point, but below the theoretically expected one. We observe indeed that the noise traders class polarizes as the days pass, as remarked by the increasing norm of the mean spin vector. For the simulation of the $O(n = 3)$ model simulation with a constant kappa value $\kappa = 1.5$ below the actual critical point, the behavior is the opposite. As presented in figures 5.12, 5.13, and 5.14, as the days pass, the idiosyncratic opinion tends to dominate the class more and more and hence the norm of the mean spin vector decreases.

This is again a representation of the effectiveness of the algorithm to simulate correctly the phase transition yet at a rescaled critical point $\kappa_c = 2$.

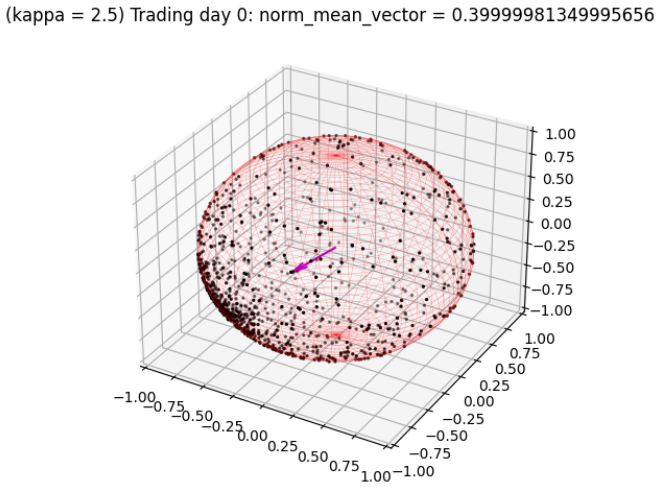

Figure 5.9: Trading day 0 of the dynamics of the $O(n = 3)$ noise traders class with a constant kappa value $\kappa = 2.5$. The class starts from a partially ordered configuration set by the initial conditions.

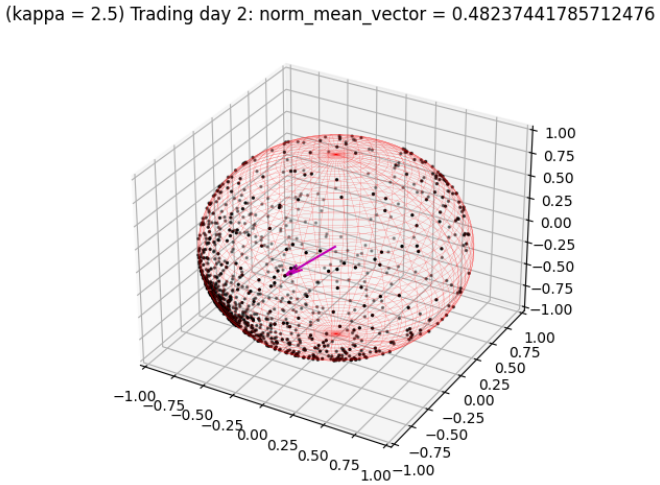

Figure 5.10: Trading day 2 of the dynamics of the $O(n = 3)$ noise traders class with a constant kappa value $\kappa = 2.5$. The class starts to polarize even more towards a specific shared opinion.

Post-submission addendum on the problem with the critical point of the symmetry-based algorithm

Eventually, the problem concerning the fact that the symmetry-based algorithm locates the phase transition always at the same value of $\kappa_c = 2$*, instead of the*

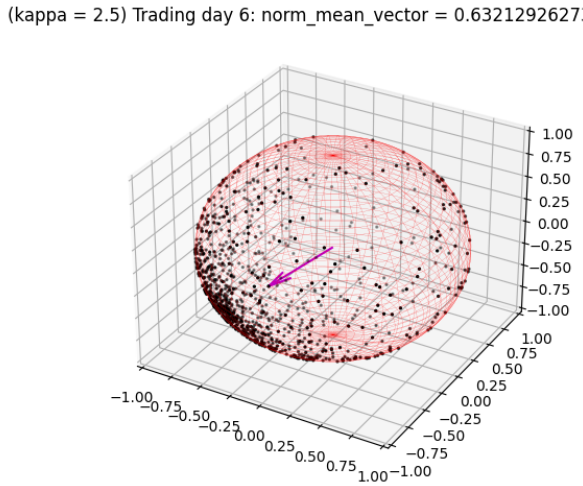

Figure 5.11: Trading day 6 of the dynamics of the $O(n = 3)$ noise traders class with a constant kappa value $\kappa = 2.5$. The class now is rather dominated by a common investment preference represented by the growing mean spin vector in magenta.

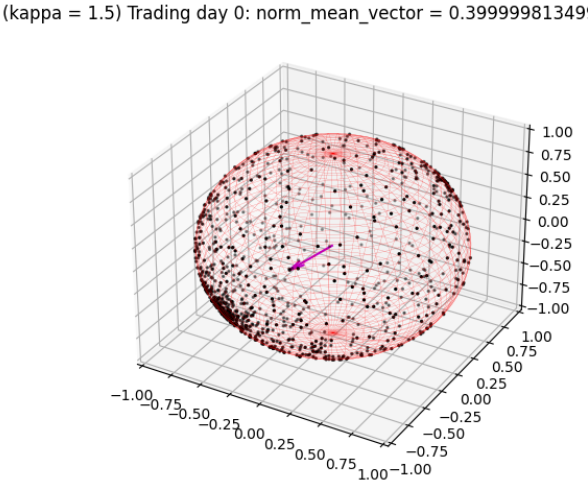

Figure 5.12: Trading day 0 of the dynamics of the $O(n = 3)$ noise traders class with a constant kappa value $\kappa = 1.5$. The class starts from a partially ordered configuration set by the initial conditions.

expected value $\kappa_{c,theory} = n$ fixed by the number of components of the spins characterizing the model, has been solved after the submission of the thesis. We report here the solution. The error has been identified in the definition of the univariate

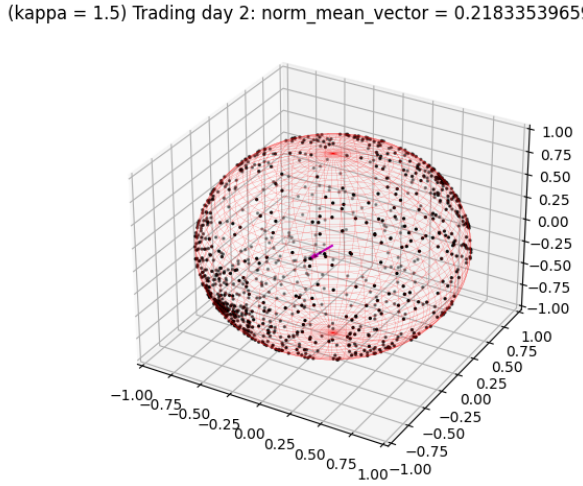

Figure 5.13: Trading day 2 of the dynamics of the $O(n = 3)$ noise traders class with a constant kappa value $\kappa = 1.5$. The class starts to randomize, the mean spin vector's norm decreases.

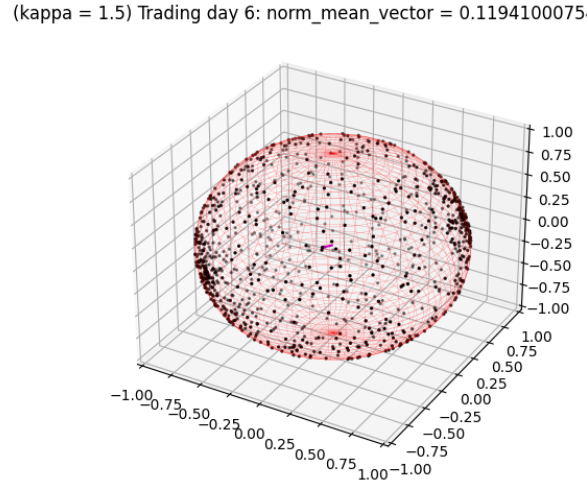

Figure 5.14: Trading day 6 of the dynamics of the $O(n = 3)$ noise traders class with a constant kappa value $\kappa = 1.5$. The idiosyncratic opinion is now dominating the class.

distribution (5.9) *of the angle* θ*. Indeed a factor*

$$(\sin\theta)^{n-2} \tag{5.17}$$

is missing. This factor accounts for the angular dependence of the surface of the $\mathbb{S}^{n-2}$ *hypersphere of equiprobability. Indeed, moving from the non-normalized*

multivariate probability density function (5.7) *to the univariate one effectively depending only on the angle* θ *we have to take into account a factor representing the surface of the hypersphere* $\mathbb{S}^{n-2}$*, that contains a term depending on* θ *and hence not negligible as a constant term in the rejection sampling procedure. In particular writing the normalization constant as c we have that the multivariate distribution reads*

$$P(\vec{A} \to \vec{B}) = \frac{1}{c} e^{\kappa_t \left(\frac{\sum_i \vec{S}_i \cdot \vec{B}}{N} + \vec{H} \cdot \vec{B} \right)}. \tag{5.18}$$

Now making explicit the dependence on the angle θ *we have*

$$\frac{1}{c} e^{\kappa_t \left(\frac{\sum_i \vec{S}_i \cdot \vec{B}}{N} + \vec{H} \cdot \vec{B} \right)} = \frac{1}{c} e^{\kappa_t \|\vec{M}\| \cos\theta} \left(\frac{2(\pi)^{\frac{n-1}{2}}}{\Gamma(\frac{n-1}{2})} (\sin\theta)^{n-2} \right), \tag{5.19}$$

where the factor in parenthesis represents the surface of the hypersphere of equiprobability $\mathbb{S}^{n-2}$*. Including the constant factors independent of* θ *in the constant c we get*

$$P(\theta) = \frac{1}{c} e^{\kappa_t \|\vec{M}\| \cos\theta} (\sin\theta)^{n-2}. \tag{5.20}$$

Finally, we can neglect the constant c term since a constant factor does not affect the rejection sampling method since does not modify the relative probabilistic weights of the possible angles. The univariate probability distribution from which we sample an angle θ *with rejection sampling is defined by*

$$P(\theta) \propto e^{\kappa_t \|\vec{M}\| \cos\theta} (\sin\theta)^{n-2}. \tag{5.21}$$

It is indeed the missing angular factor $(\sin\theta)^{n-2}$ *in* (5.9)*, leading to the incorrect location of the critical point characterizing the phase transition of the model. The absence of this term means that we are sampling many more points close to* $\vec{M}$ *than needed, enhancing the ordering forces and thus the magnetization This in turn explains the fact that the critical* κ_c *does not decrease with the dimensionality* n*. Not including the angular factor, we are wrongly removing the dimensionality dependence. All the subsequent analysis is not affected by the missing factor in the sampling procedure. All the results presented in the following are confirmed also by the implementation of the correct algorithm where the* $(\sin\theta)^{n-2}$ *is added. The only effect of wrongly not including this angular factor is an effective rescaling of the critical value* κ_c*.*

5.3 The stylized facts of the financial markets

To fully understand the financial markets, it is crucial to embrace the fact that the world economy is a constantly evolving multi-agent complex system, that can be

studied using the tools of complex systems theory. The complex systems theory can constitute the theoretical framework to explain the presence of ubiquitous statistical properties in the financial time series independent of the details of the series itself.

These emerging empirical properties have been observed across a wide range of instruments, markets, and time periods and they constitute the so-called stylized facts of the financial markets.

To test the validity of the time series generated by the simulation of our model, it is important to check if the model can reproduce some of these stylized facts.

Here we focus in particular on two of them, the fat-tailedness of assets' absolute returns and the long memory in the autocorrelation of the same quantities. We focus in particular on the simulations characterized by an Ornstein-Uhlenbeck kappa process to test the two stylized facts. We do that since we know that the simulations characterized by an Ornstein-Uhlenbeck κ_t can produce clear bubbles at odds with the constant kappa one.

We want to remark again on this point because it will be important also in the next section. The discussion on the mechanism generating the bubble in the original model, presented in section 2.6, directly applies also in the case of the $O(n)$ model. Indeed, as we have already commented, despite their differences, all the models presented, and hence the $O(n)$ one too, share the same underlying mechanism triggering and generating the bubbles. When the time-varying herding propensity parameter exceeds a certain model-dependent critical threshold, the noise traders class undergoes an actual phase transition from the disordered state dominated by the idiosyncratic opinion to the ordered state where the class polarizes towards specific investment preferences. This interaction-driven collective behavior leads to the emergence of the highly non-trivial phenomena which we identify as bubbles.

5.3.1 The fat-tailedness of absolute returns

In this section, we compare the decay of the distribution of assets' absolute returns resulting from the simulation of the $O(n)$ model to the observed leptokurtic behavior of their empirical counterparts [7], [8]. This leptokurtic trait can be understood from the point of view of extreme value theory. Indeed, the empirical distribution of absolute returns has fatter tails with respect to the Gaussian distribution. This means that rare events, represented by remarkably high or low returns (trading days characterized by booms or crashes), happen more frequently with respect to what the standard Normal distribution would predict. The relatively frequent presence of bubbles and crashes represents one distinctive feature of the financial markets.

The empirical fat-tail decay of the distribution

$$p(x) \sim x^{-1-\alpha} \tag{5.22}$$

is characterized by an exponent α in the range [2,4]. As shown in figure 5.15, the fitted parameter from the simulated time series falls in this range of values.

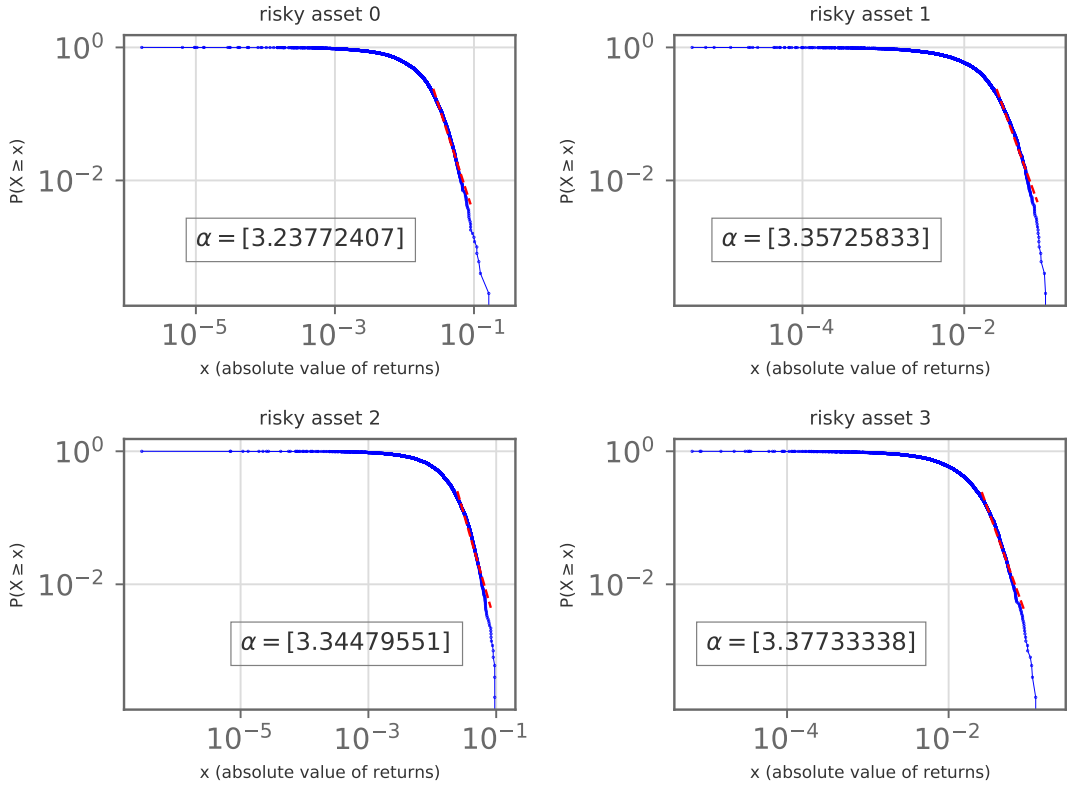

Figure 5.15: Log-log plot of the complementary cumulative distribution functions of the returns of the four risky assets from a simulation of the $O(n = 4)$ model, with Ornstein-Uhlenbeck process with mean reversion level $\mu_k = 0.98 \cdot 2$. The exponent is found fitting data from the last 20th percentile of the cumulative distribution, disregarding the largest ten values.

5.3.2 The long memory in the autocorrelation of absolute returns

The daily returns are not independent random variables. In the financial markets periods of tranquility alternate to periods of high volatility. A common observation characterizing the financial time series is the concentration of high price's exuberance in definite time windows [7], [8].

This clustering phenomenon goes under the name of volatility clustering. Its presence can be analyzed by looking for patterns in the time evolution of the market.

An effective tool to accomplish this task is constituted by the autocorrelation function. Indeed, the presence of long memory in the autocorrelation function is an indication of time inhomogeneity in the time distribution of the returns, characteristic of the volatility clustering phenomenon. The signed returns

$$\vec{r}_{p,t} = \left(\frac{P_{1,t}}{P_{1,t-1}} - 1, \ldots, \frac{P_{n,t}}{P_{n,t-1}} - 1 \right). \tag{5.23}$$

are empirically characterized by a fast-decaying autocorrelation, while the absolute returns $|\vec{r}_{p,t}|$ have instead an autocorrelation with longer memory. In figure 5.16 we check if the ABM with $O(n)$ model is able to reproduce this empirical fact. Indeed, the emerging autocorrelation functions show exactly this behavior.

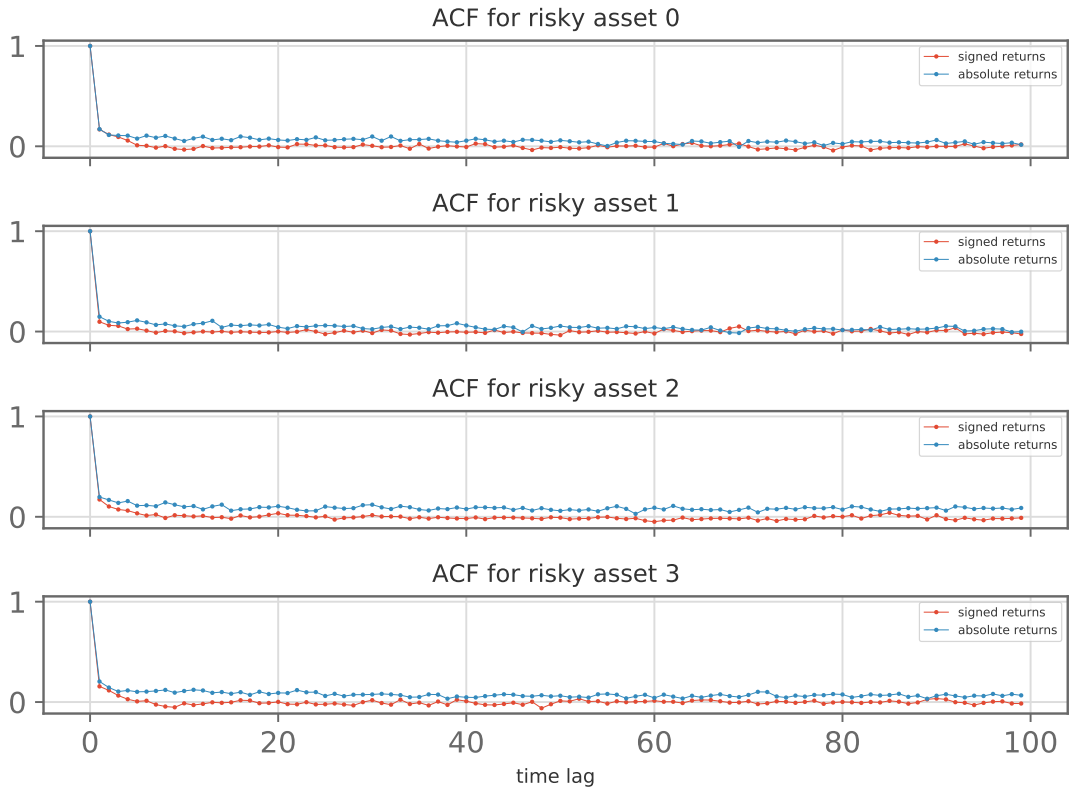

Figure 5.16: Autocorrelation function of signed and absolute returns of the four risky assets from a simulation of the $O(n = 4)$ model, with Ornstein-Uhlenbeck process with mean reversion level $\mu_k = 0.98 \cdot 2$. The autocorrelation functions are computed for the data after the 500th trading day in order to exclude possible misleading contributions due to the initial conditions.

5.4 The time synchronization of bubbles among different risky assets

In this section, we move to the application of the extended market model endowed with the $O(n)$ noise traders class to investigate interesting financial phenomena. In particular, here we are interested in analyzing the synchronous or asynchronous character of the emergence of the bubbles.

Will the assets develop faster-than-exponential growths in their prices at the same time or will the market be dominated by alternating picks in different risky assets? There exists a correlation in the prices time series between different risky assets? If it will be the case, would such a correlation be positive or negative? And still, if it is present, can we understand the mechanisms generating this endogenous correlation?

After an extensive analysis of the resulting time series and a comprehensive testing process of different speculations about the phenomena governing the time dependence between the bubbles, we can come up with a hypothesis, that in the following we will support bringing evidence in favor of it.

We hypothesize the existence of three regimes characterizing the time synchronization of the bubbles. The three regimes depend on the value of the herding propensity κ_t.

In particular, the first regime corresponds to small values of κ_t far from the critical value κ_c. In this first regime, the market model does not produce super-exponential bubbles, since the noise traders class is in the disordered phase dominated by the idiosyncratic opinion. This is true for both constant and Ornstein-Uhlenbeck kappa processes, provided that the latter moves stochastically in a range of values far from the critical point.

The second regime corresponds to values of the herding propensity near the critical one $\kappa_t \approx \kappa_c$. In this regime we observe the emergence of clear bubbles if the simulation is characterized by an Ornstein-Uhlenbeck kappa process, stochastically fluctuating near the critical threshold. The bubbles originating through this mechanism, analogous to the original model's one, are asynchronous among the different risky assets. The lack of time synchronization is confirmed by the small values of the correlations among the stocks. The prices time series follow almost uncorrelated time evolutions. We further observe that in this regime the emergence of the bubbles is mainly governed by the social imitation attitude of the noise traders.

The third and last regime is instead characterized by a large value of the herding propensity, far above κ_c. The noise traders class is deeply inside the ordered phase, being dominated by a common investment's preference. This regime was not considered in the original model discussion. First of all, remarkably, also this regime

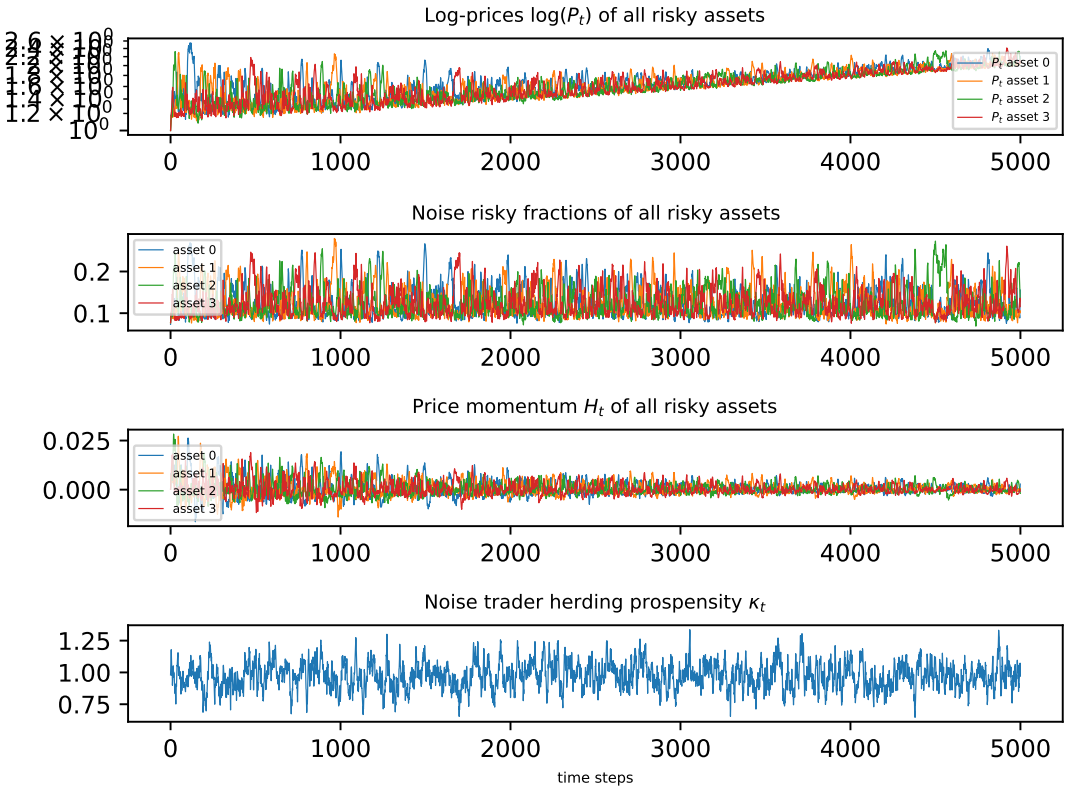

Figure 5.17: The figure presents the time series from an Ornstein-Uhlenbeck simulation of the $O(n = 4)$ model, characterized by a mean reversion level $\mu_k = 0.98 \cdot 1$, far below the critical value $\kappa_c = 2$. The systems is clearly in the disordered regime dominated by the idiosyncratic opinion. No bubble is present.

presents bubbles in the prices. We have to understand the phenomena taking place at these large values of herding propensity, indeed the bubbles characterizing these values are of an intrinsically different nature with respect to the bubbles studied until now. The discussion of this delicate point will be presented in the following subsection 5.4.1. From the point of view of the correlation among the assets, this regime presents a remarkably different situation with respect to the second one. Indeed, we observe synchronous bubbles mainly driven by the trend-following attitude of the traders.

Moreover, the trend that emerges from this analysis is that the synchronization of bubbles increases with the increasing of the range of value of the herding propensity parameter κ_t.

In figures 5.17, 5.18, and 5.19, we present respectively the three regimes. The qualitatively and quantitatively different behavior between their time series is

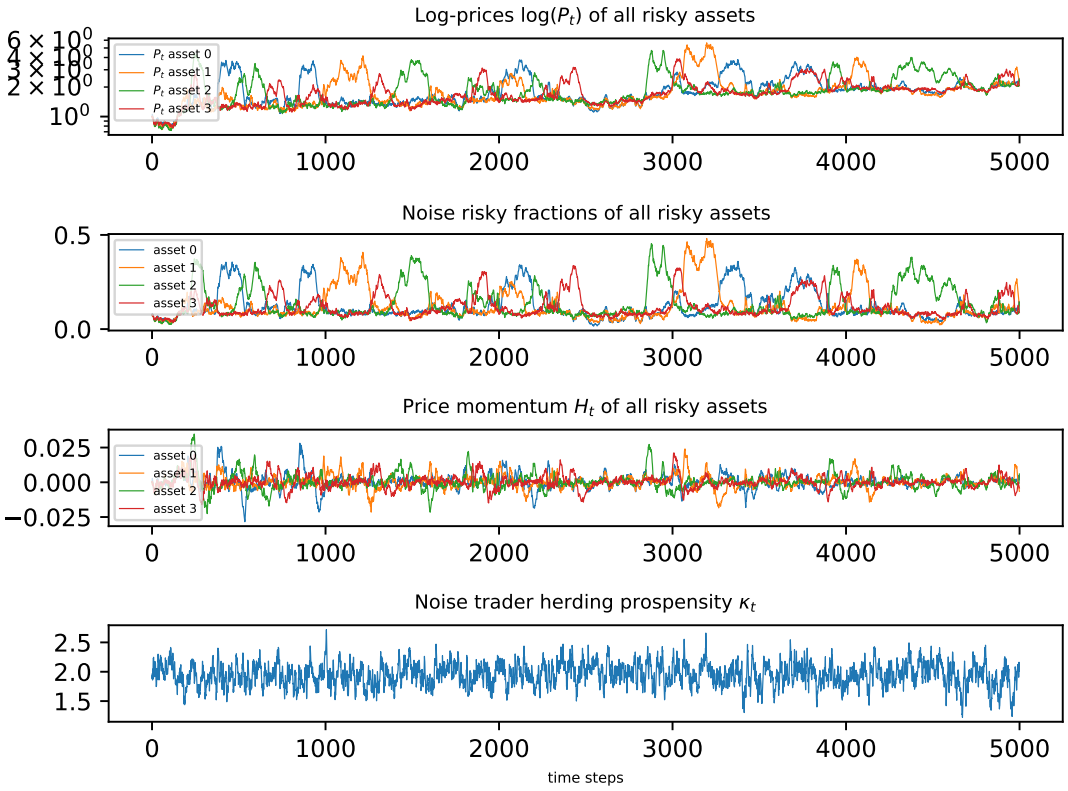

Figure 5.18: The figure presents the time series from an Ornstein-Uhlenbeck simulation of the $O(n = 4)$ model, characterized by a mean reversion level $\mu_k = 0.98 \cdot 2$, near the critical value $\kappa_c = 2$. The bubbles develop asynchronously, through an analogous process to the one described in subsection 2.6.

evident.

We start from the first regime, for which the analysis is straightforward. Indeed, as appears in figure 5.17, the prices do not present bubbles. The noise traders class is deeply in the disordered phase dominated by the idiosyncratic opinion, hence there is simply no polarization phenomenon triggering the emergence of collective phenomena capable of resulting in super-exponential-growth of the prices.

We then move to the analysis of the second regime. Here we have the clear presence of bubbles in the different assets. As we have commented, the mechanism triggering their emergence is analogous to the original model's one presented in section 2.6. The appearance of super-exponential-growths in the prices time series is asynchronous. We can understand this fact resorting to Statistical Physics. Indeed, the underlying $O(n)$ model introduces no correlation among the different components of the spin vector. The dynamics of each of this component evolves

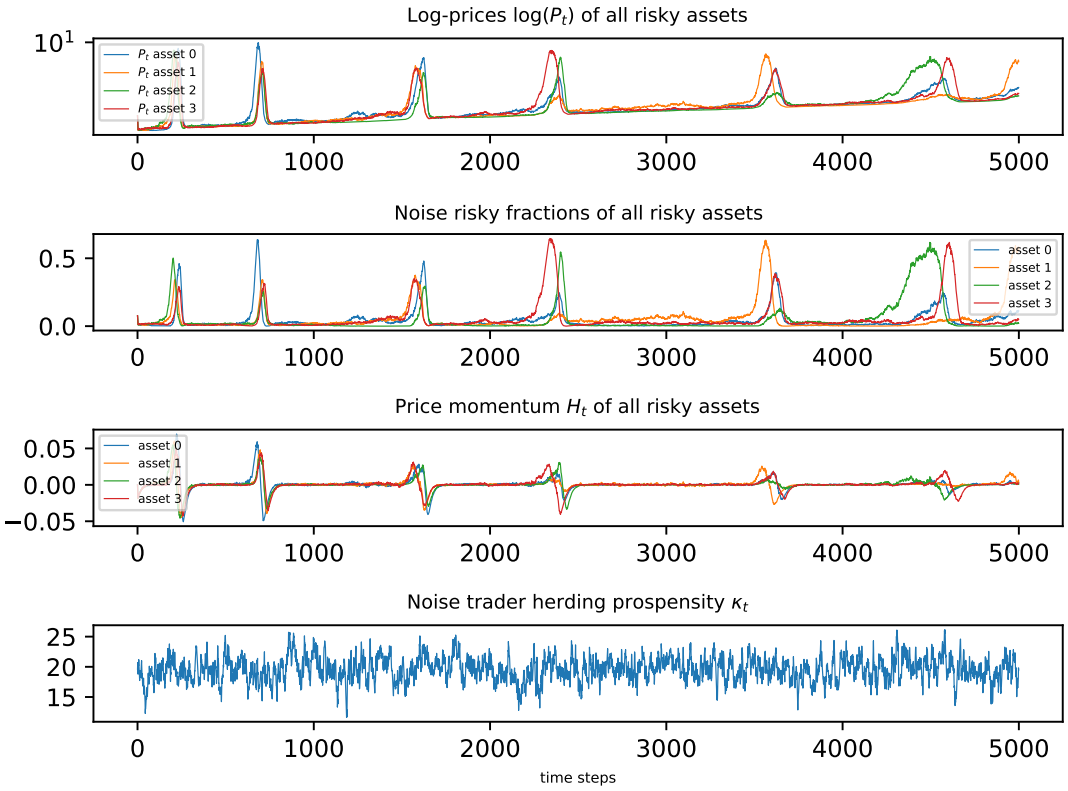

Figure 5.19: The figure presents the time series from an Ornstein-Uhlenbeck simulation of the $O(n = 4)$ model, characterized by a mean reversion level $\mu_k = 0.98 \cdot 20$, far above the critical value $\kappa_c = 2$. The noise traders class is completely polarized. Remarkably, several synchronous bubbles are identifiable. The mechanism triggering their emergence is fundamentally different from the one studied for the other bubbles until now and is discussed in subsection 5.4.1.

in a statistically uncorrelated way with respect to the others, hence we expect that the noise traders' strategy does not introduce any correlation among the asset prices.

We can further analyze this point looking at the realized correlations among the different risky assets' prices. In figure 5.20, we present the realized correlations between the prices coming from the time series of the simulation already presented in figure 5.18. We observe small but not negligible positive correlations. This is not due to the traders' strategies, instead, it is ultimately connected to the constant exponential growth characterizing the prices and the whole market model. This constant exponential growth is generated by the constant growth of the dividends processes. Hence, to focus on the analysis of the correlations coming from the

traders' strategies we have to subtract this effect from the prices time series.

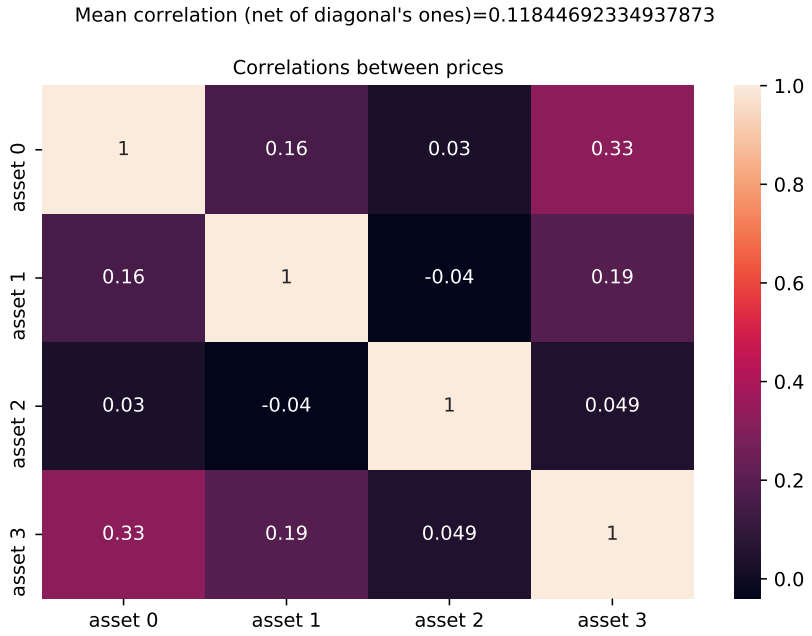

Figure 5.20: Realized prices' correlations from an Ornstein-Uhlenbeck simulation of the $O(n = 4)$ model, characterized by a mean reversion level $\mu_k = 0.98 \cdot 2$, near the critical value $\kappa_c = 2$. Their small but not negligible positive values are due to the constant exponential growth characterizing the prices, deriving from the constant growth factor present in the dividend processes. In figure 5.21 we subtract the impact of this constant growth.

Doing that, in figure 5.21 we observe vanishing values for the correlations, confirming the asynchronous character of the bubbles. Neither the fundamentalists' strategy nor the noise traders' one introduces correlation among the asset.

In the case of the fundamentalists, this is clear from the equation governing their portfolio allocation strategy (3.15) and from the fact that in these simulations we always assume that no correlation is expected between the risky asset by this type of agents

$$C^f = \begin{pmatrix} 1.0 & 0.0 & 0.0 & 0.0 \\ 0.0 & 1.0 & 0.0 & 0.0 \\ 0.0 & 0.0 & 1.0 & 0.0 \\ 0.0 & 0.0 & 0.0 & 1.0 \end{pmatrix} \tag{5.24}$$

Clearly, non-zero values in this matrix would introduce some correlation in the prices. Studying the impact of the expected correlations by the fundamentalists on the realized correlations constitutes an interesting further direction of analysis.

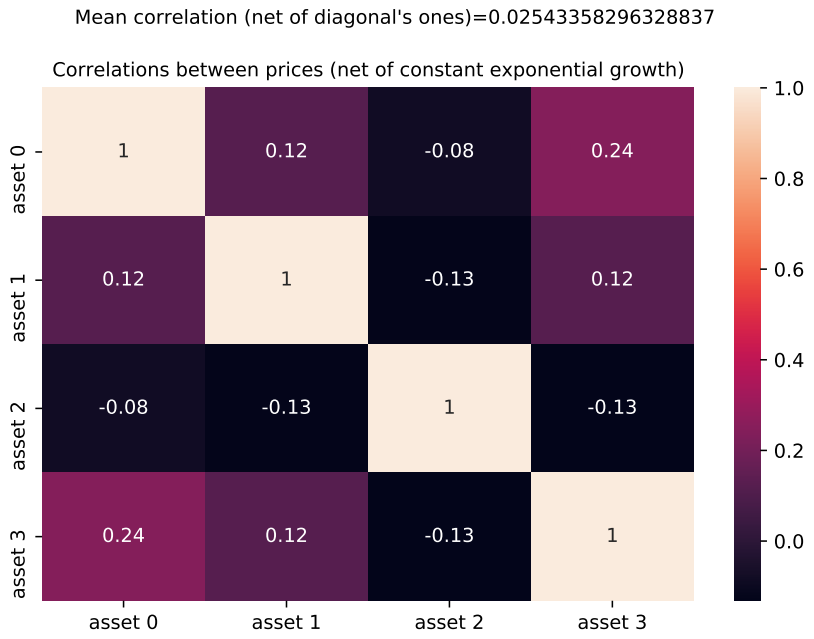

Figure 5.21: Realized prices' correlations as in figure 5.20, yet this time we subtract the constant exponential growth from the prices in order to focus on the correlations emerging from the traders' strategies. As expected the values are vanishing, confirming the asynchronous character of the bubbles. The $O(n)$ model does not introduce correlation in the prices.

Nevertheless, here we are mainly interested in the correlations introduced by the noise traders, hence we always set to zero the non-diagonal elements of matrix (5.24). For the latter agents, we know that the $O(n)$ model does not introduce correlation among different components of the spin vector, hence the vanishing values in figure 5.21 are explained.

Finally, in the following subsection, we move to the analysis of the third regime characterized by large values of κ_t, far above κ_c.

5.4.1 The supercritical herding propensity regime: Mexican hat potential and synchronous bubbles

In this subsection we deepen the analysis of the supercritical herding propensity regime, trying to gain theoretical insights into the phenomena taking place. This regime, in which the noise traders class is deep inside the ordered phase polarized towards a common investment preference, was not considered in the previous works on the original model.

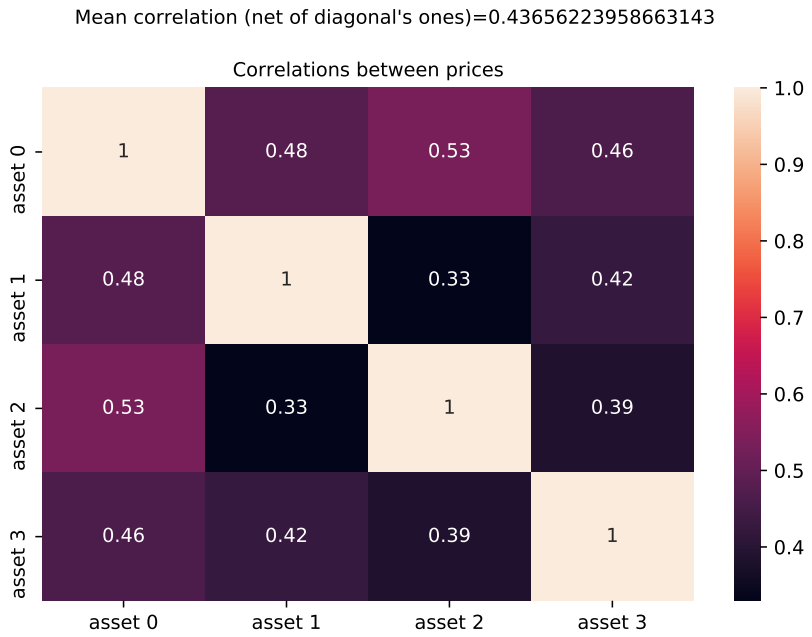

Figure 5.22: Realized prices' correlations from an Ornstein-Uhlenbeck simulation of the $O(n = 4)$ model, characterized by a mean reversion level $\mu_k = 0.98 \cdot 20$, far above the critical value $\kappa_c = 2$. At odds with the critical regime's case, we observe relatively large positive correlations.

We have anticipated that remarkably also this regime is characterized by the emergence of super-exponential bubbles, nevertheless, we will show that these bubbles are of an intrinsically different nature with respect to the ones studied until now in the present work and the other works on this model.

We have presented in figure 5.19, the time series from a setup with an Ornstein-Uhlenbeck κ_t wandering around a mean reversion level $\mu_k = 0.98 \cdot 20$, deeply inside the ordered supercritical phase. An important point is that the phenomena we are going to analyze in this regime do not depend on the nature of the kappa process.

Indeed, both constant kappa and Ornstein-Uhlenbeck one lead to the same situation, provided κ, being time-varying or not, is always deep inside the ordered phase. At odds with the critical regime with $\kappa_t \approx \kappa_c$, the time-varying nature of the herding propensity is no more important being only the supercritical nature of noise traders class the very element governing this regime.

We start presenting the realized correlations of the prices from the time series in figure 5.19. In figure 5.22 we present the full correlations, while in figure 5.23 the ones resulting from the subtraction of the constant exponential growth from the price. The correlations are always relatively large and positive, even discarding

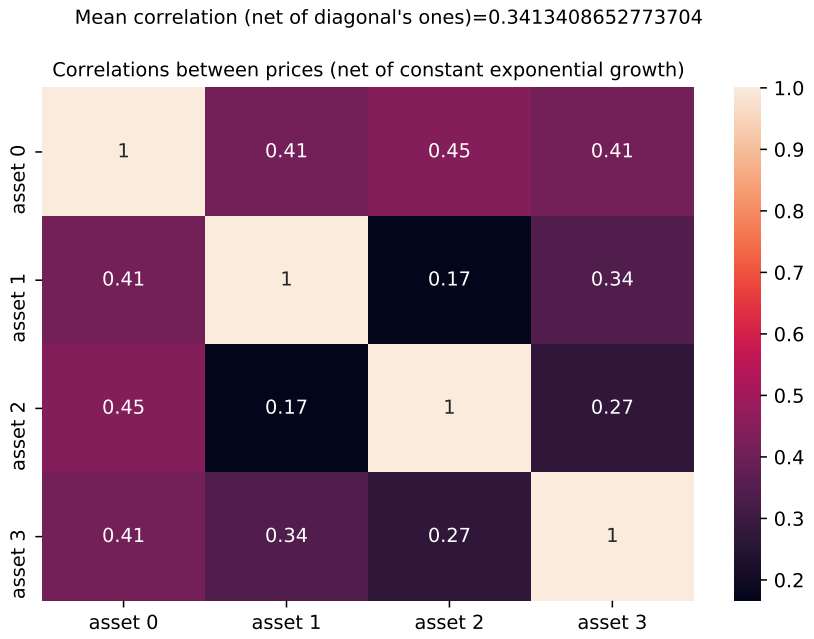

Figure 5.23: Realized prices' correlations as in figure 5.20, yet this time we subtract the constant exponential growth from the prices in order to focus on the correlations emerging from the traders' strategies. Remarkably, the correlations values are relatively large and positive. This quantifies the synchronous character of the emergence of the bubbles in the supercritical regime.

the fictitious positive correlation introduced by the constant trend. The situation is fundamentally different from the second regime's. The bubbles are indeed synchronous and the positive correlations quantify this behavior.

At this point, we have to tackle the two unknown points. First, what is the mechanism governing this type of bubbles since we know that the explanation formulated for the bubbles near criticality does no longer apply? Second, can we understand how this mechanism introduces the time synchronization feature in the emergence of the bubbles?

The bubbles' triggering mechanism in the supercritical regime

To answer the first question we resort again to Statistical Physics. We have to understand how it is possible the presence of the super-exponential-growths in the supercritical region far from the phase transition. The answer will be that these bubbles are triggered by the finite response of the system to an infinitesimal field applied in a perpendicular direction to the magnetization. In other words,

small changes in the external field of price momenta trigger a collective response of the noise traders class. Even if we are far from the phase transition, the system behaves like at criticality with respect to fluctuations parallel to the valley of minima characterizing the system's potential.

Indeed, the supercritical $O(n)$ model is characterized by the Mexican hat potential, well-known in Statistical Physics and represented, in the viewable case of $n = 3$, in figure 5.24.

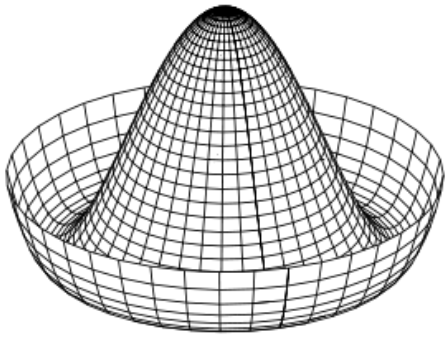

Figure 5.24: Mexican hat potential of the supercritical $O(n = 3)$ model.

The continuous phase transition from disorder to order of the $O(n)$ model is characterized by the smooth deformation of the paraboloid, constituting the subcritical potential of the system, into the Mexican hat. The single minimum located in the origin for the paraboloid, transform into a degenerate valley of minima in the supercritical case. This phase transition is the underlying mechanism triggering and governing the bubbles in the second regime.

In the supercritical regime, the situation is different and it is the very presence of the degenerate valley of minima to govern the bubbles. Indeed, even if we are inside the ordered phase far from the critical point, the system is characterized by a diverging susceptibility in the directions perpendicular to the magnetization, defining the valley. The noise traders class reacts with a collective behavior in response to small changes in the external field of price momenta. The price momenta can tilt the common investments' preferences of the class at the "macro" level.

This emerging collective behavior governed by the price momenta is ultimately the mechanism governing the super-exponential bubbles in this regime. Now we can understand why we stated that in the critical regime the bubbles are governed by the social imitation attitude, while in the supercritical one they are dominated by the trend-following attitude. In the first case, it is the transition to the ordered phase generating the bubbles, in the second instead the class is already polarized and it is the tilting effect of the external field to drive them. Indeed, these are fundamentally different mechanisms. We now move to the second question, why

are the resulting bubbles synchronous?

The supercritical bubbles' synchronization

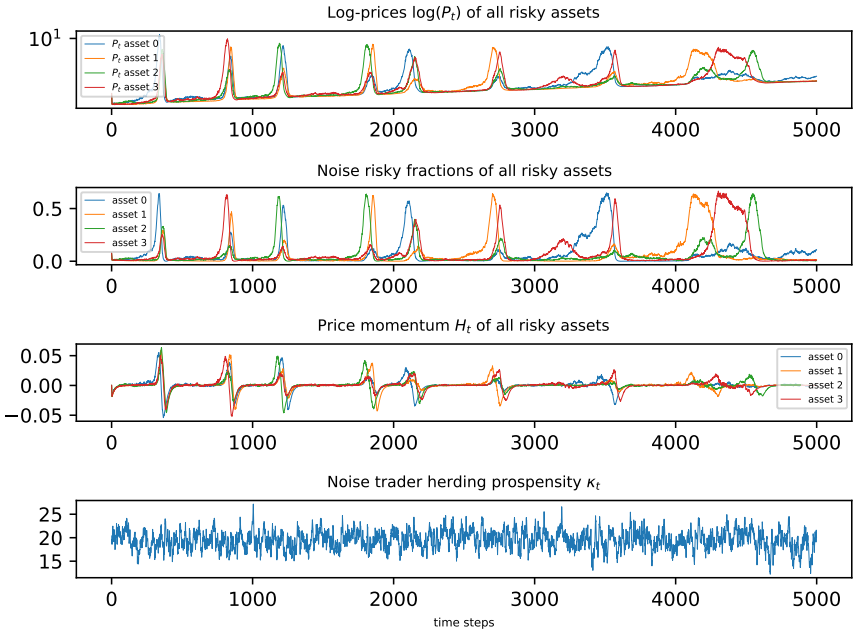

Figure 5.25: Time series from an Ornstein-Uhlenbeck simulation of the $O(n = 4)$ model, characterized by a mean reversion level $\mu_k = 0.98 \cdot 20$, far above the critical value $\kappa_c = 2$. A clear pattern emerges in the prices time series. A first bubble in an asset, cascades into synchronous bubbles in all the other assets.

In the last subsection, we have understood the mechanism underlying the emergence of the bubbles in the supercritical regime. Nevertheless, the synchronous character of their appearance is unexpected.

Indeed, on one hand, we know that the fundamentalists' strategy cannot introduce correlation among the prices since the expected correlations are set to zero and hence the system (3.15) defining their allocation strategy is constituted by independent equations for the different risky fractions. Moreover, we again explicitly state for clarity that as assumed throughout the present work no correlation has been introduced between the dividends processes.

Furthermore, we know from Statistical Physics that the components of the spin vector are uncorrelated, hence neither the noise traders' strategy can introduce correlation among the prices. Then, where does the correlation come from?

There is only one component of the model we have not considered, the price

equations. Indeed, the price equations are a set of non-linear coupled equations for the prices. The correlation can only come from the coupled character of these equations. Yet, the complex structure of the non-linear system makes an analytical study of the correlation introduced by the coupling between the equations unfeasible.

Nonetheless, after a deep analysis of the time series, we find that the large κ_t regime can give us a clue to understanding the origin of the positive correlation. Indeed, for large values of the herding propensity, a clear pattern emerges in the time series, as represented in figure 5.25.

The first bubble stochastically develops in one asset. Its price starts to grow super-exponentially. Then on average the investors, both fundamentalist and noise, get richer. Since their strategy leads to a different response to the bubble event, their increase in wealth is different. The noise traders push by the social imitation and trend following attitudes invest more on the asset undergoing the bubble the more its price rises. The fundamentalist instead decreases their exposition on the asset the more its price rises, following their risk-averse strategy. Hence is understandable how the noise traders get richer with respect to the fundamentalist investors during the bubbles. Nevertheless, both the investors get richer when a bubbles develops as we can see in figures 5.26 and 5.27, showing the traders' wealth dynamics characterizing the simulation in figure 5.25.

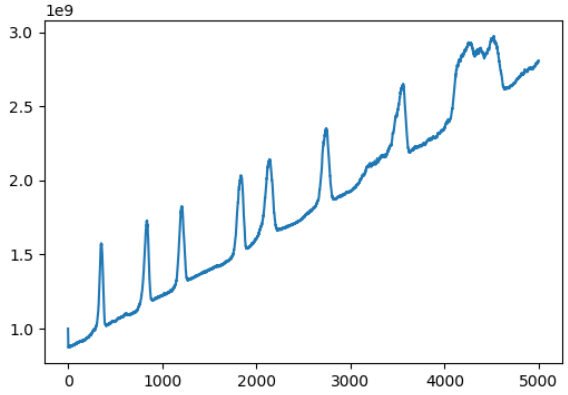

Figure 5.26: Fundamentalist traders' wealth dynamics characterizing the simulation in figure 5.25.

Since the traders' wealth increases, in order for the Walresian equilibrium to be still satisfied, the other assets' prices must grow. This is evident from the market clearing condition characterizing the Walresian equilibrium

$$\Delta D^{f,k}_{t-1\to t} + \Delta D^{n,k}_{t-1\to t} = 0 \quad \forall k \tag{5.25}$$

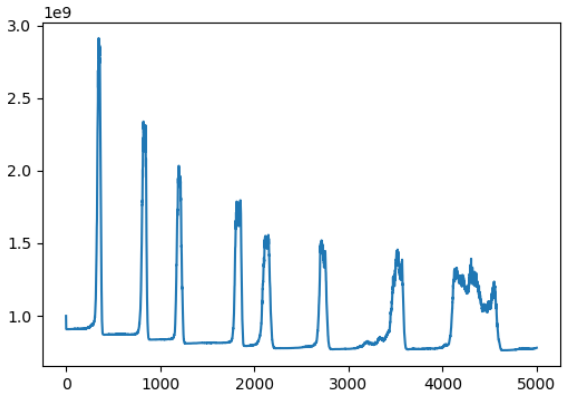

Figure 5.27: Noise traders' wealth dynamics characterizing the simulation in figure 5.25.

where $\Delta D^{f,k}_{t-1\to t}$ and $D^{n,k}_{t-1\to t}$ represent respectively the aggregate excess demands of risky asset k for each group. Expressing the equation in a more explicit form

$$W^f_t x^f_{k,t} - W^f_{t-1} x^f_{k,t-1} \frac{P_{k,t}}{P_{k,t-1}} + W^n_t x^n_{k,t} - W^n_{t-1} x^n_{k,t-1} \frac{P_{k,t}}{P_{k,t-1}} = 0 \tag{5.26}$$

and assuming constant all the quantities not dependent on the other assets prices, in particular on the one undergoing the bubble, we observe that the effect of the bubble of a specific asset on the other assets price equations, is represented by an increase of both the wealth of the fundamentalist and noise traders.

The only effect of a bubble of asset $i \neq k$ on the price equation 5.26 of any other asset k emerging from this differential analysis is an increase of the quantities W^f_t and W^n_t. The only way in which the equilibrium equation could be still satisfied is that the price $P_{k,t}$ is larger than the previous time-step's one $P_{k,t-1}$. We have indeed proved that an increase in one price triggers a positively correlated increase in all the other prices. If the increase is strong enough to have a relevant impact on the price momenta associated to the other asset, as in the case of a super-exponential bubble, the increase of the price momenta triggers the emergence of synchronous bubbles in all the other risky assets, through the tilting mechanism explained before.

Since the investment strategies of both the classes of traders do not depend on the magnitude of their total wealth but only on the characteristic of the assets, the increase of wealth from which the traders benefit during the super-exponential growth of a bubble, cascades in the synchronous emerging of bubbles in all the risky assets market.

Ultimately, this explains the pattern in figures 5.19 and 5.25, and constitutes

the mechanism at the origin of the positive correlation among the risky assets.

5.5 The limit towards the Capital Asset Pricing Model

We conclude the Chapter and with it, the work, comparing in this section the dynamics of the returns generated by the extended ABM endowed with the $O(n)$ noise traders class to the ones predicted by the Capital Asset Pricing Model (CAPM). The analysis will be shorter with respect to the wide discussion on the topic of the synchronization of the bubbles, nevertheless, it worths presenting a comparison of our model results to the classical CAPM extensively studied and used in the modern financial theory. Moreover, the introductory study here presented can constitute a first starting point for a further direction of analysis of the market model.

The Capital Asset Pricing Model is one of the pillars of the modern Portfolio Theory. It was introduced in the mid-1960s by economists Sharpe, Lintner, and Treynor in [55] as a model to price the risk associated with assets present in a portfolio. Despite more recent models have been proposed that better work with respect to the CAPM, the latter still represents the reference model in the portfolio's optimization due to its simplicity and intuitive understanding.

The risk of the stock market originates from the uncertainty in its evolution. The standard measure of this risk is the variance characterizing the stochastic nature of the assets' price and returns. From finance theory, we know that the risk permeating the stock market can be understood as composed of two parts. The first represents the specific risk of a single stock and it is called diversifiable risk. Indeed, it can be reduced or even eliminated by constructing a well-diversified portfolio. The second instead is the market risk, the risk component coming from the intrinsic uncertainty of the stock market in its entirety. This is the risk remaining in a portfolio when it reaches the limit of full diversification, i.e. it represents itself the full market.

In Portfolio Theory a measure of the risk associated with a specific stock entering a fully-diversified portfolio has been formulated, it is commonly referred to as β. The β of a specific stock represents the sensitivity of that stock to the market changes. From a statistical point of view, it is readily identifiable as the ratio of the covariance between the stock returns and the market returns divided by the variance of the market returns

$$\beta_i = \frac{\sigma_{i,m}}{\sigma_m^2} \tag{5.27}$$

Its range of values falls in the interval $[-1,1]$. A zero value of β represents a stock perfectly uncorrelated with the market and hence not sensitive at all to the

market's movements, The situation of $\beta = 1$ represents instead a stock moving exactly together with the market.

The fundamental principle on which the CAPM is built is that the investors search for high expected returns and low risk, i.e. low variance. This is also the foundation of modern Portfolio Theory, the best portfolios, commonly known as efficient portfolios, are the ones which offer the maximum expected return for a given level of risk, measured by the variance or standard deviation.

An increased risk has to be paid by higher expected returns. The risk has a price and the investors do not take risk for free. The Capital Asset Pricing Model quantifies this qualitative principle. The model boils down to a simple single formula

$$\mathbb{E}[r_i] - r_f = \beta_i(\mathbb{E}[r_m] - r_f), \tag{5.28}$$

where $\mathbb{E}[r_i]$ is the expected return of stock i, r_f is the risk-free rate and $\mathbb{E}[r_m]$ is the expected return of the market. The mathematical structure of the model is clear, we are in presence of a linear model. From the financial point of view, understanding is likewise explicit. The expected risk premium of the stock $\mathbb{E}[r_i] - r_f$, i.e. the reward from the point of view of the expected return to take the extra risk with respect to the risk-free landmark, is linearly dependent on the risk premium of the market $\mathbb{E}[r_m] - r_f$ through the coefficient β_i. The model is as simple as powerful since it embodies in a simple linear relation the risk-return trade-off characterizing the investment decision process.

In this section, we are interested in the comparison of the realized returns generated by the simulation of our market models to the one predicted by the CAPM. In particular, our question is whether the dynamics of our market model would converge to the market obeying the CAPM and under which condition.

The topic is vast and the possible directions of analysis manifold. Here we focus in particular on finding the correct definition of the limit under which we can observe the convergence of our market's dynamics to the one predicted by the CAPM and then test if the convergence is present.

First, we have to compute the quantities entering formula (5.28) from our time series. The risk-free rate is readily identified with the one introduced in our model. The expected rate of return of a stock $\mathbb{E}[r_i]$ corresponds in our model to the historical average of the returns of a specific risky asset, over a time window that we will define. The expected rate of return of the market $\mathbb{E}[r_m]$ is defined analogously, we just need to identify the market return r_m. In our model, the market return r_m simply corresponds to the arithmetic average of the returns of all the risky assets for that trading day. Finally, the β_i can be computed through their definition (5.27), where the variance of the the market returns is simply equal to the historical variance of the stochastic process r_m, $\sigma_m^2 = \mathrm{Var}(r_m)$, and the covariance $\sigma_{i,m}$, is the historical covariance between the stochastic processes r_i and r_m, $\sigma_{i,m} = \mathrm{Cov}(r_i, r_m)$.

Having defined the quantities entering the CAPM formula, we can move to the analysis of the limit procedure we could implement. The solution is found in the definition of the strategies of the two classes of traders. While the noise traders follow their social imitation and trend following attitudes, the fundamentalist traders implement a rational risk-averse strategy. Moreover, we have already commented in section 2.2 and 3.2 how the investment allocation equation for this type of agent is dominated by the risk-return trade-off. Analyzing that equation and its derivation it is clear that is indeed the fundamentalist traders class to follow the principle at the foundation of the CAPM, i.e. that the investors search for high expected returns and low risk.

Indeed, what we expect is that the more the fundamentalist rational strategy of this type of agent is important with respect to the irrational component represented by the noise traders, the more the resulting dynamics of the market will adhere to the one predicted by the CAPM.

Following this reasoning, we implement a limit procedure with respect to the initial wealth of noise traders. We expect that the more the relative importance of noise trader, represented by their initial wealth, with respect to the fundamentalist ones is small, the more the prediction of the CAPM will be correct.

In the limit of the initial wealth's value of the noise traders going to zero, the prediction of the CAPM should become exact with respect to the actual dynamics generated by our simulation.

In figures 5.28, 5.29, 5.30, 5.31, and 5.32, we present exactly this limit. The simulations are obtained from the implementation of the $O(n = 4)$ version of the ABM characterized by Ornstein-Uhlenbeck kappa process with with mean reversion level $\mu_k = 0.98 \cdot 2$.

The figures present the relative error of the CAPM prediction defined as the average (over the four risky assets) relative difference between the realized annual return and the annual return predicted by the CAPM, fitted on the previous two years returns. The initial wealth of the noise traders is decreased along the figures from a value of $W_0^n = 10^9$, equal to the fundamentalist wealth $W_0^f = 10^9$ that instead remains fixed across the figures, to a value of $W_0^n = 10^2$, negligible with respect to the fundamentalist's one.

From the comparison of the figures, it emerges that the convergence of our model dynamics to the one predicted by the CAPM is indeed present in the limit of the initial wealth of the noise traders going to zero. Indeed, the range of values of the relative errors of the CAPM prediction substantially decreases with the decreasing of W_0^n.

For completeness, we also report the plots of the realized annual return together with the annual return predicted by the CAPM for two of the above situations, in particular in figure 5.33 we present the $W_0^n = 10^6$ case and in figure 5.34 the $W_0^n = 10^9$ case.

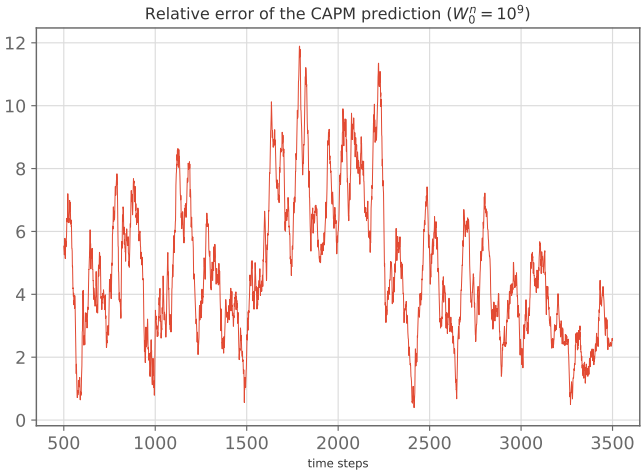

Figure 5.28: Relative error of the CAPM prediction defined as the average (over the four risky assets) relative difference between the realized annual return and the annual return predicted by the CAPM, fitted on the previous two years returns. Each point of the graph refers to the annual return of the year starting at that time-step. The CAPM fitting is done on the previous 500 time-steps. In particular, in this figure, we report the result for an initial wealth of the noise traders $W_0^n = 10^9$.

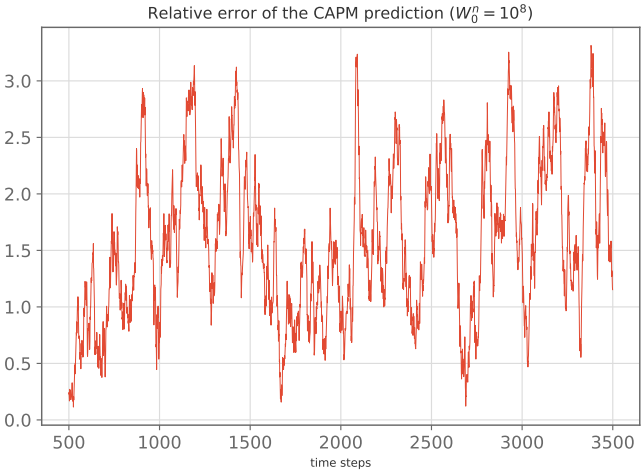

Figure 5.29: Relative error of the CAPM prediction with $W_0^n = 10^8$. We refer to figure 5.28 for a detailed description.

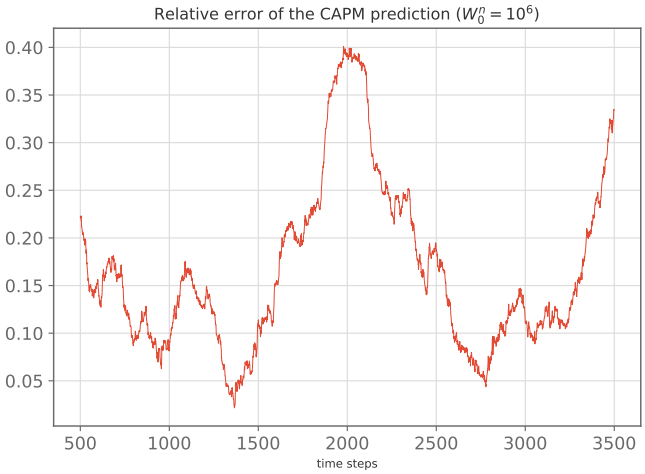

Figure 5.30: Relative error of the CAPM prediction with $W_0^n = 10^6$. We refer to figure 5.28 for a detailed description.

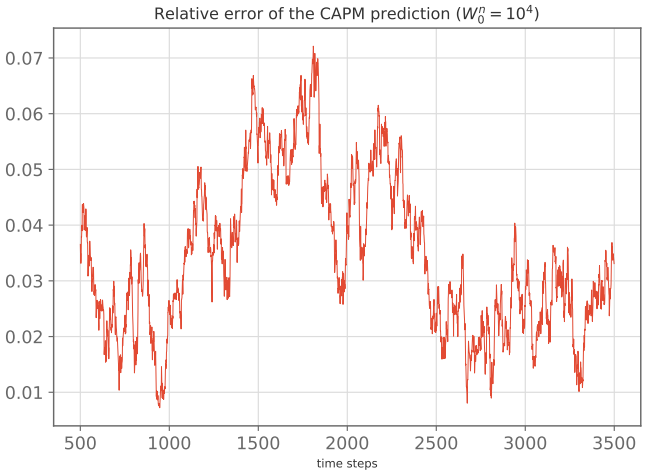

Figure 5.31: Relative error of the CAPM prediction with $W_0^n = 10^4$. We refer to figure 5.28 for a detailed description.

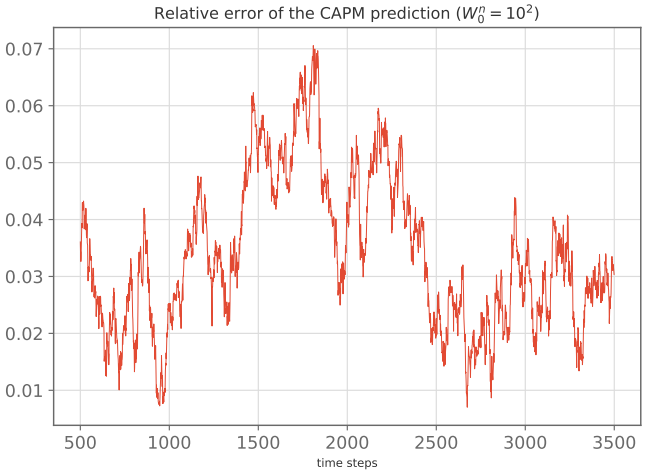

Figure 5.32: Relative error of the CAPM prediction with $W_0^n = 10^2$. We refer to figure 5.28 for a detailed description.

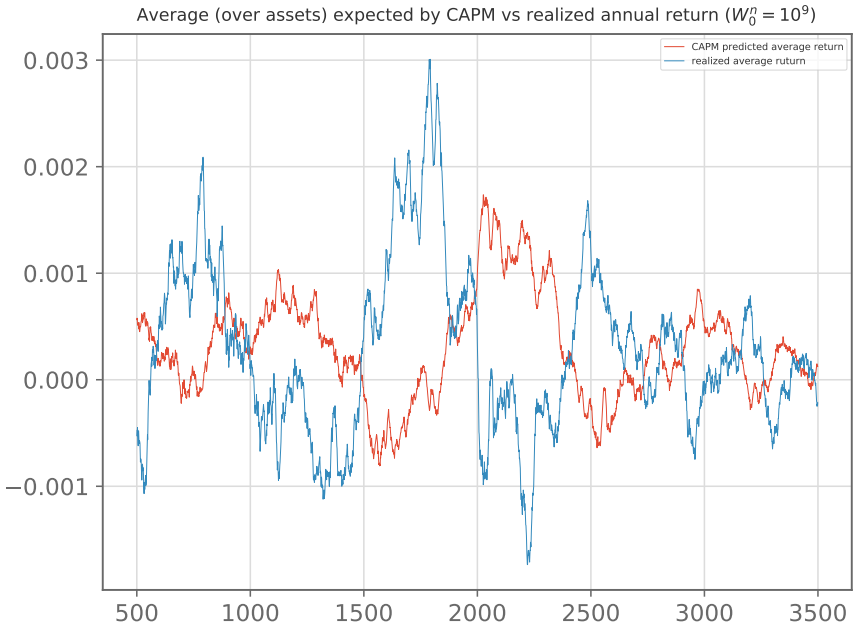

Figure 5.33: Time series of the realized annual return and the annual return predicted by the CAPM, in the case of $W_0^n = 10^9$.

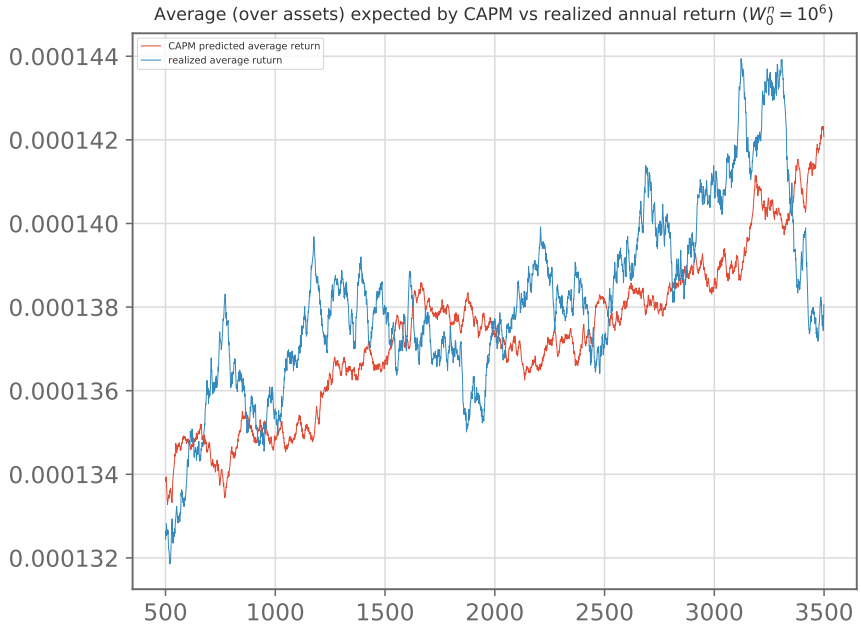

Figure 5.34: Time series of the realized annual return and the annual return predicted by the CAPM, in the case of $W_0^n = 10^6$.

Chapter 6

Conclusion

The goal of the present work has been to introduce a multi-risky-asset extension of the ABM first introduced by Kaizoji et al. [13] which is able to reproduce faster-than-exponential bubbles growth together with "stylized facts" of the financial market.

We dedicated Chapter 2 to review the original setup, composed of a risk-free asset, representing a zero-coupon government bond yielding a constant rate of return, and a risky asset, representing a stock paying a dividend to its holders. We then reviewed the other components of the model: the fundamentalist traders, rational risk-averse traders, and the noise traders guided instead by social imitation and trend following, and the price dynamics generated imposing the market clearing conditions according to Walras' theory of general equilibrium. We have also expanded the previous analysis on the model, deepening the profound connection between the noise traders class and the Ising model and discussing two features of the original transition rates which appear to be fundamental in characterizing the realistic dynamics of the bubbles.

We then moved towards the multi-asset extension of the market model discussing in Chapter 3 the presence of multiple risky investments and detailing the generalization of the fundamentalist traders' solution to the rational optimization problem characterizing their CRRA utility maximization. We then tackled the solution of the complex non-linear system characterizing the extended price equations through numerical techniques. At the end of the Chapter, we discussed the noise traders' generalization puzzle, introducing the Statistical Physics approach we have applied.

We discussed the crucial modelization point of the present work. Indeed, modeling the noise traders class boils down to defining a stochastic dynamics for their investment' decisions. Such a stochastic dynamics is completely specified by a discrete-time Markov chain, defined by the possible states, the assets in this case, and the transition rates among them. The central problem was indeed constructing well-chosen transition probabilities that govern the dynamics of our microscopic

agent, the noise trader.

We had complete freedom in defining the stochastic dynamics which best modeled the system under analysis. Yet, we have commented that this freedom could have been a double-edged sword, indeed the resulting lack of solid theoretical results regarding the emerging statistical properties could have represented an important problem in modeling a complex system such as a financial market.

For this reason, we decided to start by modeling the statistical property of the noise traders class and then derive from them the stochastic dynamics governing the time evolution of the investment decisions.

Fortunately, we found a strong ally to accomplish this task: Statistical Physics. Indeed, Statistical Physics has a history of success in modeling systems with a large number of components (in this case the traders) whose collective interactions lead to the emergence of highly non-trivial collective phenomena (in this case the bubbles). A huge amount of work has been done in the field of Statistical Physics to tackle the problem of simulating the stochastic dynamics of a system with specified statistical properties and extremely powerful tools have been developed. We extensively made use of them.

We used the powerful tool constituted by the Markov Chain Monte Carlo (MCMC) theory together with the detailed balance condition to define realistic stochastic dynamics while having complete control of the resulting statistical properties.

This Statistical Physics approach has been implemented in Chapter 4, where we have presented four statistical models, a Potts model, an $O(n)$ model, a vectorial extension of the BEG model, and an n-state extension of the BEG model and for each of them we derived the characterizing stochastic dynamics through the aforementioned method.

Despite their differences, we commented on how all the models share the same underlying mechanism triggering and generating the bubbles. When the herding propensity parameter exceeds a certain model-dependent critical threshold, the noise traders' class undergoes an actual phase transition from the disordered state dominated by the idiosyncratic opinion to the ordered state where the class polarizes towards specific investment preferences. This interaction-driven collective behavior leads to the emergence of highly non-trivial phenomena, the bubbles. This is a typical feature of complex multi-agent systems.

Then for each model, we have deeply discussed its strengths and weaknesses. We really tried to present in this Chapter the largest analysis possible regarding the Ising-like modeling of the noise traders class, we did our best to construct a collection of useful suggestions, warnings, possible dangers, and fruitful directions for anyone who would face the problem to model the social imitation and trend following attitudes in a multi-asset framework. In particular, we focused on both the theoretical aspects of the derivation of the simulation's method and its

implementation's side. We underlined the good results but also the big problems faced, some of them not yet completely solved.

Finally, in Chapter 5 we moved to the comparison of the effectiveness of the various setups in modeling a real financial market. We decided to use for the application part the ABM with the $O(n)$ model for the noise traders' class. We focused on it due to both the validity of the resulting price time series and to the high controllability of its behavior, connected to solid theoretical results on the model itself and the intuitive meaning of its parameters.

We first checked the model's ability to reproduce the "stylized facts" of financial markets, in particular, focusing on the hyperbolic decay of the autocorrelation function of the absolute returns in contrast to the exponential decay of the autocorrelation of the signed returns, together with the fat-tailed behavior of the distribution of the returns. We happily found that the model was indeed able to reproduce them. Then the analysis has been carried out in two main directions. First, the extended ABM has been applied to understand the mechanism behind the time synchronization of bubbles among the assets. The interesting analysis emerging showed the importance of the herding propensity parameter in governing the synchronous or asynchronous character of the bubbles. The second direction instead dealt with the comparison of the dynamics of the resulting returns to the one predicted by the Capital Asset Pricing Model (CAPM), we showed how the dynamics of our model converge to the one predicted by the CAPM in the limit of the negligible relative importance of the noise traders with respect to the fundamentalist ones.

The research on the extended market model is far from being over and complete. The possible further directions of analysis are manifold and in our opinion extremely interesting. Here we just mention some of them.

The dividends dynamics modelization can be expanded and made more realistic, in particular, through the covariance matrix of the dividends processes, the effect of the correlations among the assets coming from the real economy on the realized financial correlations can be studied.

The extremely challenging analysis of the possibility to construct stochastic dynamics for the noise traders through the more general global balance rule instead of the more restrictive detailed balance one could be tackled. The theoretical discussion on the relationships between detailed balance and global balance is extremely wide and in our opinion represents one of the most interesting and challenging aspects of modern Statistical Physics theory. Its application in financial modeling constitutes a frontier research topic. For a great discussion on it, we refer to Bouchaud [43].

A further analysis that could be done is the study of the rich physical picture which emerges considering also negative value for the kappa process, i.e. contrarian noise traders. For it we refer to the last part of section 4.1 on the Potts model and

on the captivating discussion in Ostilli and Mukhamedov [51].

In our opinion, one of the most appealing further directions of analysis is doubtless constituted by a deeper study of the n-state BEG model, presented in section 4.5. In particular regarding the possibility to introduce a notion of risk aversion for the noise traders and to work with the extremely rich physical picture emerging from the phase diagram of the model, characterized by phase transitions of a different order and an intriguing tricritical point.

Finally, on the application side, the interesting results concerning the Mexican hat picture presented in section 5.4 could be explored in a wider manner as well as the topic of the limit towards the CAPM.

We truly hope this work could be a reference and a starting point for further direction of analysis on this rich and effective Agent-Based Model.

Bibliography

[1] Thomas Lux. «Herd behaviour, bubbles and crashes». In: *The economic journal* 105.431 (1995), pp. 881–896 (cit. on pp. 1, 18).

[2] W Brian Arthur, John H Holland, Blake LeBaron, Richard Palmer, and Paul Tayler. «Asset pricing under endogenous expectations in an artificial stock market». In: *The economy as an evolving complex system II* 27 (1996) (cit. on p. 1).

[3] William A Brock and Cars H Hommes. «Heterogeneous beliefs and routes to chaos in a simple asset pricing model». In: *Journal of Economic dynamics and Control* 22.8-9 (1998), pp. 1235–1274 (cit. on p. 1).

[4] James J Heckman. «Micro data, heterogeneity, and the evaluation of public policy: Nobel lecture». In: *Journal of political Economy* 109.4 (2001), pp. 673–748 (cit. on p. 1).

[5] John Conlisk. «Why bounded rationality?» In: *Journal of economic literature* 34.2 (1996), pp. 669–700 (cit. on p. 1).

[6] Ariel Rubinstein. *Modeling bounded rationality*. MIT press, 1998 (cit. on p. 1).

[7] Rama Cont. «Empirical properties of asset returns: stylized facts and statistical issues». In: (2001) (cit. on pp. 1, 147, 148).

[8] Rama Cont. «Volatility clustering in financial markets: empirical facts and agent-based models». In: *Long memory in economics*. Springer, 2007, pp. 289–309 (cit. on pp. 1, 147, 148).

[9] Robert Axelrod. «Agent-based modeling as a bridge between disciplines». In: *Handbook of computational economics* 2 (2006), pp. 1565–1584 (cit. on p. 2).

[10] Cars H Hommes. «Heterogeneous agent models in economics and finance». In: *Handbook of computational economics* 2 (2006), pp. 1109–1186 (cit. on p. 2).

[11] Nicholas T Chan, Blake LeBaron, Andrew W Lo, Tomaso Poggio, Andrew W Lo Yy, and Tomaso Poggio Zz. «Agent-based models of financial markets: A comparison with experimental markets». In: (1999) (cit. on p. 2).

[12] Didier Sornette. «Physics and financial economics (1776–2014): puzzles, Ising and agent-based models». In: *Reports on progress in physics* 77.6 (2014), p. 062001 (cit. on pp. 2, 30, 62, 92).

[13] Taisei Kaizoji, Matthias Leiss, Alexander Saichev, and Didier Sornette. «Super-exponential endogenous bubbles in an equilibrium model of fundamentalist and chartist traders». In: *Journal of Economic Behavior & Organization* 112 (2015), pp. 289–310 (cit. on pp. 2, 6, 9, 10, 12, 14, 18, 19, 22, 27, 28, 30, 42, 46, 52, 59, 67, 68, 123, 169).

[14] Carl Chiarella, Roberto Dieci, and Xue-Zhong He. «Heterogeneity, market mechanisms, and asset price dynamics». In: *Handbook of financial markets: Dynamics and evolution*. Elsevier, 2009, pp. 277–344 (cit. on pp. 2, 6, 9, 42, 45).

[15] Thomas Lux and Michele Marchesi. «Scaling and criticality in a stochastic multi-agent model of a financial market». In: *Nature* 397.6719 (1999), pp. 498–500 (cit. on pp. 2, 6, 11, 13).

[16] L Walras. *Elements of Pure Economics. English translation by W. Jaffe (1954)*. 1926 (cit. on pp. 2, 7, 16, 47).

[17] Ralf Kohrt. «The market impact of exploiting financial bubbles». In: *Master's thesis, ETH Zürich* (2016) (cit. on pp. 6, 8, 14, 16, 19, 20, 22, 130).

[18] Rebecca Westphal and Didier Sornette. «Market impact and performance of arbitrageurs of financial bubbles in an agent-based model». In: *Journal of Economic Behavior & Organization* 171 (2020), pp. 1–23 (cit. on pp. 6, 19, 22, 67, 102, 122, 130).

[19] Madis Ollikainen. «Multiple market regimes in an equilibrium model of fundamentalist and noise traders». In: *Master's thesis, ETH Zürich* (2016) (cit. on pp. 6, 11, 19, 21, 22, 26, 30, 85, 130).

[20] Jean-Remy Conti. «Long-term behavior of an artificial market, composed of fundamentalists and noise traders». In: *Master's thesis, ETH Zürich* (2018) (cit. on p. 6).

[21] Emily Damiani. «Equilibrium model of fundamentalist and noise traders in a multi-asset framework». In: *Master's thesis, Politecnico di Torino* (2019) (cit. on pp. 6, 30, 42, 45, 47, 49).

[22] Antoine Kopp. «Equilibrium model of a Fixed Income market with fundamentalist and chartist traders». In: *Master's thesis, ETH Zürich* (2020) (cit. on pp. 6, 42, 45–49, 51).

[23] Sayuli Drouard. «Effects of controlling or exploiting financial bubbles on market dynamics, in the framework of an agent-based model». In: *Master's thesis, ETH Zürich* (2020) (cit. on p. 6).

[24] Rebecca Westphal and Didier Sornette. «How market intervention can prevent bubbles and crashes». In: *Swiss Finance Institute Research Paper* 12-74 (2020) (cit. on p. 6).

[25] William A Brock, Cars H Hommes, et al. «Rational animal spirits». In: (1999) (cit. on p. 9).

[26] Carl Chiarella, Xuezhong He, et al. «Asset price and wealth dynamics under heterogeneous expectations». In: *Quantitative Finance* 1.5 (2001), pp. 509–526 (cit. on p. 10).

[27] Franco Modigliani and Merton H Miller. «The cost of capital, corporation finance and the theory of investment». In: *The American economic review* 48.3 (1958), pp. 261–297 (cit. on pp. 10, 46).

[28] Franco Modigliani and Merton H Miller. «Corporate income taxes and the cost of capital: a correction». In: *The American economic review* 53.3 (1963), pp. 433–443 (cit. on pp. 11, 46).

[29] Morgan Kelly. «All their eggs in one basket: Portfolio diversification of US households». In: *Journal of Economic Behavior & Organization* 27.1 (1995), pp. 87–96 (cit. on p. 11).

[30] Jean-Philippe Bouchaud and Marc Mézard. «Wealth condensation in a simple model of economy». In: *Physica A: Statistical Mechanics and its Applications* 282.3-4 (2000), pp. 536–545 (cit. on p. 12).

[31] Georges Harras, Claudio J Tessone, and Didier Sornette. «Noise-induced volatility of collective dynamics». In: *Physical Review E* 85.1 (2012), p. 011150 (cit. on pp. 12, 13, 30).

[32] Tom Engsted and Thomas Q Pedersen. «The dividend–price ratio does predict dividend growth: International evidence». In: *Journal of Empirical Finance* 17.4 (2010), pp. 585–605 (cit. on p. 19).

[33] Didier Sornette. *Why stock markets crash: critical events in complex financial systems*. Vol. 49. Princeton University Press, 2017 (cit. on p. 21).

[34] Robert J Shiller. *Irrational exuberance: Revised and expanded third edition*. Princeton university press, 2015 (cit. on p. 26).

[35] Roy J Glauber. «Time-dependent statistics of the Ising model». In: *Journal of mathematical physics* 4.2 (1963), pp. 294–307 (cit. on p. 31).

[36] Carl Chiarella, Roberto Dieci, and Xue-Zhong He. «Heterogeneous expectations and speculative behavior in a dynamic multi-asset framework». In: *Journal of Economic Behavior & Organization* 62.3 (2007), pp. 408–427 (cit. on p. 42).

[37] Volker Böhm and Carl Chiarella. «Mean variance preferences, expectations formation, and the dynamics of random asset prices». In: *Mathematical Finance: An International Journal of Mathematics, Statistics and Financial Economics* 15.1 (2005), pp. 61–97 (cit. on p. 42).

[38] Hai-Chuan Xu, Wei Zhang, Xiong Xiong, and Wei-Xing Zhou. «Wealth share analysis with "fundamentalist/chartist" heterogeneous agents». In: *Abstract and Applied Analysis*. Vol. 2014. Hindawi. 2014 (cit. on pp. 42, 46).

[39] Christian Borghesi and Jean-Philippe Bouchaud. «Of songs and men: a model for multiple choice with herding». In: *Quality & quantity* 41.4 (2007), pp. 557–568 (cit. on p. 42).

[40] Shu-Heng Chen and Ya-Chi Huang. «Risk preference, forecasting accuracy and survival dynamics: Simulations based on a multi-asset agent-based artificial stock market». In: *Journal of Economic Behavior & Organization* 67.3-4 (2008), pp. 702–717 (cit. on p. 42).

[41] Michael JD Powell. *A Fortran subroutine for solving systems of nonlinear algebraic equations*. Tech. rep. Atomic Energy Research Establishment, Harwell, England (United Kingdom), 1968 (cit. on p. 48).

[42] Michael JD Powell. «A hybrid method for nonlinear equations». In: *Numerical methods for nonlinear algebraic equations* (1970) (cit. on p. 48).

[43] Jean-Philippe Bouchaud. «Crises and collective socio-economic phenomena: simple models and challenges». In: *Journal of Statistical Physics* 151.3-4 (2013), pp. 567–606 (cit. on pp. 59, 171).

[44] Nicholas Metropolis, Arianna W Rosenbluth, Marshall N Rosenbluth, Augusta H Teller, and Edward Teller. «Equation of state calculations by fast computing machines». In: *The journal of chemical physics* 21.6 (1953), pp. 1087–1092 (cit. on pp. 60, 91).

[45] Daniel McFadden. «Econometric models of probabilistic choice». In: *Structural analysis of discrete data with econometric applications* 198272 (1981) (cit. on pp. 63, 92).

[46] Paul Cuff, Jian Ding, Oren Louidor, Eyal Lubetzky, Yuval Peres, and Allan Sly. «Glauber dynamics for the mean-field Potts model». In: *Journal of Statistical Physics* 149.3 (2012), pp. 432–477 (cit. on p. 80).

[47] TR Kirkpatrick and PG Wolynes. «Stable and metastable states in mean-field Potts and structural glasses». In: *Physical Review B* 36.16 (1987), p. 8552 (cit. on p. 80).

[48] Massimo Ostilli and Farrukh Mukhamedov. «1D Three-state mean-field Potts model with first-and second-order phase transitions». In: *Physica A: Statistical Mechanics and its Applications* (2020), p. 124415 (cit. on p. 80).

[49] D Thirumalai and TR Kirkpatrick. «Mean-field Potts glass model: Initial-condition effects on dynamics and properties of metastable states». In: *Physical Review B* 38.7 (1988), p. 4881 (cit. on p. 80).

[50] Alessandro Pelizzola. «Statistical Physics Notes». In: *Lecture notes of the Statistical Physics course, part of the Master's Degree Physics of Complex Systems at Politecnico di Torino* (2020) (cit. on p. 80).

[51] M Ostilli and F Mukhamedov. «Continuous-and discrete-time Glauber dynamics. First-and second-order phase transitions in mean-field Potts models». In: *EPL (Europhysics Letters)* 101.6 (2013), p. 60008 (cit. on pp. 85, 86, 172).

[52] Mervin E Muller. «A note on a method for generating points uniformly on n-dimensional spheres». In: *Communications of the ACM* 2.4 (1959), pp. 19–20 (cit. on p. 93).

[53] Ognyan Ivanov Zhelezov. «N-dimensional rotation matrix generation algorithm». In: *American Journal of Computational and Applied Mathematics* 7.2 (2017), pp. 51–57 (cit. on pp. 98, 99, 136).

[54] M Blume, VJ Emery, and Robert B Griffiths. «Ising model for the λ transition and phase separation in He 3-He 4 mixtures». In: *Physical review A* 4.3 (1971), p. 1071 (cit. on p. 110).

[55] William F Sharpe. «Capital asset prices: A theory of market equilibrium under conditions of risk». In: *The journal of finance* 19.3 (1964), pp. 425–442 (cit. on p. 162).